A Synthetic Approach to Asymmetric Phthalocyanines with Peripheral Metal-Binding Sites and Their Divalent Ruthenium Complexes

Inauguraldissertation

der Philosophisch-naturwissenschaftlichen Fakultät

der Universität Bern

vorgelegt von

Marco Haas

von Muntelier FR

Leiter der Arbeit:

Prof. Dr. S. Decurtins

Departement für Chemie und Biochemie

A Synthetic Approach to Asymmetric Phthalocyanines with Peripheral Metal-Binding Sites and Their Divalent Ruthenium Complexes

Inauguraldissertation

der Philosophisch-naturwissenschaftlichen Fakultät

der Universität Bern

vorgelegt von

Marco Haas

von Muntelier FR

Leiter der Arbeit:

Prof. Dr. S. Decurtins

Departement für Chemie und Biochemie

Von der Philosophisch-naturwissenschaftlichen Fakultät angenommen.

Der Dekan:

Bern, 21. Dezember 2006   Prof. Dr. P. Messerli

Acknowledgements

First of all, I would like to thank Prof. Dr. Silvio Decurtins for giving me the opportunity to realise the present PhD work in his research group. I extremely appreciate the freedom he granted me during the work on my project. At the same time, he was always there for discussions and new ideas. He also made it possible for me to attend very interesting national and international work shops and conferences, where I could learn from other scientists.

Special thanks go to Dr. Shi-Xia Liu who supported me throughout my PhD work. She always found time for discussions and gave helpful advice. She also spent a lot of time on reviewing the present thesis and made useful suggestions to improve it.

I also thank Prof. Dr. Peter Belser for co-refereeing my dissertation and Prof. Dr. Gion Calzaferri for chairing my PhD defense.

The collaboration with several research groups made the versatility of this work possible. I would like to thank Dr. Thomas Jung, Dr. Meike Stöhr and Tomas Samuely from the University of Basel for the very interesting and instructive STM project. Many thanks go to Dr. Meike Stöhr who supported me during the writing of Chapter 4 of the present work. Then, my thanks go to Prof. Dr. Dirk Guldi and Axel Kahnt from the University of Erlangen (Germany) for the transient absorption measurements. I also thank Prof. Dr. Andreas Hauser and Dr. Claudia Leiggener from the University of Geneva for the luminescence studies. Many thanks go to Prof. Dr. Helen Stoeckli-Evans and Dr. Antonia Neels from the University of Neuchâtel for the determination of the crystal structures. Furthermore, I would like to thank Dr. Eric Levillain from the Laboratoire de Chimie, Ingénierie Moléculaire et Matériaux d'Angers (CIMMA, France) and Dr. Christine Goze for cyclic voltammetry measurements.

Special thanks go to Fredy Nydegger from the University of Fribourg for MALDI and ESI mass spectrometry. Many thanks go to Dominique Mooser and his group from the Ecole d'Ingénieurs et d'Architectes in Fribourg for elemental analyses. I also thank our in-house services, namely the NMR group of Prof. Dr. Peter Bigler, the MS group of Dr. Stefan Schürch and Beatrice Frey and Beatrice Köppel from the solid state analysis group for innumerable measurements. Furthermore, thanks go to the people from the library, the material administration and to our present and former secretaries Brigitte Oggier and Verena Scharnhorst.

Especially, I would like to thank all former and present group members of the Decurtins research group for the nice working atmosphere and their help during the last four years.

Last but not least, I would like to express my gratitude to my family and friends who always supported me during my studies.

Abstract

The present work describes synthetic routes to phthalocyanine-based multicomponent systems. In a first step, various ligand systems in the form of asymmetric phthalocyanines (Pcs) with peripheral metal-binding sites were prepared. These metal-binding sites can either be offered by flexible pyridyl groups or by a rigid phenanthroline unit. In the former case, asymmetric Pcs of the AAAB, AABB, ABAB and ABBB type were successfully isolated from the statistical mixture formed via a cyclotetramerisation reaction of a phthalonitrile bearing solubilising groups (denoted by A) and 6,7-dicyano-2,3-di(2-pyridyl)quinoxaline (denoted by B). In the latter case, an asymmetric Pc with one dipyrido[3,2-f:2',3'-h]quinoxaline unit directly fused to the Pc was synthesised according to the aforementioned strategy. Synthetic procedures for the selective coordination of metal ions, such as Co(II), Mg(II) or Zn(II), into the macrocyclic cavity of this ligand system have been developed. The resulting MPcs were then reacted with [Ru(bpy)$_2$Cl$_2$] to obtain the corresponding [MPc-Ru(bpy)$_2$]$^{2+}$ dyad systems. Transient absorption experiments revealed that these dyads exhibit very efficient intramolecular energy transfer from the Ru(II) moiety to the MPc unit upon photoexcitation. Finally, 4',5'-bis-(propylthio)tetrathiafulvaleno[4,5-i]dipyrido[3,2-a:2',3'-c]phenazine (TTF-dppz), instead of bpy, was successfully introduced to give multicomponent system [ZnPc-Ru(TTF-dppz)$_2$]$^{2+}$. This compound is composed of three photophysically active entities, but all emission features are totally quenched indicating the appearance of intriguing deactivation processes of the excited states in this complex system.

Furthermore, symmetric, octa-substituted metal-free and zinc phthalocyanines were self-assembled on Ag(111) and Au(111) substrates, respectively. STM investigations revealed the formation of highly ordered Pc monolayers. Predominantly, a rhombic packing was found in all cases. Only rarely, a more loosely packed quadratic phase was observed. Aiming at the construction of an ordered, coordinative bilayer system, pyridyl-functionalised fullerene molecules were evaporated onto the highly ordered ZnPc monolayer followed by STM investigation.
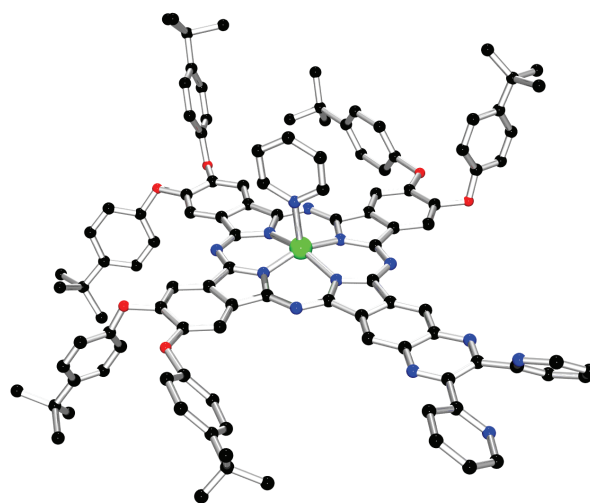
Table of Contents

Introduction

Results and Discussion

3. Synthesis of asymmetric phthalocyanines with peripherally coordinated Ru(II) complexes   **41**

Experimental Part

1. Phthalocyanine-based multicomponent systems

Phthalocyanines (Pcs) are considered as synthetic porphyrin analogues and emerge as attractive molecular building blocks due to a variety of characteristic properties. On the one hand, the electronic structure of the Pc^{2-} macrocycle represents a two-dimensional 18 π-electron system which gives rise to an intrinsic redox activity as well as two intense π-π^* transitions in the visible region. Especially the intense absorption in the red/near-infrared spectral region which, interestingly, contrasts the absorption behavior of porphyrin analogues, makes Pcs attractive for the incorporation into donor-acceptor ensembles, where they function as antennas. On the other hand, Pcs exhibit an architectural flexibility which is well exemplified by a large number of metallic complexes and importantly, a large variety of substituents can be attached to the macrocyclic core. Moreover, they offer additional advantages such as very high thermal and chemical stability. Nowadays, phthalocyanines are of great industrial importance. Many thousands of tons are produced worldwide per year. They are mainly used as pigments and dyes, in xerography, in optical data storage, in liquid-crystal displays, in solar cells, as catalysts and chemical sensors.[1,2]

The aforementioned physical and chemical properties and the increasing synthetic knowledge in attaching functional groups to the phthalocyanine periphery gathered over the last two decades has led to the incorporation of Pcs into multicomponent systems with specific properties. The study of electronic interactions in systems containing multiple redox-active centers are of fundamental importance in the development of molecular-based electronic and optoelectronic devices or multielectron redox catalysts. In addition, such systems can serve as models for the studies of photoinduced intramolecular electron or energy transfer to improve the understanding of complex, but practically useful processes such as solar energy conversion and artificial photosynthesis.[3] It has been demonstrated that Pc-based multicomponent systems exhibit higher nonlinear optical activities than monomeric Pcs.[4]

In this chapter, the functionalisation of phthalocyanines with well studied building blocks such as metal complexes, fullerenes and porphyrins will be overviewed. Despite the great scientific and technological interest in multicomponent Pc-based systems, not much effort has been devoted to their synthesis so far. The following text is mainly focused on the properties

of a variety of asymmetric phthalocyanine compounds. In the next chapter, the synthetic approach to such systems and also asymmetric Pcs in general will be described. The functionalisation of Pcs with TTF building blocks was the main project in Claudia Loosli's recent PhD thesis[5] and will therefore not be mentioned here.

1.1. Phthalocyanines with peripherally coordinated metal complexes

The main topic of the present work is the synthesis of soluble asymmetric Pcs with peripheral metal-binding sites and the introduction of divalent ruthenium complexes to their periphery in order to obtain novel materials which are expected to have interesting photophysical properties. In addition, it is a synthetic challenge to prepare such systems, which might be the reason why there are only a few examples of phthalocyanines with peripherally coordinated metal ions in the literature. All published examples are either functionalised with ruthenium(II) or iron(II) in the form of ferrocene units.

1.1.1. Phthalocyanines with peripherally coordinated ruthenium(II)

Phthalocyanines and ruthenium(II) complexes are well known for their photophysical properties. The combination of both subunits in one compound leads to new materials which are very interesting candidates for the study of energy and/or electron transfer processes.[6]

1a (R = H)
1b (R = OCH$_2$C(CH$_3$)$_3$)
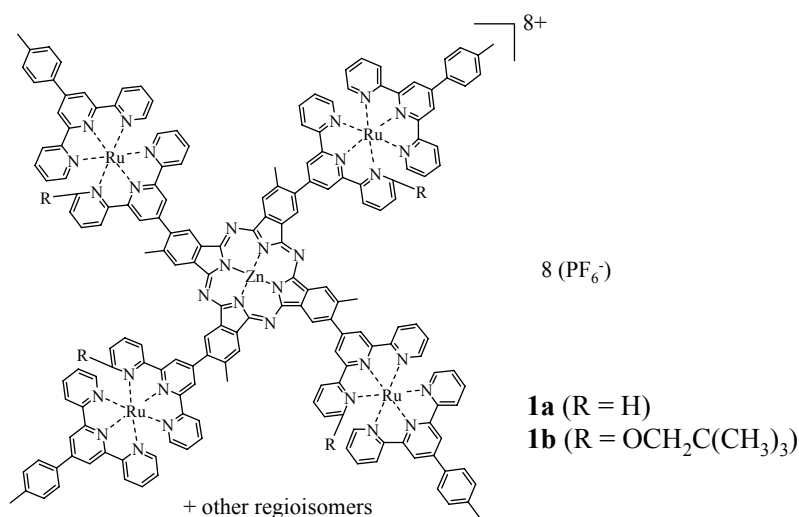
Compounds **1a** and **1b** were synthesised by Kobayashi *et al.* and their photophysical properties were investigated. Their UV-vis spectra show a slightly red shifted Q band, compared to the ZnPc ligand and a strong absorption around 500 nm (MLCT of the Ru(II) units). These molecules absorb a large part of the visible solar spectrum which could make

them interesting light harvesters. Upon excitation of the B band, fluorescence measurements showed strong quenching ($\Phi_F = 0.05$) and a red shift of the Pc fluorescence, compared to the uncomplexed ZnPcs ($\Phi_F = 0.22$). When excited at 494 nm, where only the $[Ru(tpy)_3]^{2+}$ moieties absorb, fluorescence was exclusively observed from the Pc unit. Mixtures of different ratios of uncomplexed ZnPc and $[Ru(Meph-tpy)_2](PF_6)_2$ did not show any emission upon excitation of the MLCT band of $[Ru(Meph-tpy)_2](PF_6)_2$. These results indicate a very efficient photoinduced intramolecular energy transfer from the $Ru(tpy)_3^{2+}$ units to the ZnPc moiety. In addition, the free ZnPc ligand (peripherally uncomplexed **1b**) acts as a very sensitive chemosensing material. The addition of Co^{2+}, Cu^{2+}, Fe^{2+}, Ni^{2+} and Zn^{2+} ions to a solution of uncomplexed **1b** leads to efficient fluorescence quenching. The profile of the fluorescence quenching depends on the kind of metal ion.[7,8]

2a (X = ethenyl)
2b (X = NHCO)
2c (X = ethynyl)
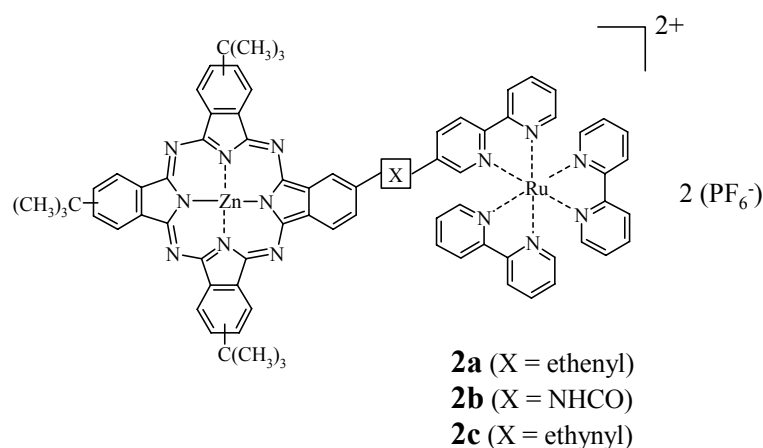
The intramolecular electronic interactions of compounds **2a-2c** have been finely tuned by variation of the spacer between the ZnPc unit and the $[Ru(bpy)_3]^{2+}$ moiety. The absorption spectra of dyads **2a** and **2c**, which have conjugated ethenyl and ethynyl bridges, respectively, show a remarkable broadening and splitting of the Q band with regard to the corresponding uncomplexed ZnPc. Moreover, the Q bands of **2a** and **2c** are significantly red shifted. This effect is indicative of some interaction in the ground state between the two photoactive subunits. The Q band absorption of **2b** and its uncomplexed ZnPc are superimposable. Dyads **2a-2c** show quenched (**2a**: $\Phi_F = 0.036$, **2b**: $\Phi_F = 0.04$, **2c**: $\Phi_F = 0.01$) and red shifted fluorescence, compared to zinc tetra-*tert*-butylphthalocyanine ($\Phi_F = 0.3$) in THF. Measuring in the more polar benzonitrile, the fluorescence is shifted to lower energies and the quenching is amplified by about a factor of two. Charge separation processes could be ruled out by transient absorption measurements. No spectral evidence was found which could be attributed to the one-electron oxidation of ZnPc or the one-electron reduction of $[Ru(bpy)_3]^{2+}$. Following the initial excitation of either chromophore, intramolecular electronic interactions between the

two subunits dominate the photophysical events. These intramolecular interactions lead, in the case of the photoexcited ZnPc unit, to faster intersystem crossing kinetics, compared to zinc tetra-*tert*-butylphthalocyanine, while photoexcited $[Ru(bpy)_3]^{2+}$ undergoes a rapid and efficient transfer of triplet excited-state energy to the ZnPc unit.[6]

3a M = 2H
3b M = Cu(II)
3c M = Ni(II)
3d M = V(IV)O
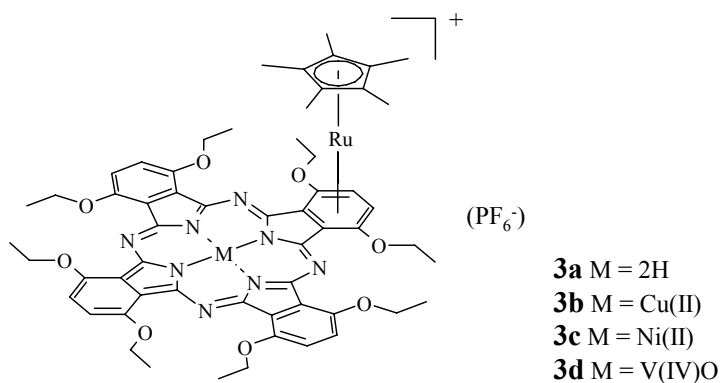
Compounds **3a-d** are systems with the phthalocyanine acting as a π-ligand. The Q band absorptions of **3a-d** show red shifts compared to the uncomplexed MPcs. In general, MPcs show strong fluorescence quenching compared to their H_2Pc analogues upon photoexcitation. In contrast, **3a** only shows a moderate decrease in emission. This indicates that π-coordination of the Ru(II)-pentamethylcyclopentadienyl cation to a phthalocyanine benzene ring (coordination mode was confirmed by X-ray analysis) has less influence on the emission properties than metallation of the Pc macrocyclic cavity.[9]

1.1.2. Phthalocyanines with peripherally attached ferrocenyl units

Ferrocene and Pc are both well known redox active units. By the combination of both, new compounds with multiple redox active centers are obtained. Such molecules can act as potential candidates for multielectron redox catalysis and serve as models for the studies of photoinduced intramolecular charge separation, which is a fundamental process in photosynthesis and the conversion of solar light into electric energy in photovoltaic cells.[3] Ferrocene units are also known to couple together when separated by a short bridge of several atoms which results in a splitting of the Fc^+/Fc redox process. They usually behave uncoupled at longer separations. An exception to this trend was found in *meso*-tetraferrocenylporphyrin[10] and *meso*-diferrocenylporphyrin[11] (ferrocenyl moieties are at opposite *meso* positions) systems, which form mixed valence species. Upon oxidation, different potentials for the Fe^{3+}/Fe^{2+} redox couples were observed, which indicate that communication between the ferrocene units occurs.[12]

Electrochemical studies of compounds **4-6** revealed that the ferrocenyl moieties attached to these phthalocyanines behave independently and are oxidised at the same potential. The electronic interaction between the ferrocenyl and Pc units seems to be insignificant in the ground state. However, the ferrocenyl units are very efficient in quenching the fluorescence of the ZnPc unit in the excited-state of **4**. This observation was assigned to a probable photoinduced electron transfer (PET) in which the ferrocene acts as an electron donor. On the basis of the electrochemical data of **4**, the overall free energy change ($\Delta G°$) for this PET was determined to be -0.48 eV, showing that it would be a thermodynamically favorable process. The alternative quenching pathway by energy transfer from the singlet excited-state of the Pc to the ferrocene is excluded because of its endothermic nature.[3] Ng and coworkers continued this work by preparing various phthalocyanines with attached ferrocenyl units, which are linked through ethynyl bridges to the Pc cores. The reason for the independence of the redox centers of the preceding systems **4-6** was thought to be the saturated nature of the oxyethylene linkers. It is known that ethynyl groups can enhance electronic coupling across a system. In addition, these linkers should impose a coplanar orientation between the Pc macrocycle and the ferrocenyl moieties, thereby enabling effective electronic interactions within the molecule. Surprisingly, these facts did not lead to communication between the ferrocenyl units, since they are undergoing electrochemical oxidation at the same potential as their oxyethylene bridged analogues.[13] Compound **7** was synthesised by Leznoff *et al.* and electrochemical studies also showed four independent one-electron oxidation processes of the four ferrocene units, which has little or no effect upon the oxidation potential of the Pc^{2-} ring even though the formal charge of the molecule has been increased by +4. Again, this strongly indicates that there is no communication between the two redox-active units in the ground state.[12]
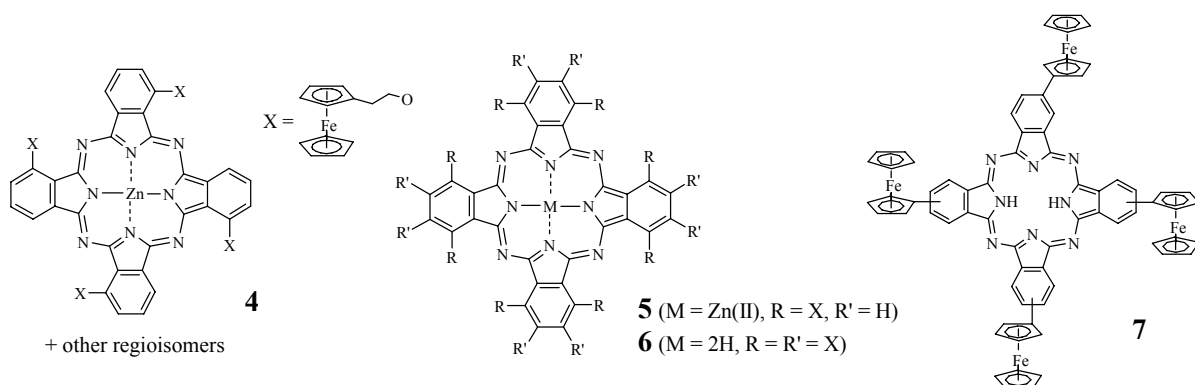
Cook and coworkers prepared compound **8** in order to study its liquid crystalline behavior. Ferrocene was chosen because of the similar distance between the cyclopentadienyl rings (3.3 Å) and the intermolecular spacing of Pc molecules within mesophase stacks. Therefore, the

ferrocenyl unit was expected to be accommodated into the mesophase packing. Indeed, compound **8** exhibits a single mesophase which is characterised by its fan type birefringence texture as a discotic columnar mesophase of hexagonal symmetry with disordered spacing within the columns.[14]
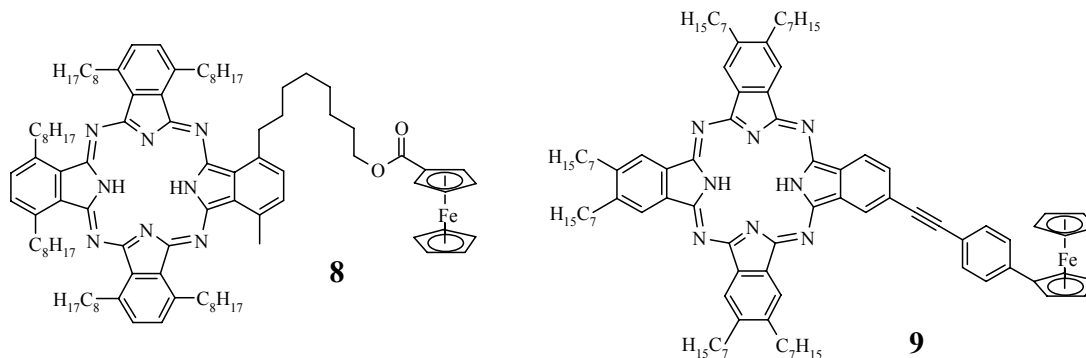
Lindsey and coworkers found that upon photoexcitation of the Q band at 662 nm, the fluorescence of the Pc unit of dyad **9** is strongly quenched ($\Phi_F = 0.09$) compared to tetra-*tert*-butylphthalocyanine ($\Phi_F = 0.77$). These experiments were also carried out after oxidation of the ferrocene unit and the Pc emission was totally quenched. These results indicate that the ferrocene cation radical serves as an extremely efficient trap for excited-state energy.[15]
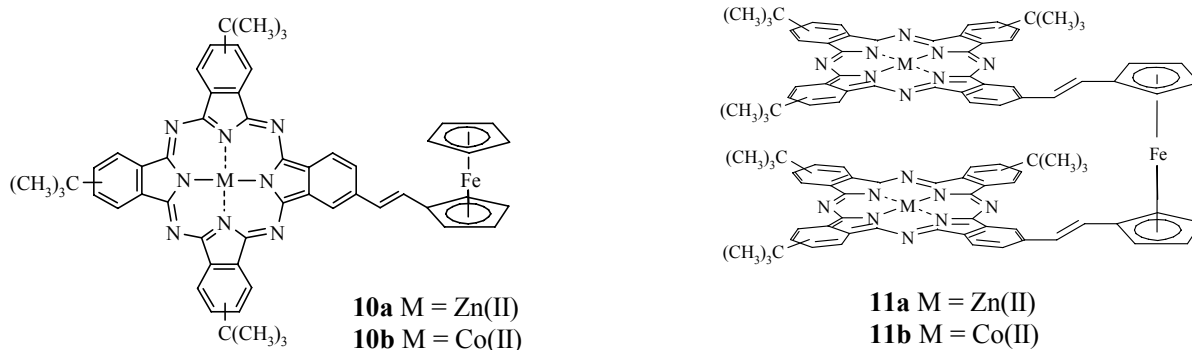
Torres *et al.* performed hyper-Rayleigh light scattering (HRS) measurements on dipolar compounds **10** and **11** to study their nonlinear optical behavior. They concluded that compounds **10** and **11** present similar dipole moments and also show similar quadratic NLO responses as measured by HRS.[16,17] For other ferrocene-functionalised Pcs mainly synthetic aspects have been published.[18,19]

All presented ferrocene-functionalised Pc systems do not show significant communication between the two units in the ground state as it has been observed for similar porphyrin ensembles, which exhibit mixed valence behavior. In compound **4** however, upon photoexcitation charge-transfer from the ferrocene to the Pc unit was assumed, but not further

investigated. In addition, dyad **9** shows communication in the excited-state in the form of the Pc fluorescence quenching.

1.2. Phthalocyanine-C$_{60}$ systems

To gain a better understanding of the processes happening in the reaction center of chlorophyll it is inevitable to mimic these charge separation events in the lab. Therefore, the combination of a donor and an acceptor unit is necessary. In addition, the donor and/or the acceptor should act as light harvesting units. Phthalocyanines can act as donors and absorb light around 300 (B band) and 680 nm (Q band) very strongly. Fullerenes are very good acceptors and exhibit very low reorganisation energies, which stabilise the C$_{60}$$^{\bullet-}$ radical anions. Therefore, the incorporation of these two molecules into dyads seems to be very promising for such studies. When, upon photoexcitation, very long-lived charge-separated states are possible, these materials can be of great interest for the application in photovoltaic cells as will be shown in the course of this chapter.

1.2.1. Peripherally fullerene-functionalised asymmetric phthalocyanines

The first phthalocyanine-C$_{60}$ dyad (**12**) was synthesised by the group of Hanack.[20] Later, the same group prepared a similar system with a larger spacer (**13**) and compared the properties of the two compounds. The UV-vis spectrum of **12** shows a split Q band (in contrast to the NiPc precursor compound), whereas **13** has one maximum (like its diene Pc precursor). Therefore, they concluded that, in contrast to **12**, the electron acceptor property of the fullerene unit in **13** has a small influence on the electronic properties of the phthalocyanine. This observation was attributed to the larger spacer of compound **13**. No excited-state photophysical studies have been carried out with these systems. CV measurements of compounds **12** and **13** revealed that the reduction potentials of the fullerene and NiPc unit do not significantly change compared to other C$_{60}$ monoaddition compounds and separated NiPcs. However, the first reduction of the fullerene unit in **12** has a pronounced influence on the optical properties of the NiPc unit, since the splitting of the Q band disappears. The fact that this was not observed in dyad **13**, was again attributed to its longer spacer.[20,21] Zhu and coworkers synthesised the CuPc-C$_{60}$ dyad **14** which is very similar to **12**.[22] The optical limiting properties of **14** in a THF solution and as nanoparticle dispersion in water were investigated. The nanoparticles had an average size of 35 nm, which was confirmed by SEM. An enhanced optical limiting performance, by excitation at 532 nm, of the nanoparticle

sample, as compared to that of the solution sample, was observed. The formation of ordered aggregates (blue shift of the Q band) with a face-to-face packing was proposed to be responsible for the enhancement of the optical limiting performance of the nanoparticle sample.[23,24]

12 (M = Ni(II), R = heptyl, R' = H)
14 (M = Cu(II), R = H, R' = *tert*-butyl)

13 (R = heptyl)

A system which was prepared and extensively studied by Torres *et al.* is the ZnPc-C$_{60}$ dyad **15a**.[25] Fluorescence and transient absorption measurements showed that in compound **15a** charge-separated states are formed upon photoexcitation. The Q band absorption of ZnPc-C$_{60}$ is red shifted by 2 nm (in *o*-dichlorobenzene) and shows a lower extinction compared to zinc tetra-*tert*-butylphthalocyanine (**ZnPc**, not shown) used as the reference. Additionally, a weak charge-transfer transition at 740 nm (in CHCl$_3$) is present. These trends suggest electronic coupling between the two units in the ground state. The fluorescence of **15a** is red shifted by 8 nm and decreased by more than one order of magnitude compared to **ZnPc**. Going from nonpolar to relatively polar solvents the quantum yields are further decreased. This is the indication for an efficient electron transfer quenching of the locally excited ZnPc unit of **15a**. Fluorescence and transient absorption measurements revealed charge-separated state lifetimes of a few nanoseconds. These charge-separated states are stabilised by large driving forces for the charge recombination (inverted region of the Marcus-parabola) and small reorganisation energies of the fullerene unit.[26] The physicochemical properties of **15a-15c** were further investigated in more detail by Guldi *et al.*[27]

15a M = Zn(II)
15b M = Cu(II)
15c M = 2H

16

The excited-state photophysical properties of ZnPc-C_{60} dyad **16** were investigated in nonpolar and polar solvents. Photophysical studies of **16** in nonpolar solvents revealed that charge recombination occurs, comparable to **15a**, within nanoseconds. When **16** is dissolved in polar solvents, perfectly ordered one-dimensional ZnPc-C_{60} nanotubules are formed. To study the aggregation properties, **16** was dispersed in water and the resulting mixture was supersonicated. The insoluble material was removed by centrifugation and one drop of the solution was analysed by transmission electron microscopy, which showed long and extremely well-organised nanorods. The fluorescence quantum yield of the ZnPc unit of dyad **16** (assembled to one-dimensional nanotubules) was determined to be lower than 10^{-5} (compared to the ZnPc reference, $\Phi = 0.3$) upon excitation either of the B or Q band. Steady-state fluorescence experiments with time-resolved measurements showed an ultrafast excited-state deactivation of the ZnPc singlet excited-state ($\sim 10^{12}$ s^{-1}). Transient absorption measurements confirmed an electron transfer state with a lifetime of 1.4 ms. Charge recombination dynamics were found to be deeply located in the Marcus inverted region, where the rate constants for electron transfer decrease with increasing driving forces.[28]

Continuing this work, Torres and coworkers published ZnPc-C_{60} dyad **17** which has, compared to **15a**, a phenylenevinylene spacer that links the two photoactive units. In compound **17**, photoexcitation leads to the formation of a charge-separated ZnPc$^{\bullet+}$-$C_{60}$$^{\bullet-}$ state, which has a lifetime of 130 ns (in THF). Electron rich compound **17** and electron deficient compound **18** were assembled to the supramolecular donor-acceptor triad **17/18**. This assembling process was monitored by absorption and fluorescence titration spectroscopy. The 1:1 stoichiometry was assertained by the Job plot method.[29] Excited-state spectroscopy of **17/18** in toluene revealed a lifetime of 475 ns for the charge-separated state. Beneficial for retarding the charge recombination is the electronic coupling of the two phthalocyanines by donor-acceptor interactions, which are expected to help in delocalising the radical cationic charge over the ZnPc and the PdPc moieties.[30]

17

18
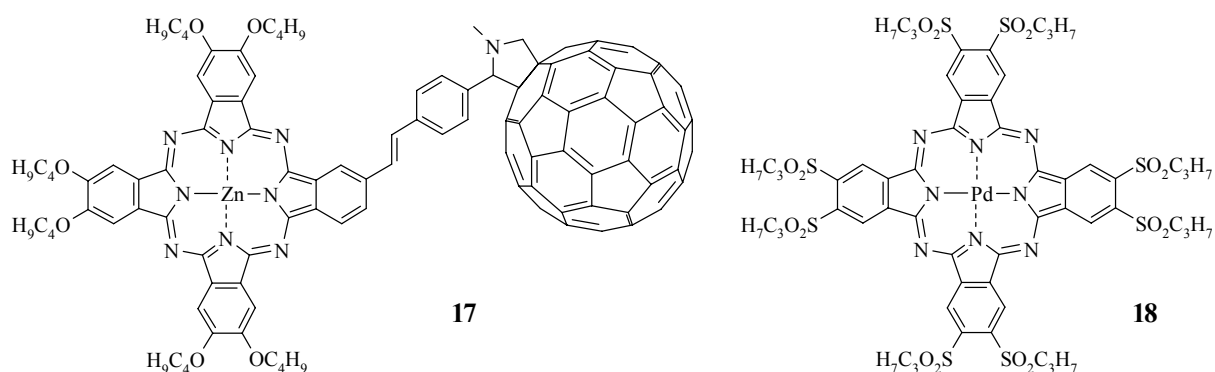
When deposited as a thin film, compound **15a** shows a very long-lived charge-separated state with a lifetime of 0.2 ms, which is several orders of magnitude higher than in solution. Such a long lifetime is essential for possible photovoltaic applications since it is necessary to avoid recombination and increase the chances of positive and negative charges reaching the electrodes. The photovoltaic devices were built on transparent indium tin oxide-coated glass. The substrate was covered with a thin film of PEDOT:PSS by spin-coating to improve the ohmic contact with the organic semiconductor. On top of it, **15a** was spin-coated and the top electrodes were vapour-deposited using LiF and Al. The power conversion efficiency under simulated solar illumination of 80 mWcm^{-2} was found to be moderate (0.02%).[31] The photocurrent of **15a** shows maxima below 400 and around 700 nm, but only a small response in the range around 500 nm. To improve the spectral match to the solar emission spectrum, an energy transfer process from the conjugated polymer MDMO-PPV to dyad **15a** was investigated. Luminescence measurements showed evidence for the above-mentioned energy transfer. In IPCE (incident photons to current efficiency) measurements, a photocurrent around 500 nm correlated with energy transfer from MDMO-PPV to ZnPc-C$_{60}$ (**15a**). In addition to the photocurrents below 400 and around 700 nm almost the full visible spectral range is covered. However, low short-circuit currents indicated charge transport problems.[32]

19
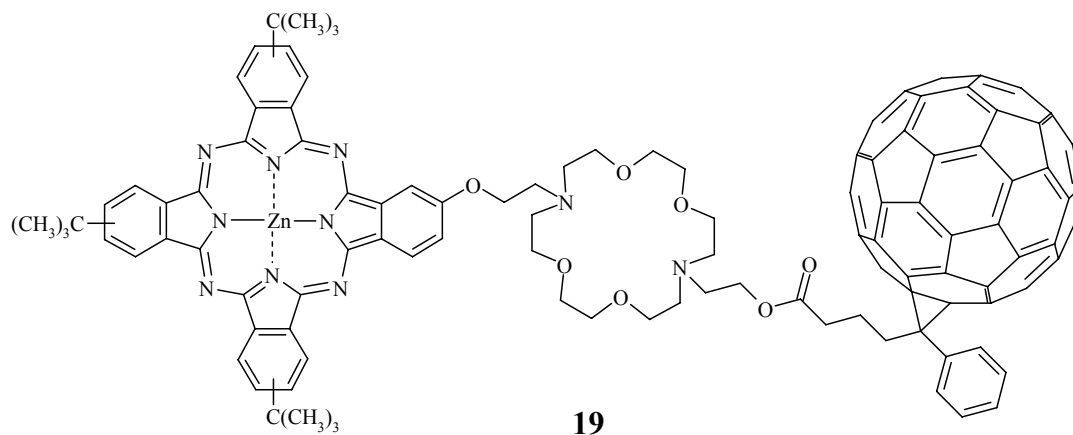
Compound **19** bearing an azacrown subunit spacer between the ZnPc and the fullerene was synthesised as a mixture of eight regioisomers. The UV-vis spectrum of **19** is a superposition of those of a zinc phthalocyanine and a typical 1,2-bridged methanofullerene, which shows that the C$_{60}$ unit has no influence on the electronic structure of the Pc ring in the ground state. Aggregation of compound **19** can have a great influence on the intermolecular photoinduced processes. Crown ethers and their derivatives are known to assemble in stacks to form ion channels upon the addition of alkali cations. Therefore, the effect of alkali cations on the aggregation of compound **19** has been studied and surprisingly, no changes in the UV-vis

spectra were found (such as a blue shift of the Q band upon aggregation of the ZnPc units). This lack of aggregation was assigned to steric hindrance of the bulky peripheral groups of the Pc unit. Excited-state photophysical studies of **19** showed no evidence for a charge separation process. In addition, electrochemical data revealed that there is no significant interaction between the two redox active units.[33]

1.2.2. Axially fullerene-functionalised phthalocyanines

Molecular dyad **20** was published independently by two research groups in short succession. Ito and coworkers performed various photophysical measurements and found evidence for the formation of the charge-separated TiPc$^{\bullet+}$-C$_{60}$$^{\bullet-}$ state, such as fluorescence quenching of the singlet excited-state of the TiPc unit of **20** in polar solvents. Additionally, transient absorption measurements after excitation at 532 nm, which excites the C$_{60}$ moiety predominantly, showed a quick raise-decay at 790 and 1020 nm. These two absorption bands were assigned to TiPc$^{\bullet+}$ and C$_{60}$$^{\bullet-}$, respectively. However, they did not determine the lifetime of the intramolecular charge-separated state.[34] Torres *et al.* confirmed the formation of an energetically low lying (around 1 eV) and very long-lived charge-separated state with a lifetime of up to 1.7 μs.[35] Another Pc compound with two axial fullerene substituents is reported in the literature, but no excited-state photophysical properties are discussed.[36]
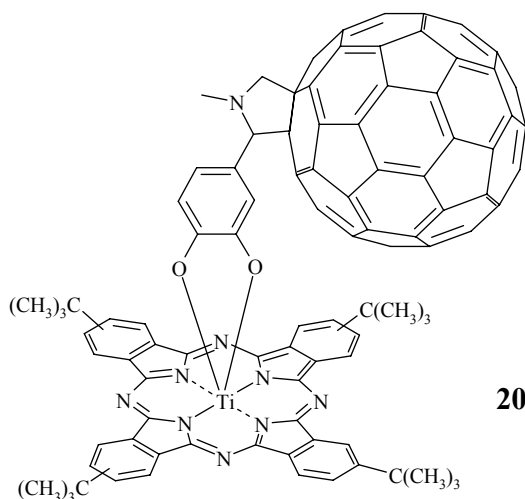
1.2.3. Noncovalently fullerene-functionalised phthalocyanines

The photophysical properties of self-assembled donor-acceptor dyad **21** were investigated in noncoordinating and coordinating solvents by D´Souza and coworkers. The formation of **21** was confirmed by UV-vis absorption spectral changes upon addition of functionalised C$_{60}$ to

the ZnPc in noncoordinating solvents, a decrease of the Q band intensity and the appearance of several isosbestic points was observed. The fluorescence intensity of **21** was decreased by 70% compared to uncomplexed ZnPc. Transient absorption experiments showed the occurrence of a very efficient charge separation. A lifetime of up to 20 ns was calculated for the supramolecular radical ion pair. The free-energy change for charge recombination was found to be -0.89 eV, which belongs to the inverted region of the Marcus parabola. In contrast to an example reported by Guldi *et al.*,[37] after photoexcitation and rapid intracomplex electron transfer, the radical ion pairs of dyad **21** do not dissociate. In benzonitrile, where the supramolecular dyad **21** is not formed, intermolecular charge-transfer was observed.[38]
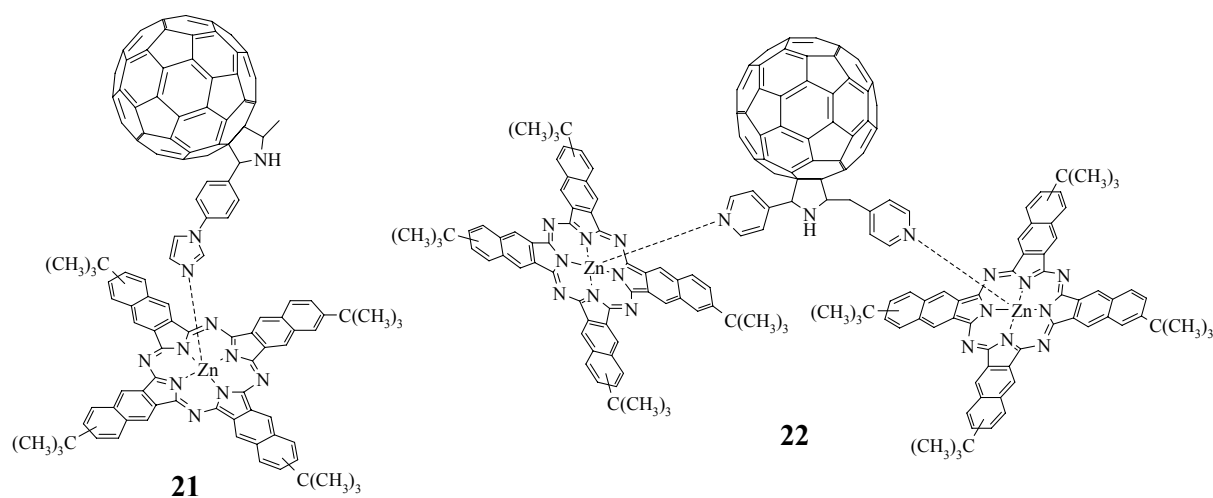
The supramolecular triad **22** was formed in a toluene solution. Its formation was confirmed in titration experiments, which showed a decreasing Q band absorption of the ZnPc unit upon addition of the bispyridine functionalised C_{60}. A Jobs plot[29] revealed the expected 2:1 composition of the supramolecular triad. The charge separation process is very efficient (Φ_{CS} = 0.93) and the lifetime of the charge-separated state is about 30 ns. In polar coordinating solvents the supramolecular triad **22** is not stable and intermolecular electron transfer from the triplet excited ZnPc to the fullerene could be observed.[39]

Zinc phthalocyanine-fullerene ensembles **23** and **24** are formed by molecular recognition of the crown ether unit and the dibenzylammonium entity.[40] Fluorescence titration experiments, in which photoexcited ZnPc or ZnPc-ZnPc are probed with variable concentrations of the dibenzylammonium-substituted fullerene, were carried out. Upon addition of the latter, a quenching of the phthalocyanine fluorescence reflects a very efficient intracomplex quenching in the formed complexes **23** and **24**. A correction for occuring intermolecular quenching between free ZnPc (ZnPc-ZnPc) molecules and dibenzylammonium substituted fullerene was performed by reference measurements with fullerene derivatives that are not

able to form supramolecular complexes such as **23** and **24**. Transient absorption measurements (excitation at 337 nm) of ZnPc and ZnPc-ZnPc, in the absence of the fullerene unit, showed that upon excitation, the resulting singlet excited-states are transformed into the long-lived triplet excited-states. After excitation of **23** and **24**, the singlet excited-state of the ZnPc moieties relax through very efficient ($\Phi = 0.9$) electron transfer processes to form charge-separated states with lifetimes of 1.5 and 1.3 μs, respectively. The charge separation process does not lead to complex dissociation as observed for a reference compound, where the C_{60} and the ZnPc unit were connected through a pyridine-ZnPc coordination bond.[37]

23   **24**
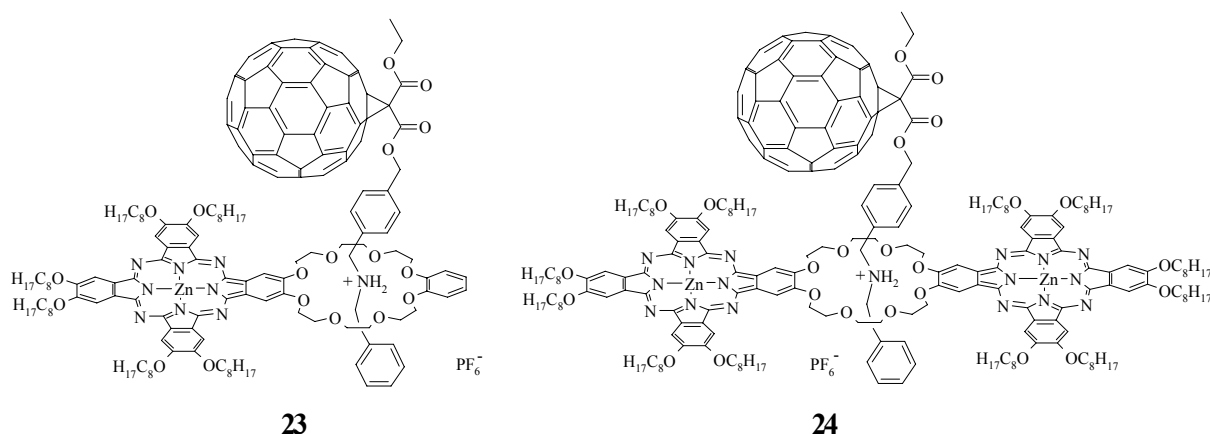
The reported charge-separated states of the above-mentioned Pc-C_{60} ensembles in solution are, compared with some porphyrin-fullerene analogues, very short-lived. In bacterial photosynthetic reaction centers for example, the radical ion pair has a lifetime of about one second.[41] Fukuzumi *et al.* observed a lifetime of 260 μs (at 298 K, in solution) in a porphyrin-fullerene dyad.[42] In a similar dyad in a frozen solution, Fukuzumi and coworkers even determined a CS state lifetime of 120 seconds (at 123 K).[43]

1.3. Light-harvesting arrays composed of phthalocyanines and porphyrins

A very important feature in the field of artificial photosynthesis is the study of light-harvesting arrays. Such constructs must incorporate a large number of closely related pigments in a well-defined three-dimensional architecture, absorb strongly across the solar spectrum, and funnel energy efficiently to a designated site – the reaction center.[44] The approach of the covalent linkage of porphyrins (Pors) to phthalocyanines turned out to be very promising for the study of such systems. In 1986, the first Por-Pc dyad was published by Maillard *et al.*[45] They observed very efficient intramolecular energy transfer from the ZnPor

to the ZnPc upon photoexcitation. In general, most such systems show this property, some of them even exhibit electron transfer from the Por to the Pc unit when photoexcited.[46-49] Systems with up to eight porphyrins per phthalocyanine have been prepared so far. Here, selected examples of the achievements in this field will be presented.
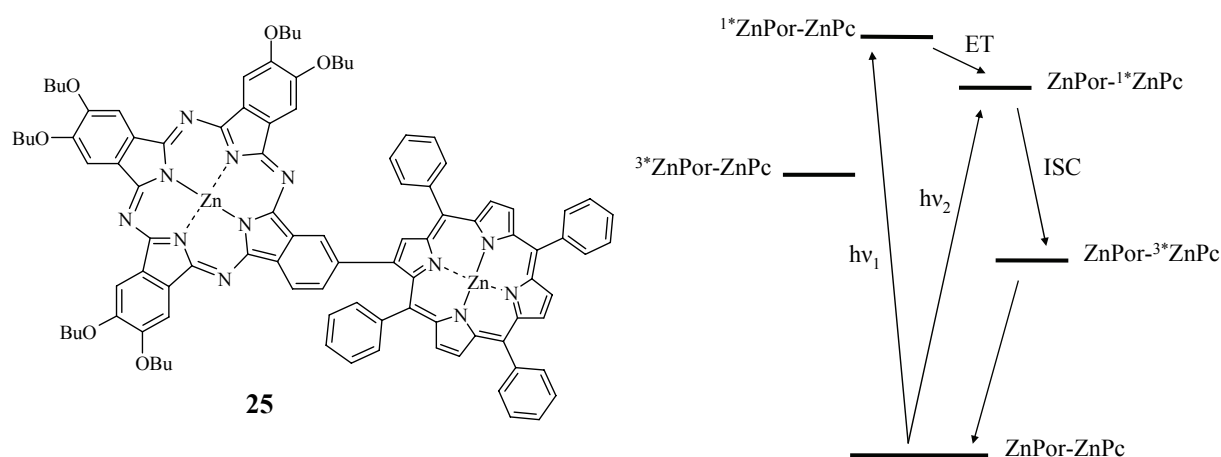
Figure 1.1. Molecular structure of ZnPor-ZnPc dyad **25** (left) and a schematic energy diagram of the predominant photophysical processes occuring in compound **25** (right).

Recently, ZnPor-ZnPc dyad **25** was synthesised by Torres and coworkers. The photophysical measurements showed very efficient energy transfer from the ZnPor unit to the ZnPc entity, which is illustrated in a schematic energy diagram in Fig. 1.1. Excitation of the Soret band (426 nm, $h\nu_1$) of the ZnPor moiety leads to strong quenching of its fluorescence compared to reference compounds. Instead, the zinc phthalocyanine unit shows strong emission around 700 nm. Fluorescence and transient absorption experiments showed that the reason for this observation is an energy transfer (ET) process from the highly energetic ^{1*}ZnPor (2.0 eV) to the ^{1*}ZnPc state (1.79 eV). From there, conventional intersystem crossing (ISC) events populate the long-lived (70 μs) ^{3*}ZnPc state (1.2 eV). ^{3*}ZnPor is not formed to any appreciable extent, which is mainly due to its unfavorable energetic positioning (1.53 eV) in dyad **25**. Going from toluene to the more polar THF no significant differences in the photophysical events could be observed. This serves as an additional proof for an all-energy transfer pathway, that is not expected to change notably with solvent polarity, in photoexcited **25**. Selective excitation of the ZnPc unit (680 nm, $h\nu_2$) leads to the photophysical processes observed for isolated phthalocyanines. The fluorescence quantum yields and lifetimes are superimposable with those recorded for zinc tetra-*tert*-butylphthalocyanine as the reference.[50] Very efficient intramolecular energy transfer from the porphyrin to the phthalocyanine units has also been observed for other dyads.[45,51,52]

+ other regioisomers

26a M = 2H
26b M = Zn(II)
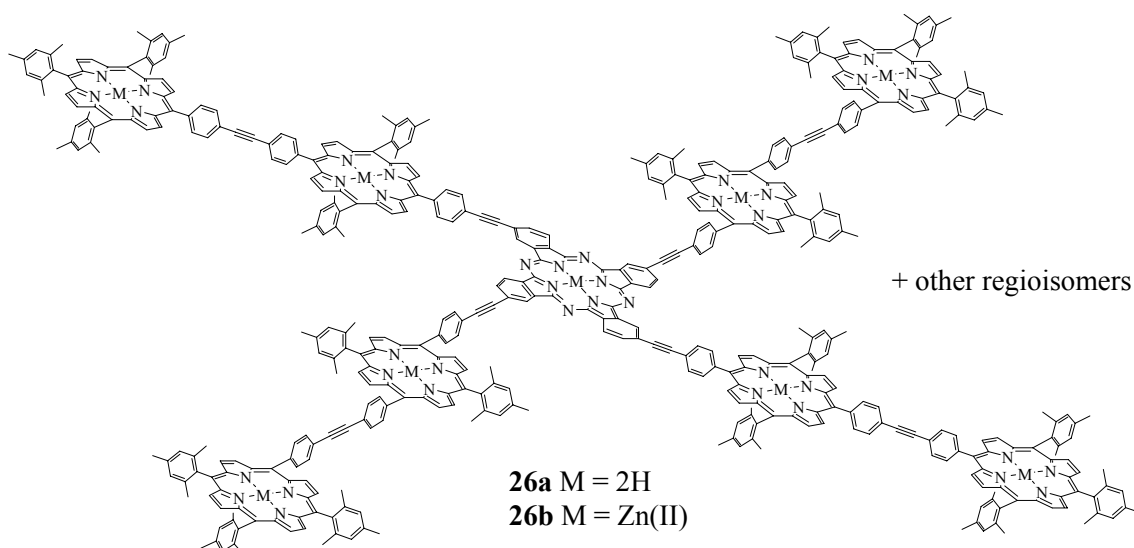
Even larger systems than **25** have been reported, such as phthalocyanines functionalised with either four[53-57] or eight[44,58] covalently attached porphyrins. Nonamers **26** and **27** show very efficient energy transfer from the Por units to the Pc moieties upon photoexcitation. Upon selective excitation of the Por units (515 nm) of compound **26a**, the fluorescence quantum yield of the Pc unit increased (Φ_F = 0.89) compared to tetra-*tert*-butylphthalocyanine (Φ_F = 0.77).[44] Despite quantitative energy transfer from the ZnPor to the ZnPc units in **27**, the fluorescence quantum yield of the ZnPc unit after photoexcitation decreases compared to a reference ZnPc.[58] This is an indication for the presence of other deactivation processes of the ZnPc singlet excited-state.

27
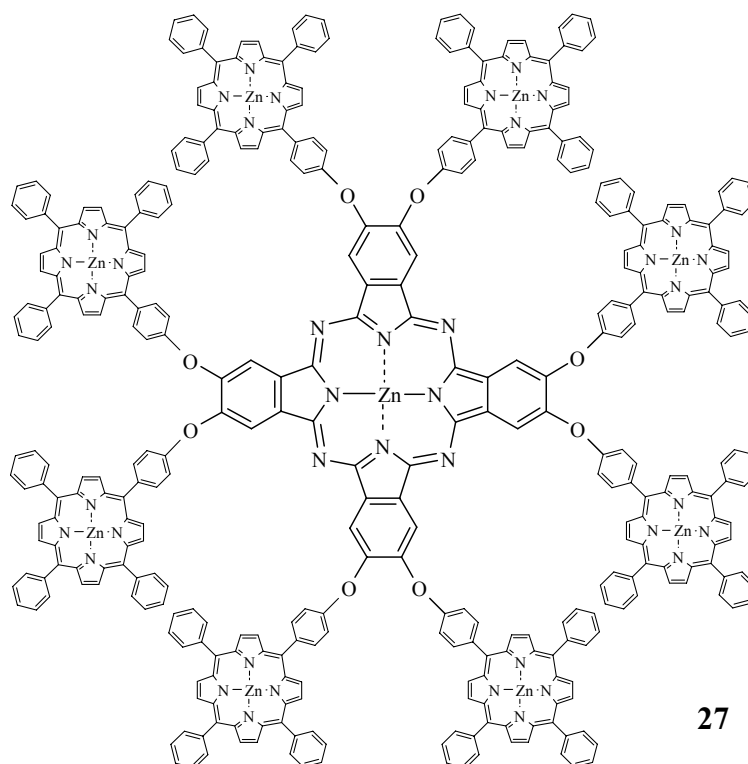
Compound **28** consists of a ZnPor-ZnPc dyad with three attached anthraquinones (Aqs) on the periphery of the ZnPc. Upon photoexcitation (355 nm), an energy transfer from the ZnPor unit to the ZnPc moiety takes place, but the phthalocyanine fluorescence is strongly quenched. Transient absorption spectra showed absorption bands of ZnPor$^{\bullet+}$, ZnPc$^{\bullet-}$ and Aq$^{\bullet-}$. Xu and coworkers suggested that the observed radical ions are generated via the excited ZnPc singlet state. After intersystem crossing to ^{3*}ZnPc charge separation to the radical pair ZnPor$^{\bullet+}$-ZnPc-Aq$^{\bullet-}$ occurs.[59]

28
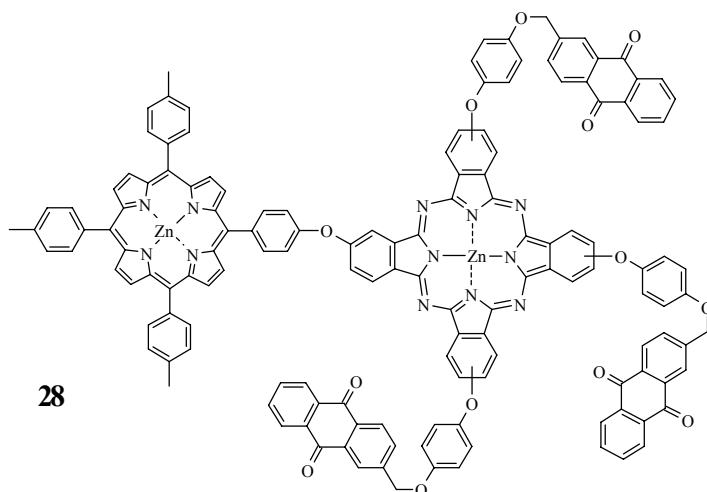
Tetrad **29** was synthesised by Lindsey *et al*. Excitation at 490 nm, where the perylene and porphyrin unit mainly absorb, leads to an emission exclusively from the Pc moiety. The perylene emission is strongly quenched and the porphyrin emission is completely absent. This again shows ultrafast and very efficient energy transfer from the perylene and the Por to the Pc unit, which emits with the same high efficiency ($\Phi_F = 0.78$) and lifetime as the isolated chromophore, indicating the absence of other quenching processes in tetrad **29**.[60]

29
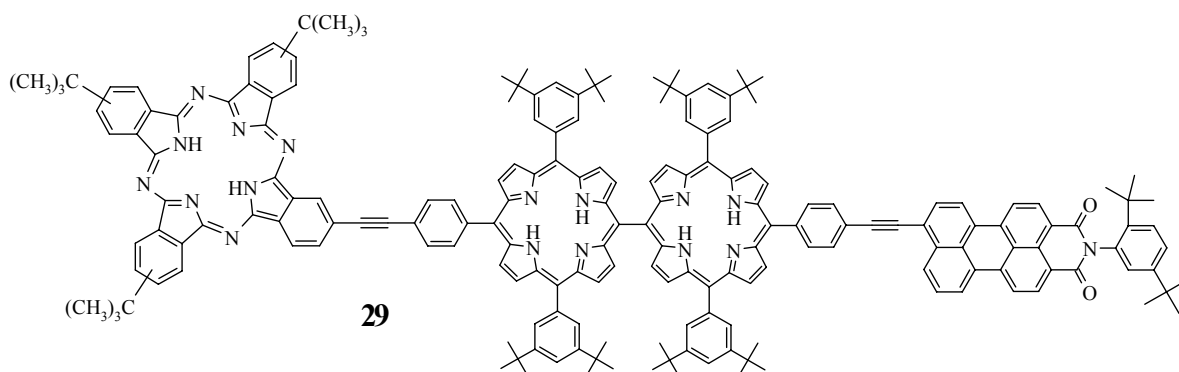
Triad **30** is an example for an optoelectronic gate. Excitation of triad **30** at 662 nm results in typical Pc emission with a quantum yield of 0.79. In this case, the ferrocene unit is farther apart from the Pc moiety compared to dyad **9**, where a strong quenching of the luminescence

is observed in the neutral state. Oxidation of the ferrocene unit in **30** results in a complete quenching of the fluorescence as in dyad **9**, where the ferrocene cation radical serves as an extremely efficient trap for the excited-state energy of the Pc unit. Accordingly, a ferrocene unit could serve as a redox switch in architectures wherein an entire component carrying a ferrocene unit could be removed from the energy transfer train, as in triad **30**.[15]

30
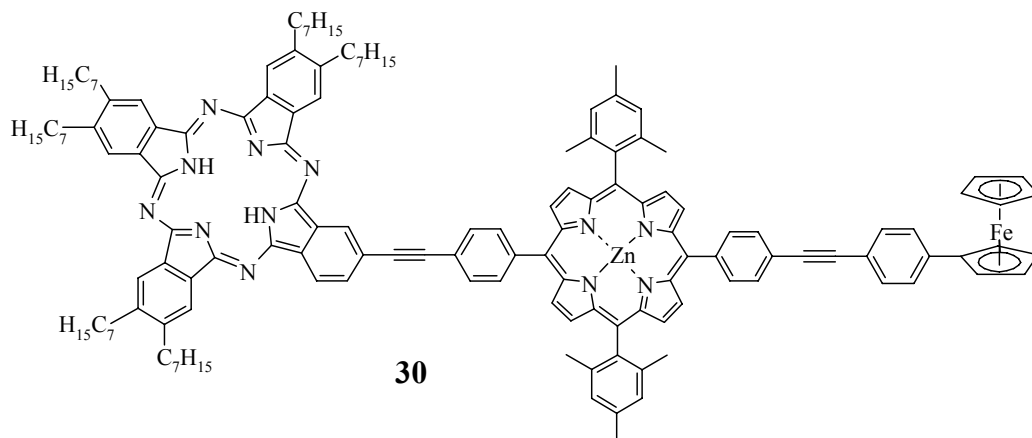
1.4. Phthalocyanines linked together through their periphery

In 1984, the first publication of a peripherally linked binuclear phthalocyanine appeared in the literature.[61] At that time, binuclear porphyrins were prepared and used in the four-electron reduction of oxygen to water.[62,63] Under operating conditions, these porphyrins lost their catalytic activity with time. For this reason, researchers synthesised similar phthalocyanine systems which are thermally and photochemically much more stable than their porphyrin analogues.[64] Due to the fact that the reduction of oxygen to water is a multi-electron process, flexible binuclear catalysts were expected to be more effective than the corresponding monomers, because the former can participate in a concerted electron process with the substrate (cofacial intramolecular aggregation by building a μ-peroxo bridge with molecular oxygen).[65] Compounds **31a** and **31b** exhibit electrocatalytic two-electron reduction of molecular oxygen to hydrogen peroxide in the pH range of 1-14. The first reduction (Co^{II}/Co^{I}) and oxidation (Pc^{-}/Pc^{2-}) couples of **31a** are split compared to the monomer. The formation of mixed-valence species indicates a high degree of coupling between the two subunits, which was not observed for **31b**.[66,67] The electrocatalytic reduction of oxygen to hydrogen peroxide has been observed in other Pc oligomers,[68-71] but the 4-electron reduction to water has not been reported for such Pc systems.[72]

31a (n = 0)
31b (n = 1)
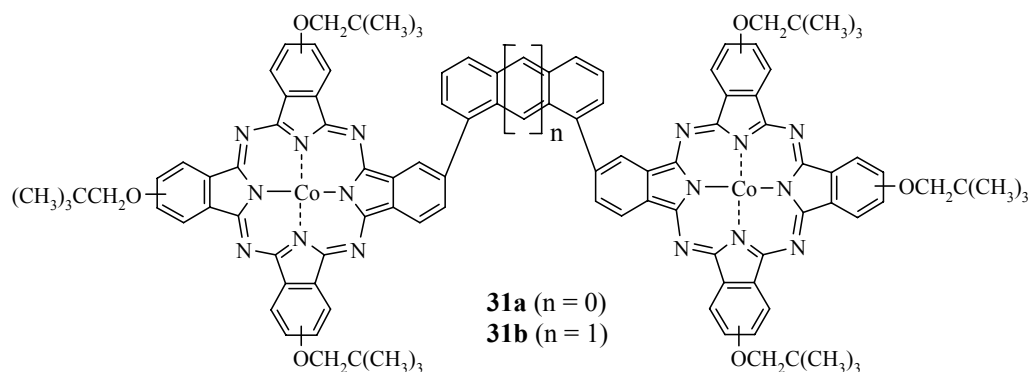
Various annulated Pc dimers[73-81] and trimers,[81] like **32** and **33** (R = 2,6-dimethylphenyl), have been synthesised. The magnetic behavior of compound **32** was investigated by Kasuga *et al*. The reciprocal magnetic susceptibility and the temperature are related by the Curie-Weiss law with a Weiss constant of θ = -7 K, which is indicative of the existence of a weak antiferromagnetic interaction.[79] Recently, annulated trinuclear Pc **33** was synthesised for the first time by Wöhrle and coworkers. In solution, Pc monomers are intensively green colored, whereas the analogous dimer of **33** (which was also obtained during the synthesis of the trimer) and **33** itself only exhibit a weak yellow-green color as a result of their low absorption intensities in the visible region. In addition, the extinction coefficient of the Q band absorption increases going from monomeric Pc to trimer **33**. These two trends are clearly attributed to the enlargement of the π-system. The fluorescence quantum yields are reduced dramatically in the order monomer-dimer-trimer. This effect is due to the decrease of the HOMO-LUMO gap and a more extended vibrational level structure of larger molecules, thus increasing the probability of nonradiative decay of the excited Pc state.[81]

32

33
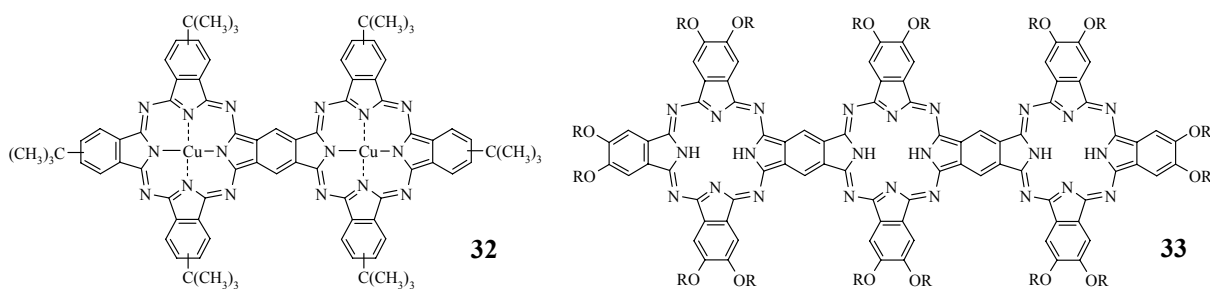
Torres *et al*. described the first Pc supramolecular assembly driven by strong donor-acceptor interactions between dinuclear ZnPc-NiPc **34**. Heteroassociation between electron-rich Zn(II)-hexabutoxyphthalocyanine and electron-deficient Ni(II)-hexa(alkylsulfonyl)phthalocyanine units was observed in ^{1}H NMR and UV-vis studies. Donor-acceptor interactions are the main driving force for the association of **34**, which forms one-dimensional nanoaggregates through intermolecular interactions in 1mM n-butanol solutions. These nanoaggregates were found to

be very monodisperse in both size and shape (typical dimensions: 290 x 90 nm^2) by investigation with TEM. The authors believe that this novel recognition motif and the formation of these novel π-π supramolecular polymers represent a useful tool to control the organisation of Pcs into functional supramolecular systems.[82]

34
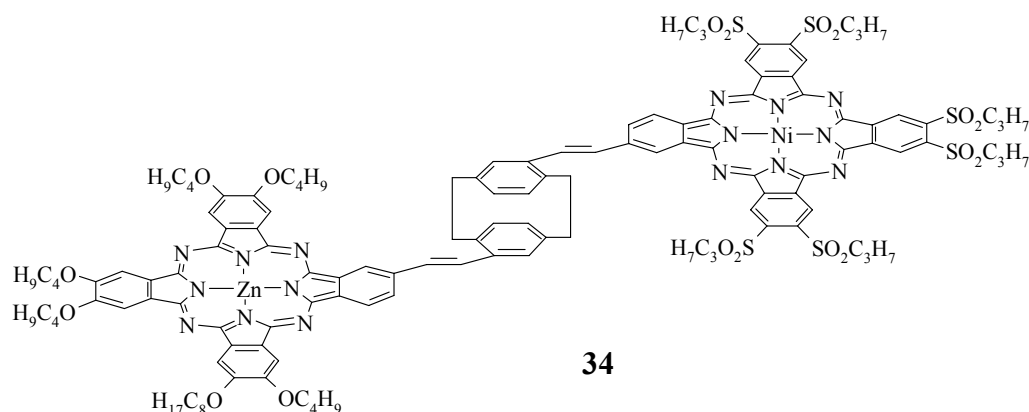
Torres and coworkers prepared trinuclear Pc systems for the study of nonlinear optical (NLO) properties. The second-order NLO responses for the octupolar trisphthalocyanine-phosphonium salt **35a** and the dipolar reference **35b** were determined through hyper-Rayleigh light scattering (HRS). The measured β$_{HRS}$ values at λ = 1.06 μm in a THF solution were 189*10^{-30} esu and 20.5*10^{-30} esu, respectively. The high first-order hyperpolarisability value of **35a** is comparable to those reported for SubPc, core-modified Pcs with octupolar character, and clearly superior to those available for related asymmetrically substituted phthalocyanines with dipolar characteristics.[83]

35a

35b
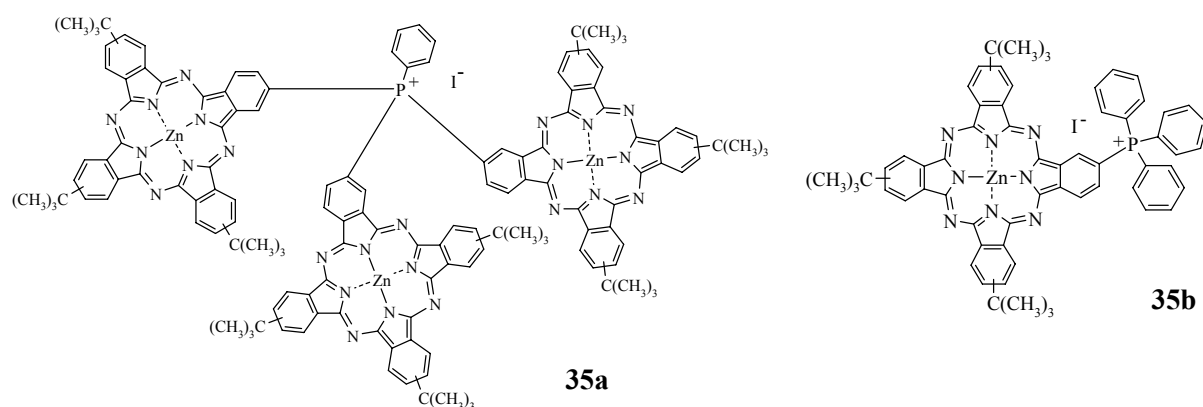
The experimental β$_{HRS}$ values for compounds **36** are quite different which may be interpreted in terms of their octupolar character and their π-conjugation. Compounds **36a** and **36c** have a β$_{HRS}$ = 144*10^{-30} esu. This large value is assigned to the octupolar enhancement, which is not observed in compound **36b** (β$_{HRS}$ = 46*10^{-30} esu). This observation was assigned to the fact that in **36b** the orthogonal relationship between the Pc moieties and the central benzene ring is

favored, whereas in the case of the other compounds the Pc units adopt a coplanar conformation to the benzene ring which was confirmed by calculations. The incorporation of a 1,3,5-triazine unit, as in the case of compound **36d** (β_{HRS} = 83*10^{-30} esu) was found to be counterproductive. Again, octupolar Pc compounds were found to have higher β_{HRS} values than dipolar systems.[4]

36a (X = C, $\boxed{Y}$ =)
36b (X = C, $\boxed{Y}$ =)
36c (X = C, $\boxed{Y}$ = CN)
37d (X = N, $\boxed{Y}$ =)
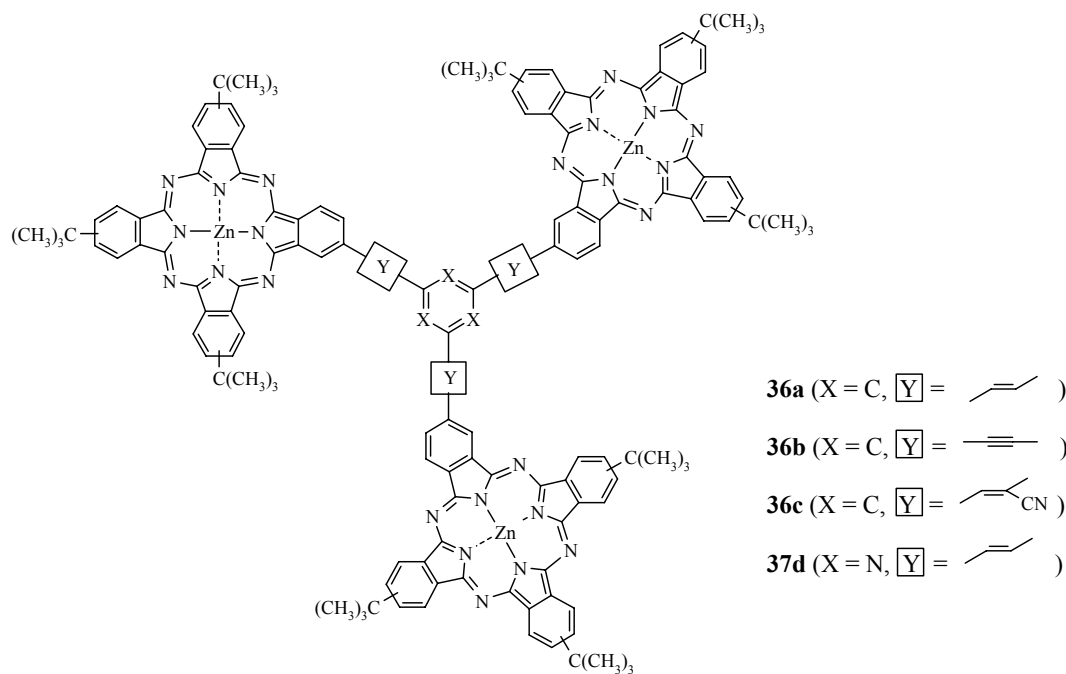
1.5. Other phthalocyanine-based multicomponent systems

Upon photoexcitation of either chromophore subunit, dyads **37a** and **37b** showed emission from the ZnPc unit with a quantum yield of 0.19 (like the ZnPc reference). The fluorescence from the SubPc moiety was strongly quenched in dyads **37a** and **37b**. Given the energy values for the singlet excited-state of both subunits (ca. 2.1 eV for SubPc and 1.7 eV for ZnPc) and the fact that excitation at 570 nm (maximum Q band absorption of SubPc unit) mainly populates the singlet SubPc state, these observations point to an efficient energy transfer

37a (R = R' = H)
37b (R = R' = SC$_8$H$_{17}$)
37c (R = H, R' = NO$_2$)
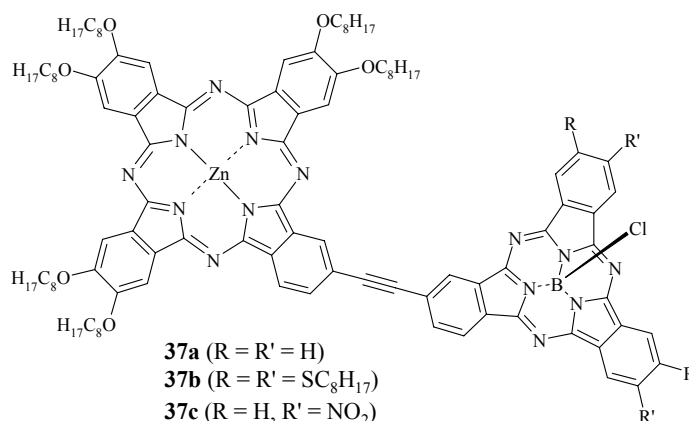
process from the ^{1*}SubPc to ^{1*}ZnPc. This energy transfer process was found to be quantitative. Therefore, these dyads behave photophysically as Pcs with the only difference being the additional strong absorption in the region below 600 nm of the SubPc moiety, which funnels energy to the Pc unit when photoexcited. For the case of compound **37c** emission spectra were strongly dependent on the solvent polarity and fluorescence emissions from both subunits were quenched. Increasing in the solvent polarity resulted in stronger quenching of the Pc emission. In addition, **37c** has the lowest reduction potential of the three dyads due to the electron-withdrawing nitro groups in the periphery of the SubPc macrocycle, which leads to a charge-transfer state lower in energy than the singlet excited-states of both chromophore subunits, in contrast to **37a** and **37b**. Nanosecond transient absorption experiments failed to detect the ZnPc$^{\bullet+}$-SubPc$^{\bullet-}$ state, which led the authors to the conclusion of very fast charge recombination (faster than the time resolution of the experiment). It was shown that by different substitution of the SubPc unit the photophysical events upon photoexcitation could be fine-tuned.[84]

38
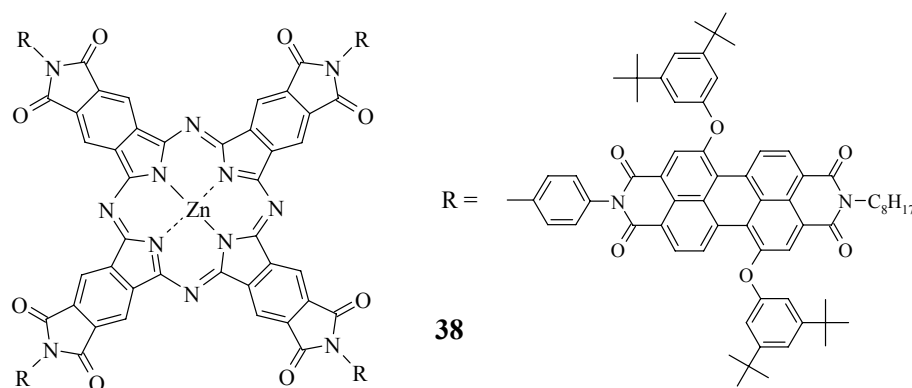
Wasielewski and coworkers synthesised a symmetric Pc with four covalently attached perylenediimide (PDI) units (**38**) which shows very interesting aggregation behavior in solution. Electronic absorption spectra show two broad bands with maxima near 500 and 645 nm belonging to the PDI and ZnPc unit, respectively, which are both strongly blue shifted compared to the corresponding monomers. To estimate the aggregate size and shape of **38** in a THF solution ($6*10^{-4}$ M) the authors performed small-angle X-ray scattering (SAXS) measurements using a high-flux synchrotron source. This experiment revealed that **38** forms monodisperse aggregates of seven cofacial molecules. Upon increasing the concentration, TEM images showed that the cylindrical stacks grow to form fibers of more than 1 μm length and different diameters. Photophysical measurements showed that photoexcitation of the PDI moieties in heptamers of **38** resulted in a quantitative energy transfer from ^{1*}PDI to ^{1*}ZnPc which then relaxes to form ^{3*}ZnPc (It is known that the fluorescence from H-aggregates of

21

ZnPcs is strongly quenched, while H-aggregates of PDI exhibit emission with quantum yields of 15-30%.). Exciton hopping between ZnPc sites within aggregates of $(ZnPc-PDI)_7$ occurs before relaxation to the ground state. The comparision between the exciton lifetime at each site (160 fs) and the total exciton lifetime (260 ps) implies that energy transfer can occur through very large aggregates of **38** before significant excited-state decay occurs. Therefore, the authors suggest that large artificial light-harvesting systems can be achieved by self-assembly of $ZnPc-(PDI)_4$ building blocks.[85]
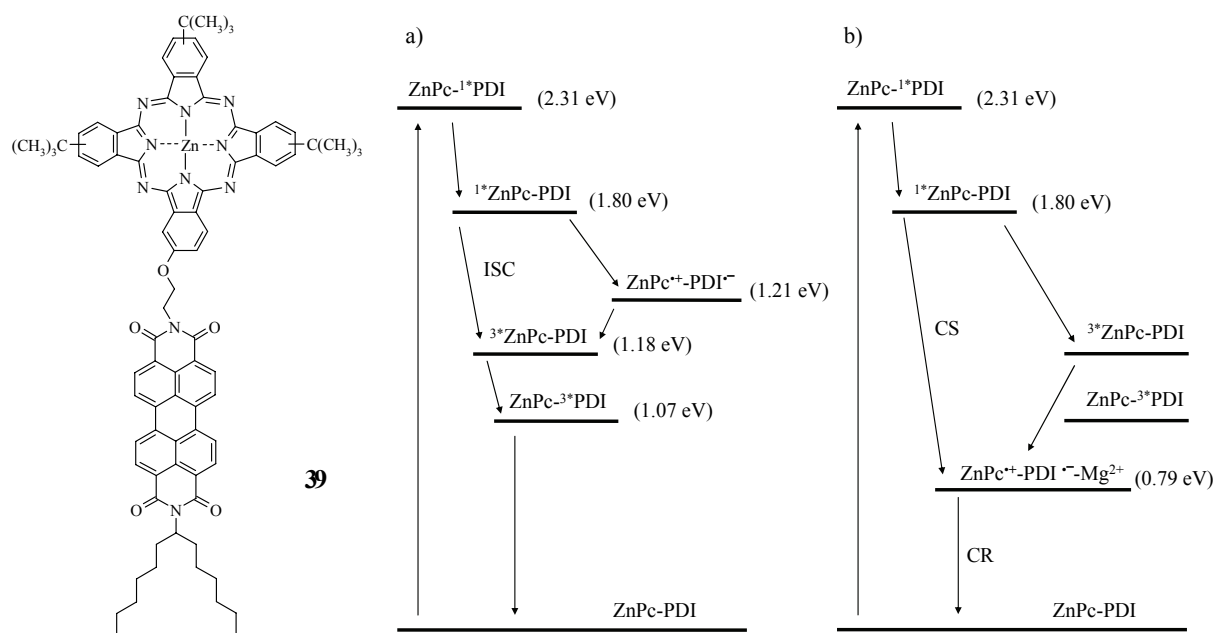
Figure 1.2. Molecular structure of **39** (left) and energy diagrams of photophysical processes in dyad **39**: a) without Mg^{2+}, b) with Mg^{2+}.

The photophysical properties of dyad **39** can be dramatically altered by the addition of Mg(II) ions. The photoexcitation of both monomeric subunits of **39** results in emissive relaxation of the excited-states. Excitation of the ZnPc or PDI subunit of dyad **39** results in selective formation of the final long-lived ZnPc-^{3*}PDI state, which exhibits non-radiative decay (Fig. 1.2a). Addition of an excess of Mg(II) to a benzonitrile solution of **39** and photoexcitation of the PDI unit at 530 nm results in the formation of the long-lived $ZnPc^{\bullet+}$-$PDI^{\bullet-}/Mg^{2+}$ state with a lifetime of 240 μs. Both radical ions, $ZnPc^{\bullet+}$ and $PDI^{\bullet-}/Mg^{2+}$ were detected in transient absorption experiments. The $PDI^{\bullet-}/Mg^{2+}$ absorption (500 nm) is significantly shifted compared to the uncomplexed $PDI^{\bullet-}$ species (720 nm), whereas no change in the absorption spectrum of PDI in the presence of Mg^{2+} is observed. It was shown that in the presence of Mg(II) the energy of the charge-separated state of **39** is lower than the energy of the ZnPc-^{3*}PDI state (Fig. 1.2b).[86]

Binuclear ZnPc **40** in which the Pc units are bridged through four covalently attached calixarene derivatives exhibits mixed-valence behavior. The mixed-valence splitting of the two redox processes Pc^{-1}/Pc^{-2} and Pc^{-2}/Pc^{-3} was determined by cyclic voltammetry and the values are 0.69 V and 0.44 V (vs. SCE), respectively. These results suggest that charge delocalisation among the cofacial ZnPc units in **40** occurs. Additionally, a large negative potential shift of the redox couple Pc^{-1}/Pc^{-2} compared to monomeric ZnPc was observed, which was assigned to HOMO-HOMO interactions between the cofacial Pc rings.[87]

40
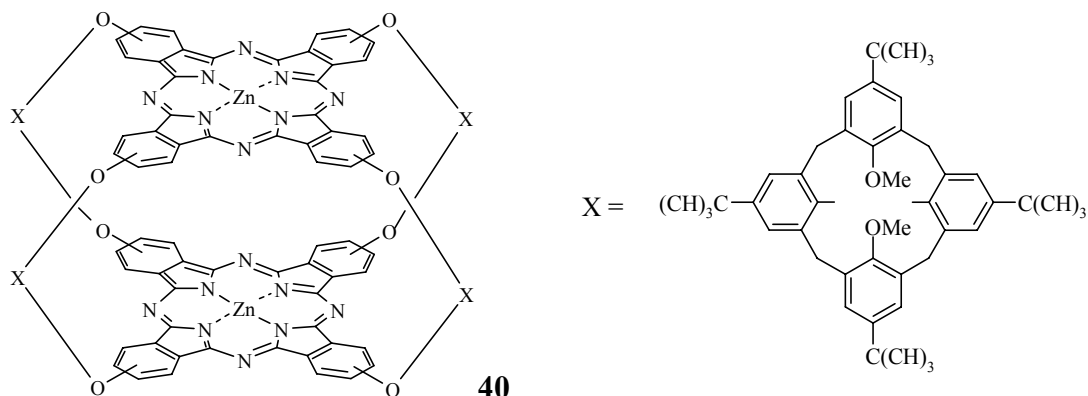
Other units such as triazolehemiporphyrazines[88] have been covalently linked to phthalocyanine macrocycles, but mainly synthetic procedures to prepare such systems have been described. A Pc with covalently attached anthraquinone (Aq) showed efficient intramolecular quenching of the phthalocyanine fluorescence,[54] whereas strong intramolecular electronic interactions between the covalently bonded electron-donating Pc and the electron-withdrawing Aq moiety in a Pc-Aq-Pc triad in the ground state was demonstrated by CV experiments.[89]

1.6. Carbon nanotubes with covalently attached phthalocyanines

The covalent linking of Pcs to carbon nanotubes is a very new topic in scientific research (with only three publications so far). Such systems are very interesting to study donor-acceptor interactions between the Pc and the carbon nanotube units. The first system was published in 2003 by Torres and coworkers. The phthalocyanines were covalently attached through amide bonds to the carbon nanotubes. Insufficient solubility of these novel compounds is problematic for their characterisation and the photophysical studies. Further efforts in order to solubilise these promising compounds have to be undertaken.[90-92]

2. Synthesis of asymmetric phthalocyanines

2.1. General synthesis of phthalocyanines

The following short introduction about Pc preparation is illustrated with unsubstituted precursors and phthalocyanines for simplicity. Obviously, the given synthetic conditions are also applied for all kinds of substituted Pc precursors. Phthalocyanines can be substituted in their peripheral or/and their non-peripheral positions as shown in Fig. 2.1. Unsubstituted Pcs are very insoluble in common organic solvents at ambient conditions due to their π-π stacking interactions. Therefore, the chosen substituents are usually bulky in their nature to decrease this behavior and thus increase solubility. The latter can also be increased by axial substitution of Pcs other than metal-free phthalocyanines (H$_2$Pcs), which will not be discussed here.
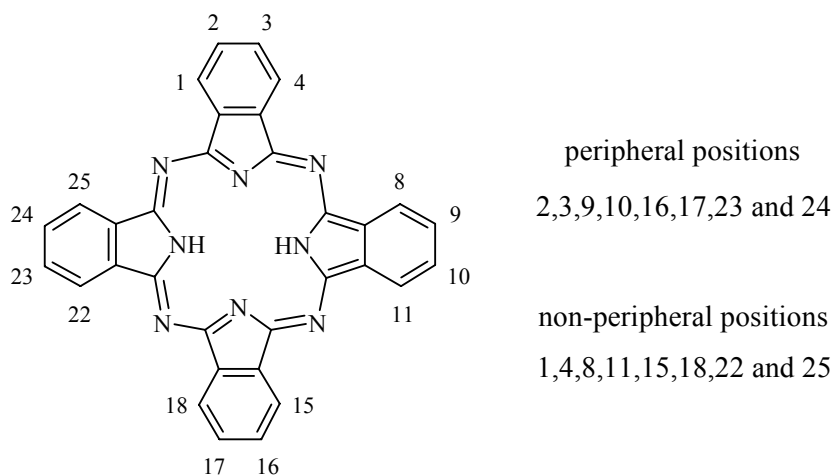
Figure 2.1. Peripheral and non-peripheral positions of the phthalocyanine macrocycle.

2.1.1. Metal-free phthalocyanines

Certain *ortho*-disubstituted benzene derivatives can act as phthalocyanine precursors, but for laboratory syntheses phthalonitrile (1,2- or *o*-dicyanobenzene) is usually used. In Scheme 2.1, several methods for the cyclotetramerisation of phthalonitriles to form H$_2$Pcs are depicted. H$_2$Pc can be prepared by adding phthalonitrile to a refluxing solution of lithium metal dissolved in 1-pentanol (lithium pentyloxide) to form Li$_2$Pc. The lithium ions are then

displaced by adding dilute acid to the reaction mixture (a).[93] Cyclotetramerisation of *o*-dicyanobenzene in a melt with hydroquinone (4:1 by weight) is another possibility to synthesise H_2Pc. Hydroquinone acts as the necessary reducing agent and therefore, it allows the preparation of the metal-free phthalocyanine in the absence of any metal ions (b).[94] Similarly, a non-nucleophilic hindered base like 1,8-diazabicyclo[5.4.0]undec-7-ene (DBU) is an efficient reagent for the cyclotetramerisation of phthalonitrile in a melt or in a 1-pentanol solution (c).[95] Another procedure is to convert 1,2-dicyanobenzene into diiminoisoindoline by the treatment with ammonia (d). Afterwards the diiminoisoindoline is refluxed in a high-boiling point alcohol to form H_2Pc via a condensation reaction under relatively mild conditions (e).[1,96]
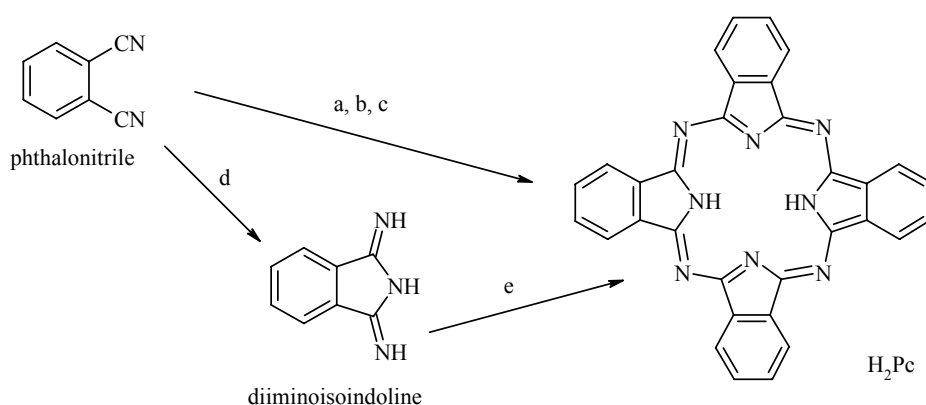
Scheme 2.1. Synthetic routes to metal-free phthalocyanines (H_2Pcs).

2.1.2. Metal phthalocyanines

Scheme 2.2 shows several synthetic strategies for the preparation of metal phthalocyanines (MPcs). The most simple MPcs are prepared from phthalonitrile or diiminoisoindoline by a template synthesis with the appropriate metal ion in high-boiling point solvents like 1-pentanol, quinoline, DMAE, DMF or 1-chloronaphthalene (a). In addition, phthalic anhydride or phthalimide can be used as precursors in the presence of a metal salt (e.g. copper(II) acetate or nickel(II) chloride) and urea (acting as nitrogen source) in a refluxing high-boiling point solvent (b). Alternatively, the reaction between H_2Pc or Li_2Pc and an appropriate metal salt produces most MPcs (c, d). The insolubility of H_2Pc in most organic solvents requires the use of a high-boiling-point aromatic solvent such as 1-chloronaphthalene or quinoline in order to ensure complete metallation (c). The use of Li_2Pc as a precursor is simpler owing to the solubility of this complex in acetone and ethanol and the insoluble MPc product is readily collected on completion of the metal-ion-exchange reaction (d).[1]
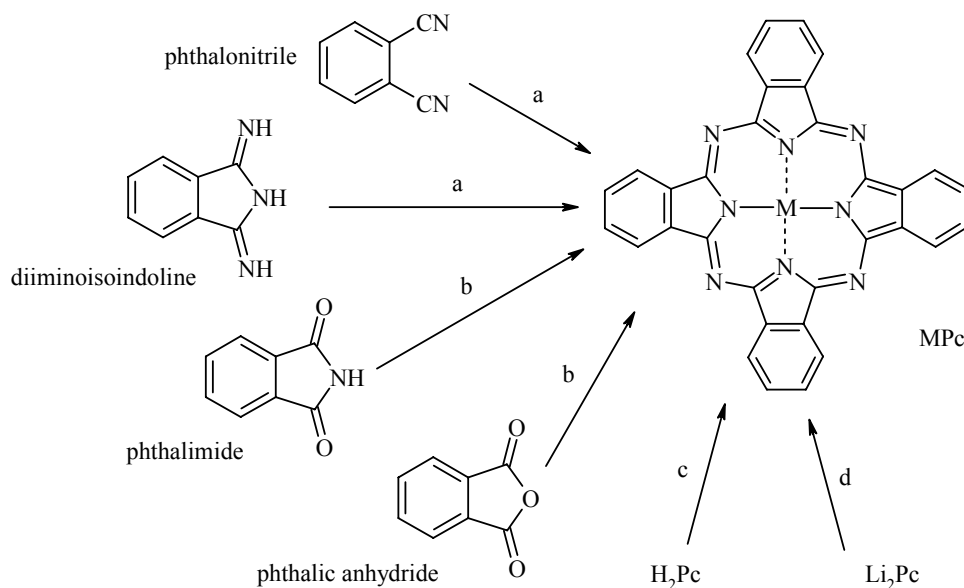
Scheme 2.2. Synthetic routes to metal phthalocyanines (MPcs).

2.1.3. Phthalocyanine double deckers (MPc$_2$)

Lanthanide metal ions form complexes in which two Pc rings complex with the same ion. These so-called sandwich complexes can be prepared via a melt reaction or a reaction of phthalonitrile and the appropriate lanthanide(III) acetate salt in solution. The crude product mixture contains the diphthalocyanine MPc$_2$ (Fig. 2.2), a monophthalocyanine M(OAc)Pc, some H$_2$Pc and also some triphthalocyanine M$_2$Pc$_3$ (triple decker). The composition of the product mixture strongly depends on the conditions and the used lanthanide salt. Since these sandwich complexes are soluble in common organic solvents, chromatographic purification, prior to sublimation, isolates the desired product from M(OAc)Pc, M$_2$Pc$_3$ and H$_2$Pc by-products.[1]
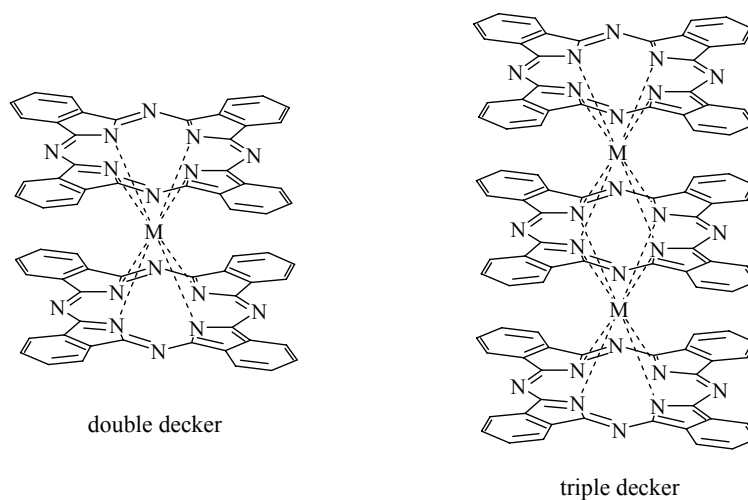
Figure 2.2. Molecular structures of double (left) and triple decker phthalocyanines (right).

2.2. Synthetic strategies to asymmetric phthalocyanines

Asymmetric phthalocyanines are usually prepared when a certain functionality needs to be incorporated into the periphery of a soluble Pc macrocycle. One Pc precursor is substituted with solubilising groups and the other is functionalised with the desired functional group or unit as will be shown later in this chapter.

The following part was prepared by following the contribution of Torres and coworkers in *The Porphyrin Handbook* (Design and Synthesis of Low-Symmetry Phthalocyanines and Related Systems).[97] First, the statistical condensation reaction will be explained, followed by the selective preparation of different asymmetric Pc (aPc) compounds such as **AAAB**, **ABAB** and **AABB** (Scheme 2.3), which will be illustrated by a selected example. The last part will then show strategies to prepare chosen multicomponent aPc systems described in the previous chapter.

2.2.1. Statistical condensation reaction

The statistical condensation reaction is usually used to prepare phthalocyanines of the **AAAB** type. During this non-selective reaction two differently substituted phthalonitriles or 1,3-diiminoisoindolines are reacted together to afford a mixture of six Pc compounds (Scheme 2.3). Therefore, chromatographic separation is essential to isolate the desired product(s) from the statistical mixture. Due to the strong tendency of Pcs to form aggregates, the isolation of the Pc products can be very difficult. For this reason, one of the phthalonitriles usually contains bulky substituents that increase solubility and suppress aggregation. Functionality can be introduced into the Pc macrocycle with the other phthalonitrile. Although this method is mainly used to prepare **AAAB** Pcs, there are a few publications where the **AABB** and **ABAB** compounds have been isolated as well.[98-105] Their separation is a demanding task since these isomers only differ in the location of their substituents.

Stoichiometry is one of the most determinant factors which can be manipulated in order to direct the reaction towards the maximal amount of **AAAB** Pc. The ratio of 3:1 (**A**:**B**) would be the best choice according to statistical considerations. However, the reactivities of the phthalocyanine precursors **A** and **B** play a very important role for the formation of the different Pc compounds. Assuming **B** is much more reactive than **A**, a molar ratio higher than 3:1 may be used to obtain **AAAB** in the largest possible amount. In the case of very reactive **A**, the ratio has to be decreased. In some cases, the molar ratio of **A** to **B** was increased to 9:1

in order to obtain **AAAA** and **AAAB** as the only phthalocyanine products, which enormously facilitates the isolation of pure **AAAB**.
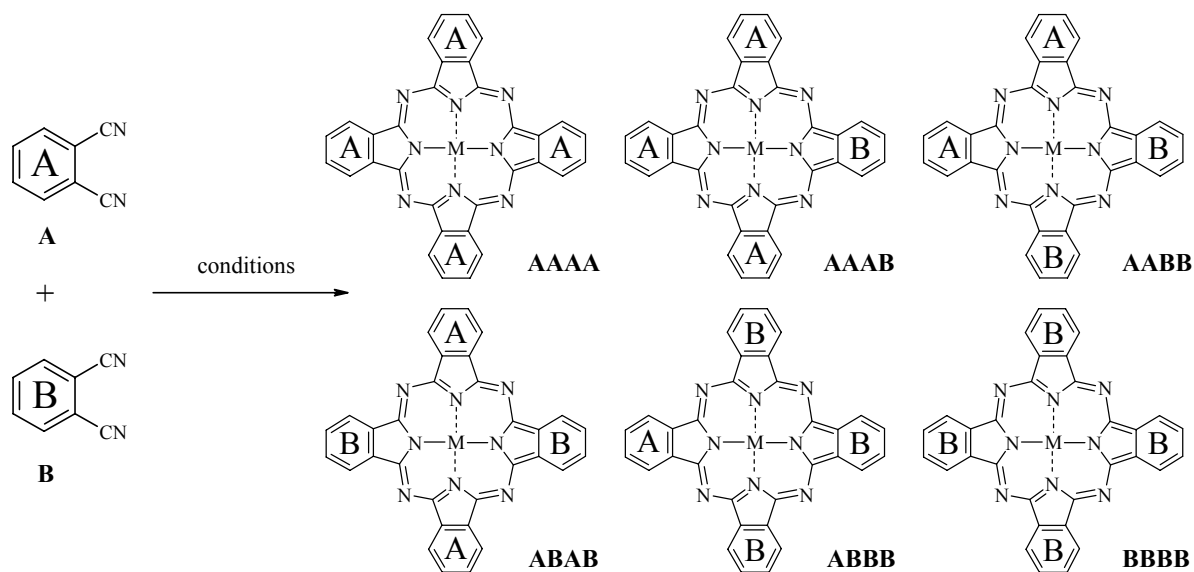
Scheme 2.3. Products of a statistical condensation reaction of two different phthalonitriles.

The non-peripheral (3,6-positions) substitution with rigid and bulky groups (e.g. phenyl) of phthalonitrile **A** can lead to a reduced number of Pc products due to steric hindrance between two adjacent units of **A**.[97,99,103,106-109]

2.2.2. Selective synthesis of AAAB phthalocyanines

2.2.2.1. Ring expansion of subphthalocyanines

Subphthalocyanines (SubPc) can be treated with diiminoisoindoline derivatives to obtain phthalocyanines of the **AAAB** type in a ring expansion reaction (Scheme 2.4). This reaction is highly dependent on the reactants and the experimental conditions. So it can either be a very selective method or can lead to mixtures of statistical products. **AAAB** can be obtained in yields ranging from 3-80%.[58,110-120] In non-selective cases the SubPc obviously decomposes followed by statistical ring closure of the fragments, which can lead to all six possible Pc compounds.[117] The addition of a metal salt to the reaction mixture or the treatment of the SubPc with a low reactive phthalonitrile in the presence of a strong base (e.g. DBU) seems to increase the yield of the desired **AAAB** Pc. The best yields have been achieved in the case of reactions between unsubstituted SubPcs or SubPcs with electron-withdrawing substituents and diiminoisoindolines bearing electron-donating groups.[97]
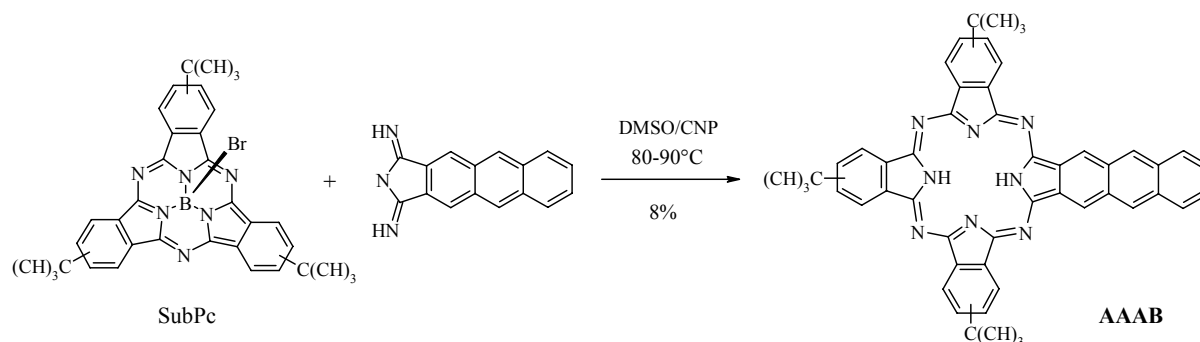
Scheme 2.4. Example of a ring expansion reaction of a SubPc to an **AAAB** Pc.

2.2.2.2. Synthesis of AAAB Pcs on polymeric supports

Phthalocyanines of the **AAAB** type can also be synthesised via solid phase synthesis.[72,121-123] Leznoff and coworkers usually used polymers bearing alcohol groups which react with 4-nitrophthalonitrile to give the polymer-bound precursor. This precursor can then be converted to the 1,3-diiminoisoindoline analogue (**B**) which reacts with a differently substituted 1,3-diiminoisoindoline (**A**). After the reaction, the soluble by-product **AAAA** is removed from the reaction mixture by washing. The desired **AAAB** Pc can then be released from the polymer by acid treatment. An example of such a synthetic procedure is shown in Scheme 2.5.[121] While
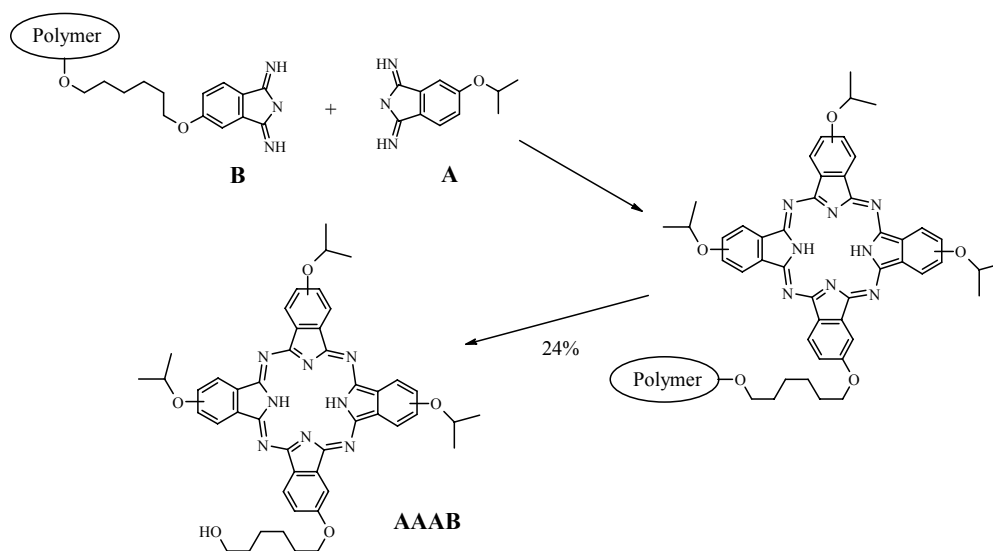
Scheme 2.5. Synthesis of asymmetric Pc **AAAB** on a polymeric support.

applying this procedure, yields of approximately 20% are achieved. Wöhrle *et al.* covalently bound a phthalonitrile bearing a phenoxybenzoic acid group to silica which was modified with aminopropyl groups. The bound phthalonitrile was then reacted with a differently substituted phthalonitrile and the **AAAB** Pc was removed from the silica by cleaving the amide bond.[123]

The main advantage of the solid phase synthesis is the quite simple purification procedure compared to above-mentioned synthetic strategies for the preparation of **AAAB** Pcs.[97]

2.2.3. Selective synthesis of ABAB phthalocyanines

The reaction of substituted 1,3,3-trichloroisoindolenine (**A**) with substituted 1,3-diiminoisoindoline (**B**) in the presence of a base and a reductive agent offers an effective route to selectively synthesise **ABAB** Pcs (Scheme 2.6).[18,124-128] This reaction type can lead to very high selectivity and yields of up to 72% have been reported for a copper derivative.[124] However, other reactions did not lead to such high yields and selectivity, because **ABBB** by-products were formed.
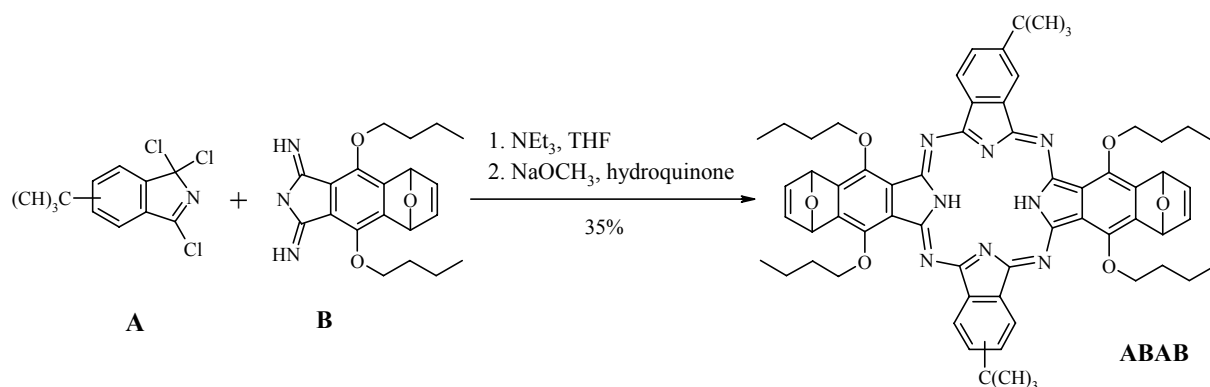
Scheme 2.6. Synthesis of an **ABAB** phthalocyanine derivative.

Another cross-condensation procedure was developed by Leznoff and coworkers which is not as selective as the aforementioned, since traces of all other possible Pc compounds were obtained and the isolation of pure **ABAB** turned out to be impossible. The reaction of 1,3-diiminoisoindoline (**A**) and 1*H*-isoindole-1,3(2*H*)-dithione (**B**) derivatives led to the major formation of **ABAB** (Scheme 2.7).[129]
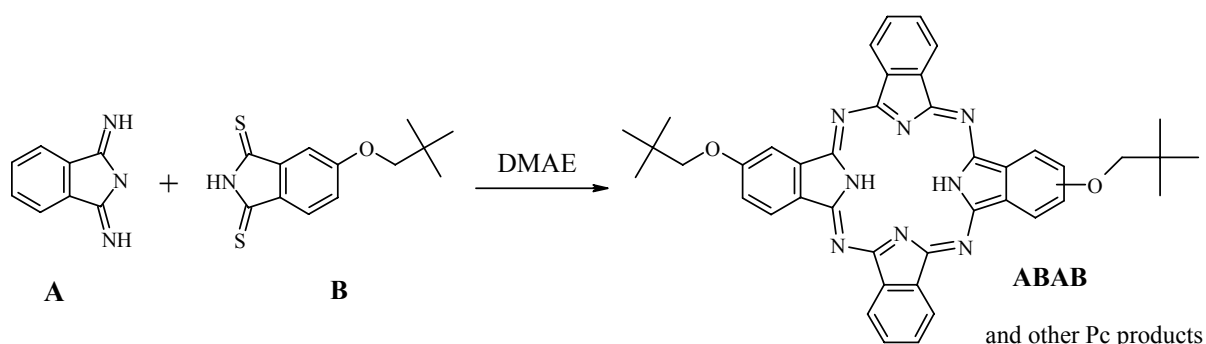
Scheme 2.7. Less selective method to prepare **ABAB** Pcs.

In addition, a statistical condensation reaction including sterically hindered precursors, such as 3,6-diphenylphthalonitrile, can also facilitate the formation and separation of **ABAB** phthalocyanines as mentioned above.[97]

ABAB type Pcs have been employed by Hanack *et al.* for the successful synthesis of ladder-type oligomers based on Pc units by Diels-Alder reactions or by Youngblood as a building block for the polymerisation to rodlike Pc polymers.[126-128]

2.2.4. Selective synthesis of AABB phthalocyanines

AABB Pcs can be selectively prepared via a "half-Pc" intermediate (Scheme 2.8). The method, reported by Oliver and Smith, was used to convert **A** to the "half-Pc" intermediate **AA** in refluxing lithium methoxide.[130] Leznoff and coworkers attempted to purify **AA** by chromatographic techniques but partial demetallation was observed. Therefore, crude intermediate **AA** was directly reacted with **B** in 1-octanol with subsequent metallation to exclusively obtain **AABB** in 28% yield.[131]
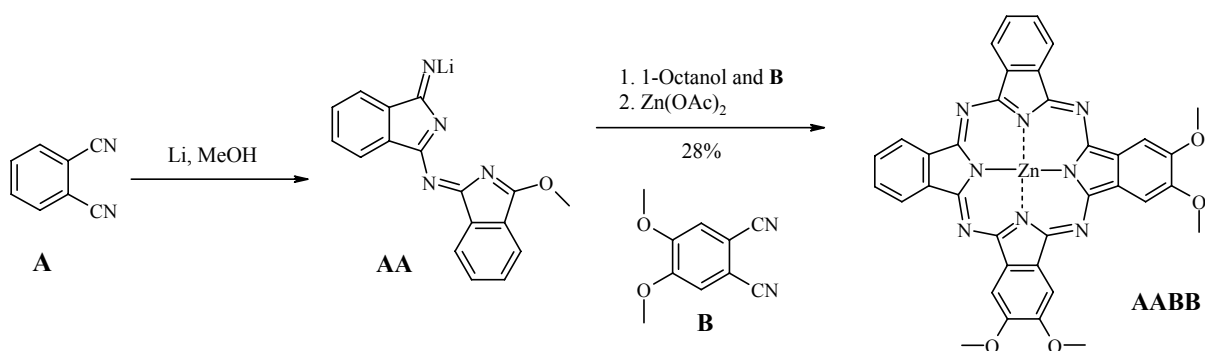
Scheme 2.8. Synthesis of **AABB** Pcs involving a "half-Pc" intermediate.

Another approach to obtain **AABB** Pcs was developed by Kobayashi *et al.* They reacted *bis*-(1,3-diiminoisoindoline) **AA** with a substituted 1,3-diiminoisoindoline to obtain pure **AABB** in 26% yield (Scheme 2.9). Additionally, **AAAA** and **BBBB** were obtained as by-products, which could easily be removed by chromatographic techniques from **AABB**. In the presented reaction in Scheme 2.9, **AA** was either reacted as pure (S)- or (R)-enantiomer. These compounds do not racemise under Pc reaction conditions. Since the distance between the two phenoxy groups of **AA** is close to the minimum to link two adjacent benzene rings of the phthalocyanine, the formation of Pc oligomers or even polymers is suppressed.[97,109,132-135]
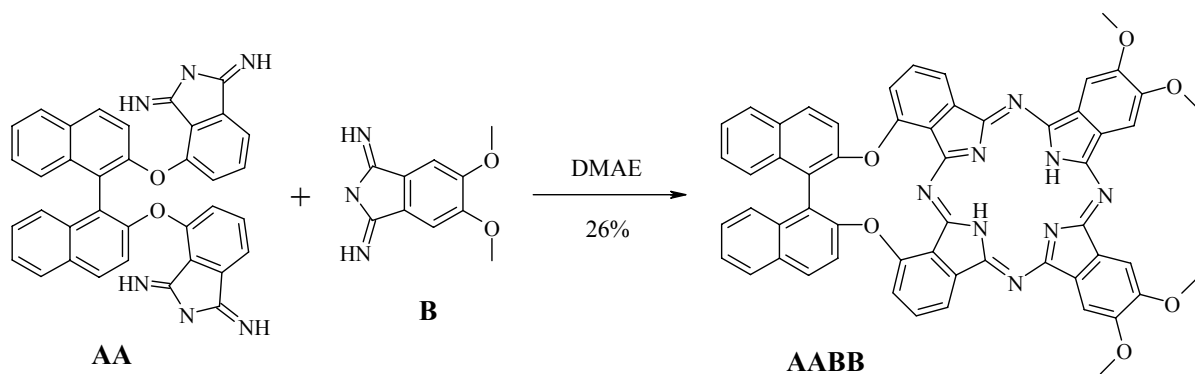
Scheme 2.9. Preparation of **AABB** Pc via bis-(1,3-diiminoisoindoline) **AA**.

2.3. Synthesis of asymmetric phthalocyanine-based multicomponent systems

Most multicomponent Pc-based systems described in Chapter 1 are composed of asymmetric phthalocyanines of the AAAB type. There are two main strategies to prepare such materials. An asymmetric phthalocyanine bearing peripheral functionality in the form of a formyl, ethynyl, iodo or amino group can be reacted with the appropriate counterpart to form complex Pc systems. The second main strategy is the statistical condensation reaction of two differently substituted phthalonitriles, one carrying the desired subunit. In this part, synthetic routes to selected compounds, described in Chapter 1, will be explained. The numbering of the final products is in accordance with the previous chapter.

2.3.1. Covalent linkage of a desired subunit after phthalocyanine formation

Dienes always add to the 6-6 double bonds of the fullerene core, which was the strategy for the preparation of dyads **12-14**. Non-peripherally substituted **Pn1** was reacted with diene-functionalised **Pn2** via a statistical condensation reaction. **Pc1** was then isolated from other Pc products by column chromatography. The synthesis of dyad **12** was accomplished in a Diels-Alder reaction of **Pc1** with C_{60} in four days, affording **12** as the major product in 75% yield (Scheme 2.10).[20] Dyads **13** and **14** were prepared according to similar procedures.[21,22]
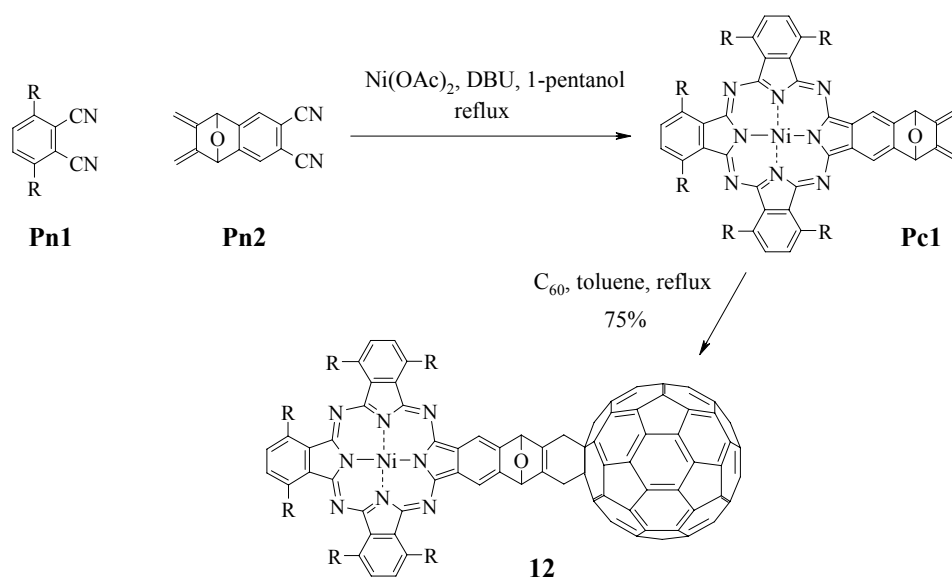
Scheme 2.10. Synthesis of Pc-C_{60} dyad **12** via a Diels-Alder reaction (R = heptyl).

The synthetic route to phthalocyanine dyad **15a** is depicted in Scheme 2.11. A statistical condensation reaction of 4-iodophthalonitrile (**Pn3**) with 4-*tert*-butylphthalonitrile (**Pn4**) produced **Pc2** in 15% yield. Then, a Stille coupling reaction of **Pc2** with tributyl(vinyl)tin using [Pd(PPh$_3$)$_4$] as a catalyst afforded tri-*tert*-butyl-vinyl-phthalocyanine **Pc3**, which underwent an oxidative cleavage reaction using osmium tetroxide and sodium periodate as oxidising agents to give formylphthalocyanine **Pc4**. The subsequent functionalisation of C_{60}, based on the 1,3-dipolar cycloaddition of the azomethine ylide generated *in situ* from **Pc4**, led to the formation of dyad **15a**.[25] Similar synthetic procedures were applied for the preparation of compounds **16** and **17**.[28,30]
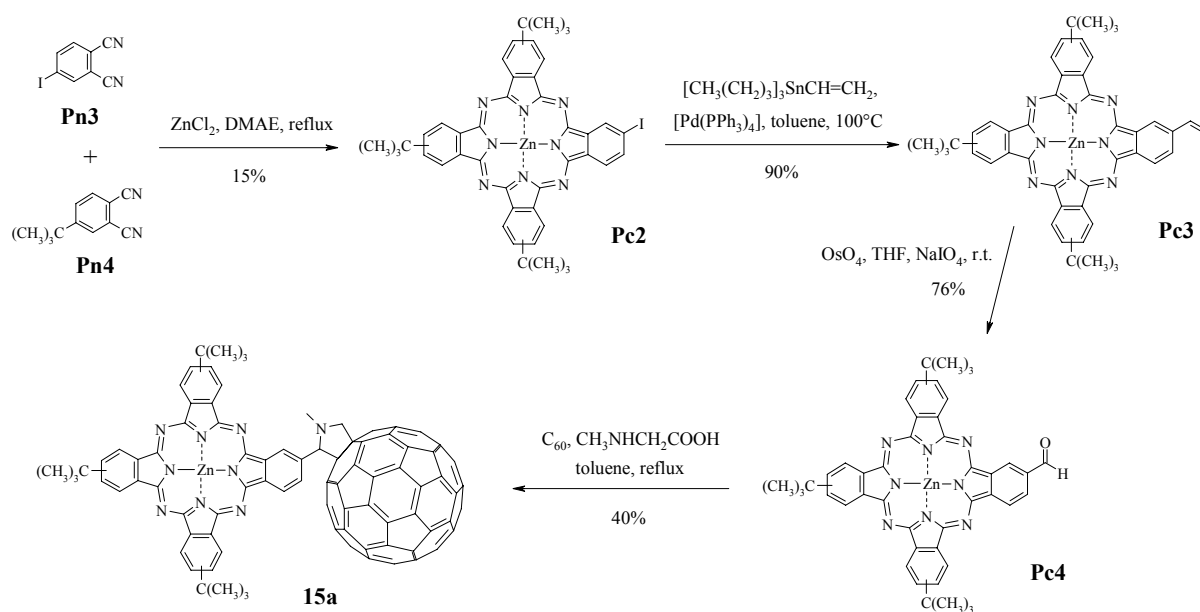
Scheme 2.11. Synthetic procedure for the preparation of Pc dyad **15a**.

An alternative synthetic approach to **15a** involved the statistical condensation reaction of **Pn4** with the appropriate C_{60}-functionalised phthalonitrile. The crude reaction mixture was only composed of tetra-*tert*-butylphthalocyanine and **15a**. This can be explained due to steric hindrance between two closely spaced fullerene units, which might inhibit the macrocyclisation. Despite the purification advantage, this procedure is not suitable for the preparation of **15a** due to very low yields.[25]
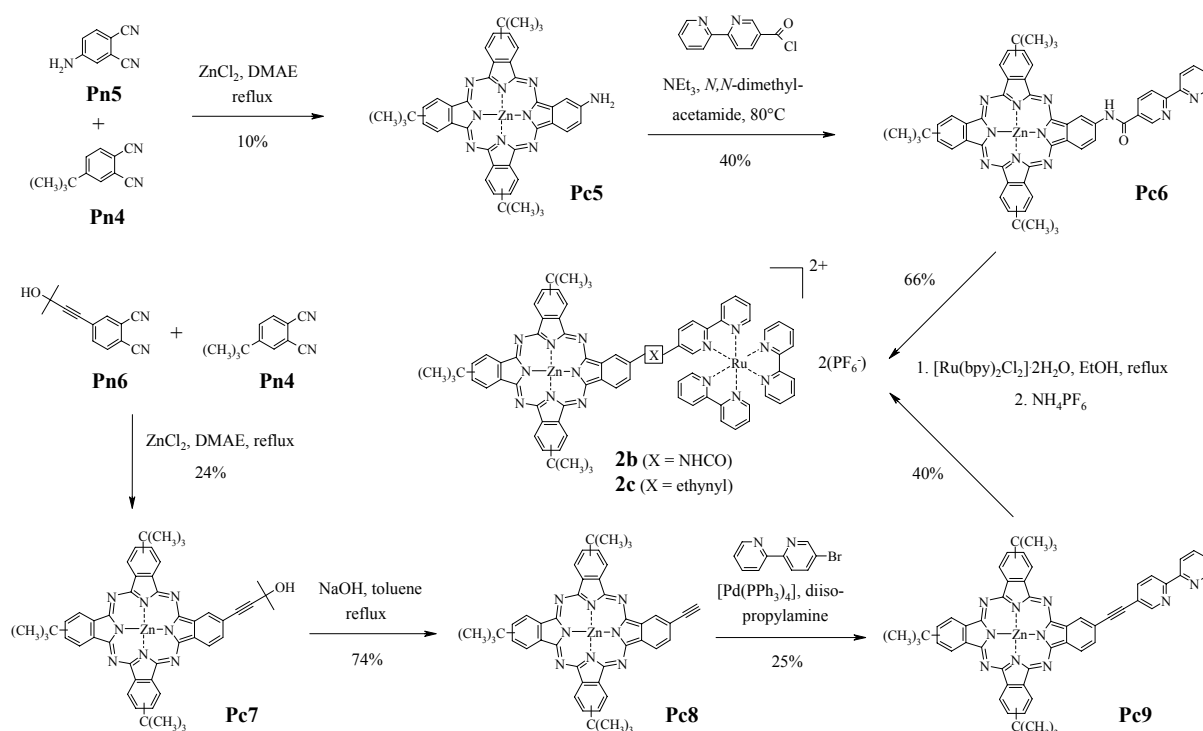
Scheme 2.12. Synthetic pathway to dyads **2b** and **2c**.

Dyad **2b** with the amide linker between the two photoactive units was synthesised via tri-*tert*-butylaminophthalocyanine **Pc5**, which was prepared via a statistical condensation reaction (Scheme 2.12). The synthesis of **Pc6** was carried out by coupling 5-chlorocarbonyl-2,2'-bipyridine to **Pc5** in *N,N*-dimethylacetamide. After chromatographic purification, compound **Pc6** was treated with [Ru(bpy)$_2$Cl$_2$]·2H$_2$O in refluxing EtOH to yield dyad **2b**. The analogous compound **2c**, bearing an ethynyl instead of an amide bridge, was prepared via three Pc intermediates. After a statistical condensation reaction between **Pn4** and **Pn6** and purification of **Pc7** by column chromatography, the latter was treated with sodium hydroxide in toluene to remove the –C(CH$_3$)$_2$OH protecting group in the form of acetone to obtain **Pc8**. **Pc9** was then prepared via a palladium(0)-promoted cross-coupling reaction between 5-bromo-2,2'-bipyridine and **Pc8** in freshly distilled and deaerated diisopropylamine followed by chromatographic purification. Finally, dyad **2c** was synthesised analogous to the procedure for

2b.[6] The key-precursors for dyads **2b** and **2c** were asymmetric aminophthalocyanine **Pc5** and asymmetric ethynylphthalocyanine **Pc8**, respectively.

For the synthesis of octupolar Pc-based systems **36a-d**, asymmetric iodophthalocyanine **Pc2** and formylphthalocyanine **Pc4** are key precursors (Scheme 2.13). Compound **36a** was synthesised in 61% yield under standard Heck conditions by heating 1,3,5-trivinylbenzene (**C1**) and **Pc2** in DMF in the presence of lithium chloride, tetrabutylammonium bromide, potassium carbonate and catalytic amounts of palladium(II) acetate at 90°C for 24h. Compound **36b** was obtained in 70% yield under standard Sonogashira cross-coupling conditions by reacting 1,3,5-triethynylbenzene (**C2**) with **Pc2** in triethylamine in the presence of catalytic amounts of both [Pd(PPh$_3$)$_4$] and copper(I) iodide at 80°C for 65h. The Knoevenagel condensation was applied to the synthesis of compounds **36c** and **36d**. The reaction of **Pc4** with 1,3,5-tris(cyanomethyl)benzene (**C3**) using tetrabutylammonium hydroxide and potassium *tert*-butoxide as bases in THF at 50°C led to **36c** in 59% yield. In the same way, the preparation of **36d** was achieved in 24% yield by condensation of **C4** with **Pc4** in the presence of potassium hydroxide in a refluxing solvent mixture of methanol and toluene.[4]
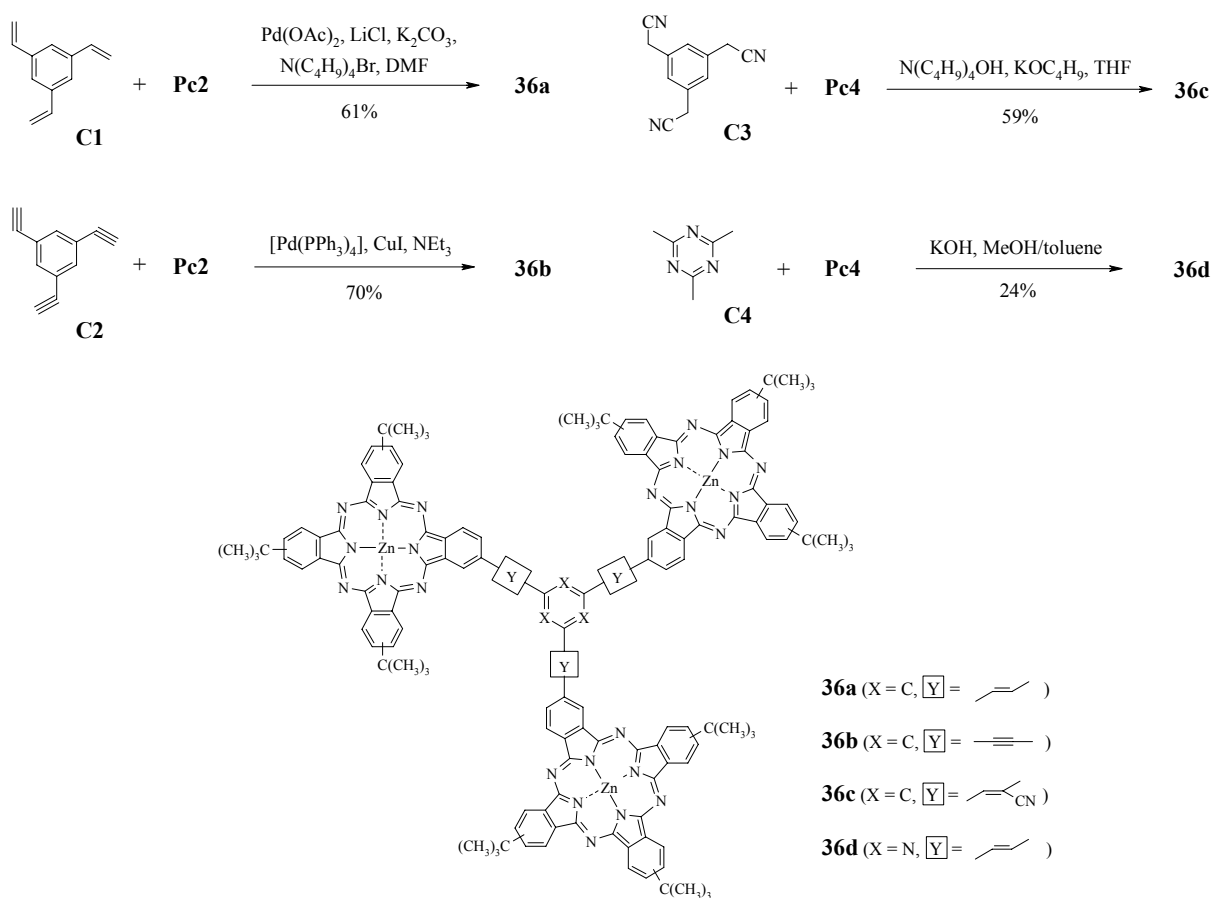
Scheme 2.13. Synthetic pathways to octupolar systems **36a-d**.

Triad **30** was synthesised by employing a mixed Pd-coupling reaction of ethynyl-substituted **Pc10**, **Por1** and 4-ethynylphenylferrocene (**C5**) as shown in Scheme 2.14. A mixture of trimeric, dimeric and monomeric materials was obtained. Pure **30** was obtained in 15% yield after adsorption and size exclusion chromatography.[15]
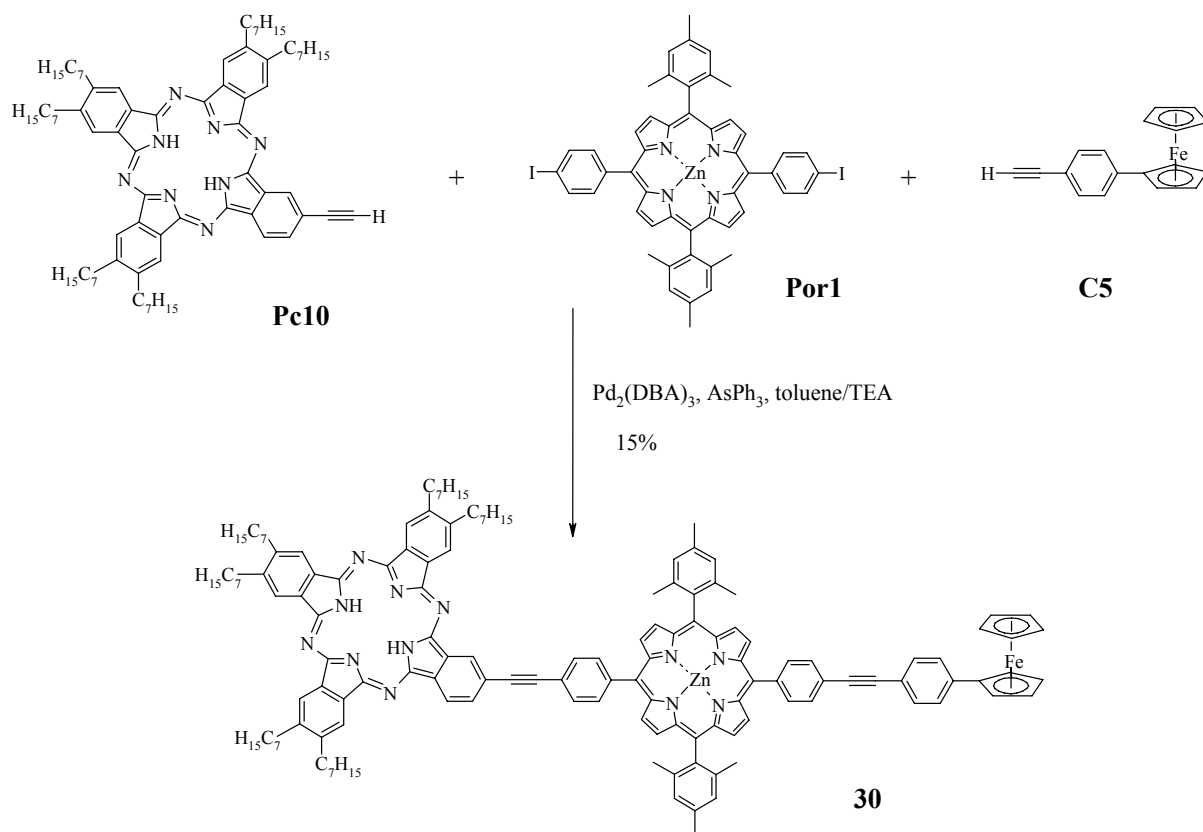
Scheme 2.14. Covalent linkage of the three subunits of triad **30** in a one step reaction procedure.

Bekaroğlu and coworkers reported the selective synthesis of an ABAB type ferrocene-functionalised phthalocyanine (Scheme 2.15). Cyclotetramerisation of 5-dodecylsulfanyl-diiminoisoindoline (**C6**) and 6-nitro-1,3,3-trichloroisoindolenine (**C7**) was accomplished in THF in the presence of triethylamine and sodium methoxide as the bases and hydroquinone as the reductant to yield **Pc11**, which underwent reduction using sodium sulfide as reducing agent to obtain **Pc12**. In the last step, the latter was reacted with ferrocenylaldehyde and a catalytic amount of *p*-toluene sulfonic acid in refluxing toluene to give target **Pc13** in 60% yield.[18]
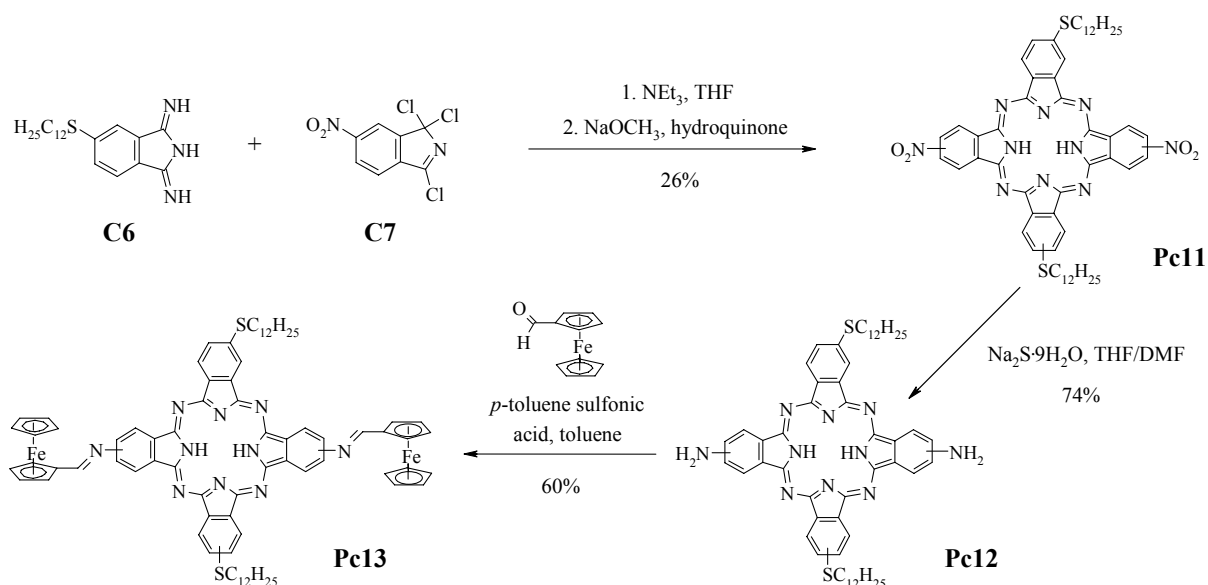
Scheme 2.15. Synthetic strategy to diferrocenyl-substituted phthalocyanine **Pc13**.

It has been shown that functionalised asymmetric phthalocyanines are very important precursors to multicomponent Pc-based systems. Asymmetric Pcs with peripheral amino groups have been used for the preparation of compounds **2b**, **39**, **Pc13** and others.[6,18,86,90,136] Asymmetric Pcs with covalently attached ethynyl groups on the periphery have been used as precursors for the synthesis of asymmetric phthalocyanines bearing a ferrocenyl unit,[19] Por-Pc ensembles (like **30**),[15,51] the covalent linkage of a SubPc to a Pc unit (compounds **37a-c**)[84] and ethynyl-bridged di- and trinuclear Pcs.[137-141] Asymmetric iodo-substituted Pcs have been involved in the synthesis of compounds **34-36b**[4,82,83] and ethynyl-bridged Por-Pc[142] and Pc-Pc[143] dimers. Asymmetric phthalocyanines bearing formyl groups are very useful precursors for the covalent linkage of fullerenes to a Pc unit as discussed above. Additionally, Por-Pc[52] and Pc-Pc[144,145] systems built from this precursor are described in the literature.

2.3.2. Statistical condensation reactions

In the following part, examples of statistical condensation reactions with phthalonitriles functionalised with desired subunits to form phthalocyanine-based multicomponent systems will be presented.

In contrast to **2b** and **2c**, compound **2a** was directly synthesised via a statistical condensation reaction of **Pn4** with a phthalonitrile bearing a 2,2'-bipyridine unit (**Pn7**) using DMAE as solvent in the presence of zinc(II) chloride (Scheme 2.16). The product (**Pc14**) was then refluxed with [Ru(bpy)$_2$Cl$_2$]·2H$_2$O in EtOH, followed by anion exchange to give dyad **2a** in 71% yield.[6]
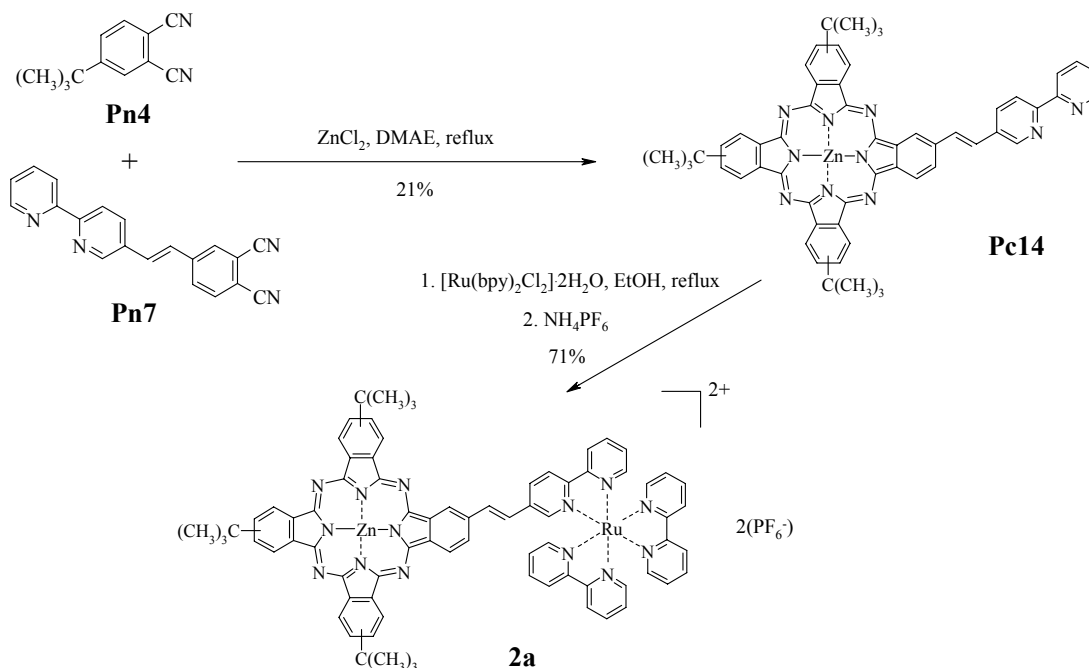
Scheme 2.16. Synthetic strategy to prepare compound **2a**.

Annulated dinuclear phthalocyanines, like **Pc15**, are usually prepared as depicted in Scheme 2.17.[73-81] A statistical condensation reaction of substituted phthalonitrile **Pn8** with bis-(diiminoisoindoline) **C8** in a 7:1 ratio produced binuclear **Pc15** in 11% yield. Besides symmetric Pc (composed of four **Pn8** units), Wöhrle and coworkers were able to isolate trinuclear Pc **33** in a very low yield. Attempts to use other molar ratios of **Pn8** and **C8** did not
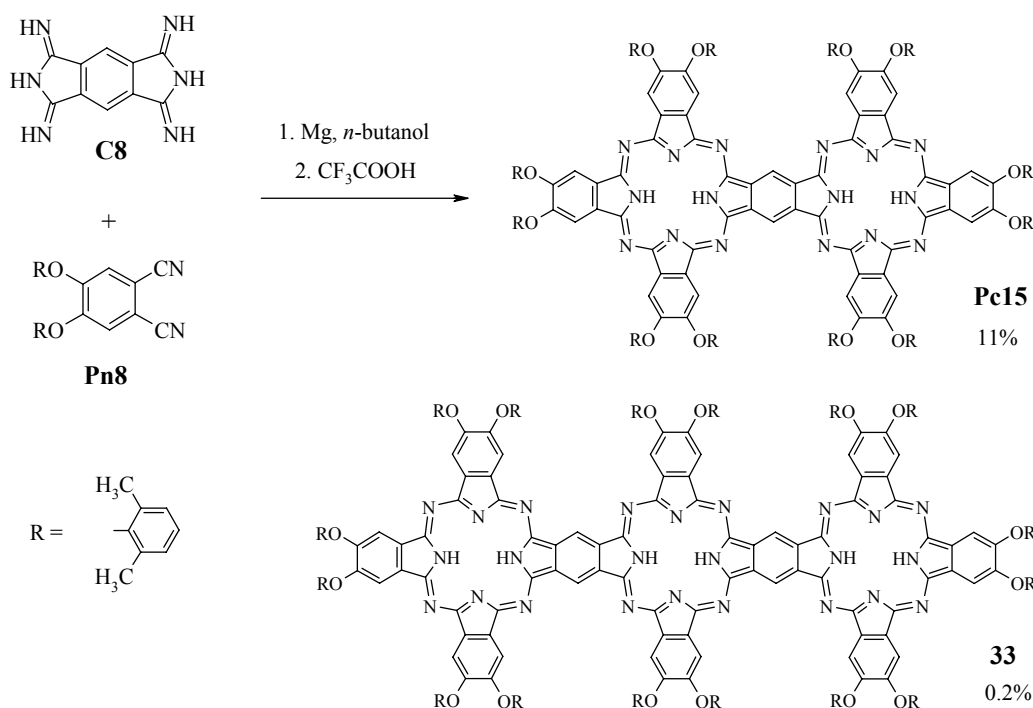
Scheme 2.17. Preparation of annulated di- and trinuclear phthalocyanines (R = 2,6-dimethylphenyl).

lead to the isolation of compound **33**. For example, the theoretical molar ratio of 4:1 led to a larger amount of higher oligomeric Pcs, thus preventing the isolation of **33**.[81]

Most of the asymmetric Por-Pc systems (such as dyad **25**, compound **28** and tetrad **29**) have been prepared by a statistical cyclotetramerisation reaction of a porphyrin-functionalised phthalonitrile with a differently substituted *o*-dicyanobenzene.[45,49,50,59,60] Furthermore, some of the ferrocene-Pc systems (such as compounds **10** and **11**) have been prepared following this method.[13,16]

For the synthesis of triad **28** both aforementioned strategies were involved (Scheme 2.18). In a first step, porphyrin-substituted **Pn9** was reacted with 4-(4-hydroxyphenoxy)phthalonitrile (**Pn10**) via a statistical condensation reaction around a zinc(II) template to yield crude **Pc16**. After column chromatography, dyad **Pc16** was coupled with 2-bromomethyl-anthraquinone to yield target phthalocyanine **28**.[59] The synthetic protocol of the cited communication is very shallow. The cyclotetramerisation to **Pc16** is usually carried out in solvents such as 1-pentanol or DMAE with the option of adding catalytic amounts of a base like DBU. A typical procedure for the nucleophilic substitution for the synthesis of **28** is the reaction of the two starting materials in a basic solution (e.g. K_2CO_3 in DMF).
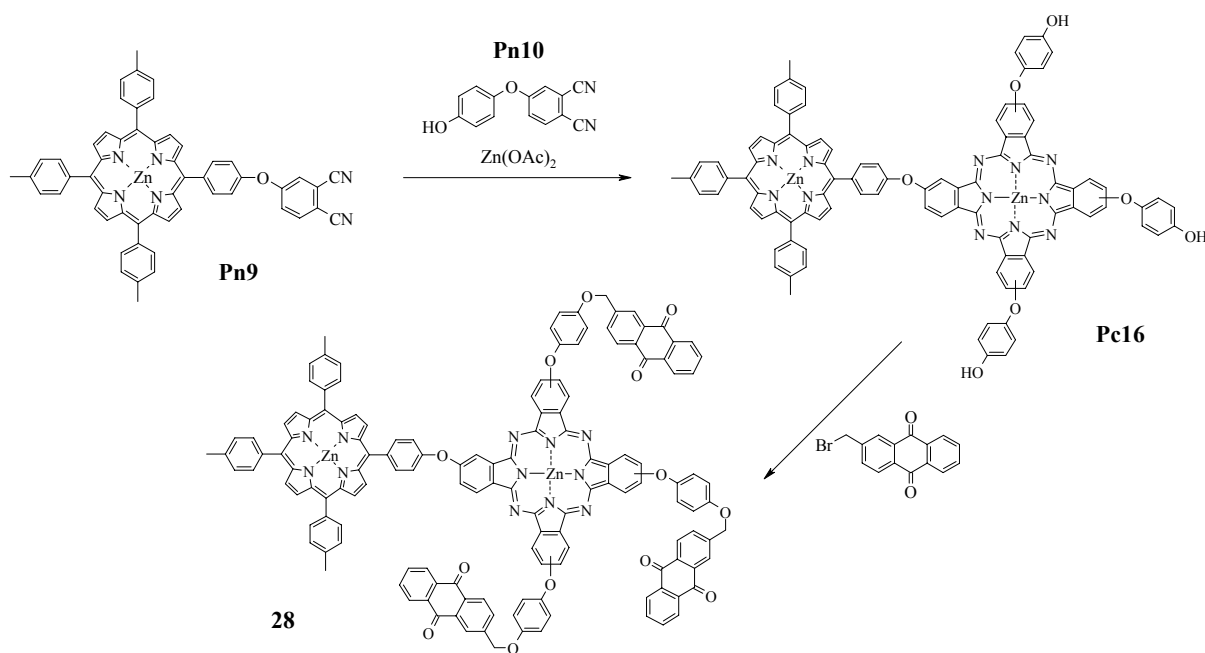
Scheme 2.18. Synthetic pathway for the preparation of triad **28**.

3. Synthesis of asymmetric phthalocyanines with peripherally coordinated Ru(II) complexes

The interest in the use of peripherally functionalised phthalocyanines as ligands to form Pc-based multicomponent systems with multiple functions, as described in the first chapter, has led to the synthetic investigation of asymmetric Pcs with peripheral metal-binding sites. Thereby, 6,7-dicyano-2,3-di(2-pyridyl)quinoxaline (**1**) and 7,8-dicyanodipyrido[3,2-*a*:2',3'-*c*]phenazine (**2**) have been chosen as key precursors. Molecules like **1** possess conformational flexibility which allows them to bind to metal ions either through the nitrogen atoms of the pyridine and the pyrazine rings, forming five-membered rings, or through the nitrogen atoms of both pyridine rings disposed in a cis-conformation, forming seven-membered rings as evidenced by X-ray analyses.[146-155] The phenanthroline unit of phthalonitrile **2** is rigid and therefore, the complexation of metal ions can be controlled in a better way. In addition, the phenanthroline unit is fused to the phthalocyanine π-system through a pyrazine bridge. This means that peripherally coordinated photoactive metal ions have no rotational degrees of freedom with respect to the phthalocyanine core which is expected to lead to a better communication between the two photoactive units after photoexcitation since nonradiative relaxation of excited state energy is less favored. Many examples of phenanthroline derivatives coordinated to photoactive metal ions, such as Ir(III), Os(II), Pt(II) or Ru(II), are reported in the literature.[5,156-164]

Consequently, these ligands have been used for the construction of elaborate metal complexes which show interesting photophysical and redox properties as well as intercalation interactions with DNA duplexes.

3.1. Synthesis of phthalocyanine precursors with metal-binding sites

Both phthalonitrile derivatives, either with two flexible pyridyl rings (**1**) or a rigid phenanthroline unit (**2**), were obtained via a Schiff's base condensation of 4,5-diaminophthalonitrile (**C1**) and 2,2'-pyridil or 1,10-phenanthroline-5,6-dione, respectively, in an equimolar ratio using ethanol as solvent (Scheme 3.1). The target compounds precipitated after formation and were isolated by filtration as pure products.
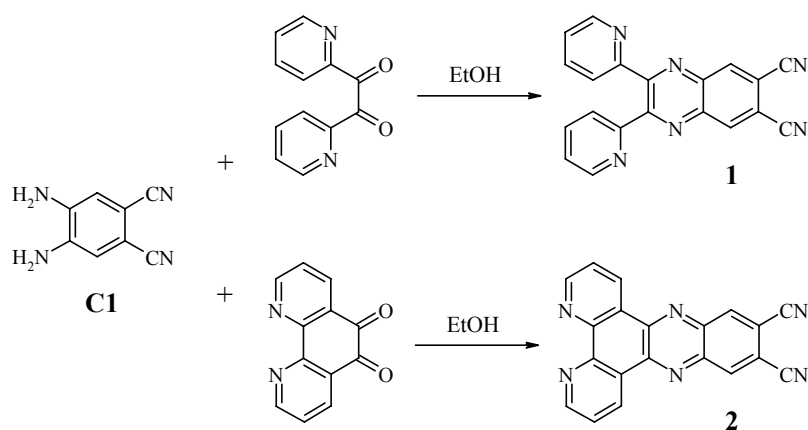
Scheme 3.1. Synthesis of phthalonitriles **1** and **2** with metal-binding sites.

3.2. Symmetric and asymmetric phthalocyanines with peripheral pyridyl groups

In the following part, the synthesis and characterisation of a symmetric octa-substituted H_2Pc bearing eight pyridyl groups and asymmetric, peripherally octa-substituted H_2Pcs and ZnPcs which contain a combination of 2,3-di(2-pyridyl)pyrazino and *p*-pentylphenoxy or *p-tert*-butylphenoxy substituent groups will be described. Taking into account that exploitation of Pcs in materials science demands good solubility and low aggregation, it is noted that the *p*-pentylphenoxy and bulky *p-tert*-butylphenoxy groups provide the resulting Pc compounds with sufficient solubility in organic solvents for that purpose. These asymmetric Pc compounds were synthesised by a statistical condensation reaction between two different phthalonitriles, and the mixed products were finally separated by chromatographic techniques.

3.2.1. Synthesis of a symmetric H_2Pc with eight peripheral pyridyl groups

Previously, our research group reported a synthetic route to a symmetric, fully conjugated phenanthroline-appended phthalocyanine (**Pc1**) which was obtained via a cyclotetramerisation reaction of phthalonitrile **2**.[165] However, this planar, extended Pc system exhibits a high degree of insolubility in common organic solvents. As a continuation of that work, phthalocyanine **3** with eight conformationally flexible pyridyl groups at the periphery was obtained by a direct cyclotetramerisation of 6,7-dicyano-2,3-di(2-pyridyl)quinoxaline (**1**) in the presence of lithium pentoxide at 100°C under nitrogen, followed by the treatment with glacial acetic acid (Scheme 3.2). Although H_2Pc **3** shows less π-π stacking and a slightly better solubility in organic solvents compared to its phenanthroline-appended analogue, it was still not possible to perform purification by chromatographic techniques or by

recrystallisation. Thus, the crude product had to be purified by thoroughly washing with various solvents of different polarity to afford pure H_2Pc **3** in 66% yield.

Pc1
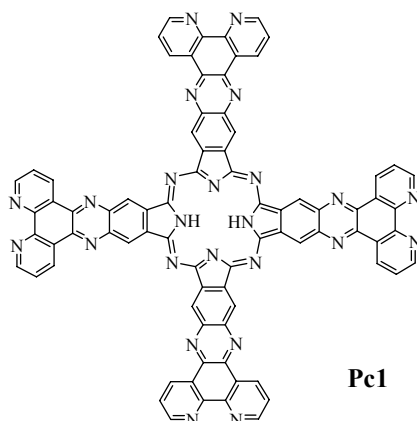
As a further step, following our aim to probe coordination chemistry with **3** as a ligand system, it turned out that its still limited solubility prevented the successful isolation of corresponding Pcs with peripherally coordinated metal ions.
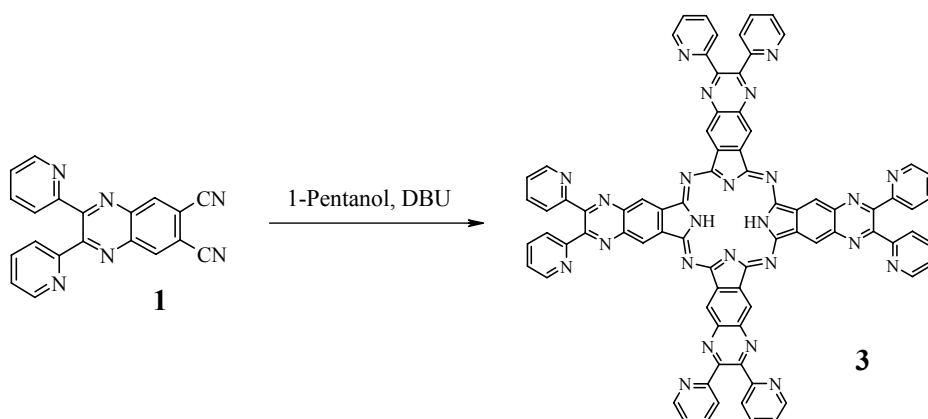
Scheme 3.2. Preparation of symmetric phthalocyanine **3** bearing eight flexible pyridyl groups at its periphery.

Therefore and alternatively, the Pd(II) complex **4** was prepared according to Scheme 3.3 in order to test the direct cyclotetramerisation of a metal complex in the form of a phthalonitrile precursor. However, although the reaction conditions have been varied to a large extent with respect to different solvents, catalytic bases and different metal ion templates, no phthalocyanine product from the Pd(II) complex **4** could be characterised so far.
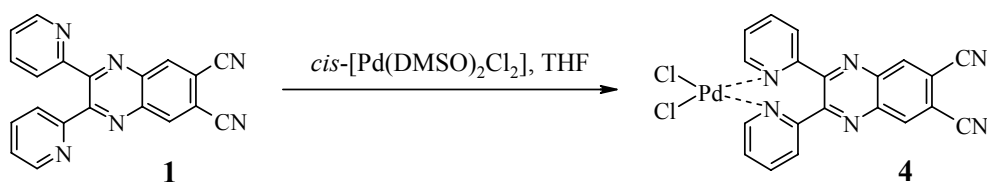
Scheme 3.3. Synthetic procedure to palladium(II) complex **4**.

In general, cyclotetramerisation reactions of various metal-coordinated phthalonitriles (with Pt^{2+}, Ru^{2+} and Pd^{2+}), prepared in our group,[5,166] did not produce the appropriate Pc systems. The suspicion of heavily altered electronic structure of the cyano groups of the metal-coordinated phthalonitriles can be ruled out by ^{13}C NMR and IR studies of various phthalonitrile metal complexes and differently substituted phthalonitriles which are easily reacted to phthalocyanines under various conditions. The ^{13}C NMR study of all compounds in DMSO-d_6 revealed that all the ^{13}C resonances of the cyano groups appear between 114 and 116 ppm (The ^{13}C resonances of the cyano groups of the phthalonitriles which can be tetramerised to Pcs are randomly distributed in the same region of 114-116 ppm). Similar results were obtained in an IR study showing that all the cyano stretch vibrations resonate in the range of 2231-2241 cm^{-1}. Obviously, the electronic structure of the phthalonitrile is not dramatically altered upon complexation with metal ions and therefore, it cannot be the reason of failing cyclotetramerisation to Pcs. When Pcs are synthesised from phthalonitriles, a two-electron reduction takes place to form the Pc^{2-} macrocycle. A possible reason for the unsuccessful tetramerisation of metal ion-functionalised phthalonitriles could be the fact that these metal ions (in this case Pt^{2+}, Ru^{2+} and Pd^{2+}) somehow disturb this two-electron reduction during phthalocyanine formation. In contrast to the aforementioned difficulties, some ferrocene-functionalised phthalocyanines described in the first chapter were prepared from phthalonitriles bearing covalently linked ferrocenyl groups.[3,12,13,16]

Due to the aforementioned problems, alternative strategies towards phthalocyanines with peripherally coordinated metal complexes have to be developed. The following part describes the synthetic approach to various asymmetric Pcs with peripheral metal-binding sites and their successful coordination with Ru(II) complexes.

3.2.2. Synthesis of asymmetric H$_2$Pcs with peripherally attached pyridyl groups

The interest in asymmetrically substituted Pcs, for instance in AAAB type Pcs, where three of the benzenoid rings are substituted with solubilising groups and the fourth with ligating groups, is primarily based on the gain of solubility of the Pcs and at the same time on the availability of peripheral coordination sites for binding metal ions. Additionally, the distinctly reduced aggregation of the Pc cores allows easier chromatographic separation of the different, in part isomeric, phthalocyanine products as discussed in the second chapter.

Phthalonitriles **5-8** bear different bulky groups in order to increase the solubility and decrease π-π stacking properties of the resulting asymmetric Pc products. They were prepared via

nucleophilic substitution reactions. In a typical reaction procedure, commercially available 4,5-dichlorophthalonitrile (**C2**) was reacted with six equivalents of the corresponding phenol derivative in DMSO in the presence of an excess of potassium carbonate (Scheme 3.4).[95] The phenol derivative was added to the reaction in excess in order to completely convert **C2** into product. Otherwise, the purification of the crude product is very problematic since unreacted **C2** is difficult to separate from the phthalonitrile product. After extraction, **5** and **8** were purified by column chromatography, while **6** and **7** were washed with plenty of methanol. The work-up procedure of **6** and **7** was slightly different from that described in the literature.[167,168] During the course of this work, compounds **5-7** were successfully used to prepare various asymmetric phthalocyanines that could be isolated by chromatographic techniques, whereas asymmetric phthalocyanines prepared from **8** and **1** do not exhibit the desired solubility.
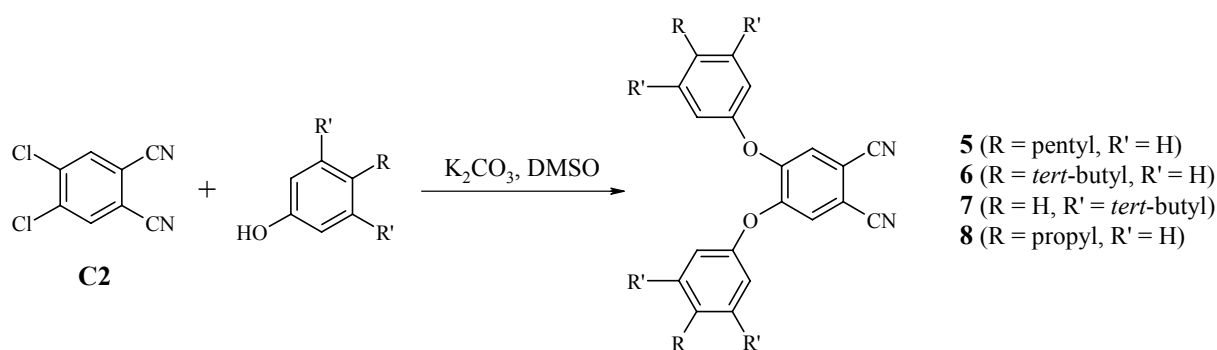
Scheme 3.4. Synthetic procedure to phthalonitriles **5-8**.

Phthalonitrile derivative **1** and 4,5-bis(*p*-pentylphenoxy)phthalonitrile **5** were reacted via a statistical condensation reaction. As expected, this procedure leads to the formation of a mixture of H_2Pcs (**9-13**), as shown in Scheme 3.5 (the formation of H_2Pc **3** may also occur). As mentioned earlier, central theme and challenge of such a strategy lies in the work-up protocol for the mixed products. In the actual case, separation of the H_2Pcs **9** and **10** from the reaction mixture was successfully achieved by column chromatography, since Pcs with a larger number of the more polar pyridyl groups elute distinctly slower through the silica column. The remaining H_2Pc products **11-13** were separated by preparative thin layer chromatography. In the case of H_2Pc **12** with the four pyridyl groups located on adjacent benzo positions (AABB), it was noticed that it is retained longer on alumina than the ABAB type H_2Pc **11**. This illustrates what is still quite rare and therefore remarkable, namely to perform isomer separation of Pcs simply based on alumina preparative thin layer chromatography. Finally, H_2Pcs **9-13** were purified by refluxing in CH_3CN followed by filtration.
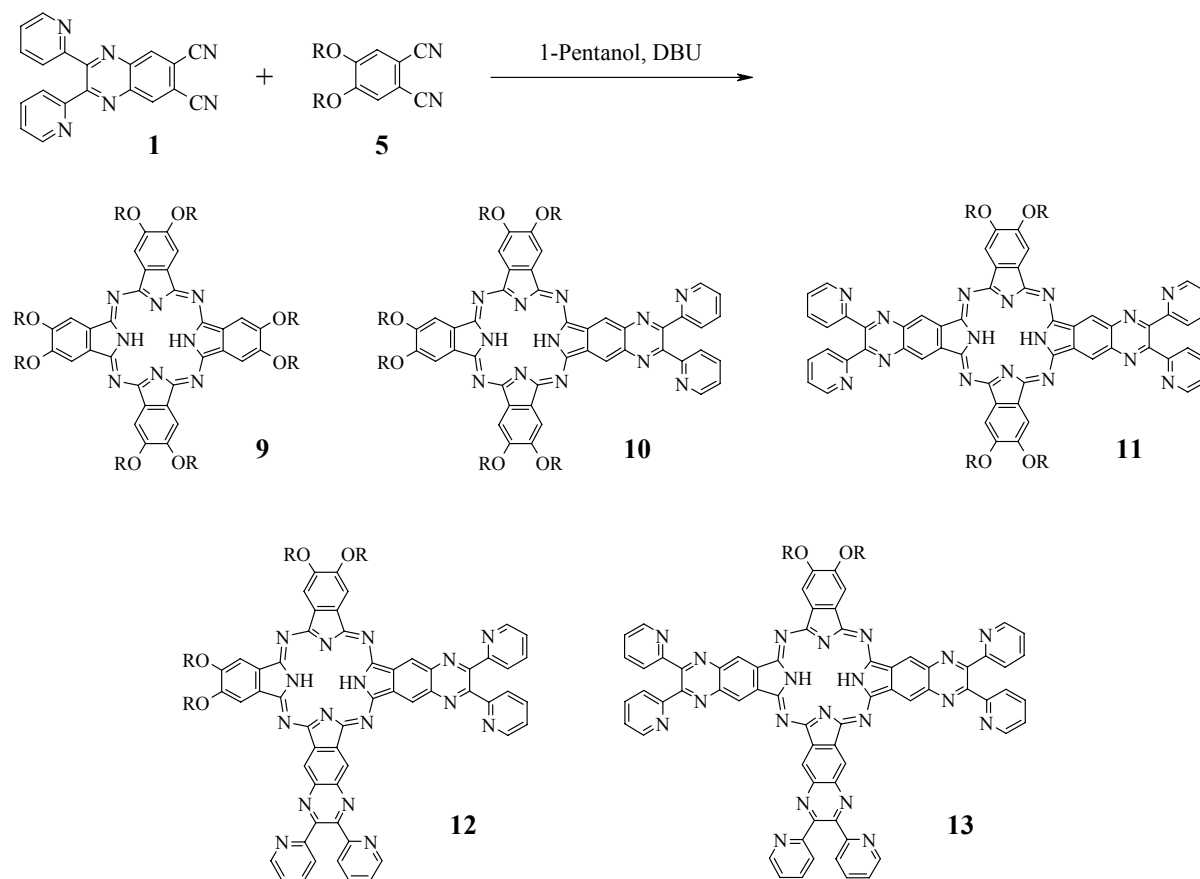
Scheme 3.5. Isolated Pc products **9-13** from the statistical condensation reaction of phthalonitriles **1** and **5** (R = *p*-pentylphenyl).

In general, by varying the molar ratio of the two different types of phthalonitrile precursors, it is to some extent possible, to influence the relative amounts of the individual species which are present within the reaction mixture.[97] In our study it was found that the 3:1 ratio of compounds **5** and **1** optimises the conditions for a formation of the asymmetrical H_2Pc **10**. The yields of H_2Pcs **9** and **10** are 26% and 21%, respectively, quite comparable to values reported in the literature.[97]

3.2.3. Synthesis of asymmetric zinc phthalocyanines

The reaction of H_2Pc **10** with zinc(II) acetate dihydrate in 1-pentanol under mild conditions gave ZnPc **14** in a fairly good yield (Scheme 3.6). **14** exhibits a high enough solubility in common organic solvents for an investigation by ^1H NMR and UV-vis spectroscopy; however, the obtained crystals were of rather poor quality for a single crystal X-ray study. Therefore, in order to elucidate the X-ray structure of such an asymmetrically octa-substituted system, the analogous AAAB type ZnPc **15** was prepared via the cyclotetramerisation reaction of 4,5-bis(*p-tert*-butylphenoxy)phthalonitrile **6** and phthalonitrile derivative **1** by

using a zinc(II) template (Scheme 3.6). The exchange of the peripheral substituents, namely *p*-pentylphenoxy with *p-tert*-butylphenoxy, was expected to give rise to a different crystallisation behavior. Clearly, the reaction afforded a mixture of different Pc compounds from which, **15** was isolated in 18% yield after performing column chromatography for several times. Indeed, suitable single crystals for an X-ray analysis have been obtained by slow evaporation of a pyridine solution of **15**.
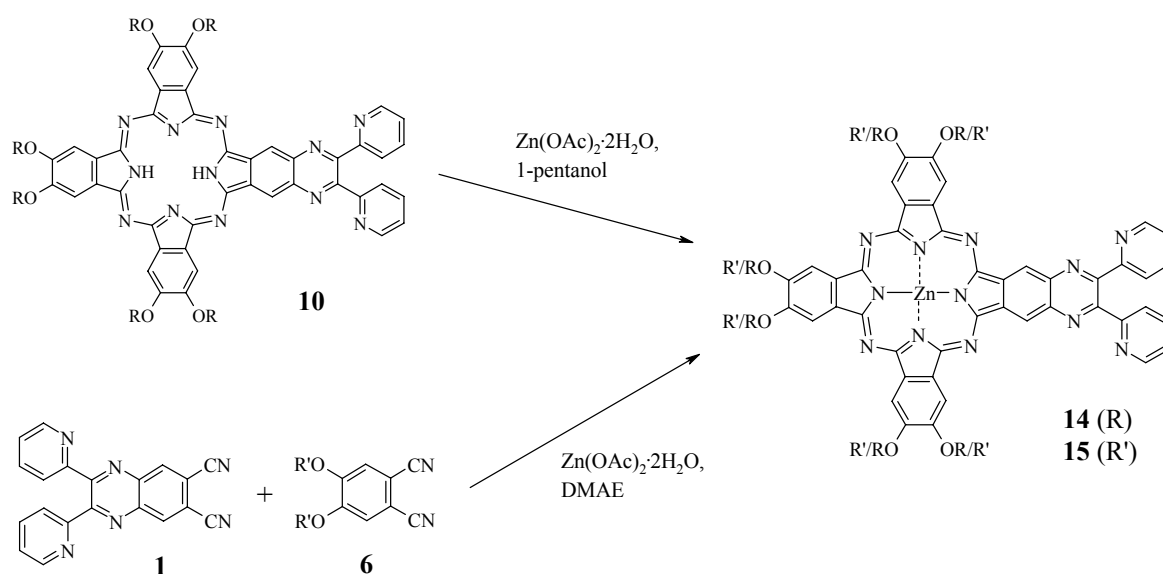
Scheme 3.6. Synthetic route to asymmetric zinc phthalocyanines **14** (R = *p*-pentylphenyl) and **15** (R' = *p-tert*-butylphenyl).

3.2.4. Solution properties of asymmetric metal-free phthalocyanines

The presence of the *p*-pentylphenoxy groups in H_2Pcs **9-13** leads to a fairly good solubility which allows for ^{1}H NMR and UV-vis spectroscopy in chloroform. Their ^{1}H NMR spectra clearly show that H_2Pcs **9-13** are all well separated and represent pure compounds in accordance with their proposed molecular formula. Particularly, the ^{1}H NMR spectra are quite informative since they differentiate between the constitutional isomers **11** and **12**, while both show the same molecular ion peaks in their MALDI-MS spectra. As depicted in Fig. 3.1, isomer **11** exhibits only two doublets attributed to the two protons of the pyridyl groups (in *ortho* position to the N atom and in *ortho* position to the C linked to the quinoxaline unit), designated by c and d, respectively. Similarly, only one set of resonances is observed for methylene protons of the pentylphenoxy chain closest to the Pc core (see Chapter 5). Additionally, there are only two singlets assigned to the protons of the phthalocyanine core (a and b). Obviously, the spectrum of **11** indicates magnetically equivalent environments for these substituents, which conforms to a structure exhibiting in good approximation D_{2h}

symmetry. Accordingly, in the case of the less symmetrical isomer **12** approximated by C_s symmetry, two types of methylene protons (see Chapter 5) and two types of protons (c and d) of the pyridyl groups lead to separate triplets and doublets, respectively. Similarly, four types of Pc aromatic protons result in two separate singlets (a and b) in the case of isomer **11**, whereas for isomer **12**, each one of them additionally splits into two separated singlets (a/a' and b/b').
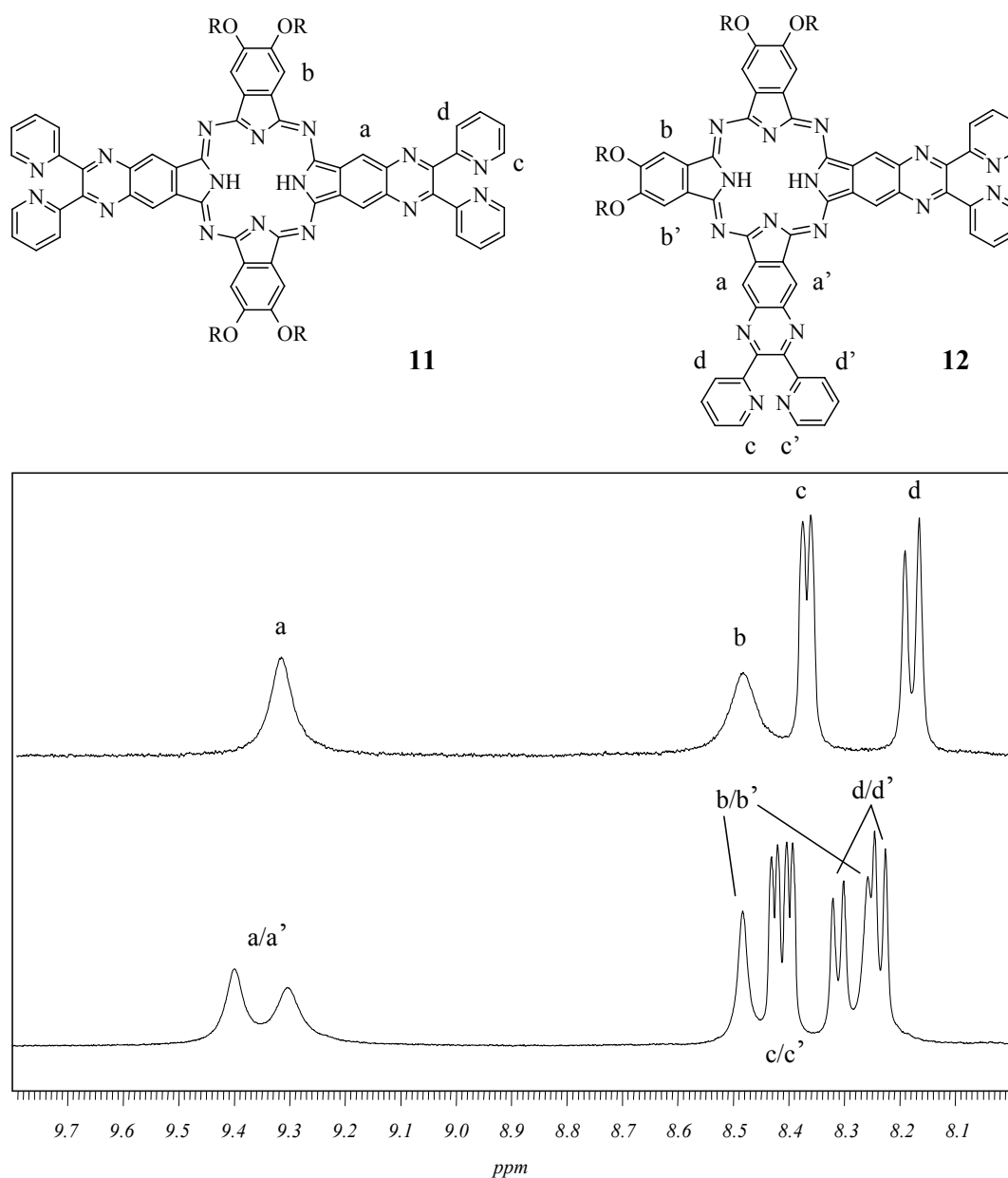
Figure 3.1. The ^{1}H NMR spectra (part of the resonance range of the aromatic protons) of H_2Pc compounds **11** (above) and **12** (below).

The UV-vis spectra within the Q band range of H_2Pcs **9-13** are shown in Fig. 3.2. To recall, in general, the Q band absorption of phthalocyanines is assigned to the transition from the HOMO to the LUMO, whereas for ring-expanded systems, the percentage of pure HOMO-

LUMO character increases with enlargement of the π–system; with the same trend, due to the lowering of the LUMO, the Q band also shifts to longer wavelengths. Furthermore, substituted species concomitantly split, which means that the degeneracy of the LUMO depends on the symmetry of the macrocyclic system, and this splitting becomes larger the larger the size of the fused aromatic molecules. As expected, compound **9**, the symmetrically substituted H_2Pc that shows approximately D_{2h} symmetry, exhibits a Q band with distinct splitting. In a recognisable manner, going from compounds **11** to **13**, the Q bands show a pronounced increase of their red shift and, from **9** to **11**, also an increase in their splitting. In contrast, compound **12** reveals only a small splitting. However, this observation is rationalised by MO calculations, which show that the Q band splitting of adjacent ring-expanded 2:2 phthalocyanines is smaller, if occurring at all, than for opposite ring-expanded 2:2 Pcs.[169]
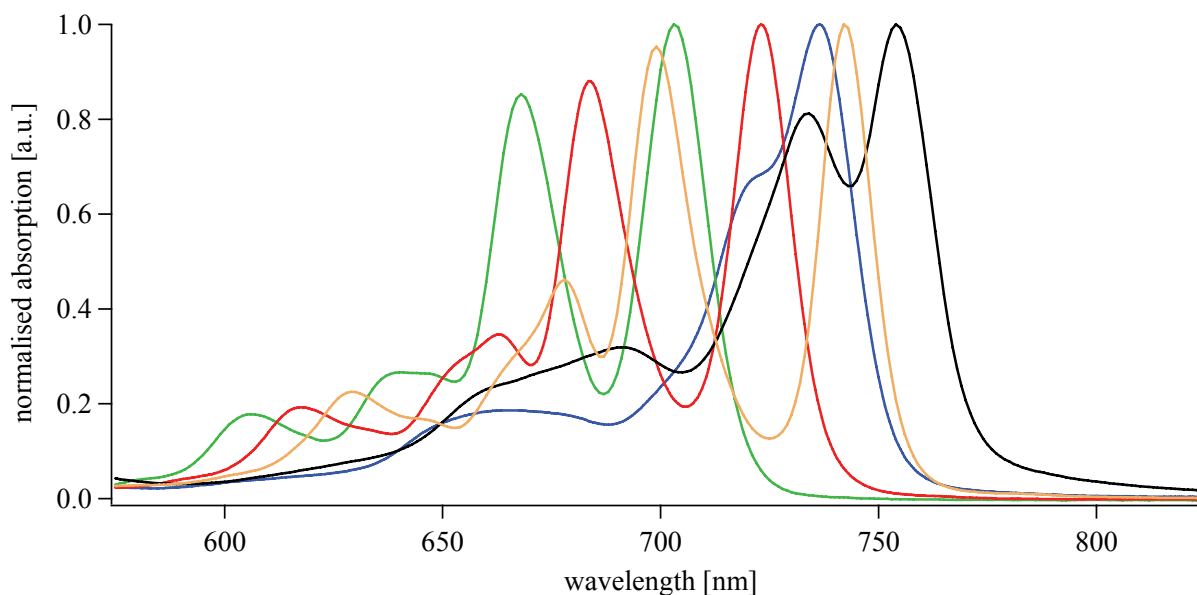
Figure 3.2. Q band range of UV-vis spectra of H_2Pc compounds **9** (green), **10** (red), **11** (yellow), **12** (blue) and **13** (black) in $CHCl_3$. The Q band absorption maxima are normalised.

3.2.5. X-ray single crystal structures

Crystal data of ligand **1**, its Pd(II) complex **4** and ZnPc **15** are listed in Table A1. (see Appendix). Compound **1**, the 6,7-dicyano-2,3-di(2-pyridyl)quinoxaline ligand, crystallises in the triclinic space group $P\bar{1}$ with one molecule per asymmetric unit. The molecular structure, together with selected bond lengths and bond angles is shown in Fig. 3.3. The structural parameters found for **1** are comparable to those found for similar ligands.[170,171] The benzene ring of the quinoxaline unit is nearly planar, whereas the pyrazine ring shows a slight distortion with the largest torsion angle being 6.8(3)° for N2-C3-C4-N1. Due to steric reasons,
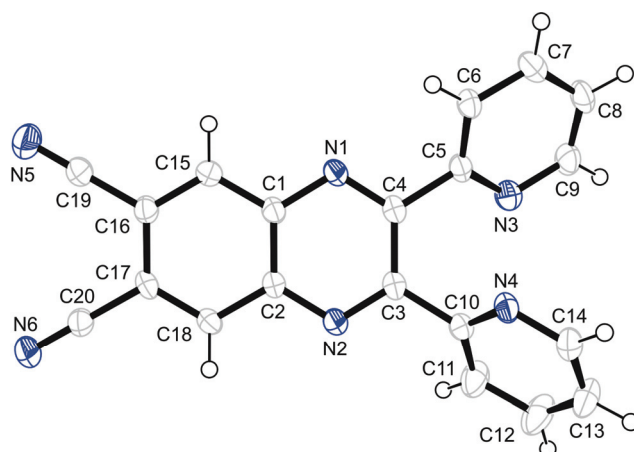
Figure 3.3. ORTEP representation (ellipsoids at 50% probability) of the molecular structure of **1**. Selected bond lengths [Å] and angles [°]: C3-C10 1.491(2), C4-C5 1.491(2), C16-C19 1.442(3), C19-N5 1.137(2), C17-C20 1.447(2), C20-N6 1.148(2); C3-C4-C5 121.42(15), C4-C3-C10 121.41(15), C16-C17-C20 119.19(15), C17-C16-C19 119.75(15).

the pyridine rings are not coplanar to the quinoxaline entity and the torsion angles C3-C4-C5-N3 and C4-C3-C10-N4 are 35.6(3) and 47.7(2)°, respectively. The pyridine nitrogen atoms are above and below the plane defined by the quinoxaline unit, and the dihedral angle between the pyridine rings is 49.9(1)°. Fig. 3.4 shows the crystal packing of compound **1**. C-H···N hydrogen bonds are present, resulting in the formation of dimers [C18-H···N6a 3.474(2) Å]. In addition, the molecules exhibit a head-to-tail arrangement which is stabilised by π-π-stacking interactions, with the shortest C···C contact being 3.379(2) Å.
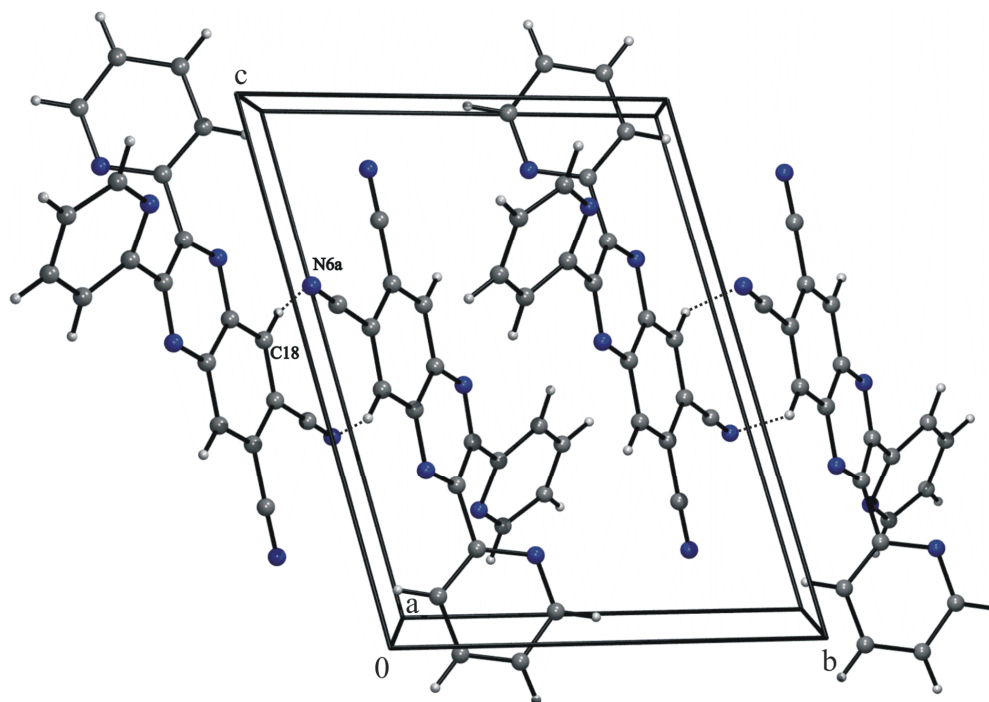
Figure 3.4. Crystal packing of **1** showing the formation of hydrogen bonded dimers, C18-H···N6a 3.474(2) Å with symmetry operation a: 2-x, -y, 1-z.

Compound **4**, the Pd(II) complex of ligand **1**, crystallises in the triclinic space group P$\bar{1}$ with one complex molecule and one co-crystallised acetonitrile molecule per asymmetric unit. The molecular structure together with selected bond distances and bond angles is shown in Fig. 3.5. The Pd(II) ion is coordinated through both pyridine N atoms disposed in a *cis*-conformation and through two terminal Cl atoms. The metal ion adopts a square planar coordination geometry with a deviation of 0.008(4) Å from the least-squares plane defined by the four donor atoms. Consequently, the pyrazine N atoms are non-coordinating and ligand **1** adopts a seven-membered boat-conformation, or equivalently, the pyridine rings are rotated with respect to the quinoxaline plane to show a butterfly wings arrangement.[172,173] The torsion angles C4-C3-C10-N4 and C3-C4-C5-N3 are -55.3(6) and 61.8(5)°, respectively, and the plane defined by the quinoxaline group is nearly perpendicular [81.9(5)°] to that of the square-planar Pd(II) coordination entity. Due to the coordination of both pyridine units, both pyridine nitrogen atoms are above the plane defined by the quinoxaline system, and the dihedral angle between the pyridine rings is 87.0(2)°. The Pd-Cl and the Pd-N bond lengths are comparable to those of related compounds reported in the literature.[172,173] Fig. 3.6 shows the crystal packing of complex **4**. The complexes exhibit a head-to-tail arrangement stabilised by π-π-stacking interactions and hydrogen bonds which results in the formation of dimers [C6-H···N6a 3.368(6) Å and C11-H···N5a 3.543(7) Å; the shortest C···C contact in the π-π stacking is 3.460(6) Å].
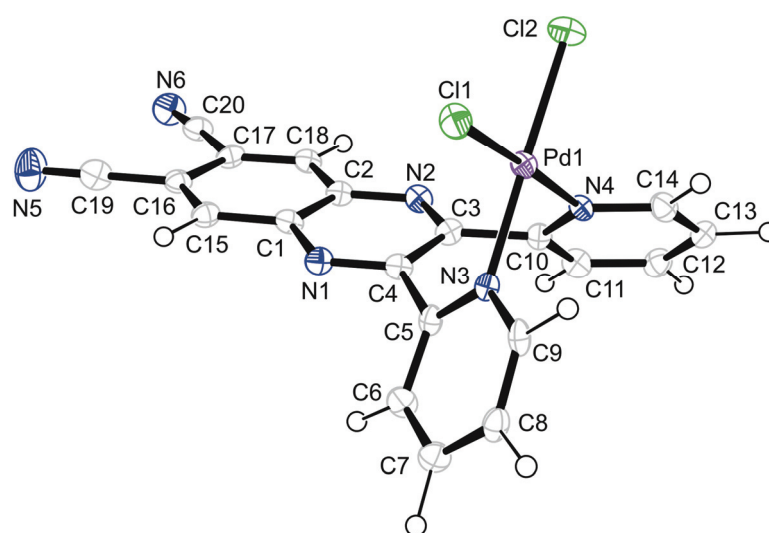
Figure 3.5. ORTEP representation (ellipsoids at 50% probability) of the molecular structure of **4**. The co-crystallised CH$_3$CN molecule is omitted for clarity. Selected bond lengths [Å] and angles [°]: Pd1-Cl1 2.2834(10), Pd1-Cl2 2.2863(12), Pd1-N3 2.010(4), Pd1-N4 2.028(3); Cl1-Pd1-Cl2 93.92(4), Cl2-Pd1-N4 89.23(10), N4-Pd1-N3 86.95(13), N3-Pd1-Cl1 89.95(9).
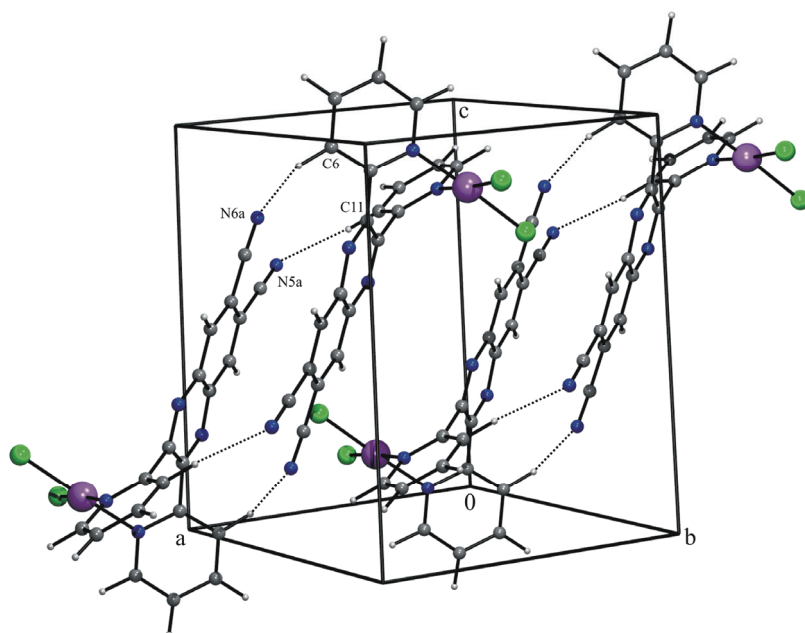
Figure 3.6. Crystal packing of complex **4** showing the formation of hydrogen bonded and π-π stacked dimers, C6-H···N6a 3.368(6) Å and C11-H···N5a 3.543(7) Å with symmetry operation a: -x, 1-y, 1-z. CH$_3$CN molecules are omitted for clarity.

Compound **15** crystallises in the monoclinic space group P2$_1$/c with one ZnPc molecule axially ligated by a pyridine molecule and an additional 7.5 co-crystallised pyridine molecules per asymmetric unit. Fig. 3.7 shows the molecular structure of the ZnPc complex, together with selected bond distances and bond angles. The zinc(II) ion is coordinated in a distorted
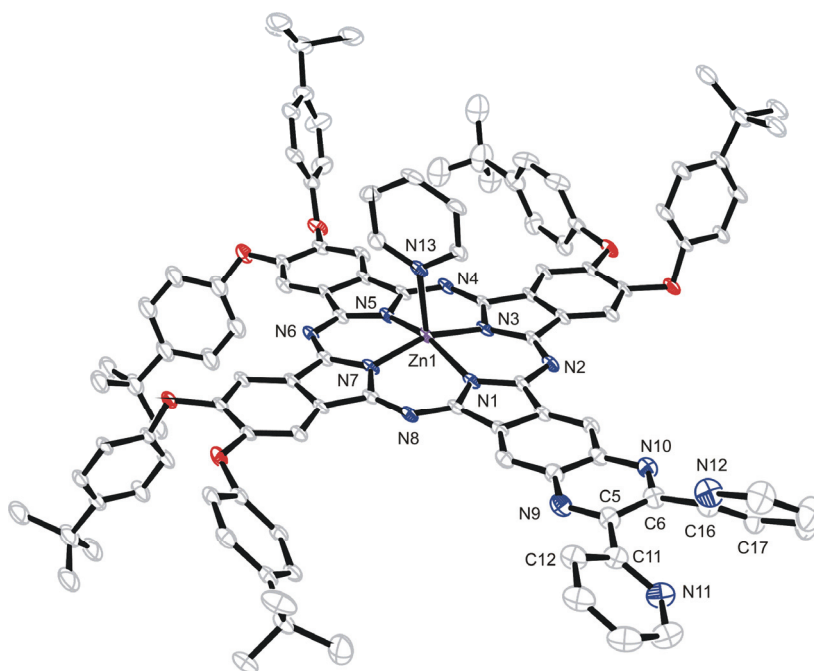
Figure 3.7. ORTEP representation (ellipsoids at 20% probability) of the molecular structure of **15** with an axial pyridine ligand. Hydrogen atoms are omitted for clarity. Selected bond lengths [Å] and angles [°]: Zn1-N1 2.240(3), Zn1-N3 1.904(3), Zn1-N5 2.197(3), Zn1-N7 1.846(3), Zn1-N13 2.068(3); N1-Zn1-N3 84.32(13), N3-Zn1-N5 89.84(13), N5-Zn1-N7 86.91(12), N7-Zn1-N1 90.64(13), N1-Zn1-N13 105.38(12).

square-pyramidal coordination geometry and situated out of the least-squares plane of the four coordinating Pc nitrogen atoms (N1, N3, N5 and N7) by 0.388(2) Å. The corresponding Zn-N bond lengths vary by 0.39 Å which reflects the distortion of the coordination geometry around the Zn(II) ion originating from the asymmetric peripheral substitution of the Pc core. The bond length of the axially coordinated pyridine nitrogen to the zinc(II) is 2.068(3) Å, which is similar to that of a previously reported structure.[174] The pyridine ring is slightly tilted from an orthogonal position with respect to the phthalocyanine plane with a dihedral angle of 81.0(1)°.
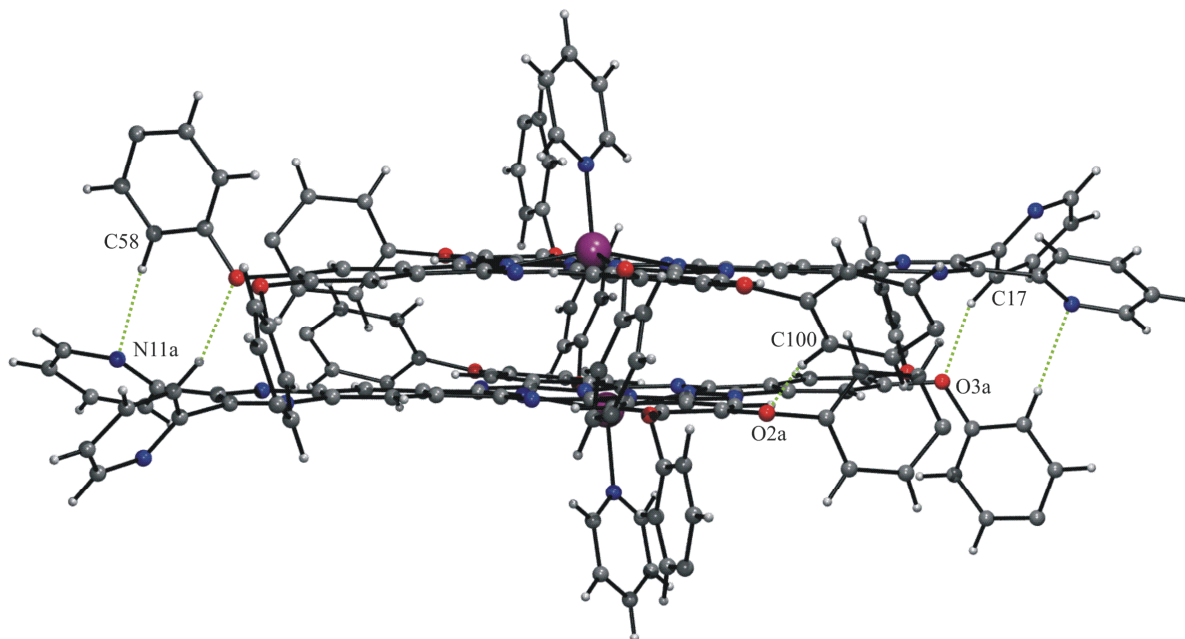
Figure 3.8. Hydrogen bonded dimers of **15** with axial pyridine ligands. *Tert*-butyl groups are omitted for clarity. Hydrogen bond distances [Å]: C17-H···O3a 3.135(6), C58-H···N11a 3.536(8), C100-H···O2a 3.442(5) with symmetry operation a: -1-x, -y, -1-z.

The aromatic Pc skeleton is distorted from perfect planarity by 0.063 Å from its best least-squares plane. The pyridine rings at the periphery of the phthalocyanine show a butterfly wings arrangement. The torsion angles C6-C5-C11-N11 and C5-C6-C16-N12 are -36.4(7) and -49.1(7)°, respectively, with the nitrogen atoms above and below the Pc plane. Fig. 3.8 shows the formation of hydrogen bonded dimers. Two Pc complexes form a head-to-tail arrangement with respect to the quinoxaline unit. The interplanar distance between these two Pcs is 3.187(4) Å and the Zn···Zn distance is 5.458(5) Å. The Pc dimers are arranged in a zigzag pattern, exhibiting an angle of 57.50(1)° as shown in the crystal packing diagram in Fig. 3.9. A similar example of an asymmetric porphyrazine with bulky substituents that also forms analogous dimers in the solid state is reported in the literature.[175]
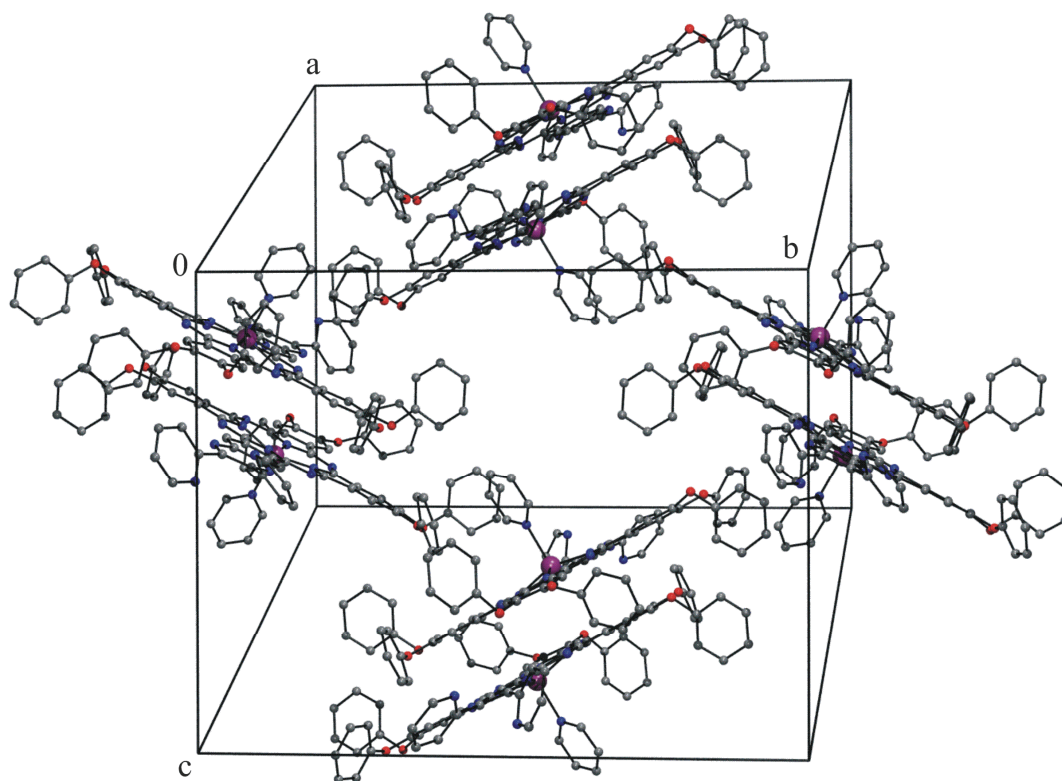
Figure 3.9. Crystal packing of compound **15** with an axial pyridine ligand. Hydrogen atoms and *tert*-butyl groups are omitted for clarity.

3.3. Asymmetric phenanthroline-appended phthalocyanines

As mentioned above, a large variety of phenanthroline derivatives coordinated to various transition metal ions has been published. Therefore, a Pc ligand with peripheral phenanthroline units is a promising candidate for the introduction of different transition metal ions to the periphery and into the cavity of the Pc core, respectively. In order to overcome the high degree of insolubility exhibited by **Pc1**, asymmetric phthalocyanine **17** bearing one peripheral phenanthroline unit (Scheme 3.7) was synthesised. Furthermore, ligand **17** was used to obtain several Ru(II)-MPc systems as shown in section 3.4.

3.3.1. Synthesis of an asymmetric phenanthroline-appended H$_2$Pc

The statistical condensation reaction of **7** with **2** afforded the desired AAAB type Pc **17** (Scheme 3.7). Both, the lithium-pentoxide and the DBU method could be applied to produce **17** in similar yields. In the former case, an additional red impurity, which shows green luminescence in solution upon photoexcitation with UV light, was formed. Since this impurity and **17** have similar polarities, it proofed very difficult to separate them. In the latter case, only a brown impurity (which was also observed in the former case) with similar polarity as

17 was present in the crude product. However, this impurity was partly separated from the product by chromatography. The remaining brown impurity was then removed by washing the crude product with boiling MeCN to yield pure **17**. Column chromatography using silica leads to purer **17** since on alumina, traces of A_2B_2 type products were eluted together with **17** as detected by MALDI-MS. A molar ratio of 1:4.5 (**2**:**7**) was found to give the highest yield of **17** (16%) during an overnight reaction of **2** with **7** in 1-pentanol using DBU in catalytic amounts at 148°C. Besides **17**, symmetric phthalocyanine **16** was obtained in 44% yield. The UV-vis spectra (Fig. 3.10) of both compounds are similar to those of **9** and **10**, respectively (Fig. 3.2). Again, the Q band of **17** is, compared to that of **16**, shifted to the red by 29 nm due to the increased π-system.
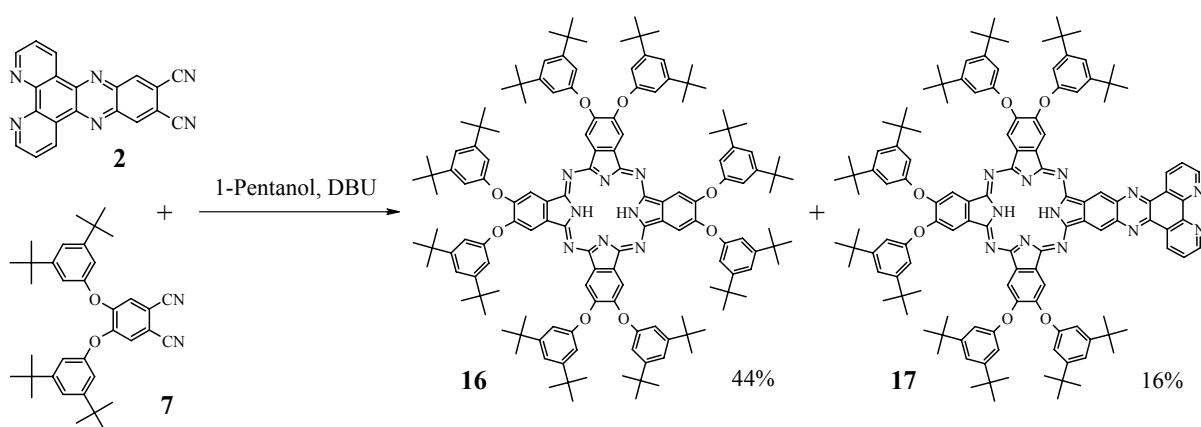
Scheme 3.7. Synthetic strategy to asymmetric Pc **17**.

It is worth noting that for the separation of an AAAB type Pc - with B representing the directly to the Pc fused dipyrido[3,2-*f*:2',3'-*h*]quinoxaline (dpq) entity as in compound **17** - from the mixture of different Pcs formed during the cyclotetramerisation reaction, it turned out to be crucial which phthalonitrile with solubilising groups (denoted by A) was used for the synthesis. The reaction of **2** with **5** led to the formation of a green reaction mixture with very low solubility. The UV-vis spectrum of the crude product shows a Q band which indicates the presence of the desired AAAB type Pc. Two of three maxima are assigned to the symmetric Pc of the AAAA type, and the third, more red shifted maximum corresponds to the AAAB type Pc due to its increased π-system. However, the low solubility of the crude product made the isolation of the desired product impossible. The use of **6** instead of **5** leads to an increased solubility of the crude product. Hence, column chromatography was performed, but only symmetric H_2Pc (AAAA) could be isolated. The AAAB type Pc could not be eluted although very polar solvents, such as CH_2Cl_2:MeOH (1:1) or acidified eluents, were used.
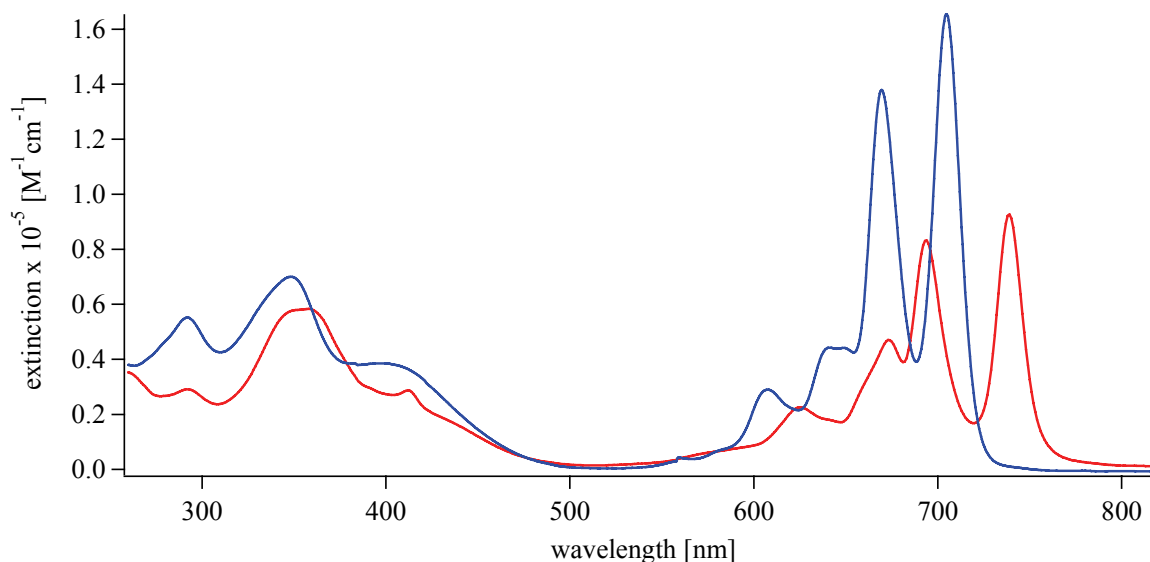
Figure 3.10. UV-vis spectra of phthalocyanines **16** (blue) and **17** (red) in CHCl$_3$.

3.3.2. Metallation of asymmetric phenanthroline-appended H$_2$Pc

Asymmetric phthalocyanine **17** was reacted with various metal salts to obtain the corresponding MPcs **18-20** (Scheme 3.8). For the preparation of MgPc **18**, **17** was reacted with 30 equivalents of magnesium chloride hexahydrate in DMF at 150°C overnight. However, complete metallation of **17** was not achieved. As a consequence, **18** was separated from unreacted **17** by column chromatography. After heating the solid in a water-methanol mixture followed by filtration, pure **18** was obtained in 84% yield.
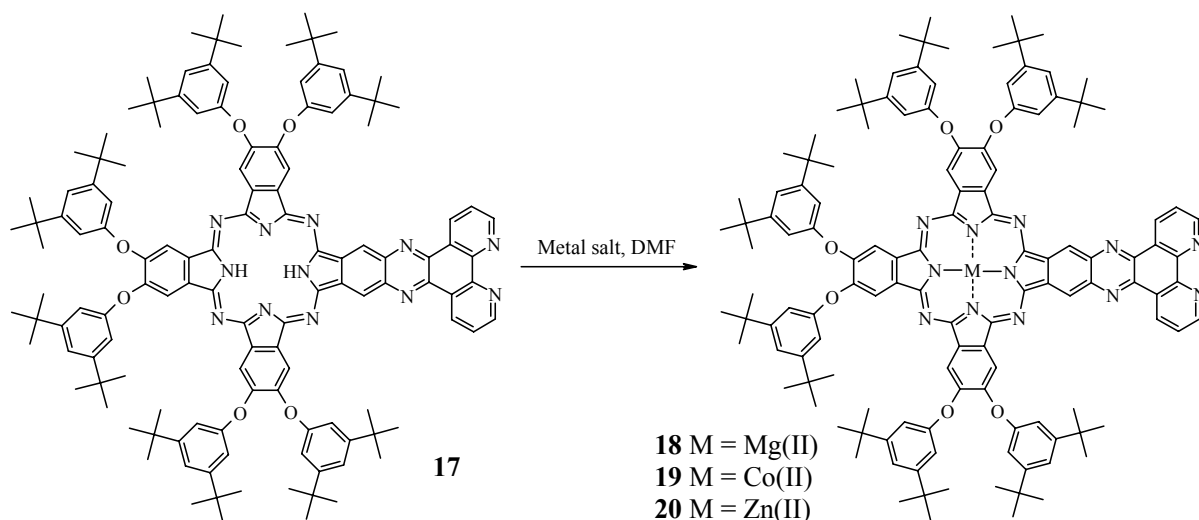
Scheme 3.8. Preparation of metal phthalocyanines **18-20**.

For the synthesis of CoPc **19**, 11 equivalents of anhydrous cobalt(II) chloride were reacted with **17** under similar conditions as for the preparation of **18**. MALDI-MS and UV-vis measurements showed that complete metallation of **17** occured. The metallation of **17** with transition metal ions could lead to the problem of peripheral coordination to the phenanthroline unit. Crossley and coworkers reported on similar problems with phenanthroline-functionalised zinc porphyrin systems. They were able to remove peripherally coordinated Zn(II) ions, but kept Zn(II) bound to the macrocyclic cavity, by treatment with an excess of ethylenediaminetetraacetic acid (EDTA) in boiling DMF.[176] The "EDTA method" was applied to remove all free and possibly peripherally coordinated Co^{2+} ions since compound **19** is not soluble enough to perform chromatographic purification. For that purpose, the crude product was heated in the presence of ethylenediaminetetraacetic acid disodium salt dihydrate (Na$_2$EDTA) for one day. The reaction mixture was then heated in a water-methanol mixture followed by filtration to obtain pure **19** in 94% yield.

Metallation of **17** with Zn(II) was a very delicate procedure since Zn(II) does not selectively coordinate to the macrocyclic cavity of the Pc. MALDI-MS measurements revealed that Zn(II) coordinates to the peripheral phenanthroline unit as well. **17** was reacted with 1.02 equivalents of zinc(II) acetate dihydrate in DMF at 100°C overnight followed by applying the "EDTA method" as described for **19**, yielded pure **20** quantitatively. It is worth noting that higher temperatures and a large excess of Zn(II) favors the coordination at the periphery of **17** as shown by MALDI-MS experiments with dithranol as the matrix. Besides the [MH]$^+$ signal, a signal which could be assigned to the [M-Zn(II)-matrix]$^+$ species was observed with intensities depending on the synthetic conditions.

3.4. Asymmetric phthalocyanines with peripherally coordinated Ru(II) complexes

The ZnPc-Ru(II) dyads **2a-2c** (see Chapter 1) show very efficient energy transfer from the ruthenium(II) unit to the ZnPc moiety upon photoexcitation. There are two main differences between these systems and dyads **21-23**. In the latter, the ruthenium(II) units are directly linked to the phthalocyanine π-systems and hence, the entire systems are rigid which is expected to affect the photophysics of dyads **21-23** with respect to **2a-2c**. Hoffman and coworkers reported on porphyrazine dyads **Pz1a** and **Pz1b** which are very similar to compounds **21-23**.[177] However, the authors did not publish any photophysical measurements besides UV-vis absorption spectra.

Pz1a M = Zn(II)
Pz1b M = Mg(II)
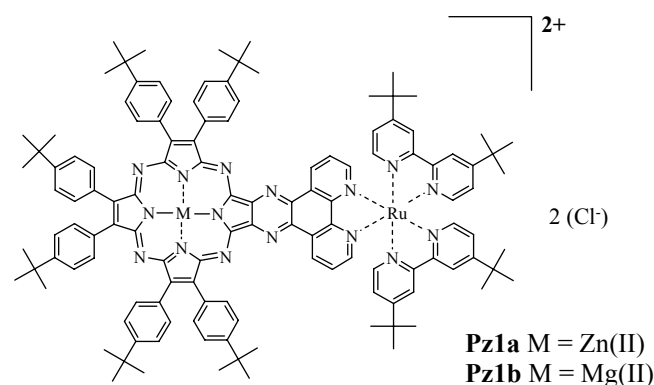
3.4.1. Synthesis of MPcs with peripherally coordinated bis(2,2'-bipyridine)-ruthenium(II)

Dyads **21** and **22** can be synthesised following two different strategies. They can be formed in a one-pot reaction from **17**, where the asymmetric MPcs **18** and **20** are prepared *in situ* followed by the reaction with *cis*-[Ru(bpy)$_2$Cl$_2$] (Scheme 3.9). Another procedure involves a time-consuming two step synthesis, namely the isolation of the asymmetric MPcs **18** and **20** and subsequent reaction with *cis*-[Ru(bpy)$_2$Cl$_2$] to obtain dyads **21** and **22**. Interestingly, the two synthetic approaches lead to the formation of **21** and **22** in similar yields. In a typical reaction protocol, **17** was reacted with four equivalents of M(II) chloride in DMF for three hours. Then, two equivalents of *cis*-[Ru(bpy)$_2$Cl$_2$] were added and the reaction mixture was refluxed for another four hours. The resulting dyad was then isolated by column chromatography, and the chloride anions were exchanged by hexafluorophosphate anions as a further step of purification. However, dinuclear system **23** could not be synthesised via the *in situ* procedure. Therefore, CoPc **19** was reacted with two equivalents of *cis*-[Ru(bpy)$_2$Cl$_2$] in refluxing DMF (Scheme 3.9). The work-up procedure was similar as for compounds **21** and **22**. It is worth noting that the reaction of metal-free Pc **17** with *cis*-[Ru(bpy)$_2$Cl$_2$] did not lead to the formation of the desired H$_2$Pc with peripherally coordinated divalent ruthenium.

17 M = 2H
19 M = Co(II)

1) Metal(II) chloride, DMF (except for **23**)
2) *cis*-[Ru(bpy)$_2$Cl$_2$], DMF
3) NH$_4$PF$_6$

21 M = Zn(II)
22 M = Mg(II)
23 M = Co(II)
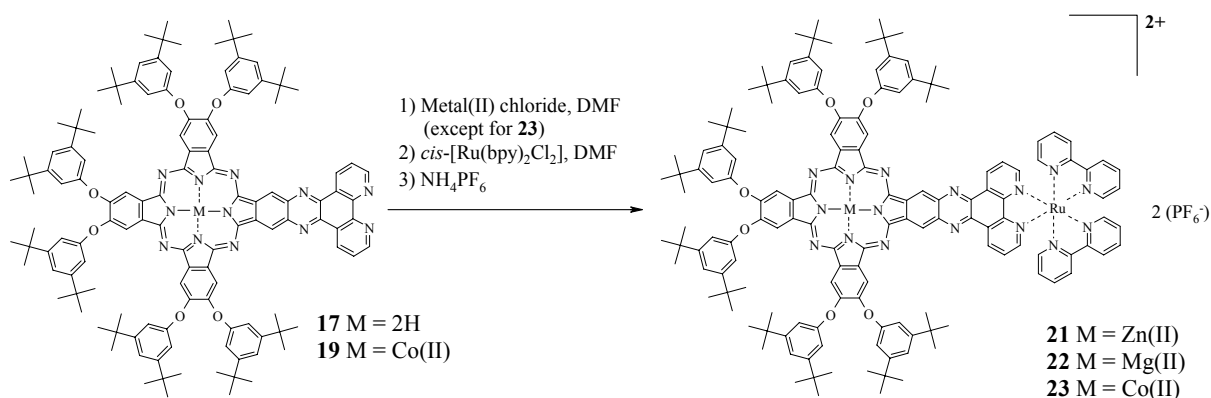
Scheme 3.9. Preparation of MPc-Ru(II) dyads **21-23**.

3.4.2. Photophysical properties of dyads 21-23

Recently, Guldi and coworkers published the photophysical studies of compounds **2a-2c** (see Chapter 1) which exhibit a very efficient intramolecular energy transfer from the photoexcited $[Ru(bpy)_3]^{2+}$ unit to the ZnPc moiety as the governing photophysical event.[6] These compounds are very similar to dyads **21-23**. As mentioned above, the ruthenium(II) units of the latter are directly linked to the phthalocyanine π-systems and hence, they are rigid and cannot rotate as in compounds **2a-2c**. Compounds **21-23** bear different metal ions in their Pc cavity in the form of Zn^{2+}, Mg^{2+} and paramagnetic Co^{2+} (d^7), respectively. Their influence on the photophysical properties of dyads **21-23** were examined as well.

3.4.2.1. Optical ground state properties

For the present photophysical study of dyads **21-23**, metal phthalocyanines **18-20** were used as reference compounds. Their UV-vis spectra are shown in Fig 3.11. These compounds exhibit a set of Q bands in the form of a strong maximum around 700 nm flanked by a weak maximum around 630 nm. The B band absorption of the Pc unit (around 370 nm) and the π-π* transition features arising from the dpq entity and the 3,5-di-*tert*-butylphenoxy groups are observed between 250 and 400 nm. The nature of the Q and B band corresponds to the S_0-S_1 and S_0-S_2 transitions, respectively.[178]
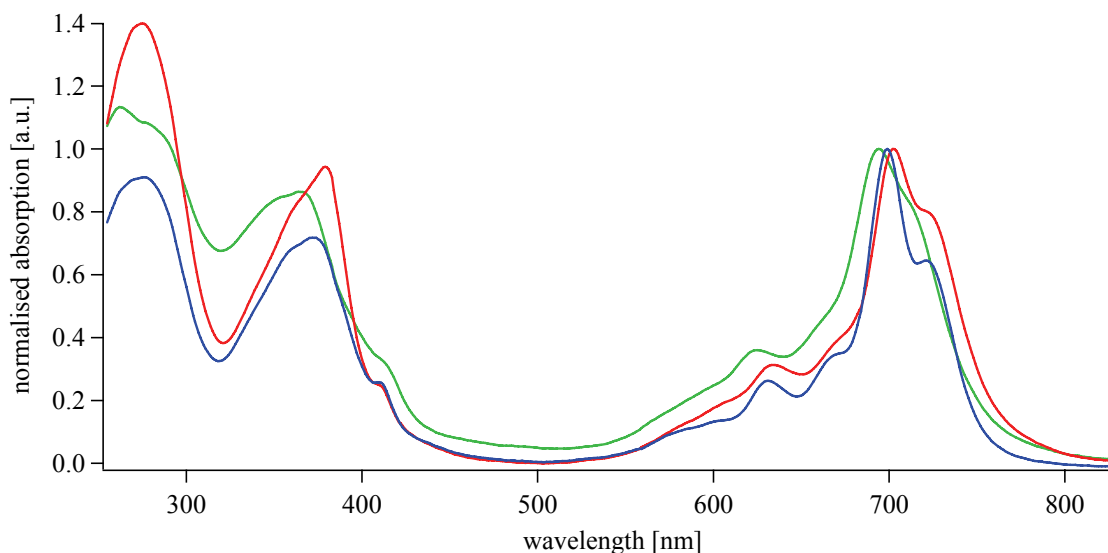
Figure 3.11. UV-vis spectra of MgPc **18** (red), CoPc **19** (green) and ZnPc **20** (blue) in THF. The Q band absorption maxima are normalised.

Dyads **21-23** show a Q band absorption and similar features between 250 and 400 nm as observed for the reference compounds (Fig. 3.12). Compared to the reference Pcs, the dyads

exhibit an additional shoulder around 450 nm which is assigned to the characteristic MLCT transition of the Ru(II) unit.
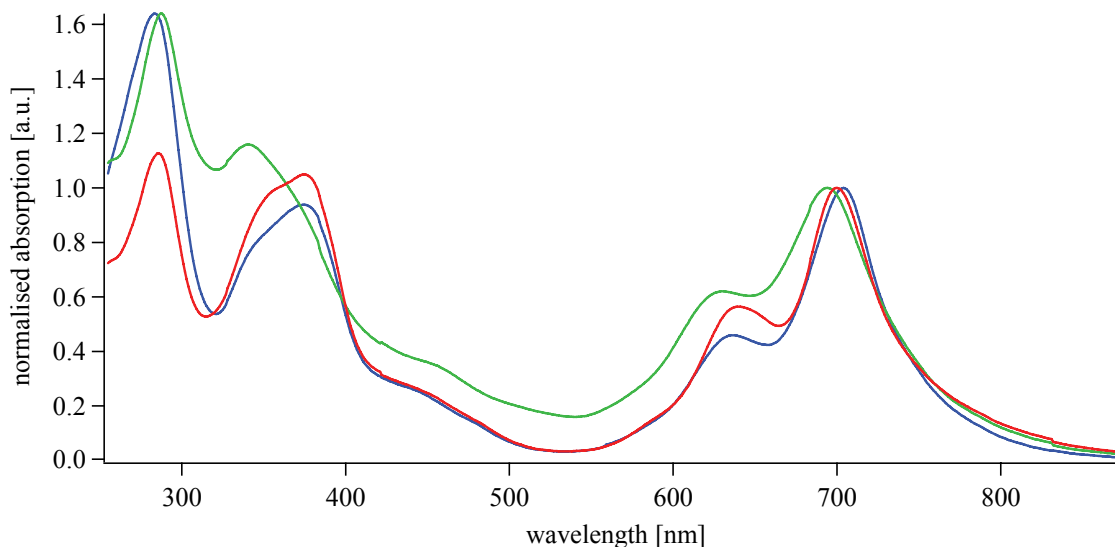
Figure 3.12. UV-vis spectra of ZnPc dyad **21** (blue), MgPc dyad **22** (red) and CoPc dyad **23** (green) in THF. The Q band absorption maxima are normalised.

Comparing the Q bands of compounds **18-23** with the Q band of symmetric ZnPc **27** (Fig 3.13), which does not exhibit aggregation, reveals that the former are much broader. Furthermore, compounds **18-23** exhibit lower Q band extinction coefficients than **27**. These observations are a clear indication for aggregate formation in compounds **18-23**.[179] An additional argument comes into play for dyads **21-23** since an eventual ground state communication between the two subunits may as well influence the nature of the Q band absorptions.[6] However, it is not possible to determine which of the aforementioned features has the bigger influence on the appearance of the Q bands of compounds **21-23**.
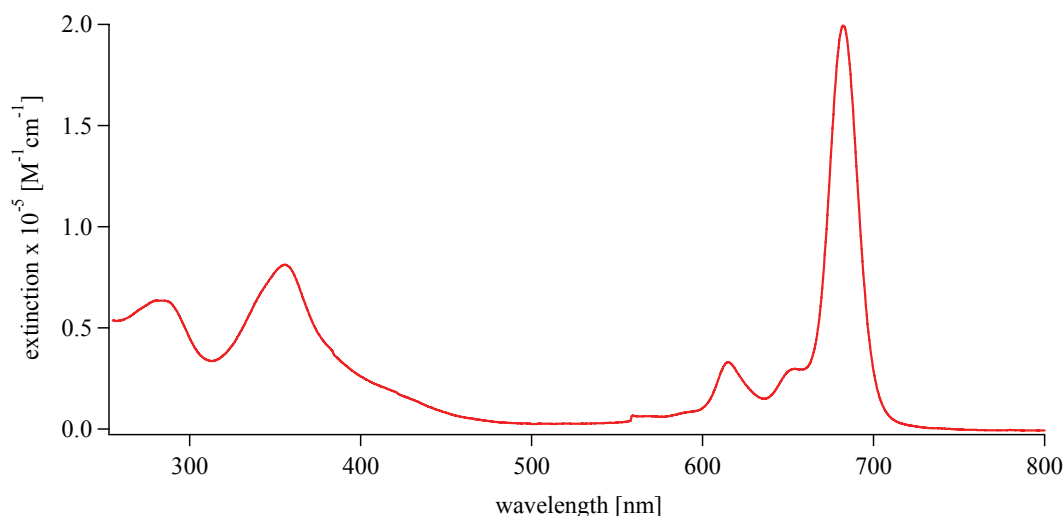
Figure 3.13. UV-vis spectrum of symmetric ZnPc **27** in CHCl$_3$.

3.4.2.2. Luminescence measurements

Upon photoexcitation at 380 nm, ZnPc dyad **21** exhibits dual-luminescence in the form of two overlapping signals with their maxima around 630 and 690 nm, respectively (Fig. 3.14). The former is assigned to the ^{3*}MLCT emission,[166] and the latter to the fluorescence of the ZnPc unit.[178] This indicates that both subunits are excited upon irradiation at 380 nm. Selective excitation of the MLCT transition at 480 nm mainly leads to ^{3*}MLCT state emission, together with a weak luminescence from the ^{1*}ZnPc state. The presence of the ZnPc emission is a clear indication for an energy transfer from the Ru(II) moiety to the ZnPc unit which was further investigated by transient absorption measurements (see sections 3.4.2.3. and 3.4.2.4.). Upon photoexcitation of the Q band at 630 nm, only the ZnPc luminescence is observed. The emission properties of MgPc dyad **22** are very similar to those of **21**. However, in both cases, the MLCT emission is strongly quenched [Φ(**21**) = 0.0015 and Φ(**22**) = 0.0055] compared to [Ru(bpy)$_3$](PF$_6$)$_2$ (Φ = 0.029). CoPc dyad **23** does not exhibit luminescence due to the paramagnetic nature of the Co(II) ion. In general, CoPcs are known to be nonluminescent.[178]
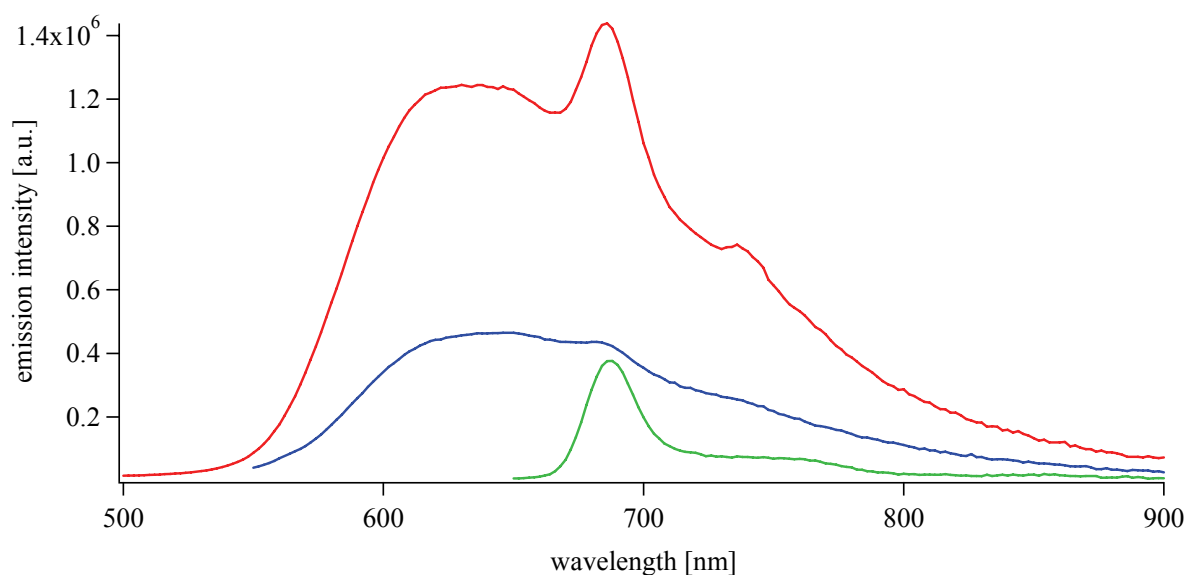
Figure 3.14. Luminescence spectra of ZnPc dyad **21** after excitation at 380 nm (red), 480 nm (blue) and 630 nm (green) in CH$_2$Cl$_2$ (c = 2 μM) at room temperature.

3.4.2.3. Femtosecond transient absorption measurements

To shed light onto the nature and dynamics of a possibly formed charge-separated radical ion pair state in dyads **21-23** upon photoexcitation, femtosecond transient absorption spectroscopy was employed.

Differential absorption changes of reference compound **20** reveal two minima around 630 and 700 nm which nicely correspond to the S_0-S_1 absorptions of the ZnPc. Additionally, two maxima around 500 and 1000 nm are observed for both excitation energies at 387 and 680 nm, respectively (Fig. 3.15 and 3.16). The two maxima belong to the S_1-S_n absorption of the first excited singlet state of the ZnPc. Differential absorption spectra recorded after approximately one nanosecond reveal a shift of the maximum around 500 to 530 nm. This new transient has a significantly longer lifetime than the excited singlet-singlet absorption. It was identified to belong to excited ^{3*}ZnPc state by nanosecond transient absorption measurements as shown in section 3.4.2.4. The singlet lifetimes were fitted monoexponentially and determined to be 1195 ps for the excitation at 387 nm (Fig. 3.17) and 897 ps for the Q band excitation (Fig. 3.18).

Figure 3.15. Differential absorption spectra of reference ZnPc **20** after excitation at 387 nm.

Figure 3.16. Differential absorption spectra of reference ZnPc **20** after excitation at 680 nm.

Figure 3.17. Time profiles at 530 (red) and 950 nm (black) of **20** after excitation at 387 nm.

Figure 3.18. Time profiles at 530 (red) and 950 nm (black) of **20** after excitation at 680 nm.

In the case of dyad **21**, three femtosecond laser photolysis experiments were performed which all revealed bleaching of the Q band absorption as observed for reference compound **20**. Photoexcitation at 387 nm mainly leads to the S_0-S_2 transition of the ZnPc unit. As shown in luminescence measurements, the Ru(II) unit is excited as well. Two maxima were found around 950 and 530 nm (Fig. 3.19). Compared to **20**, these two maxima are shifted and the decay to the long-lived ^{3*}ZnPc state is much more accelerated. Then, the MLCT transition of the Ru(II) entity of **21** was selectively excited at 480 nm (Fig. 3.20). The same features, but with lower intensities as after excitation at 387 nm were observed. However, the maximum at 530 nm, which is partly buried under the laser beam, is decaying much slower than the one after excitation at 387 nm (Fig 3.19). Therefore, this transient is assigned to the excited triplet ZnPc state. Finally, photoexcitation at 680 nm was performed to achieve the S_0-S_1 transition of the ZnPc moiety. In general, the transient absorption spectra after excitation at 680 nm (Fig. 3.21) show the same features as those after excitation at 387 nm. The only, but important difference between both series of spectra is that upon photoexcitation at 680 nm, the intensity of the remaining signal belonging to the first excited triplet ZnPc state is much lower than in the case of the excitation at 387 nm. Fitting the time profiles monoexponentially at 530 and 950 nm for the excitation at 387 (Fig. 3.22) and 680 nm (Fig. 3.23), gives the first excited singlet state lifetimes of 107 ps and 67 ps, respectively.

Figure 3.19. Differential absorption spectra of dyad **21** after excitation at 387 nm.

Figure 3.20. Differential absorption spectra of dyad **21** after excitation at 480 nm.

Figure 3.21. Differential absorption spectra of dyad **21** after excitation at 680 nm. The Q band bleaching is partly buried under the excitation laser beam.
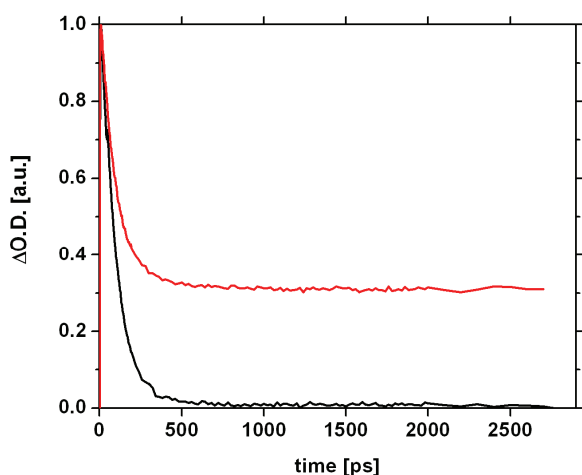
Figure 3.22. Time profiles at 530 (red) and 950 nm (black) of **21** after excitation at 387 nm.
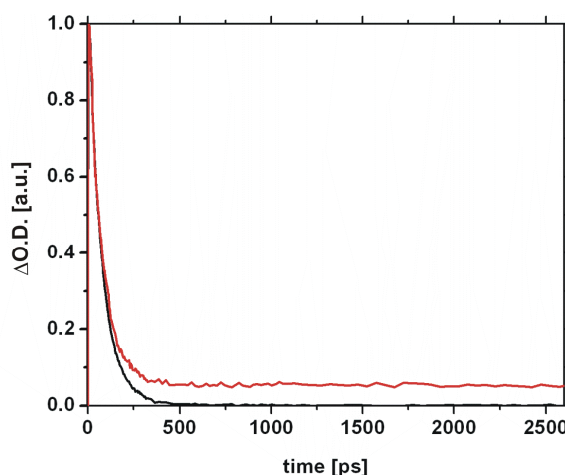
Figure 3.23. Time profiles at 530 (red) and 950 nm (black) of **21** after excitation at 680 nm.

Upon excitation at 387 and 680 nm, the magnesium phthalocyanine **18** shows analogous features as observed for ZnPc **20**. Again, bleaching of the Q band absorption and two maxima around 500 and 1000 nm were observed (Fig. 3.24 and 3.25). The absorption around 500 nm is repeatedly shifted to lower energy with time and is assigned to the T_1-T_n transition of the MgPc. The ^{1*}MgPc state lifetimes are 727 (excitation at 387 nm, Fig. 3.26) and 639 ps (excitation at 680 nm, Fig 3.27).
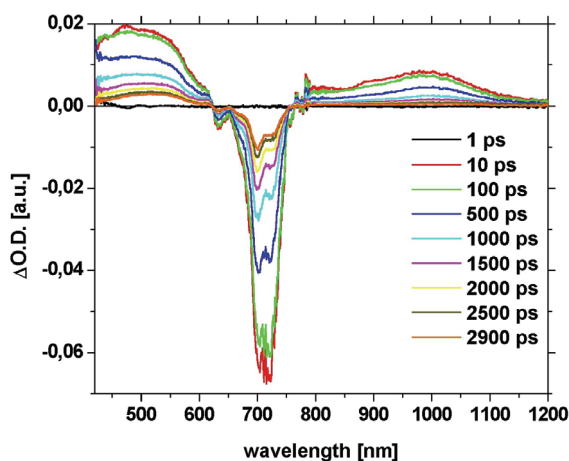
Figure 3.24. Differential absorption spectra of reference compound **18** after excitation at 387 nm.
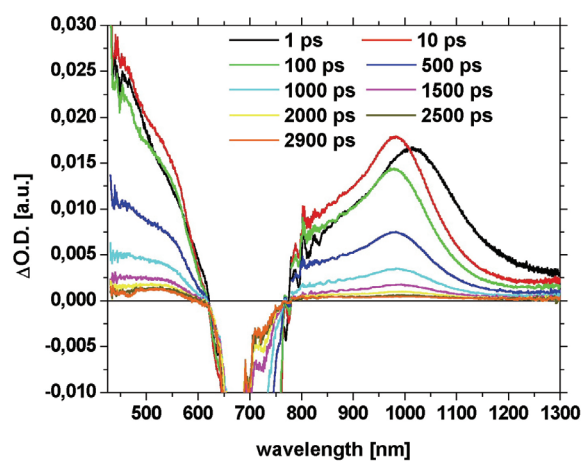
Figure 3.25. Differential absorption spectra of reference compound **18** after excitation at 680 nm.
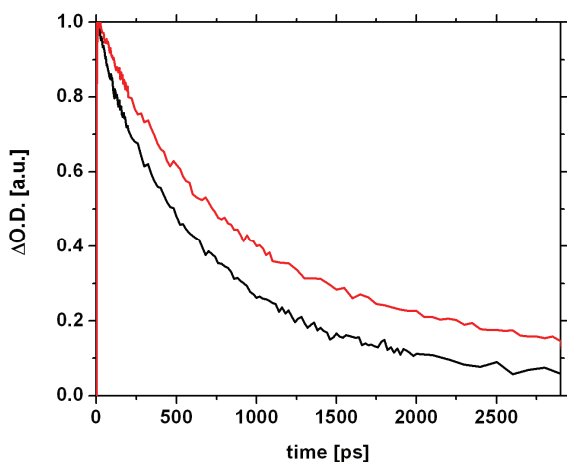
Figure 3.26. Time profiles at 530 (red) and 950 nm (black) of **18** after excitation at 387 nm.
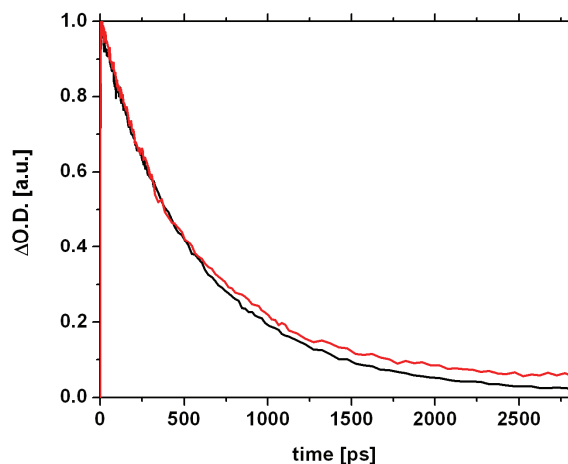
Figure 3.27. Time profiles at 530 (red) and 950 nm (black) of **18** after excitation at 680 nm.

MgPc dyad **22** shows a very similar behavior as ZnPc dyad **21**. The two minima around 630 and 700 nm, which correspond to the ground state Q band absorption of the MgPc moiety, were repeatedly observed upon excitation at three different wavelengths. After excitation at 387 nm (Fig. 3.28), the two maxima around 530 and 950 nm, which belong to the first excited singlet state, decay to the ^{3*}MgPc state as confirmed later in nanosecond transient absorption measurements. Selective excitation of the MLCT transition of the Ru(II) moiety leads to the transient absorption of the excited triplet MgPc state (Fig. 3.29). Upon excitation of the Q band of **22** (Fig. 3.30), analogous photophysical events as found for dyad **21** were observed. Fitting the time profiles monoexponentially at 530 and 950 nm for the excitation at 387 (Fig. 3.31) and 680 nm (Fig. 3.32), yielded the ^{1*}MgPc state lifetimes of 58 and 53 ps, respectively.
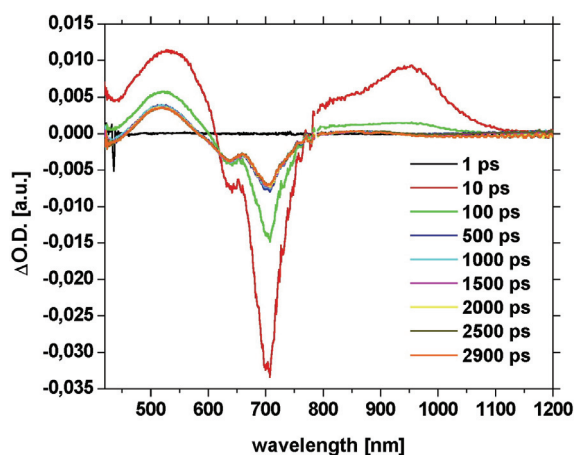
Figure 3.28. Differential absorption spectra of dyad **22** after excitation at 387 nm.
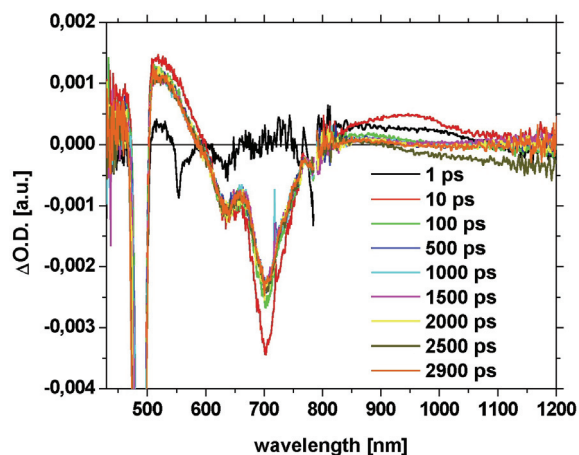
Figure 3.29. Differential absorption spectra of dyad **22** after excitation at 485 nm.
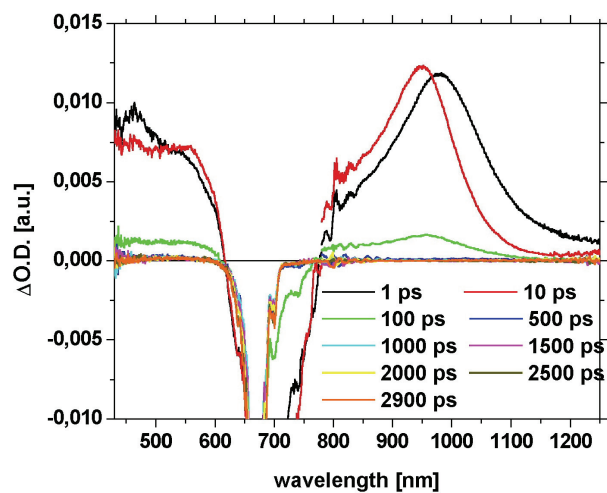
Figure 3.30. Differential absorption spectra of dyad **22** after excitation at 680 nm.
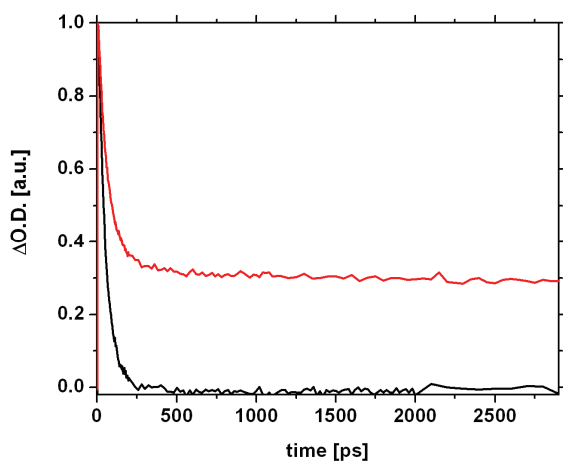
Figure 3.31. Time profiles at 530 (red) and 950 nm (black) of **22** after excitation at 387 nm.
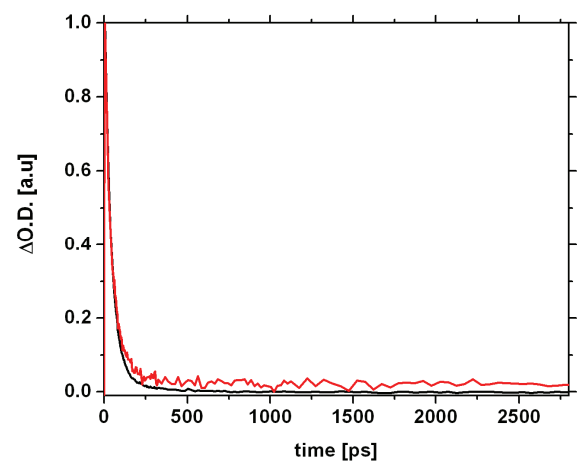
Figure 3.32. Time profiles at 530 (red) and 950 nm (black) of **22** after excitation at 680 nm.

The CoPc **19** shows different photophysical behavior from MPcs **18** and **20**. After photoexcitation (387 or 680 nm), the ^{1*}CoPc state lifetime is much shorter than those of the closed-shell analogues (Fig. 3.33 and 3.34). The lifetimes of the first excited singlet state are 1.2 (excitation at 387 nm, Fig. 3.35) and 1.3 ps (excitation at 680 nm, Fig. 3.36). Similar lifetimes were observed for other CoPc systems.[180,181] Therefore, no evidence for the formation of the ^{3*}CoPc state was found.
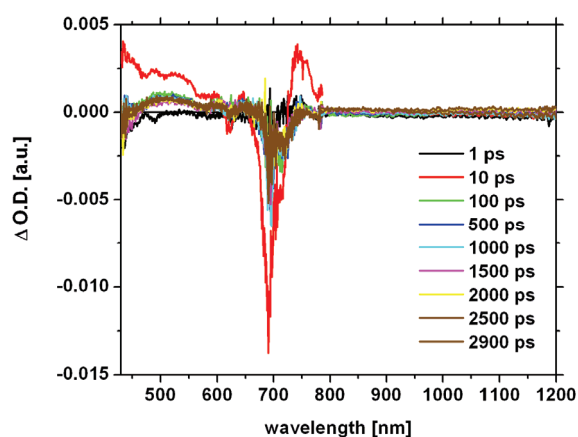
Figure 3.33. Differential absorption spectra of reference compound **19** after excitation at 387 nm.
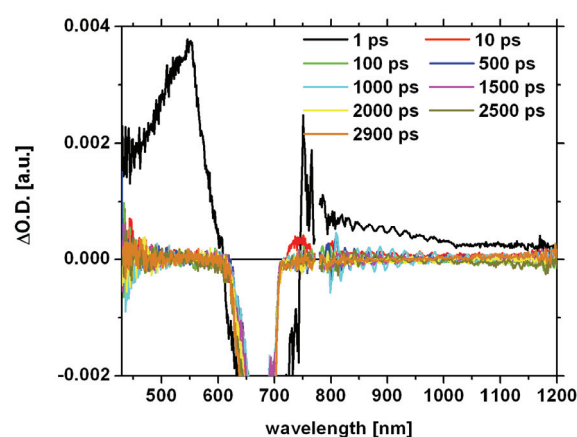
Figure 3.34. Differential absorption spectra of reference compound **19** after excitation at 680 nm.
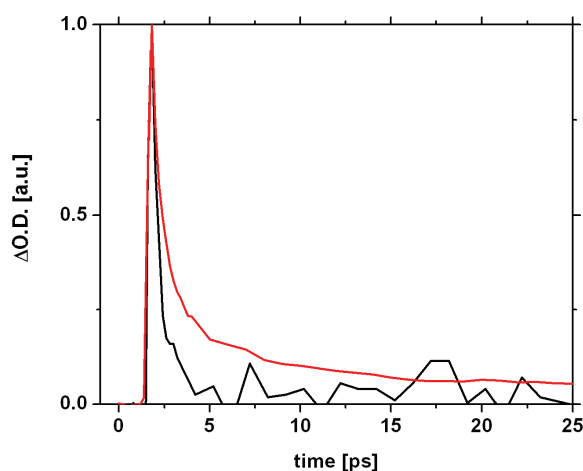
Figure 3.35. Time profiles at 530 (red) and 950 nm (black) of **19** after excitation at 387 nm.
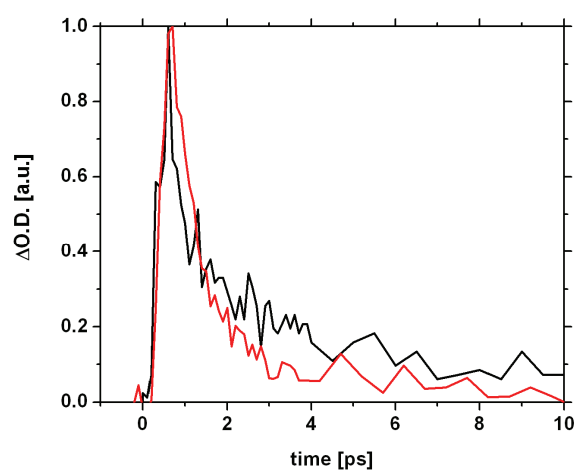
Figure 3.36. Time profiles at 530 (red) and 950 nm (black) of **19** after excitation at 680 nm.

In general, dyad **23** exhibits a very similar behavior as reference compound **19**. The decay of the first excited singlet state is extremely fast and there is no clear evidence for a formation of an excited triplet CoPc state (Fig. 3.37-3.39). The decay of the first excited singlet CoPc state was fitted monoexponentially and values of 1.2 ps (excitation at 387 nm, Fig. 3.40) and 1.1 ps (excitation at 680 nm, Fig. 3.41) were obtained.
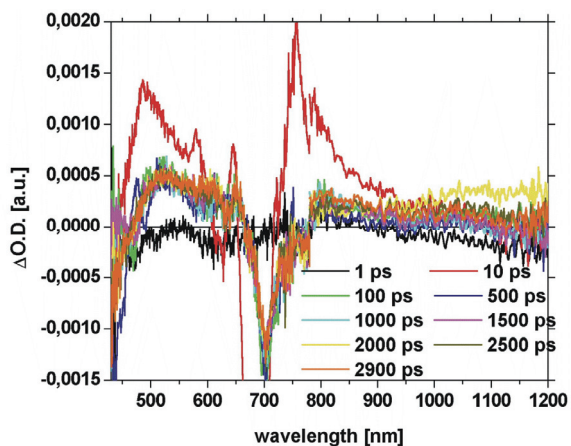
Figure 3.37. Differential absorption spectra of dyad **23** after excitation at 387 nm.
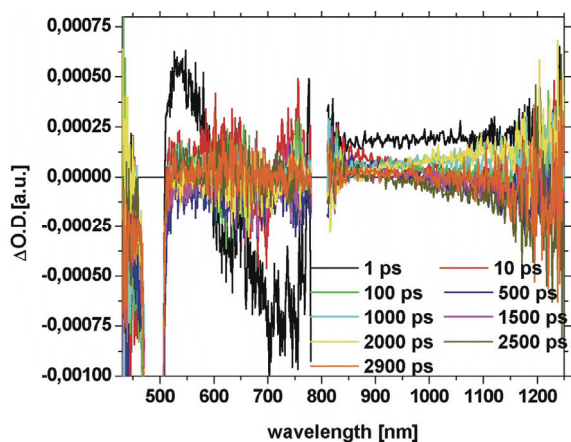
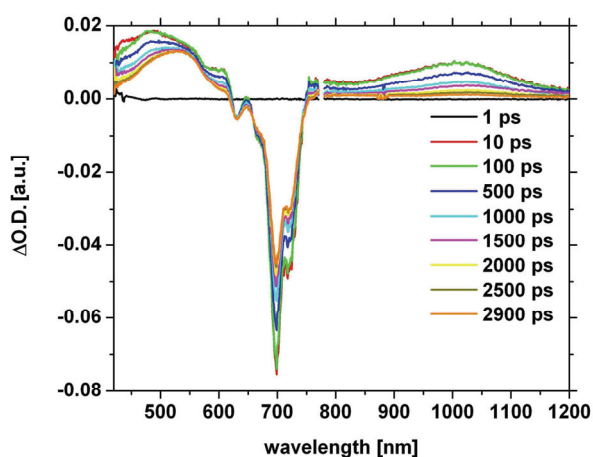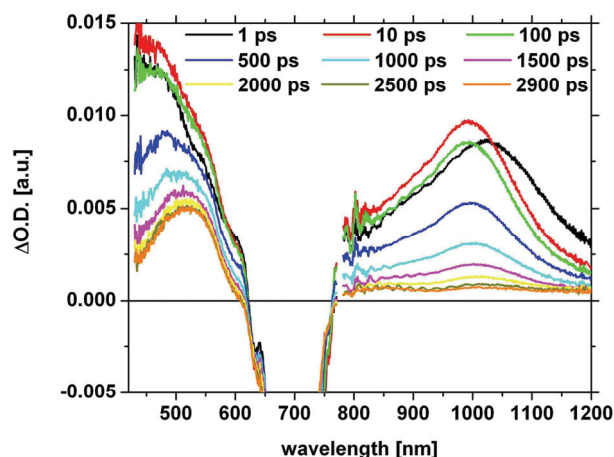**Figure 3.38.** Differential absorption spectra of dyad **23** after excitation at 485 nm.
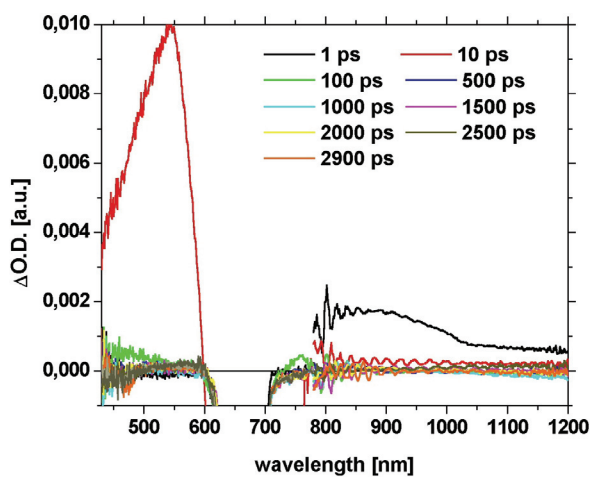
Figure 3.39. Differential absorption spectra of dyad **23** after excitation at 680 nm.
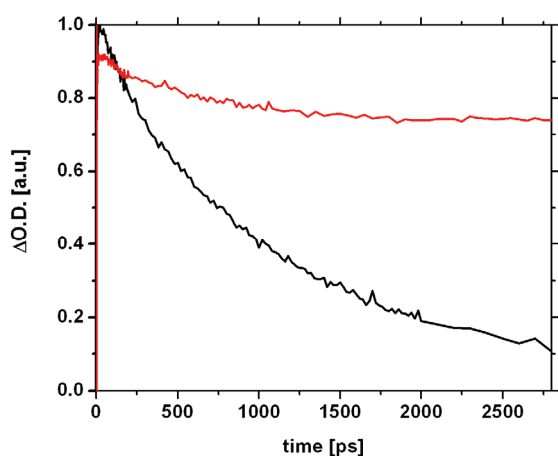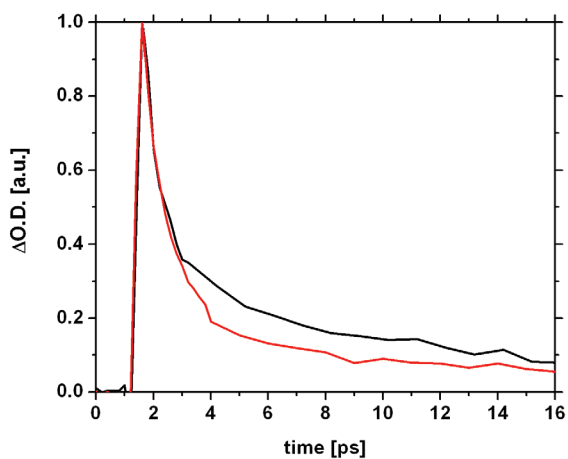

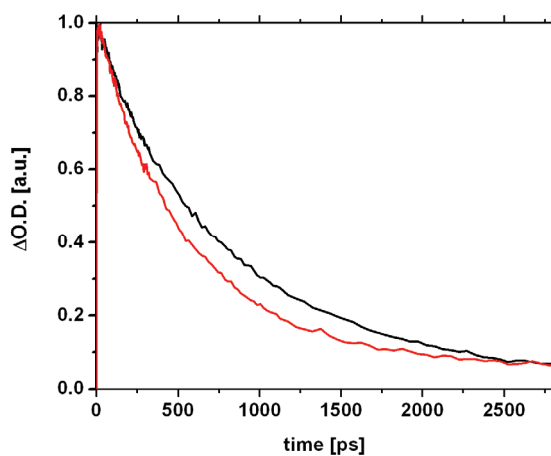**Figure 3.40.** Time profiles at 530 (red) and 950 nm (black) of **23** after excitation at 387 nm.
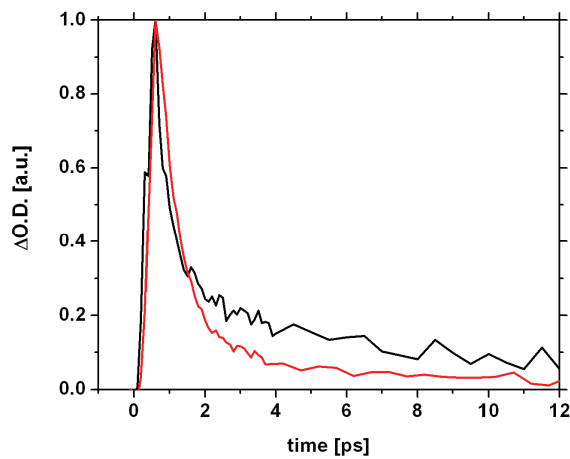
Figure 3.41. Time profiles at 530 (red) and 950 nm (black) of **23** after excitation at 680 nm.

3.4.2.4. Nanosecond transient absorption measurements

Finally, nanosecond transient absorption measurements were employed to detect and characterise long-lived transients like excited triplet and/or radical ion pair states. Tetra-*tert*-butylphthalocyaninato zinc (**ZnPc**) was tested as the reference compound to establish the excited triplet state features of ZnPc in THF (Fig. 3.42). The transient absorption around 500 nm is assigned to the excited triplet ZnPc state since its nature was confirmed by quenching with molecular oxygen (Fig. 3.43).[182]
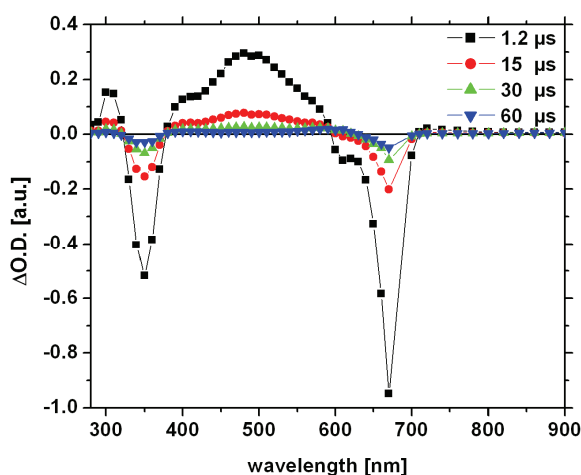
Figure 3.42. Differential absorption spectra of **ZnPc** in THF after excitation at 355 nm.
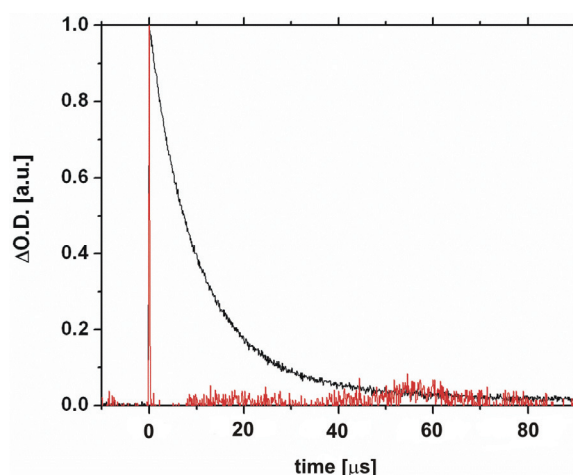
Figure 3.43. Time profiles at 500 nm of **ZnPc** in THF saturated with nitrogen (black) or oxygen (red) after excitation at 355 nm.

Compounds **21** and **22** were photolysed under the same conditions as **ZnPc**, and very similar differential absorption spectra were obtained as shown in Fig. 3.44 and 3.45, respectively. They show two minima around 350 and 700 nm which are assigned to the B and Q band ground state transition. The maximum around 530 nm is attributed to the T_1-T_n absorption of the MPc units. Again, this excited triplet state was confirmed by quenching it with molecular oxygen. The lifetimes of the excited triplet MPc states of **21** and **22** are 79 and 86 μs, respectively. They are in the same order of magnitude as those observed for other MPcs.[178] No nanosecond transient absorption signals were obtained due to the very short lifetime of the excited singlet CoPc state of **23**.
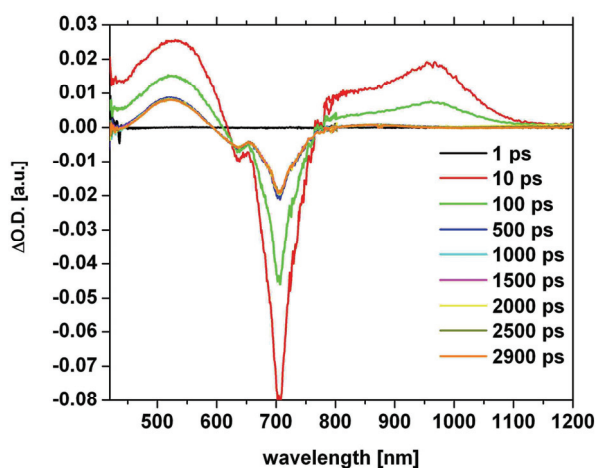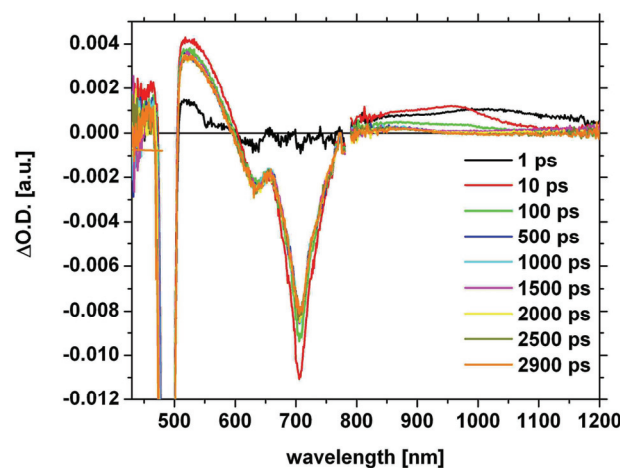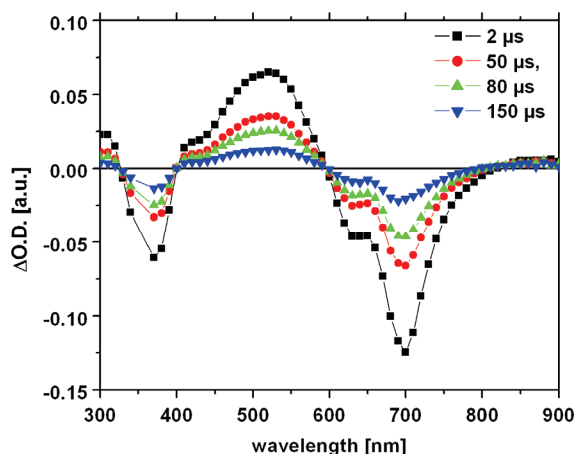
Figure 3.44. Differential absorption spectra of **21** in THF after excitation at 355 nm.

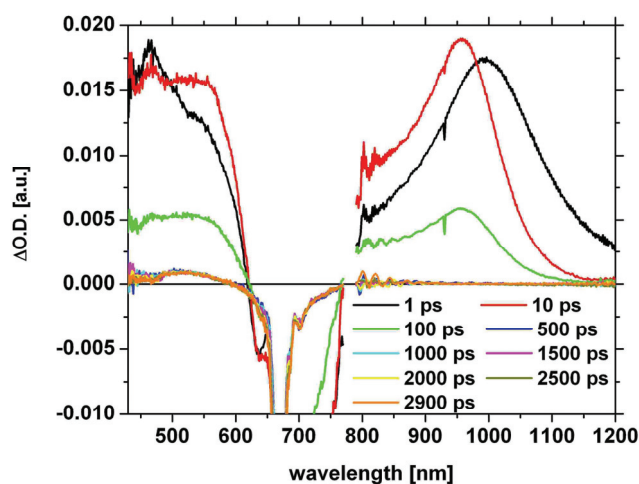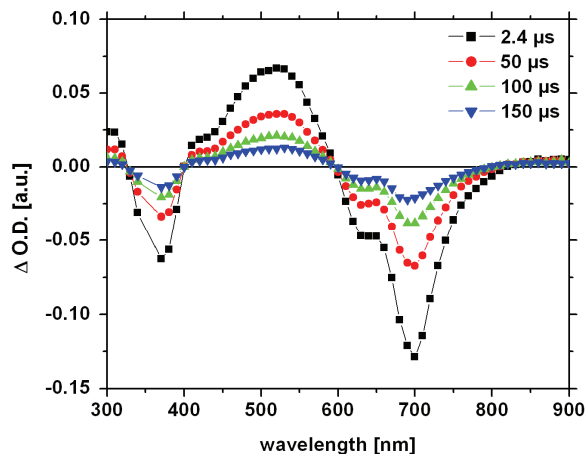**Figure 3.45.** Differential absorption spectra of **22** THF after excitation at 355 nm.

In conclusion, the current study demonstrates that an intramolecular energy transfer from the photoexcited Ru(II) moiety to the electron-accepting MPc unit governs the photoreactivity of dyads **21-23**. The main evidence in support of the energy transfer hypothesis came from the femtosecond transient absorption measurements. Selective excitation of the MLCT transition at 480 nm leads to the formation of the first excited triplet state of the MPc moieties in dyads **21** and **22**, which show very similar photophysical behavior. The nature of the excited triplet MPc state was confirmed by quenching with molecular oxygen in nanosecond transient absorption measurements. In addition, the bleaching of the Q band suggests consumption of MPc as a result of converting the singlet MPc ground state to the corresponding ^{1*}MPc state.[6] Excitation at 387 nm of either sample, results in the rapid formation of the second excited singlet state followed by a very fast internal conversion into the first excited singlet state. Finally, the intersystem crossing into the first excited triplet state was observed. Photoexcitation of the Q band leads to the corresponding ^{1*}MPc states which decay through intersystem crossing into the ^{3*}MPc states with the triplet quantum yield being qualitatively lower than that observed after excitation at 387 nm. Irradiation at 387 nm leads to higher quantum yields of the excited triplet MPc state since both subunits are excited as shown in luminescence measurements and hence, they both contribute to its formation due to an energy transfer from the Ru(II) to the MPc unit. At the same time, it should be mentioned that the lifetimes of the first excited singlet states of dyads **21** and **22** are quenched and the formation of the first excited triplet states is accelerated compared to the corresponding reference compound. Thus, intersystem crossing events are more probable in compounds **21** and **22** due to the heavy-atom effect exhibited by the coupled Ru(II) core (spin-orbit coupling). In general, dyad **23** shows the same photophysical features as **21** and **22**. The excited states were

quenched by orders of magnitude and no clear evidence for the formation of a first excited triplet state was found due to the paramagnetic nature of the Co(II) in **23**. The lifetime of the first excited singlet state is quite short, around 1.1 ps. Hence, no intersystem crossing into the first excited triplet state can take place and for that reason, it was not possible to detect any differences in the photophysical behavior compared to **21** and **22**.

It is to emphasise that no spectral evidence for an electron transfer was found (e.g. the characteristic sharp transient absorption band of the ZnPc[•+] at 840 nm).[183] Therefore, dyads **21-23** show the same photophysical processes upon photoexcitation as observed for multicomponent systems **2a-2c** (see Chapter 1).[6]

3.4.3. Synthesis of a ZnPc with peripherally coordinated bis(TTF-dppz)ruthenium(II)

Recently, compounds **C3a-C3c** were synthesised by Goze in our laboratories. Photophysical studies revealed that these compounds exhibit an additional charge transfer absorption from the TTF to the dppz unit around 610 nm besides the typical π-π* and the MLCT transition known for [Ru(bpy)$_3$]$^{2+}$ derivatives. Upon photoexcitation at 450 nm, compound **C3a** exhibits a strong MLCT triplet state emission of the Ru(II) entity around 600 nm with an intensity of approximately 50% of that of [Ru(bpy)$_3$](PF$_6$)$_2$. However, this emission is strongly quenched in compounds **C3b** and **C3c** which suggests an additional quenching mechanism when more than one TTF-dppz ligand is coordinated to Ru(II). Interestingly, all compounds show a weak TTF-dppz charge transfer state emission around 900 nm, which is red shifted and lower in intensity compared to the uncomplexed TTF-dppz ligand.[184] It is not yet clear why the MLCT emission of compounds **C3b** and **C3c** is strongly quenched and hence, a more detailed study of these systems is currently in progress. For example, cyclic voltammetry measurements could reveal whether a potential electron transfer is thermodynamically favored or not. If this process is considered to be possible, transient absorption experiments could detect the radical ion pairs.

C3a (X = 1, Y = 2)
C3b (X = 2, Y = 1)
C3c (X = 3, Y = 0)
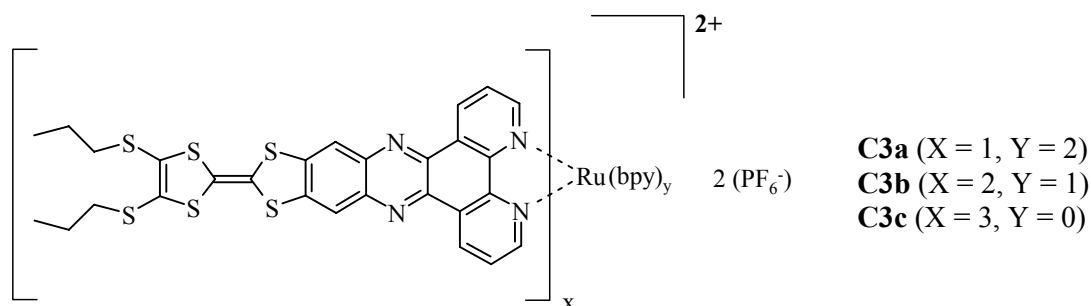
A similar multicomponent system in the form of **26**, in which the ZnPc unit can act as an additional light harvesting or redox-active entity, was prepared (Scheme 3.10) due to the exciting photophysical properties exhibited by compounds **C3a-C3c**.

The synthesis of **25** requires *cis*-[Ru(1,10-phenanthroline-5,6-dione)$_2$Cl$_2$] (**24**) as a starting material which is described in the literature.[185] The authors claim that they synthesised **24** according to the same procedure as described for the preparation of *cis*-[Ru(bpy)$_2$Cl$_2$] by Meyer and coworkers implying the reaction of RuCl$_3$ with the appropriate diimine ligand in the presence of LiCl in refluxing DMF at 160°C.[186] When RuCl$_3$ was reacted with 1,10-phenanthroline-5,6-dione under the same reaction conditions, the ^{1}H NMR spectrum showed a lot of impurities besides the desired product **24** after purification. However, by decreasing the reaction temperature to 140°C, very pure **24** was obtained according to ^{1}H NMR spectroscopy.
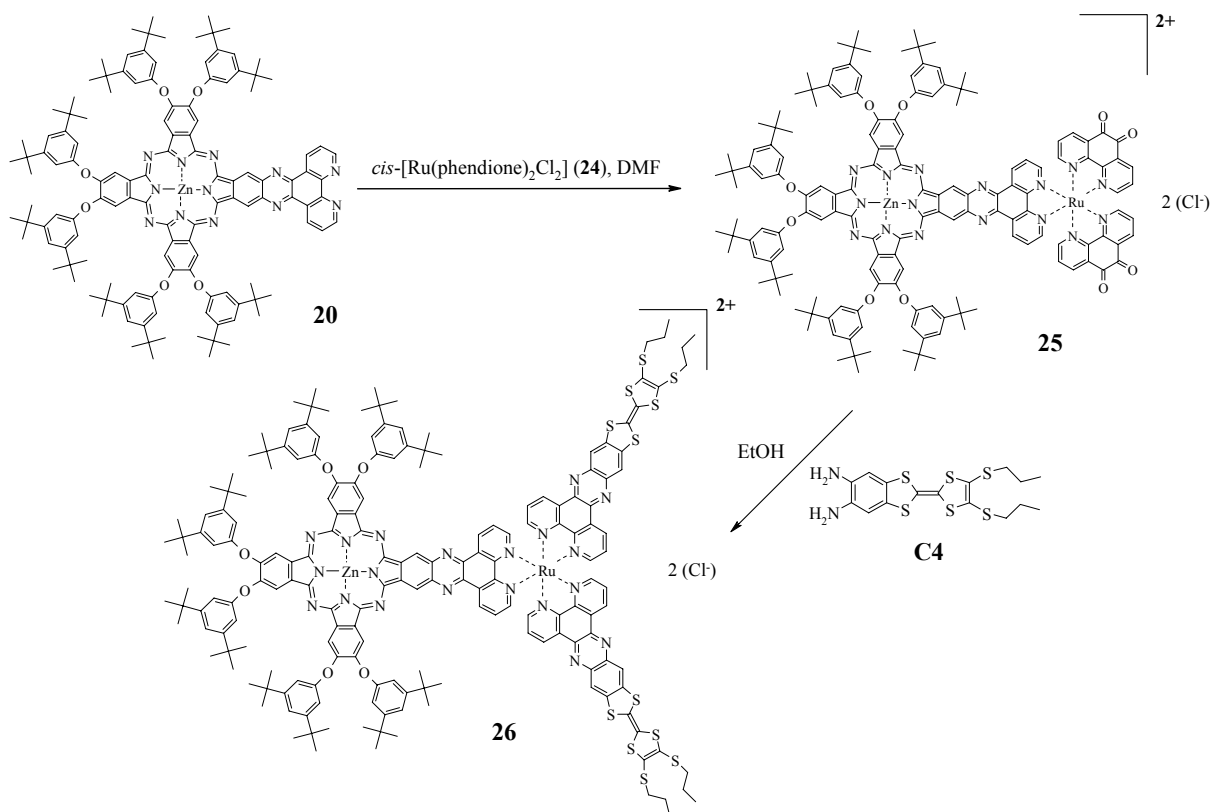
Scheme 3.10. Synthetic route to multicomponent Pc-based system **26**.

Compound **25** was obtained by the reaction of ZnPc **20** with **24** in DMF at 140°C (Scheme 3.10). In contrast to **21**, compound **25** cannot be purified by adsorption chromatography on alumina or silica due to the presence of four polar keto groups. Finally, size exclusion chromatography (SEC) made it possible to separate **25** from unreacted **20**. After redissolving **25** in a minimum amount of toluene followed by the precipitation with hexane gave pure **25** in

70% yield. Higher reaction temperatures than 140°C led to impurities that were detected by ESI mass spectrometry, while at lower temperatures (130°C), lower yields were obtained. **25** was then reacted with **C4** via a Schiff's base condensation in refluxing ethanol overnight. Column chromatography followed by the precipitation by adding hexane to a CH_2Cl_2 solution gave compound **26** in 32% yield. Since Schiff's base condensation reactions are known to be almost quantitative, this yield is quite low. Several modifications of the reaction conditions such as the addition of acetic acid to the ethanol solution or a reaction in toluene using a Dean-Stark apparatus to remove the formed water from the equilibrium, did not help to improve the yield. Additionally, the reaction of **25** in the form of a PF_6-salt (**25** was dissolved in EtOH and aqueous NH_4PF_6 was added followed by the isolation of the precipitate) with **C4** even led to a lower yield because of the poorer solubility of **25** in the form of the PF_6-salt than **25** in EtOH.

3.4.4. Photophysical properties of compound 26

The UV-vis absorption spectrum of compound **26** exhibits a Q band with a maximum around 700 nm, which is comparable to reference compound **21** (Fig. 3.46). However, **26** shows an additional feature in the form of a shoulder around 600 nm which is assigned to a charge transfer absorption from the TTF to the dppz unit as observed in compound **C3b**. Compounds **21** and **26** both show the MLCT transition around 450 nm in the form of a shoulder. Again, the Q band is quite broad which is an indication for aggregate formation and probable ground state communication between the ZnPc and the Ru(II)-(TTF-dppz)$_2$ unit.
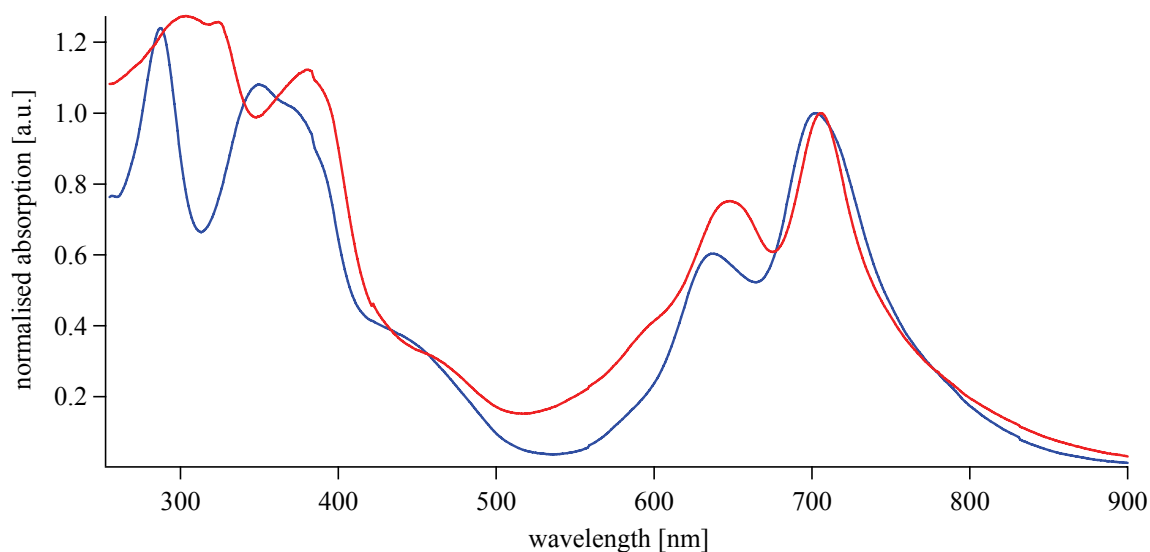
Figure 3.46. UV-vis spectra of compounds **21** (blue) and **26** (red) in CH_2Cl_2. The Q band absorption maxima are normalised.

Compound **26** is a very complex system since it bears three different photoactive units. Luminescence measurements revealed that all three possible emission features, namely the Pc, the MLCT and the TTF-dppz emissions, are totally quenched. The disappearance of the phthalocyanine and the weak TTF-dppz luminescence at room temperature might be explained by the size of the molecule and the resulting vibrational degrees of freedom and/or the aforementioned heavy-atom effect. The MLCT emission could be quenched due to an electron transfer process as supposed in the case of compound **C3b**. Cyclic voltammetry measurements - which could reveal whether an electron transfer is thermodynamically favored - of reference compound **21** and multicomponent Pc-based system **26** show very complicated and overlapping redox potentials (Fig. 3.47). They could not yet be assigned to the different units of these compounds. Further experiments are necessary in order to be able to understand the complicated electrochemistry of multicomponent systems **21** and **26**.
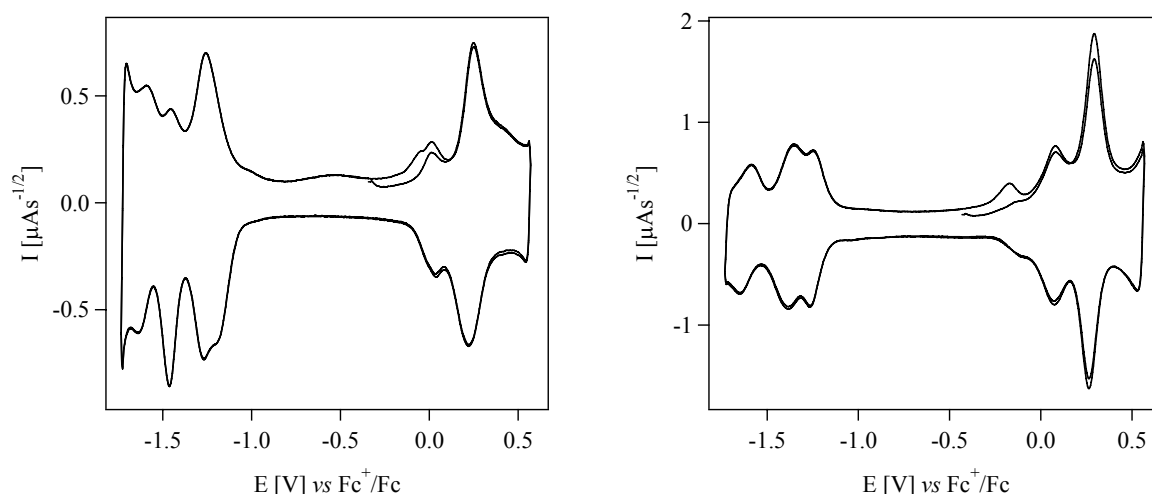
Figure 3.47. Deconvoluted cyclic voltammograms of **21** (left, c = $2.2 \ast 10^{-4}$ M) and **26** (right, c = $1.4 \ast 10^{-4}$ M). The scan rates for both measurements were 200 mV/s.

3.5. Conclusions and Outlook

The present work describes the synthetic access to asymmetric, octa-substituted phthalocyanines with peripheral metal binding sites. At the beginning, the symmetric phthalocyanine **3** with eight flexible pyridyl groups was obtained by a cyclotetramerisation reaction of phthalonitrile **1**. However, due to its insufficient solubility in organic solvents, it was impossible to investigate its coordination ability to different metal ions at the periphery. Furthermore, the direct cyclotetramerisation of metal diimine complexes under a variety of reaction conditions did not lead to the isolation of the corresponding peripherally metallated Pc products. Consequently, an alternative strategy involving the synthesis of asymmetric Pcs

has been adopted. As a result, Pcs **10-15** containing combinations of 2,3-di(2-pyridyl)pyrazino and *p*-pentylphenoxy or *p*-*tert*-butylphenoxy substituents were synthesised by means of statistical condensation reactions between two different types of phthalonitriles, and most importantly, they were successfully isolated by chromatographic techniques. The aforementioned concept was also applied to prepare asymmetric Pc **17** bearing a rigid dpq unit directly fused to the Pc core. The main advantage over systems **10-15** is the fact that peripheral metal complexation can be controlled in a better way due to the rigid nature of the phenanthroline unit of compound **17**. Synthetic procedures for the selective metallation of the macrocyclic cavity and the periphery of **17** were developed. As a result, MPcs **18-20** were prepared by selective coordination of Mg(II), Co(II) or Zn(II) into the macrocyclic cavity of **17**. The MPc-Ru(II) dyads **21-23** were then synthesised by reacting the corresponding MPcs with [Ru(bpy)$_2$Cl$_2$]. Transient absorption experiments revealed that these dyads exhibit very efficient intramolecular energy transfer from the Ru(II) unit to the MPc moiety upon photoexcitation as observed for dyads **2a-2c** (see Chapter 1). Finally, Pc-based multicomponent system **26**, which contains three photophysically active entities, was synthesised. However, all three potential emission features were found to be totally quenched. In our ongoing study, a detailed investigation will be carried out in order to understand these complex photophysical deactivation processes.

As shown in Chapter 1, phthalocyanine-based multicomponent systems show very interesting physical properties. Phthalocyanine **17** bearing a peripheral diimine metal-binding site is a very useful precursor for such systems. During this work, several Ru(II) complexes of **17** were successfully synthesised. However, the introduction of other metal ions at the periphery, such as Pt(II) and Fe(II), did not lead to a successful characterisation of a corresponding dyad system.

During this work, another strategy to build multicomponent Pc-based systems was tentatively investigated. The cyclotetramerisation of phthalonitriles **C1** and **7** is a straightforward synthetic route to **Pc2**. Various conditions have been tried during the course of this work, but **Pc2** was not prepared successfully. Stuzhin and coworkers encountered similar problems when they intended to get octaaminoporphyrazine via a cyclotetramerisation reaction of the similar diaminomaleonitrile.[187] Phthalonitrile **C1** is prepared by the reduction of 5-amino-4-nitrophthalonitrile (**C5**) using SnCl$_2$ in concentrated hydrochloric acid.[165] The reaction of **C5** with **7** led to the formation of **Pc3** (Scheme 3.11) and symmetric Pc **16** as confirmed by MALDI mass spectrometry. The UV-vis spectrum of the crude product showed an additional

Pc2
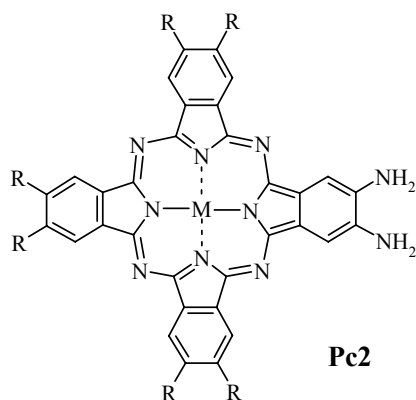
shoulder in the Q band of **16**, confirming the formation of another Pc compound. The isolation of **Pc3** from the crude product by column chromatography was not performed due to a lack of time. Chromatographic purification of **Pc3** followed by the conversion of the nitro to an amino group under reducing conditions is promising synthetic route to asymmetric phthalocyanine **Pc2**. This compound is considered to be a very versatile key precursor to form Pc-based multicomponent systems (Scheme 3.12) since a wide range of α-diketones is available.
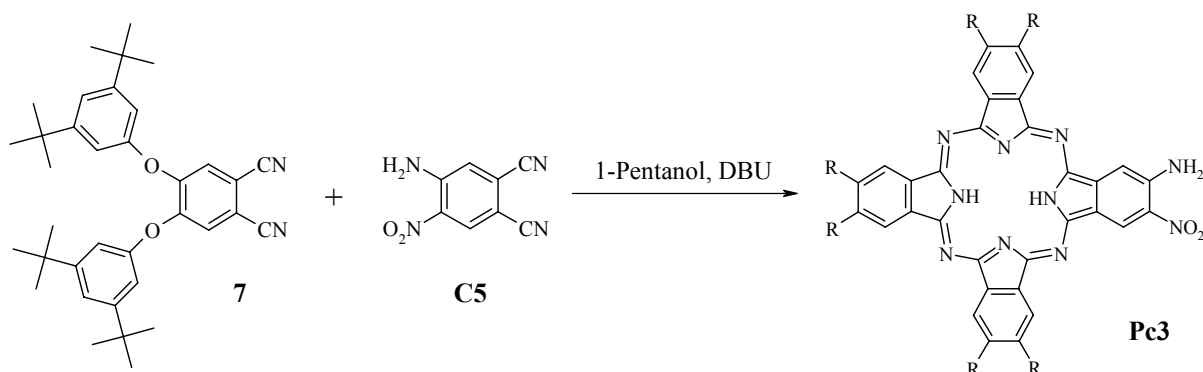
Scheme 3.11. Preparation of asymmetric amino-nitrophthalocyanine **Pc6**.

The synthesis of an asymmetric Pc with two peripheral amino groups (**Pc2**) followed by a Schiff's base condensation of an appropriately functionalised α-diketone could generate multicomponent Pc-based systems with different physical properties. Scheme 3.12 shows possible synthetic routes to three different Pc-based dyad systems. There are several examples of mono-, bis- and tris(1,10-phenanthroline-5,6-dione) metal complexes, such as Co(II), Fe(II), Os(II), Pt(II) and Ru(II), reported in the literature.[185,188] The reaction of the latter compounds with **Pc2** is expected to produce **Pc4**. This synthetic strategy is considered a promising approach to obtain phthalocyanines with peripherally coordinated metal ions other than Ru(II). The reaction of **Pc2** with an α-diketone-functionalised fullerene (**C6**), prepared *in situ*, is expected to give dyad **Pc5** (Scheme 3.12). The *in situ* preparation of **C6** and its

participation in Schiff's base condensation reactions with α-diamine derivatives are described in the literature.[189] Dyad **Pc5** is of prime interest to study intramolecular electron transfer processes as described in Chapter 1.
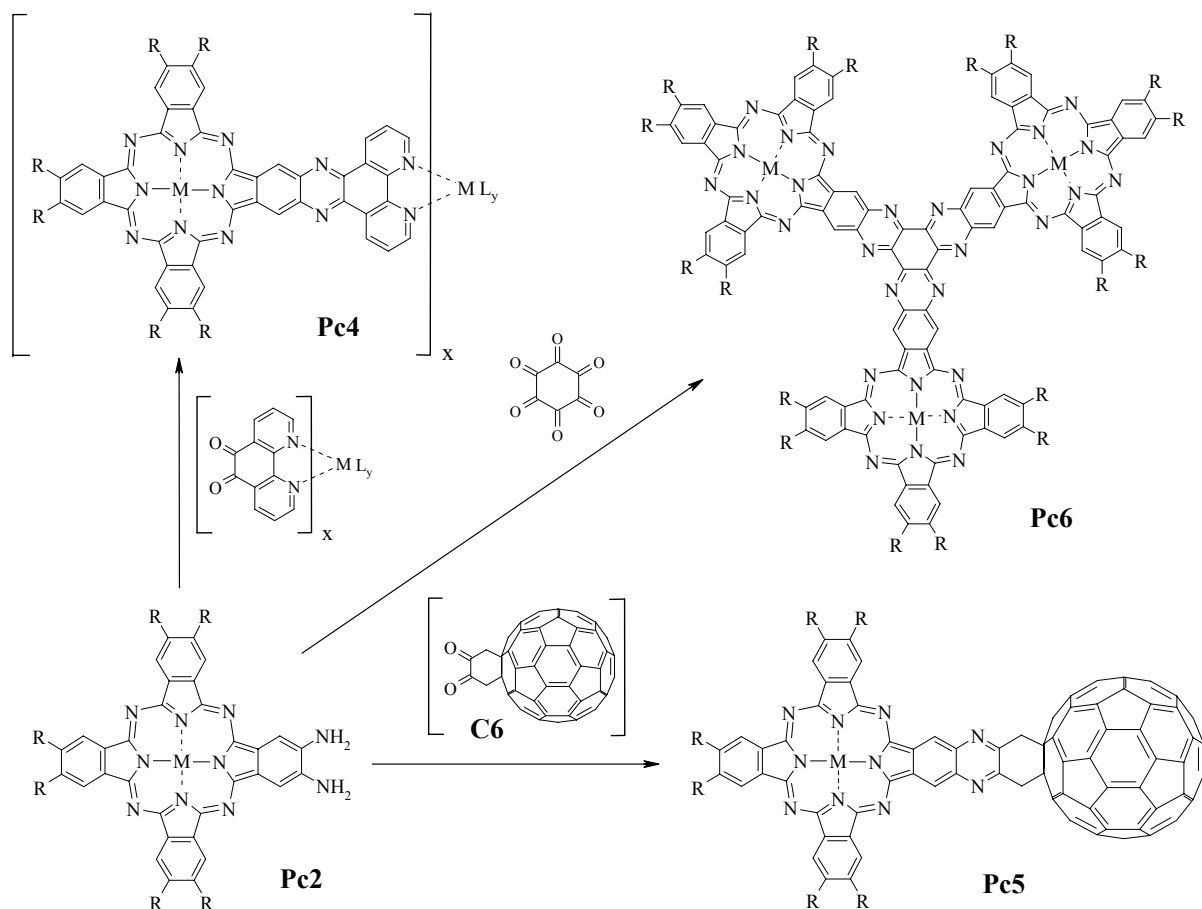
Scheme 3.12. Proposed synthetic routes to various phthalocyanine-based dyad systems (R = e.g. 3,5-di-*tert*-butylphenoxy).

Recently, our research group published an example of a hexaazatriphenylene (HAT) functionalised with three fused TTF units.[190] The phthalocyanine analogue **Pc6** could be prepared by the reaction of three equivalents of **Pc2** with one equivalent of hexaketocyclohexane (Scheme 3.12). Several attempts have been made to synthesise **Pc6** via a statistical condensation reaction of **C7** with **7** as depicted in Scheme 3.13. **C7** was prepared via a Schiff's base condensation of hexaketocyclohexane with **C1**, which was confirmed by MALDI mass spectrometry. This compound was, as expected, completely insoluble in common organic solvents. The statistical condensation reaction of **C7** with **7** did not afford the desired product **Pc6**. Instead, only symmetric Pc **16**, formed by the cyclotetramerisation of **7,** was detected by MALDI mass spectrometry. In addition, **Pc6** is expected to show a very large red shifted Q band due to its huge fully delocalised π-system (similar to trinuclear **Pc33**

mentioned in Chapter 1), which could not be observed as well. Therefore, the synthetic route to **Pc6** depicted in Scheme 3.12 seems very promising since all starting materials exhibit good solubilities. Similar to Pcs **36a-36d** (see Chapter 1), **Pc6** is expected to show enhanced nonlinear optical activity with respect to monomeric Pcs.
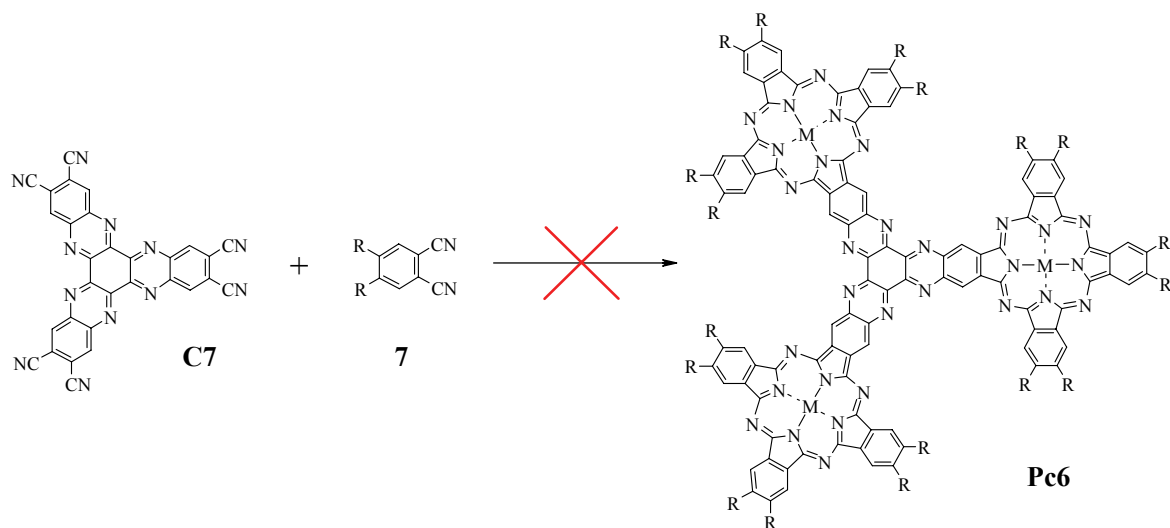
Scheme 3.13. Synthetic attempt to prepare trinuclear **Pc6** (R = 3,5-di-*tert*-butylphenoxy).

4. Scanning tunneling microscopy investigations of phthalocyanines

4.1. Introduction

One of the main goals of nanotechnology is the fabrication of nanodevices by using single atoms or molecules in the bottom-up approach. With this strategy, the limitations of the top-down approach, as applied in traditional industrial methods, could be overcome. In general, self-assembly is considered to be a very valuable method, as it can efficiently form nanostructures by means of non-covalent interactions, such as van der Waals interactions, hydrogen bonds, electrostatic or donor-acceptor interactions and π-π stacking. The formation of nanostructures using organic functional molecules and the study of adsorbate-adsorbate and adsorbate-substrate interactions in molecular self-assembled structures have become an important research field since nanoscience emerged in the last century. Phthalocyanines (Pcs) have attracted special interest because of their wide use in gas-sensing devices, photovoltaic applications, light-emitting diodes, solar and fuel cells, field effect transistors and as pigments and dyes. Additionally, the exceptional thermal and chemical stability and the low vapor pressure at room temperature make them optimal candidates for the deposition under ultrahigh vacuum (UHV) conditions. To achieve applications in the above-mentioned fields, the understanding of the influence of molecular packing, defects and domain boundaries on the overall properties of self-assembled monolayers (SAMs) is very important. Scanning tunneling microscopy (STM) is therefore a very powerful surface analytical tool to investigate surface phenomena on an atomic or molecular scale.[191]

CuPc was among the first molecules that were studied by STM.[192,193] Hipps and coworkers contributed to the interpretation of STM image contrast of MPcs by investigating different d-metal phthalocyanines with STM on a Au(111) substrate under UHV conditions. They found that the macrocyclic cavities of FePc (d^6) and CoPc (d^7) appear bright due to a strong tunneling current. In contrast, the MPc centers of NiPc (d^8) and CuPc (d^9) are dark. In other words, the macrocyclic cavity of FePc and CoPc appears higher than the rest of the molecule. This is interpreted as indication that the d^6 and d^7 systems have a greater metal d-orbital participation in molecular orbitals near the Fermi surface, while the d^8 and d^9 systems do not

show such a participation and therefore, the Pc centers appear as holes. By studying mixed MPc layers (Fig. 4.1), the processes associated with film formation and diffusion in two dimensions can be imaged and followed.[194-196]
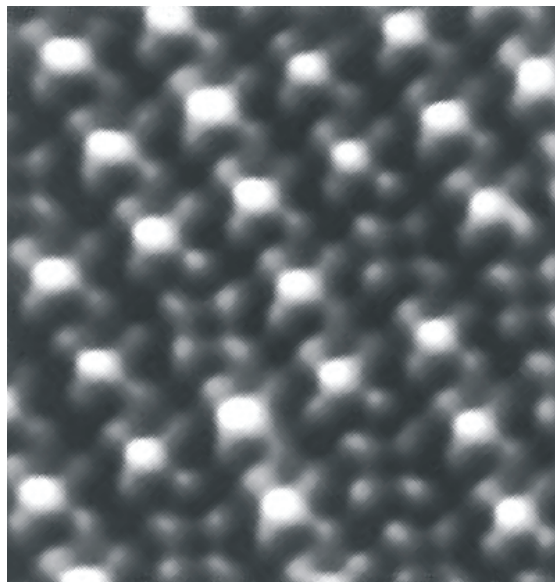
Figure 4.1. STM image of a mixed layer of CoPc and CuPc on Au(111) (9 nm x 9 nm; -0.10 V, 1 nA). The cobalt(II) ions in the macrocyclic center appear bright, whereas the copper(II) ions are dark (Source: reference 195).

By making use of the STM as manipulation tool, Ho *et al.* created a metal-molecule-metal bridge with STM methods (Fig. 4.2). The bridge consists of one CuPc molecule, to which two gold atomic chains (each consisting of three Au atoms) are attached. The created structure serves as a model for molecular junctions formed by a single molecule adsorbed across the gap between two metallic nanoelectrodes.[197] Many other STM studies of unsubstituted MPcs, mainly CuPcs, and naphthalocyanines are reported in the literature.[198-207]

Bai and coworkers reported on STM studies on copper phthalocyanines with eight peripheral octyloxy chains which act as molecular anchors or immobilisers. They observed high layer stabilities and closed packed assemblies which are attributed to van der Waals interactions between the alkyl chains and the highly oriented pyrolytic graphite (HOPG) substrate. The similarity between the image of alkylated CuPc and previous results of CuPc indicates that the alkyl substituents have little influence on the image contrast of the Pc macrocycle.[208,209]

Crown-ether-substituted CoPc (CoPcCE) was successfully self-assembled on Au(111) and Au(100) substrates. In the presence of Ca^{2+}, the CoPcCE adlayer on Au(111) trapped Ca^{2+} ions in two oppositely located 15-crown-5-ether moieties, whereas CoPcCE-modified Au(100) did not encapsulate Ca^{2+} ions. Thus, the host-guest recognition strongly depends on the crystallographic orientation of the gold substrate.[210] With another crown-ether-substituted

Pc, Rabe and coworkers were able to show that the switching between different nanostructures co-existing at the surface can be stimulated with the STM tip with a resolution on the molecular scale.[211] Various STM studies of asymmetric Pcs have also been reported in the literature.[212-214]
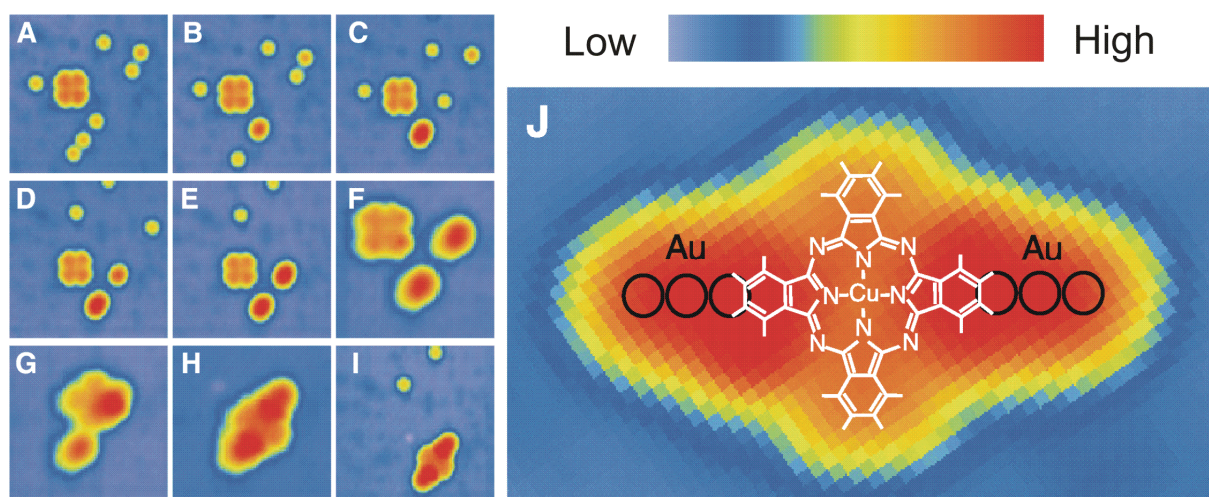
Figure 4.2. Assembly sequence and schematic for a structure consisting of a CuPc molecule and two Au$_3$ chains (1 V, 1 nA). (**A**) A CuPc molecule (appears as four-leaf clover) on the NiAl surface together with seven Au atoms. (**B**) One of the atoms was manipulated to create a Au$_2$ chain. (**C**) The first Au$_3$ chain is created. (**D**) A second Au$_2$ chain is built. (**E**) Assembly of the second Au$_3$ chain and the junction, consisting of two Au$_3$ chains, is completed. Zoom-in image of the two Au$_3$ chains and the CuPc molecule. (**G**) The CuPc was moved into the junction. (**H**) The position of the molecule was adjusted. The molecule is adsorbed symmetrically between the two Au$_3$ chains, forming Au$_3$-CuPc-Au$_3$. The image size of pictures **A-E** and **I** is 74 Å x 74 Å and **F-H** is 47 Å x 47 Å. (**J**) Schematic showing the relation between the internal molecular structure and adsorption geometry (Source: reference 197).

Several research groups reported on STM experiments of binary systems in the form of phthalocyanines and other molecules self-assembled on the same substrate. Bai and coworkers found that differently substituted Pcs can form uniform assemblies with alkane derivatives[191,215-217] (see example in Fig. 4.3) or the latter can act as templates for the adsorption, diffusion and assembling of substituted CuPcs or double decker phthalocyanines, which then exhibit enhanced lattice stability compared to other substrates.[218-221] Moreover, some publications report on mixed phthalocyanine-porphyrin adlayers.[222-225] For example, Hipps and coworkers described the self-assembly of nickel *meso*-tetraphenylporphyrin (NiTPPor) and cobalt hexadecafluorophthalocyanine (CoPcF$_{16}$) forming 1:1 adlayers, where every porphyrin has four Pc neighbors and vice versa. The main driving forces for this pattern are the H···F interactions and the reduced electrostatic repulsion between CoPcF$_{16}$ molecules due to the increased spacing forced by the NiTPPor units.[222,223] Bai *et al.* were able to trap individual phthalocyanine, porphyrin and calix[8]arene molecules on a monolayer of octaalkoxy-substituted Pc under ambient conditions on HOPG. This shows that the cavities in

the monolayer of octaalkoxy-substituted Pc can be used to immobilise organic species on substrates. The trapping efficiency was found to be significantly higher at the domain boundaries than within domains.[226] The investigation of the binary system CuPc and fullerene on Au(111) did not reveal ordered mixed layers of both molecules. Instead, the boundaries of the CuPc domains are often decorated by C_{60} molecules and for a particular choice of parameters during film preparation, individual CuPc molecules may adsorb on top of a fullerene layer.[227]
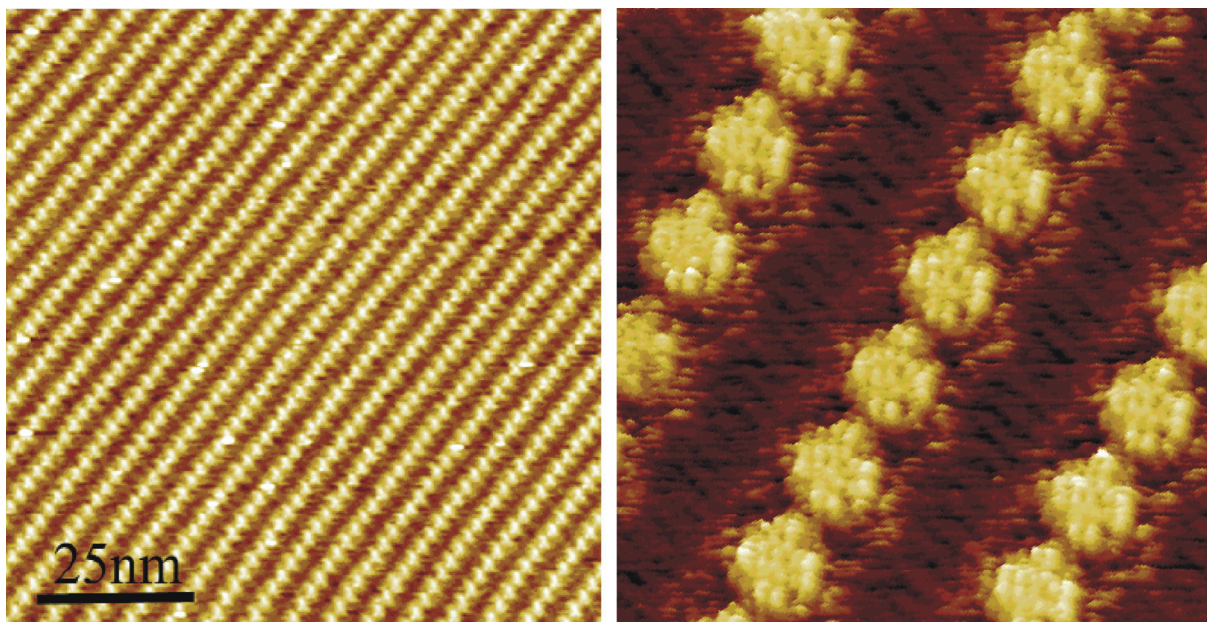
Figure 4.3. On the left: Large scale view of the uniform assembly formed by 1-iodooctadecane (dark contrast) with 1,4,8,11,15,18,22,25-octabutoxyphthalocyanine (bright contrast). On the right: High resolution STM image (12 nm x 12 nm) of the same assembly (Source: reference 216).

In the present study, assemblies of octa-substituted phthalocyanines **16** and **27** were investigated by scanning tunneling microscopy. Once highly ordered monolayers of both phthalocyanine compounds could be prepared, the idea of depositing other molecules on top of them was followed. Pyridyl-functionalised fullerene **C1** was used as an axial ligand to bind to the zinc(II) ion of a ZnTPPor through its pyridyl nitrogen.[228] Therefore, this compound is expected to be a very promising candidate for the deposition onto monolayers of ZnPc **27** in order to form an ordered, coordinative bilayer system on a metal substrate, which then can be investigated by means of STM. Lambert and coworkers investigated similar assemblies of zinc *meso*-tetra-(3,5-di-*tert*-butylphenyl)porphyrin, which were coordinated to nitrogen donor molecules through their Zn(II) ions, by STM methods.[229,230]

16 M = 2H
27 M = Zn(II)

C1

C1-27
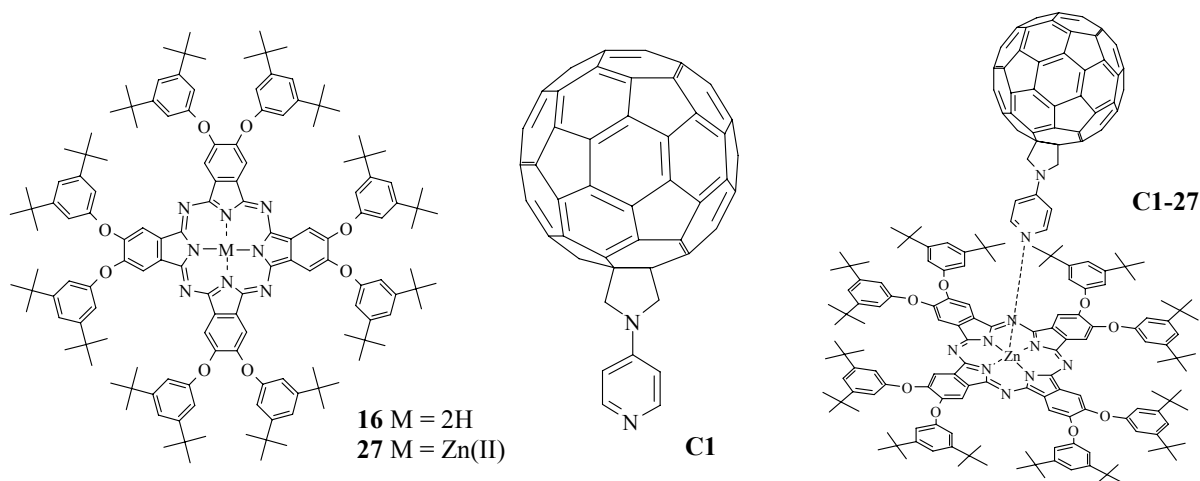
4.2. Monolayers of phthalocyanines 16 and 27

Phthalocyanines **16** and **27** were assembled on a Ag(111) substrate and investigated using a home-built STM. In the case of H$_2$Pc **16**, two different arrangements of the molecules, that are separated by a mobile phase, were observed as shown in Fig. 4.4. The left side displays a dense packing in a rhombic arrangement, whereas the right one represents a quadratic arrangement which is less dense than the rhombic one.

2.8 nm x 1.9 nm, 61°

3.2 nm x 3.2 nm, 90°
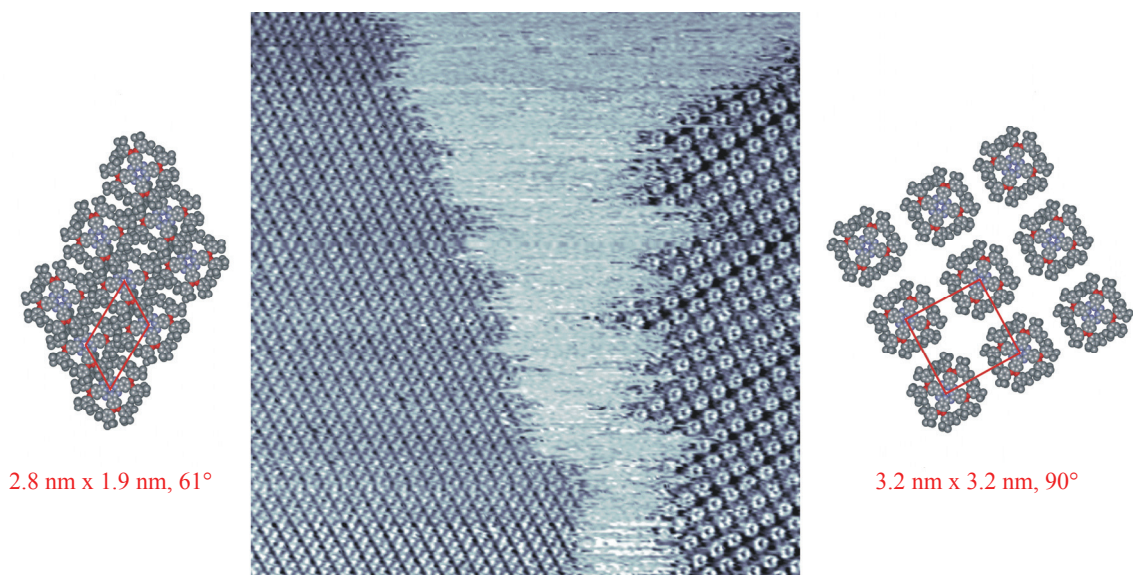
Figure 4.4. H$_2$Pc **16** annealed to 110°C on Ag(111). STM image (90 nm x 90 nm; -2.1 V, 10 pA) of two differently ordered phases which are separated by a mobile phase.

For the closer packed arrangement three rotationally different phases, having an angle of 120° with respect to each other, were found (Fig. 4.5). The occurrence of these three rotationally different phases is an indication that the substrate influences the ordering of the Pc molecules, and that the molecule-substrate interaction is important for the observed ordering. For each

molecule the substituents (3,5-di-*tert*-butyl-phenoxy) appear brighter and therefore higher than the Pc core. Most likely, this observation can be assigned to the combination of a geometric and electronic effect. On the one hand, the height of the substituents is larger than that of the core (geometric effect). On the other hand, the tunneling probability of the substituents may be larger than that of the core (electronic effect).

Within a domain the Pc substituents appear brighter than at domain boundaries. This is assigned to the fact that at boundaries the substituents are not as closely packed as within a domain. Furthermore, the interaction of neighboring substituents can also lead to a higher tunneling probability.
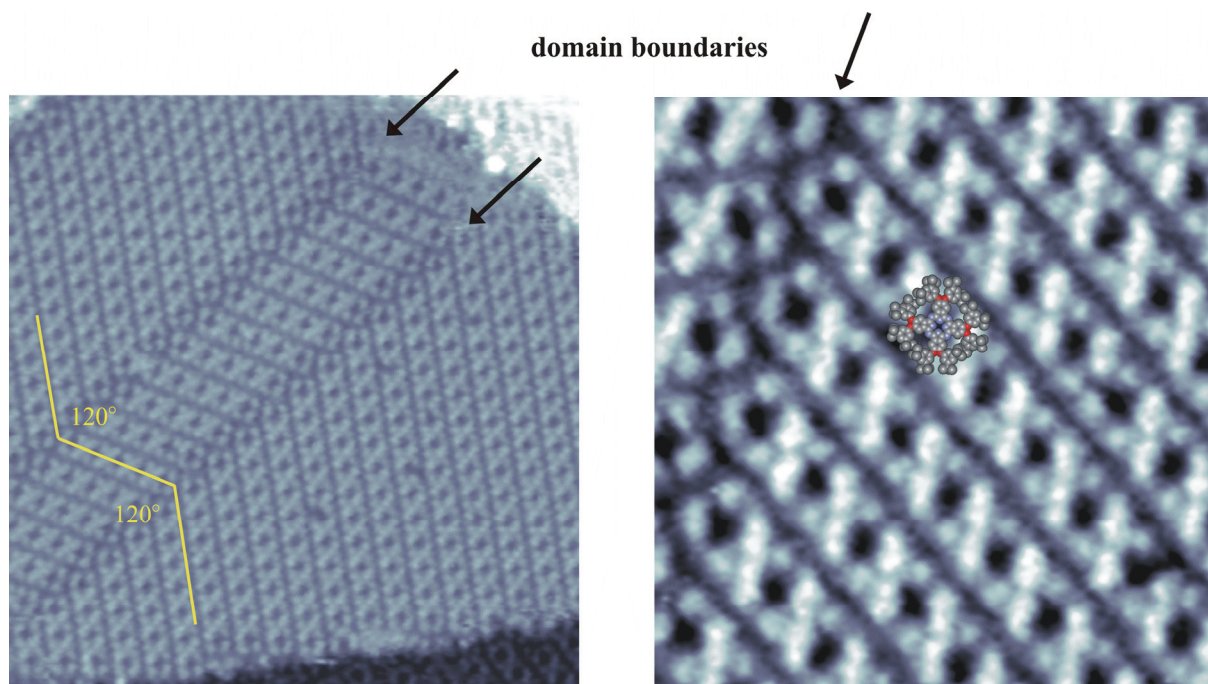
Figure 4.5. On the left side: STM image of the rhombic phase displaying two rotationally different domains (47 nm x 47 nm; 2.3 V, 8 pA). On the right side: STM image of the rhombic phase (15 nm x 15 nm , 2.1 V, 8 pA) showing the domain boundary in more detail. One H_2Pc **16** was drawn in to illustrate its position.

The ZnPc **27** on Ag(111) shows the same rhombic arrangement as H_2Pc **16** (Fig. 4.6). Again, the 3,5-di-*tert*-butyl-phenoxy groups appear higher than the Pc core. A proposed arrangement of **27** with differently rotated substituents in order to match the appearance of the molecule in the STM image is shown in Fig. 4.6. The substituents can rotate around the C-O-C bonds and therefore, it is possible that one bright spot belongs to either one or two *tert*-butyl groups as recently reported for similar compounds.[231,232] If the phenyl ring is planar to the substrate surface, two bright spots are imaged with the STM: one for each of the attached *tert*-butyl groups. If the position of the phenyl ring is orthogonal to the surface, only one bright spot for both *tert*-butyl groups is observed.

Both phthalocyanine compounds were as well deposited on Au(111) substrates, but no significant differences compared to Ag(111) were observed. It has to be mentioned that the lattice constants for Ag(111) and Au(111) are the same.
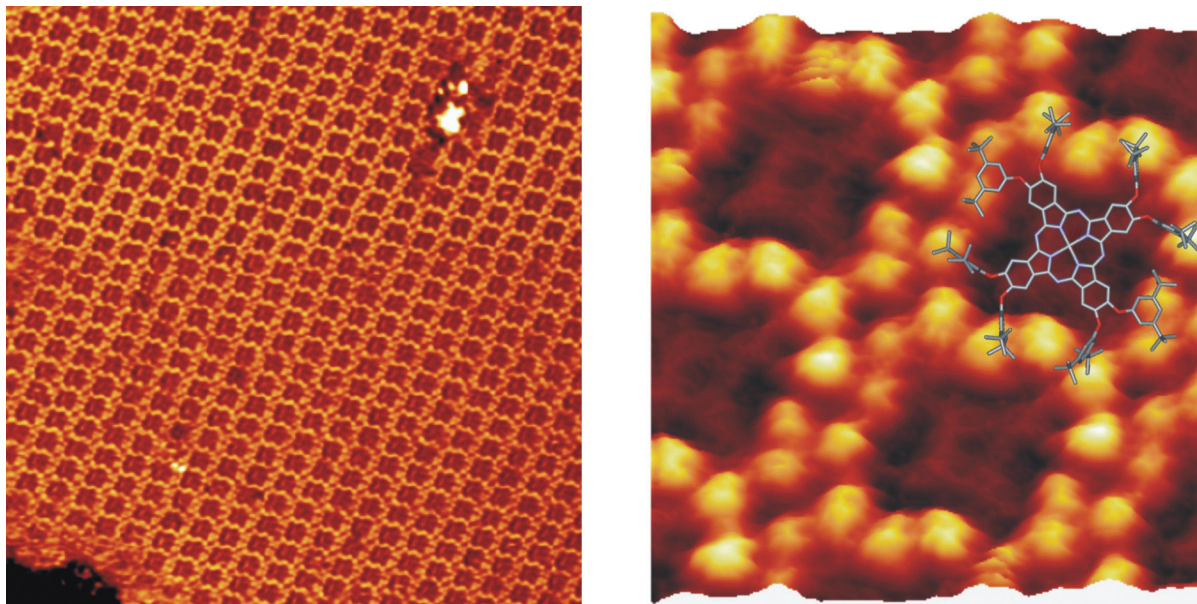
Figure 4.6. ZnPc **27** annealed to 150°C on Ag(111). On the left side: Overview of the rhombic packing of ZnPc **27** (50 nm x 50 nm; 0.8 V, 63 pA). On the right side: High resolution STM image with proposed arrangement of ZnPc **27** and its substituents (5 nm x 5 nm, 0.8 V, 63 pA).

4.3. STM investigation of a ZnPc monolayer with deposited pyridyl-functionalised fullerene molecules

The evaporation of **C1** onto **27** was found to be a very delicate process. If the Au(111) substrate is covered with less than a monolayer of **27**, the evaporation of only small amounts of **C1** already results in a collapse of the ZnPc network due to very strong interactions of the substrate with the strongly electron-accepting fullerene derivative **C1**. The evaporation of large amounts of **C1** onto a complete monolayer of **27** destroys the highly ordered ZnPc arrangement as well. Only the deposition of small amounts of **C1** onto a full monolayer of **27** can keep the ordering of the zinc phthalocyanine molecules intact (Fig. 4.7). The bright spots are assigned to the fullerene cores. The STM imaging of one fullerene unit results in two bright spots (a small one and a bigger one) which can be explained by a tip artefact – in this case with a double tip. It is rather difficult to obtain high quality pictures because there is a large height difference between the ZnPc monolayer and the top of the fullerene derivatives. Therefore, the exact location of the latter on the ZnPc monolayer cannot be determined

unambiguously. Furthermore, it cannot be detected by STM whether deposited **C1** is still intact or if decomposition during evaporation occurred.
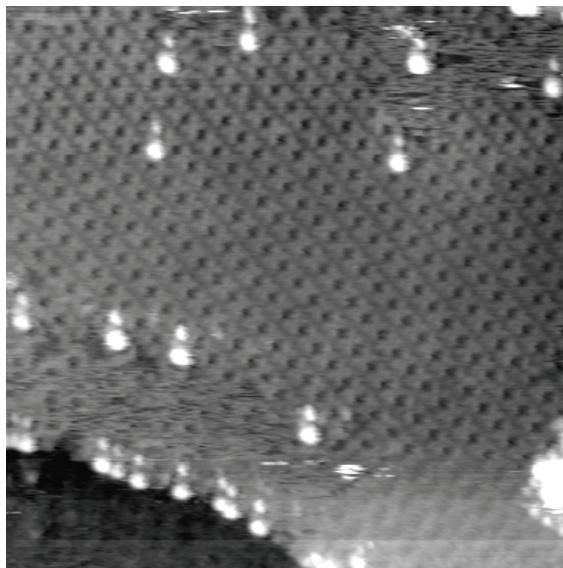
Figure 4.7. STM image after evaporation of **C1** onto a full monolayer of **27** (Au(111), 50 nm x 50 nm; 2 V, 7 pA).

4.4. Conclusions and outlook

It was shown that metal-free phthalocyanine **16** and its ZnPc analogue **27** form highly ordered monolayers on Ag(111) and Au(111), respectively. The predominantly found phase for both compounds was the rhombic one. Only rarely, a more loosely packed quadratic phase appeared.

The deposition of **C1** onto full monolayers of ZnPc **27** is only possible in small quantities. Since it is not possible to confirm by STM if the pyridyl-functionalised fullerene molecules are still intact after deposition onto the ZnPc monolayer, another surface sensitive technique will be applied to answer this question. X-ray photoelectron spectroscopy (XPS) could clarify whether the pyridyl and pyrrolidine groups are still attached to the fullerene molecule or not. This investigation will be carried out with a sample onto which only **C1** is evaporated. If the molecules are still intact after evaporation, typical XPS signals for the pyridyl and pyrrolidine nitrogen atoms are expected.

If XPS measurements reveal that **C1** is unchanged after deposition, the use of RuPc (instead of ZnPc) is thought to increase the stability of the coordination bond between the pyridyl nitrogen of **C1** and the metal ion of the MPc. There are various reports on isolated RuPcs with axial ligands coordinating through their nitrogen atoms to the Ru(II) ions.[233,234] The isolation of ZnPcs with axially coordinated pyridyl derivatives is according to own experience rather

difficult. This shows that the macrocyclic ruthenium(II) ion exhibits stronger interactions with axial nitrogen donors than the zinc(II). Therefore, RuPc is considered the better candidate for deposing **C1** onto MPc monolayers. If the interaction between the pyridyl nitrogen of **C1** and Ru(II) is even stronger than the one between the metal substrate and the fullerene derivative, the RuPc monolayer may be covered with a larger amount of **C1** compared to the ZnPc monolayer.

Chapter 5
Experimental Part

5. Experimental

5.1. General Experimental

5.1.1. Chemicals, reaction conditions and chromatography

All solvents and reagents were of commercial quality and used without further purification. 4,5-Diaminophthalonitrile,[165] *cis*-[dichloro-bis(dimethylsulfoxide)-palladium(II)],[235] *cis*-[bis-(2,2'-bipyridine)-dichlororuthenium(II)],[186] 1,10-phenanthroline-5,6-dione[236] and 5,6-di-amino-2-[4,5-bis(propylthio)-1,3-dithio-2-ylidene]-benzo[*d*]-1,3-dithiole[190] were synthesised according to literature procedures. All reactions were carried out, unless mentioned, under normal laboratory conditions in air.

Silica gel 60 (Fluka), neutral and basic aluminium oxide (CAMAG) were used to perform column chromatography. Thin layer chromatography was run on silica (0.20 mm, ALUGRAM® SIL G/UV$_{254}$, Macherey-Nagel) or alumina plates (0.20 or 0.25 mm, POLYGRAM® ALOX N/UV$_{254}$, Macherey-Nagel). Size exclusion chromatography was carried out using Bio-Beads® S-X1 beads (200-400 mesh, Bio-Rad Laboratories).

5.1.2. Measurements

Melting points were determined using a Büchi 510 instrument and are uncorrected. ^{1}H and ^{13}C NMR spectroscopy were performed either on a Bruker Avance300, a Bruker DRX400 or a Bruker DRX500 instrument. Chemical shifts δ are reported in ppm and were calibrated against TMS as an internal (CD$_2$Cl$_2$, CDCl$_3$, TFA-d$_1$) or external (DMSO-d$_6$) standard unless mentioned otherwise. Infrared spectra were recorded on a Perkin-Elmer Spectrum One FT-IR spectrometer. UV-vis spectra were measured on a Perkin-Elmer Lambda 10 spectrometer. Mass spectra were obtained on an AutoSpecQ spectrometer for the EI ionisation method and on a FTMS 4.7T BioAPEX II for the ESI and MALDI methods. Elemental analyses were performed on a Carlo Erba EA 1110 CHNS instrument. TGA measurements were recorded on a Mettler STARe system.

Data for the crystals of compounds **1** and **4** were measured on a Stoe IPDS I, and for compound **15** on a Stoe IPDS II, using MoK_α graphite monochromated radiation. The structures were solved by direct methods using the program SHELXS-97.[237] The refinement with full-matrix least squares techniques and all further calculations were carried out using SHELXL-97.[238] All non-H atoms were refined with anisotropic displacement parameters. For **1** and **4**, the hydrogen atoms could be located from Fourier difference maps while for **15**, the hydrogen atoms were included in calculated positions. Finally, all hydrogen atoms were treated as riding atoms using SHELXL default parameters. An empirical absorption correction was applied to **4**, using the DELrefABS routine in PLATON03 ($T_{min} = 0.299$, $T_{max} = 0.739$).[239] Compound **15** contains a high number of co-crystallised pyridine molecules. It was not possible to locate these molecules due to a strong disorder and/or partial occupation. Therefore, the SQUEEZE instruction in PLATON03 was used to calculate the potential solvent accessible volume in the unit cell; 4736 $Å^3$ were calculated containing about 1248 electrons. 30 pyridine molecules (30 x 42 electrons) per unit cell were included in all further calculations. In addition, four *tert*-butyl groups of the ZnPc are disordered over two positions and refined with occupancies of 0.5 for the participating methyl groups and with the thermal parameter constrained to be equal in each *tert*-butyl group. Details of crystal and experimental data are given in the appendix and CCDC 615083 - 615085 contain the supplementary crystallographic data for this work. These data can be obtained on the web site of the Cambridge Crystallographic Data Centre (www.ccdc.cam.ac.uk/data_request/cif).

For nanosecond transient absorption experiments the samples were photolysed with the output of the third harmonic (355 nm) coming from a Quanta-Ray GCR-11 Nd:YAG laser (Spectra Physics). Moreover, pulse widths of < 5 ns with an energy of up to 7 mJ were selected. The optical detection was based on a pulsed Xenon lamp (XBO 150, Osram), a monochromator (SpectraPro-275, Acton Research), a R9220 photomultiplier tube (Hamamatsu Photonics) or a fast silicon photodiode (FND-100 Q, Laser Components) with a 1 GHz amplification and a 500 MHz digital oscilloscope (DSA 602A, Tektronix). The laser power of every laser pulse was registered using a bypath with a fast silicon photodiode. The experiments were performed in THF (c = 20 μM) using 5 mm quartz flow cells, and the solutions were saturated with nitrogen unless mentioned else. The femtosecond transient absorption measurements were carried out with a CPA-2001 femtosecond laser (Clark MXR). The excitation wavelength was either generated by second harmonic generation (387 nm) or with a NOPA (Clark MXR). The THF solutions (c = 30 μM) were measured in 2 mm quartz cells. Fluorescence measurements were performed on degassed CH_2Cl_2 solutions at room temperature. Emission spectra were

measured on a FluoroLog®-3 spectrofluorometer (Horiba). Luminescence lifetime measurements were performed by exciting the samples with a pulsed Quantel Brilliant Nd:YAG laser using the second harmonic at 532 nm. The system used for detection consisted of a Spex 270M monochromator, a photomultiplier tube (H957-08, Hamamatsu Photonics) and a TDS-540B oscilloscope (Tektronix). The signals were detected at 620 nm.

Cyclic voltammetry was carried out with an EGG PAR 273A potentiostat (with positive feedback compensation) in a three-electrode cell equipped with a platinum millielectrode, a platinum wire counter-electrode and a silver wire used as quasi-reference electrode. The electrochemical experiments were performed in an inert argon atmosphere in a glove box in 0.1 M Bu_4NPF_6 in CH_2CH_2 at room temperature. Potentials were calibrated against Fc^+/Fc and the voltammograms were deconvoluted using the Condecon[TM] software.

The STM experiments were carried out in an ultrahigh vacuum (UHV) system composed of several chambers for sample preparation and characterisation with a base pressure of $2*10^{-10}$ mbar. The Ag(111) and Au(111) substrates were prepared by subsequent cycles of sputtering with Ar^+ ions and annealing at 600°C and 550°C, respectively. The molecules were evaporated from a crucible and the evaporation rate was controlled with a quartz crystal microbalance, while the substrate was held at room temperature. After annealing at given temperatures, the samples were investigated using a home-built STM which was operated at room temperature.[240]

5.2. Synthesis of phthalonitrile derivatives with metal-binding sites

6,7-Dicyano-2,3-di(2-pyridyl)quinoxaline (1). To a mixture of 4,5-diaminophthalonitrile (689 mg, 4.36 mmol) and 2,2'-pyridil (1.00 g, 4.71 mmol), ethanol (40 mL) and glacial acetic acid (6 mL) were added. The reaction mixture was stirred at 85°C for 4 h and then cooled to 0°C. The precipitate was filtered and washed with plenty of ice cold ethanol. The product was collected and dried at 50°C to yield a brass crystalline solid (1.30 g, 3.89 mmol, 89%). Suitable single crystals for X-ray analysis were obtained in the form of pale yellow rods by slow evaporation of a saturated DMSO solution.

1
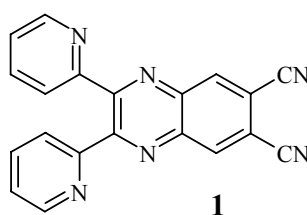
M.p. 243-244°C. ^{1}H NMR: δ_H (300 MHz, DMSO-d_6): 9.12 (s, 2H), 8.31 (d, J = 4.4 Hz, 2H), 8.07-7.98 (m, 4H), 7.44-7.40 (m, 2H). ^{13}C NMR: δ_C (75.5 MHz, DMSO-d_6): 114.06, 115.55, 124.04, 124.12, 137.10, 137.14, 141.03, 148.31, 155.59, 155.62. IR (KBr): ν/cm^{-1}: 3435, 3055, 2239 (-CN), 1586, 1569, 1475, 1397, 1347, 1078, 1002, 922, 898, 795, 759, 748, 536. MS (EI): m/z: 333 ([M-H]$^+$, 100%). CHN analysis: calcd. (%) for $C_{20}H_{10}N_6$: C, 71.85; H, 3.01; N, 25.14, found: C, 71.77; H, 2.97; N, 25.29.

7,8-Dicyanodipyrido[3,2-*a*:2',3'-*c*]phenazine (2). A mixture of 4,5-diaminophthalonitrile (1.18 g, 7.48 mmol) and 1,10-phenanthroline-5,6-dione (1.57 g, 7.48 mmol) in EtOH (130 mL) and glacial acetic acid (8 mL) was refluxed overnight. The suspension was filtered hot and washed with plenty of boiling EtOH. The product was collected and dried at 50°C to yield a yellow solid (2.36 g, 7.09 mmol, 95%).[165]

2
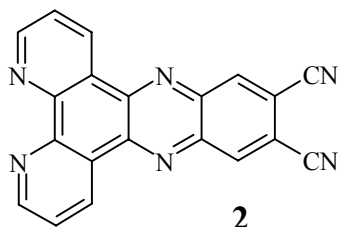
M.p. > 250°C. ^{1}H NMR: δ_H (400 MHz, TFA-d_1): 10.22 (dd, J = 8.3 and 1.2 Hz, 2H), 9.43 (dd, J = 5.1 and 1.2 Hz, 2H), 9.20 (s, 2H), 8.45 (dd, J = 5.1 and 8.3 Hz, 2H). IR (KBr): ν/cm^{-1}: 3007, 2238 (-CN), 1584, 1476, 1451, 1404, 1360, 1073, 1030, 896, 817, 742, 619, 537, 409. MS (EI): m/z: 332 (M$^+$, 100%). CHN analysis: calcd. (%) for $C_{20}H_8N_6\cdot0.1H_2O$: C, 71.89; H, 2.47; N, 25.15, found: C, 71.57; H, 2.35; N, 25.25. TGA shows an overall weight loss of 0.5% (calcd. for 0.1 molecules of water: 0.5%)

5.3. Preparation of a symmetric H$_2$Pc with eight peripheral pyridyl groups

Tetrakis[2,3-di(2-pyridyl)pyrazino][5,6-*b*:5',6'-*k*:5'',6''-*t*:5''',6'''-*c$_1$*]phthalocyanine (3). Lithium metal (36 mg, 5.19 mmol) was dissolved in 1-pentanol (3 mL) at 80°C under nitrogen. To this lithium-pentoxide solution, **1** (100 mg, 0.30 mmol) was added and the reaction mixture was heated at 100°C for 17 h under nitrogen. On cooling, the dark blue-green solution was treated with glacial acetic acid (5 mL) and acetone (70 mL). The resultant precipitate was collected by centrifugation, washed thoroughly with water, MeOH, THF and Et$_2$O and then dried at 50°C to yield **3** as a dark blue-green powder (66 mg, 49 µmol, 66%).

3
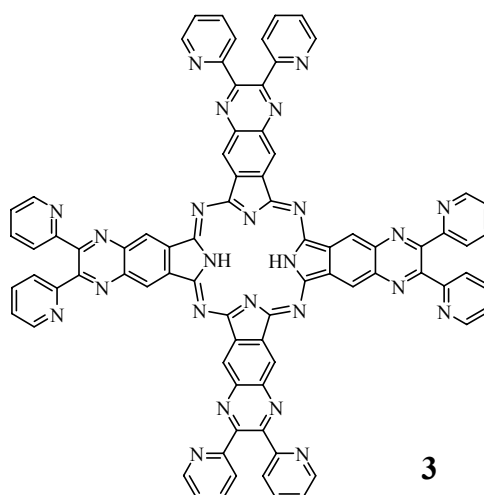
M.p. > 250°C. ^{1}H NMR: δ_H (500 MHz, D$_2$SO$_4$, TSPA as internal standard set to 0 ppm): 10.87 (s, 8H), 9.27 (d, *J* = 5.1 Hz, 8H), 8.93-8.92 (m, 8H), 8.57-8.54 (m, 8H), 8.40 ppm (d, *J* = 6.2 Hz, 8H). IR (KBr): ν/cm^{-1}: 3433, 1586, 1568, 1473, 1434, 1346, 1098, 1078, 1028, 999, 790, 743, 705. UV-vis (pyridine): λ_{max}/nm: 377, 765. MS (MALDI, dithranol as matrix): *m/z*: calcd. for [M+H]$^+$: 1339.41, found: 1339.40. CHN analysis: calcd (%) for C$_{80}$H$_{42}$N$_{24}$·3H$_2$O: C, 68.96; H, 3.47; N, 24.12, found: C, 68.67; H, 3.19; N, 23.82. TGA shows an overall weight loss of 3.2% (calcd. for three molecules of water: 3.9%).

5.4. Synthesis of a phthalonitrile-palladium(II) complex

Dichloro[6,7-dicyano-2,3-di(2-pyridyl)quinoxaline]palladium(II) (4). A mixture of *cis*-[dichloro-bis(dimethylsulfoxide)-palladium(II)] (201 mg, 0.60 mmol) and **1** (149 mg, 0.45 mmol) in THF (20 mL) was refluxed for 2.5 h. The resulting yellow suspension was filtered hot, washed with THF, water and diethyl ether and dried at 50°C to yield **4** as a pale yellow solid (207 mg, 0.40 mmol, 91%). Suitable crystals for X-ray diffraction were obtained as yellow blocks by dissolving **4** in hot acetonitrile followed by slow evaporation of the solvent.

4
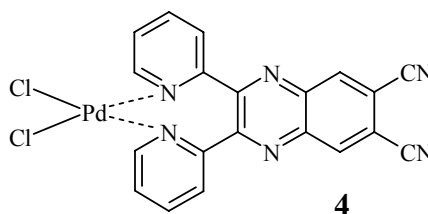
M.p. > 250°C. ^{1}H NMR: δ_H (300 MHz, DMSO-d$_6$): 9.35 (s, 2H), 9.09 (d, *J* = 5.5 Hz, 2H), 8.27 (t, *J* = 7.7 Hz, 2H), 7.95 (d, *J* = 7.7 Hz, 2H), 7.87-7.82 (m, 2H); IR (KBr): ν/cm^{-1}: 3438, 2241 (-CN), 1601, 1488, 1351, 1084, 1061, 774, 762, 539. MS (ESI, CH$_3$CN): *m/z*: calcd. for

[M+Na]$^+$: 532.93, found: 532.94 and calcd. for [2M+Na]$^+$: 1042.87, found: 1042.88. CHN analysis: calcd. (%) for $C_{20}H_{10}N_6Cl_2Pd\cdot0.8CH_3CN$: C, 47.65; H, 2.30; N, 17.49, found: C, 47.38; H, 2.16; N, 17.17. TGA shows an overall weight loss of 6.2% (calcd. for 0.8 molecules of acetonitrile: 6.0%).

5.5. Synthesis of phthalocyanine precursors with solubilising groups

4,5-Bis(*p*-pentylphenoxy)phthalonitrile (5). To a suspension of 4,5-dichlorophthalonitrile (500 mg, 2.54 mmol) and potassium carbonate (2.00 g, 14.5 mmol) in DMSO (10 mL), 4-pentylphenol (2.6 mL, 15.2 mmol) was added. The mixture was heated to 85°C for 15 min under nitrogen, followed by the addition of another portion of potassium carbonate (2.00 g). The reaction mixture was stirred at 85°C for an additional 3 h, then cooled to r.t. and poured into water (100 mL). The water phase was extracted with CH_2Cl_2 (50 mL) for three times. The combined CH_2Cl_2 phases were dried over Na_2SO_4 and filtered. The volume of the filtrate was reduced and the crude product was chromatographed through a neutral alumina column (CH_2Cl_2, R_f = 0.9) to afford **5** as a turquoise viscous oil. The oily compound was dried in high vacuum and solidified (988 mg, 2.18 mmol, 86%).

5
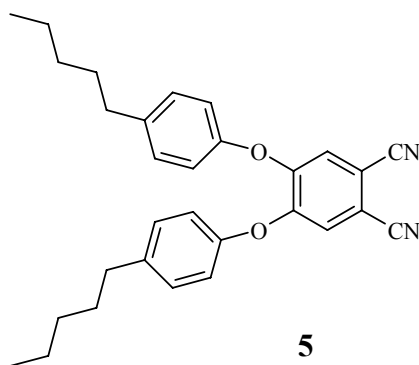
M.p. 74-75°C. ^{1}H NMR: δ_H (300 MHz, CD_2Cl_2): 7.18 (d, *J* = 8.6 Hz, 4H), 7.08 (s, 2H), 6.92 (d, *J* = 8.6 Hz, 4H), 2.55 (t, *J* = 7.5 Hz, 4H), 1.60-1.51 (m, 4H), 1.31-122 (m, 8H), 0.82 (t, *J* = 6.8 Hz, 6H). ^{13}C NMR: δ_C (75.5 MHz, $CDCl_3$): 13.98, 22.47, 31.10, 31.44, 35.26, 109.91, 115.13, 119.84, 121.37, 130.33, 140.87, 151.86, 152.24. IR (KBr): v/cm^{-1}: 3433, 2957, 2930, 2858, 2231 (-CN), 1587, 1568, 1501, 1402, 1340, 1292, 1254, 1223, 1210, 1160, 1074, 1018, 879, 855. MS (EI): *m/z*: 452 (M$^+$, 68%). CHN analysis: calcd. (%) for $C_{30}H_{32}N_2O_2$: C, 79.61; H, 7.13; N, 6.19, found: C, 79.51; H, 7.30; N, 6.17.

4,5-Bis(*p-tert*-butylphenoxy)phthalonitrile (6). A mixture of 4,5-dichlorophthalonitrile (801 mg, 4.07 mmol), 4-*tert*-butylphenol (3.64 g, 24.2 mmol) and K_2CO_3 (6.00 g, 43.4 mmol) in DMSO (8 mL) was heated to 90°C under nitrogen. After 3.5 h the mixture was added to water (100 mL) and extracted with CH_2Cl_2 (50 mL) for three times. The combined organic phases were dried over $MgSO_4$, filtered and the solvent was removed by rotary evaporation. After that, methanol (100 mL) was added to the greenish solution and the precipitate was filtered. The product was washed with plenty of MeOH and dried at 50°C to yield a pale turquoise crystalline solid (1.36 g, 3.21 mmol, 79%).[167]

6
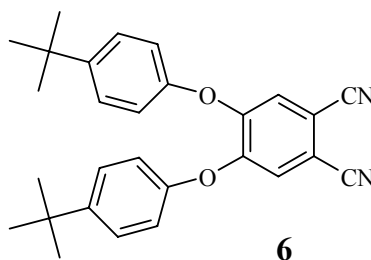
M.p. 187-188°C. ^{1}H NMR: δ_H (300 MHz, CDCl$_3$): 7.42-7.37 (m, 4H), 7.07 (s, 2H), 6.98-6.93 (m, 4H), 1.29 (s, 18H). ^{13}C NMR: δ_C (75.5 MHz, CDCl$_3$): 31.39, 34.56, 109.85, 115.17, 119.54, 121.40, 127.39, 149.07, 151.59, 152.23. IR (KBr): v/cm^{-1}: 2964, 2870, 2225 (-CN), 1583, 1502, 1400, 1346, 1294, 1255, 1225, 1213, 1171, 1108, 1076, 1017, 877, 853, 837, 575. MS (EI): *m/z*: 424 (M$^+$, 27%) and 409 ([M-CH$_3$]$^+$, 100%). CHN analysis: calcd. (%) for $C_{28}H_{28}N_2O_2$: C, 79.22; H, 6.65; N, 6.60, found: C, 79.01; H, 6.84; N, 6.64.

4,5-Bis(3,5-di-*tert*-butylphenoxy)phthalonitrile (7). A mixture of 4,5-dichlorophthalonitrile (2.00 g, 10.2 mmol), 3,5-di-*tert*-butylphenol (12.56 g, 60.9 mmol) and K_2CO_3 (16.00 g, 116 mmol) in DMSO (40 mL) was heated to 90°C under nitrogen. After 4 h the mixture was added to water (200 mL) and extracted with CH_2Cl_2 (50 mL) for three times. The combined organic phases were dried over Na_2SO_4, filtered and the solvent was removed by rotary evaporation. After that, methanol (100 mL) was added to the greenish solution and the precipitate was filtered. The solid was washed with plenty of MeOH and dried at 50°C to yield a white crystalline solid (5.05 g, 9.41 mmol, 93%).[168]

M.p. 225-226°C. ^{1}H NMR: δ_H (300 MHz, CDCl$_3$): 7.28 (t, *J* = 1.7 Hz, 2H), 7.03 (s, 2H), 6.87 (d, *J* = 1.7 Hz, 4H), 1.26 (s, 36H). ^{13}C NMR: δ_C (75.5 MHz, CDCl$_3$): 31.34, 35.15, 109.65, 114.37, 115.34, 120.03, 120.76, 152.34, 153.45, 153.87. IR (KBr): v/cm^{-1}: 2962, 2230 (-CN), 1611, 1576, 1505, 1421, 1399, 1343, 1292, 1220, 1209, 1078, 945, 881, 706. MS (EI): *m/z*:

536 (M$^+$, 71%). CHN analysis: calcd. (%) for C$_{36}$H$_{44}$N$_2$O$_2$: C, 80.56; H, 8.26; N, 5.22, found: C, 80.51; H, 8.44; N, 5.13.

7
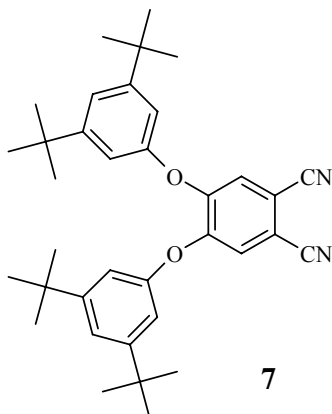
4,5-Bis(*p*-propylphenoxy)phthalonitrile (8). To a suspension of 4,5-dichlorophthalonitrile (602 mg, 3.06 mmol) and potassium carbonate (4.00 g, 28.9 mmol) in DMSO (6 mL), 4-propylphenol (2.5 mL, 18.0 mmol) was added. The reaction mixture was heated at 90°C for 4 h under nitrogen. After that, the greenish suspension was cooled to r.t. and poured into water (100 mL). The water phase was extracted with CH$_2$Cl$_2$ (40 mL) for three times. The combined CH$_2$Cl$_2$ phases were dried over Na$_2$SO$_4$ and filtered. The volume of the filtrate was reduced and the crude product was chromatographed through a neutral alumina column (CH$_2$Cl$_2$, R_f = 0.9) to afford **8** as a turquoise solid (1.01 g, 2.55 mmol, 83%).

8
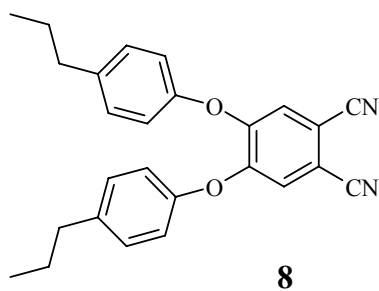
M.p. 92-93°C. ^{1}H NMR: δ_H (300 MHz, CD$_2$Cl$_2$): 7.27 (d, J = 8.7 Hz, 4H), 7.17 (s, 2H), 7.01 (d, J = 8.7 Hz, 4H), 2.62 (t, J = 7.6 Hz, 4H), 1.73-1.60 (m, 4H), 0.96 (t, J = 7.3 Hz, 6H). ^{13}C NMR: δ_C (75.5 MHz, CDCl$_3$): 13.75, 24.49, 37.35, 109.93, 115.14, 119.85, 121.38, 130.41, 140.63, 151.91, 152.24. IR (KBr): v/cm^{-1}: 2958, 2928, 2860, 2226 (-CN), 1587, 1568, 1500, 1402, 1341, 1289, 1255, 1222, 1210, 1160, 1073, 1016, 887, 877, 862, 851. MS (EI): *m/z*: 396 (M$^+$, 61%) and 367 ([M-CH$_2$CH$_3$]$^+$, 100%). CHN analysis: calcd. (%) for C$_{30}$H$_{32}$N$_2$O$_2$: C, 78.76; H, 6.10; N, 7.07, found: C, 78.18; H, 6.09; N, 6.73.

5.6. Synthesis of asymmetric phthalocyanines with peripheral metal-binding sites

Phthalocyanines 9-13: To a mixture of **1** (123 mg, 368 μmol) and **5** (500 mg, 1.1 mmol) in 1-pentanol (9 mL), DBU (156 μL, 1.0 mmol) was added. The reaction mixture was refluxed at 148°C for 17 h under nitrogen and then poured into MeCN (100 mL). The green precipitate was filtered, washed with MeCN and dried at 50°C. The product mixture was dissolved in a minimum of chloroform and the solution subjected to column chromatography (SiO$_2$), eluting with a gradient of 1-10 % CH$_3$OH in CH$_2$Cl$_2$. The first fraction (eluent: CH$_2$Cl$_2$-CH$_3$OH, 100:1, R_f = 1.0) was collected. After removal of the solvent under reduced pressure, the green precipitate was refluxed in CH$_3$CN, filtered hot, washed with plenty of CH$_3$CN and dried at 50°C to afford **9**. The second fraction (eluent: CH$_2$Cl$_2$-CH$_3$OH, 90:1, R_f = 0.7) was collected and purified by the same procedure as for **9** to afford **10**. The third fraction was eluted with CH$_2$Cl$_2$-MeOH (10:1) as a mixture. After removal of the solvent, this mixture was initially applied to a basic alumina column eluting with chloroform to remove a trace amount of **10**, and then separated on an alumina preparative TLC plate using chloroform. Phthalocyanines **11** (R_f = 0.8), **12** (R_f = 0.5) and **13** (R_f = 0.1) were extracted from the aluminium oxide with CHCl$_3$-MeOH (5:1). **13** was again subjected to an alumina preparative TLC plate using CHCl$_3$-MeOH (400:1), and then extracted from the aluminium oxide. After separation, all of them were further purified following the same procedure as for **9**.

9

10 M = 2H
14 M = Zn(II)
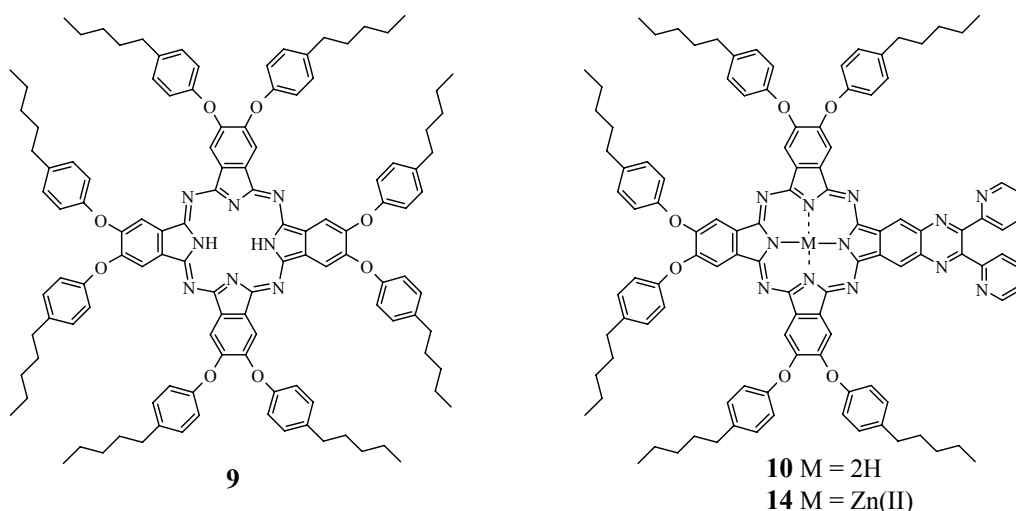
2,3,9,10,16,17,23,24-Octakis(*p*-pentylphenoxy)phthalocyanine (9). Grass-green powder; yield: 131 mg (72 μmol, 26%). ^{1}H NMR: δ$_H$ (400 MHz, CDCl$_3$): 8.53 (s, 8H), 7.15-7.10 (m, 32H), 2.52 (t, *J* = 7.70 Hz, 16H), 1.61-1.54 (m, 16H), 1.34-1.27 (m, 32H), 0.87 (t, *J* = 6.5 Hz, 24H). IR (KBr): ν/cm^{-1}: 3437, 2926, 1607, 1506, 1440, 1399, 1275, 1219, 1166, 1086, 1016,

878, 751. UV-vis (CHCl$_3$): λ_{max}/nm (log ε): 291 (4.7), 347 (4.8), 606 (4.4), 640 (4.6), 668 (5.1), 703 (5.2). MS (MALDI, dithranol as matrix): *m/z*: calcd. for [M+H]$^+$: 1812.01, found: 1812.00. CHN analysis: calcd. (%) for C$_{120}$H$_{130}$N$_8$O$_8$: C, 79.53; H, 7.23; N, 6.18, found: C, 79.58; H, 7.37; N, 6.12.

2,3-Di(2-pyridyl)pyrazino[5,6-*c$_1$*]-2',3',9',10',16',17'-hexakis(*p*-pentylphenoxy)phthalo-cyanine (10). Green powder; yield: 133 mg (79 μmol, 21%). ^{1}H NMR: δ_H (400 MHz, CDCl$_3$): 9.34 (br s, 2H), 8.59 (br s, 2H), 8.47 (br s, 2H), 8.44 (s, 2H), 8.41 (d, *J* = 4.52 Hz, 2H), 8.25 (d, *J* = 7.80 Hz, 2H), 7.85 (dt, *J* = 7.7 Hz, 1.7 Hz, 2H), 7.31-7.25 (m, 14H), 7.19-7.17 (m, 4H), 7.10-7.02 (m, 8H), 2.66 (t, *J* = 7.7 Hz, 4H), 2.54 (t, *J* = 7.7 Hz, 8H), 1.71-1.63 (m, 4H), 1.63-1.53 (m, 8H), 1.37-1.30 (m, 24H), 0.91-0.85 (m, 18H). IR (KBr): ν/cm^{-1}: 3435, 2926, 1605, 1506, 1472, 1400, 1273, 1205, 1167, 1089, 1015, 880, 745. UV-vis (CHCl$_3$): λ_{max}/nm (log ε): 348 (5.0), 618 (4.6), 663 (4.8), 684 (5.2), 723 (5.3). MS (MALDI, dithranol as matrix): *m/z*: calcd. for [M+H]$^+$: 1693.86, found: 1693.86. CHN analysis: calcd. (%) for C$_{110}$H$_{108}$N$_{12}$O$_6$: C, 77.99; H, 6.43; N, 9.92, found: C, 77.88; H, 6.53; N, 9.80.

Bis[2,3-di(2-pyridyl)pyrazino][5,6-*k*:5',6'-*c$_1$*]-2,3,16,17-tetrakis(*p*-pentylphenoxy)phtha-locyanine (11). Green powder. ^{1}H NMR: δ_H (300 MHz, CDCl$_3$): 9.32 (br s, 4H), 8.49 (br s, 4H), 8.37 (d, *J* = 4.3 Hz, 4H), 8.18 (d, *J* = 7.7 Hz, 4H), 7.81 (dt, *J* = 7.7, 1.3 Hz, 4H), 7.41-7.31 (m, 16H), 7.28-7.24 (m, 4H), 2.67 (t, *J* = 7.6 Hz, 8H), 1.73-1.62 (m, 8H), 1.37-1.33 (m, 16H), 0.90 (t, *J* = 6.7 Hz, 12H). IR (KBr): ν/cm^{-1}: 3436, 2924, 1587, 1505, 1473, 1404, 1356, 1273, 1206, 1168, 1096, 1014, 998, 880, 744. UV-vis (CHCl$_3$): λ_{max}/nm (log ε): 349 (4.9), 630 (4.4), 678 (4.7), 699 (5.0), 742 (5.0). MS (MALDI, dithranol as matrix): *m/z*: calcd. for [M+H]$^+$: 1575.71, found: 1575.65.

11　　　　**12**
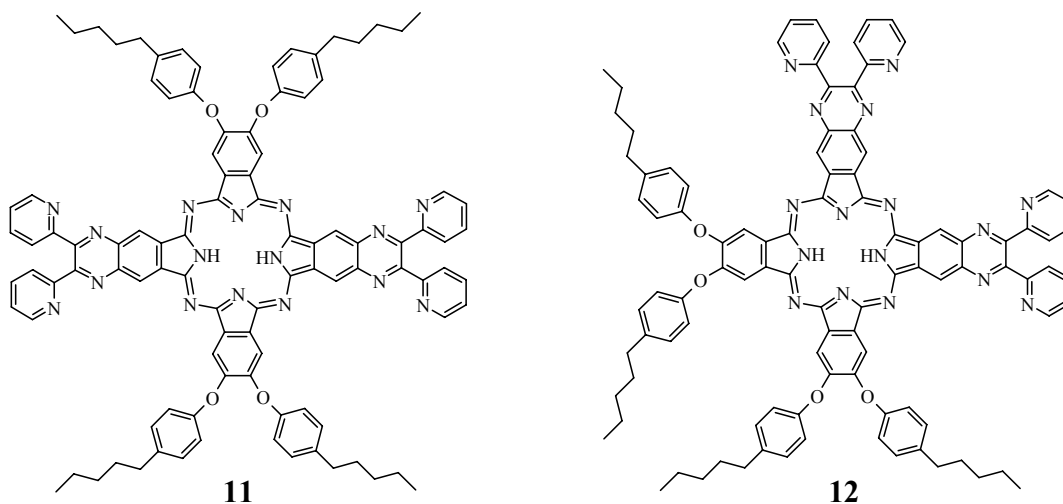
Bis[2,3-di(2-pyridyl)pyrazino][5,6-*t*:5',6'-*c$_1$*]-2,3,9,10-tetrakis(*p*-pentylphenoxy)phthalo-cyanine (12). Dark green powder. ^{1}H NMR: δ_H (400 MHz, CDCl$_3$): 9.40 (br s, 2H), 9.31 (br s, 2H), 8.49 (s, 2H), 8.43 (d, *J* = 4.3 Hz, 2H), 8.41 (d, *J* = 4.3 Hz, 2H), 8.32 (d, *J* = 7.6 Hz, 2H), 8.27 (s, 2H), 8.24 (d, *J* = 7.8 Hz, 2H), 7.84 (dt, *J* = 7.6, 1.2 Hz, 4H), 7.30-7.25 (m, 4H), 7.23-7.13 (m, 16H), 2.66 (t, *J* = 7.83 Hz, 4H), 2.57 (t, *J* = 7.83 Hz, 4H), 1.69-1.56 (m, 8H), 1.36-1.30 (m, 16H), 091-0.86 (m, 12H). IR (KBr): ν/cm^{-1}: 3435, 2925, 1586, 1505, 1446, 1346, 1273, 1204, 1166, 1090, 1071, 1013, 880, 742. UV-vis (CHCl$_3$): λ_{max}/nm (log ε): 352 (5.0), 665 (4.6), 736 (5.3). MS (MALDI, dithranol as matrix): *m/z*: calcd. for [M+H]$^+$: 1575.71, found: 1575.65.

2,3-Bis(*p*-pentylphenoxy)-tris[2,3-di(2-pyridyl)pyrazino][5,6-*k*:5',6'-*t*:5'',6''-*c$_1$*]phthalo-cyanine (13). Bluish green powder. ^{1}H NMR: δ_H (400 MHz, CDCl$_3$): 9.41 (br s, 2H), 9.02 (br s, 2H), 8.98 (br s, 2H), 8.40 (d, *J* = 4.0 Hz, 2H), 8.36-8.26 (m, 8H), 8.09-8.05 (m, 4H), 7.82 (t, *J* = 7.2 Hz, 2H), 7.75 (t, *J* = 7.3 Hz, H), 7.28-7.19 (m, 14H), 2.68 (t, *J* = 7.4 Hz, 4H), 1.70-1.63 (m, 4H), 1.37-1.33 (m, 8H), 0.90 (t, *J* = 6.4 Hz, 6H). IR (KBr): ν/cm^{-1}: 3436, 2926, 1729, 1631, 1587, 1505, 1469, 1346, 1273, 1204, 1097, 1071, 999, 891, 744. UV-vis (CHCl$_3$): λ_{max}/nm: 352, 691, 734, 753. MS (MALDI, dithranol as matrix): *m/z*: calcd. for [M+H]$^+$: 1457.56, found: 1457.56.
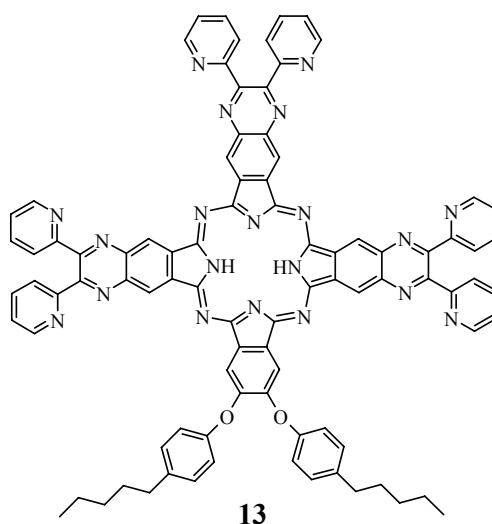
13

{2,3-Di(2-pyridyl)pyrazino[5,6-*c$_1$*]-2',3',9',10',16',17'-hexakis(*p*-pentylphenoxy)phthalo-cyaninato}zinc(II) (14). A mixture of **10** (50 mg, 30 μmol) and zinc(II) acetate dihydrate (32 mg, 146 μmol) in 1-pentanol was heated at 140°C overnight under nitrogen. Upon the addition of CH$_3$CN (50 mL), a precipitate was formed from the dark reaction mixture, filtered, washed with CH$_3$CN and dried at 50°C. The crude product was dissolved in a

minimum of CHCl$_3$ and subjected to column chromatography (SiO$_2$) eluting with CH$_2$Cl$_2$-MeOH (10:1). After removal of the solvent by rotary evaporation, the solid was refluxed in CH$_3$CN (30 mL), filtered hot and washed with boiling CH$_3$CN. The product was collected and dried at 50°C to yield a greenish blue solid (39 mg, 22 μmol, 75%).

^{1}H NMR: δ$_H$ (400 MHz, CD$_2$Cl$_2$): 9.36 (br s, 2H), 9.03 (s, 2H), 8.92 (s, 2H), 8.61 (br s, 2H), 7.30-7.06 (m, 28H), 6.87 (br s, 2H), 6.51 (br s, 2H), 2.68-2.58 (m, 12H), 1.67-1.58 (m, 12H), 1.37-1.18 (m, 24 H), 0.90-0.86 (m, 12H), 0.74 (t, *J* = 6.9 Hz, 6H). IR (KBr): ν/cm^{-1}: 3436, 2925, 1603, 1506, 1450, 1402, 1348, 1270, 1205, 1168, 1090, 1026, 887, 745. UV-vis (CHCl$_3$): λ$_{max}$/nm (log ε): 366 (5.0), 711 (5.2). MS (MALDI, dithranol as matrix): *m/z*: calcd. for [M+H]$^+$: 1755.77, found: 1755.77. CHN analysis: calcd. (%) for C$_{110}$H$_{106}$N$_{12}$O$_6$Zn·H$_2$O: C, 74.41; H, 6.13; N, 9.47, found: C, 74.14; H, 6.07; N, 9.30. TGA shows an overall weight loss of 0.4% (calcd. for one molecule of water: 1.0%)

{2,3-Di(2-pyridyl)pyrazino[5,6-*c$_1$*]-2',3',9',10',16',17'-hexakis(*p-tert*-butylphenoxy)-phthalocyaninato}zinc(II) (15). A mixture of **1** (17 mg, 51 μmol), **6** (63 mg, 148 μmol) and zinc(II) acetate dihydrate (15 mg, 68 μmol) in N,N'-dimethylaminoethanol was heated at 110°C overnight under nitrogen. To the reaction mixture water and methanol were added and the resulting suspension was centrifuged. The blue solid was collected and dried at 50°C. The crude product was dissolved in a minimum of CH$_2$Cl$_2$ and subjected to column chromatography (SiO$_2$) eluting with CH$_2$Cl$_2$-MeOH with a gradient of 0.25-1 % CH$_3$OH in CH$_2$Cl$_2$. The greenish blue fraction (eluent: CH$_2$Cl$_2$-CH$_3$OH, 100:1) was proven to be the desired zinc phthalocyanine. Solvents were removed by rotary evaporation and the product was dried at 50°C to afford **15** as a greenish blue solid (15 mg, 9 μmol, 18%). Single crystals suitable for an X-ray diffraction measurement were obtained as pink blocks by slow evaporation of a pyridine solution of **15**.

15
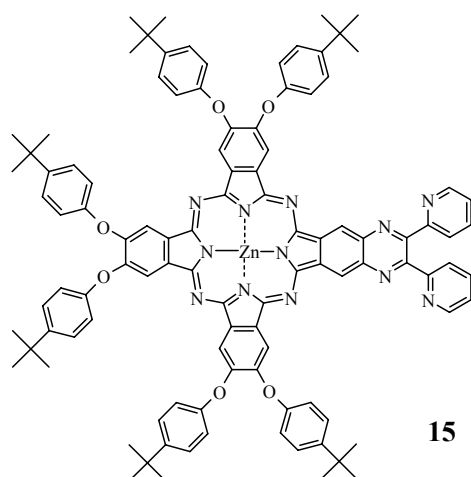
IR (KBr): v/cm^{-1}: 3437, 2924, 1628, 1508, 1440, 1268, 1217, 1179, 1090, 1027, 890, 859. UV-vis (CH$_2$Cl$_2$): λ_{max}/nm: 370, 646, 725. MS (MALDI, dithranol as matrix): *m/z*: calcd. for [M+H]$^+$: 1671.68, found: 1671.69.

Phthalocyanines 16 and 17. To a mixture of **2** (300 mg, 903 μmol) and **7** (2.18 g, 4.06 mmol) in 1-pentanol (20 mL), DBU (370 μL, 2.47 mmol) was added. The yellow suspension was reacted at 148°C for 17 h under nitrogen. The green reaction mixture was then poured into CH$_3$OH (50 mL) and water (30 mL). The suspension was centrifuged, washed with CH$_3$OH-H$_2$O (3:2) and the pellet was dried at 50°C. After that, the green solid was dissolved in CHCl$_3$ and subjected to column chromatography (silica). Elution with CH$_2$Cl$_2$ gave **16** (R_f = 1.0). After removal of the solvent under reduced pressure, the green precipitate was refluxed in CH$_3$CN, filtered hot, washed with plenty of CH$_3$CN and dried at 50°C to afford **16**. **17** was eluted with CH$_2$Cl$_2$-CH$_3$OH (10:1, R_f = 0.2) and purified by the same procedure as for **16**.

2,3,9,10,16,17,23,24-Octakis(3,5-di-*tert*-butylphenoxy)phthalocyanine (16). Grass-green powder; yield: 958 mg (446 μmol, 44% with respect to **7**). ^{1}H NMR: δ_H (300 MHz, CDCl$_3$): 8.97 (s, 8H), 7.18 (t, *J* = 1.7 Hz, 8H), 7.06 (d, *J* = 1.7 Hz, 16H), 1.26 (s, 144H). IR (KBr): v/cm^{-1}: 2963, 1608, 1588, 1461, 1440, 1423, 1395, 1316, 1298, 1270, 1198, 1087, 1012, 961, 706. UV-vis (CHCl$_3$): λ_{max}/nm (log ε): 292 (4.7), 348 (4.8), 396 (4.6), 608 (4.5), 641 (4.6), 670 (5.1), 705 (5.2). MS (MALDI, dithranol as matrix): *m/z*: calcd. for [M+H]$^+$: 2148.38, found: 2148.38. CHN analysis: calcd. (%) for C$_{144}$H$_{178}$N$_8$O$_8$: C, 80.48; H, 8.35; N, 5.21, found: C, 80.82; H, 8.58; N, 5.07. TGA shows no loss of solvent.
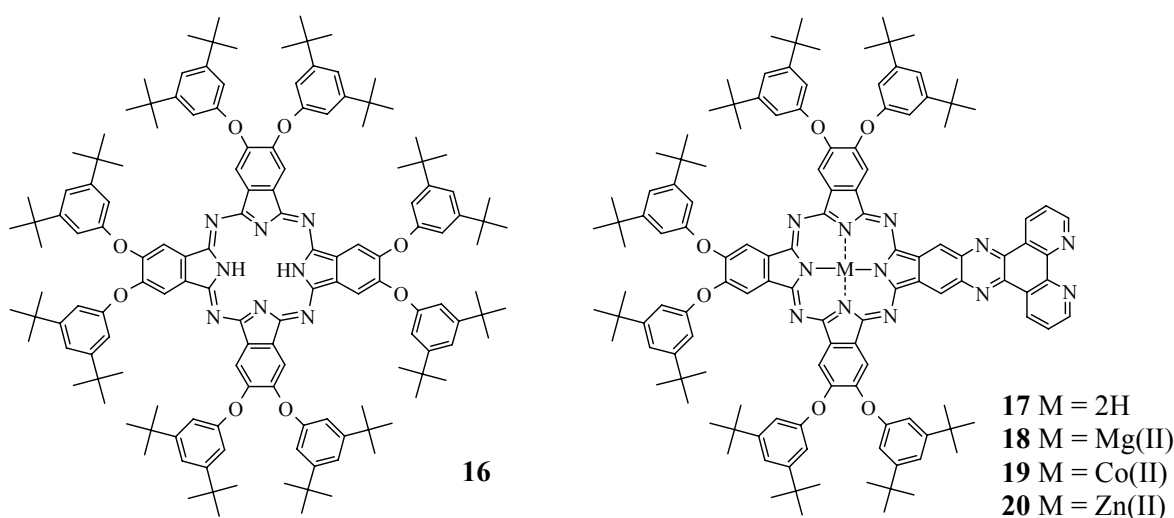
16

17 M = 2H
18 M = Mg(II)
19 M = Co(II)
20 M = Zn(II)

2,3,9,10,16,17-Hexakis(3,5-di-*tert*-butylphenoxy)-1',4',8',9'-tetraazatriphenyleno[2,3-*c$_I$*]-phthalocyanine (17). Green powder; yield: 274 mg (141 μmol, 16% with respect to **2**). ^{1}H NMR: δ_H (300 MHz, CDCl$_3$): 9.40 (s, 2H), 9.26-9.23 (m, 2H), 9.02 (s, 2H), 9.00 (s, 2H), 8.76 (s, 2H), 8.61 (s, 2H), 7.30 (t, J = 1.5 Hz, 2H), 7.25-7.18 (m, 8H), 7.15-7.13 (m, 6H), 7.02 (d, J = 1.7 Hz, 4H), 1.38 (s, 36H), 1.29 (s, 36H), 1.26 (s, 36H). IR (KBr): ν/cm^{-1}: 3436, 2963, 1608, 1588, 1477, 1461, 1443, 1422, 1401, 1363, 1297, 1270, 1246, 1197, 1088, 1012, 960, 705. UV-vis (CHCl$_3$): λ_{max}/nm (log ε): 292 (4.5), 358 (4.8), 412 (4.5), 625 (4.4), 673 (4.7), 694 (4.9), 739 (5.0). MS (MALDI, DCTB as matrix): m/z: calcd. for [M+H]$^+$: 1944.13, found: 1944.11. CHN analysis: calcd. (%) for C$_{128}$H$_{142}$N$_{12}$O$_6$·1.5H$_2$O: C, 77.98; H, 7.41; N, 8.53, found: C, 78.21; H, 7.39; N, 8.27. TGA shows an overall weight loss of 1.4% (calcd. for 1.5 molecules of water: 1.4%).

[2,3,9,10,16,17-Hexakis(3,5-di-*tert*-butylphenoxy)-1',4',8',9'-tetraazatriphenyleno[2,3-*c$_I$*]phthalocyaninato]magnesium(II) (18). A mixture of **17** (34 mg, 17.5 μmol) and MgCl$_2$·6H$_2$O (106 mg, 521 μmol) in DMF (5 mL) was heated at 150°C overnight under nitrogen. Afterwards, the solvent was removed and the blue crude product was dissolved in CHCl$_3$ and chromatographed through a neutral alumina column eluting with CH$_2$Cl$_2$-CH$_3$OH (100:1). After removing the solvents, the product was heated in CH$_3$OH-H$_2$O (1:1; 100 mL) at 70°C. The blue suspension was then filtered, washed with plenty of CH$_3$OH and dried at 80°C to yield a blue solid (29 mg, 14.7 μmol, 84%).

IR (KBr): ν/cm^{-1}: 3437, 2962, 1608, 1587, 1481, 1447, 1422, 1400, 1353, 1297, 1267, 1196, 1087, 1035, 961. UV-vis (CHCl$_3$): λ_{max}/nm: 270, 380, 641, 714, 727. MS (MALDI, dithranol as matrix): m/z: calcd. for [M+H]$^+$: 1966.09, found: 1966.10. CHN analysis: calcd. (%) for C$_{128}$H$_{140}$N$_{12}$O$_6$Mg·4.5H$_2$O: C, 75.07; H, 7.33; N, 8.21, found: C, 74.70; H, 7.10; N, 7.93. TGA shows an overall weight loss of 4.1% (calcd. for 4.5 molecules of water: 4.0%).

[2,3,9,10,16,17-Hexakis(3,5-di-*tert*-butylphenoxy)-1',4',8',9'-tetraazatriphenyleno[2,3-*c$_I$*]phthalocyaninato]cobalt(II) (19). A mixture of **17** (60 mg, 31 μmol) and CoCl$_2$ (44 mg, 339 μmol) in DMF (6 mL) was heated at 150°C for 16 h under nitrogen. Then, ethylenediaminetetraacetic acid disodium salt dihydrate (504 mg, 1.35 mmol) was added to the blue reaction mixture, which was kept at 150°C for a further day. The reaction mixture was then poured into CH$_3$OH-H$_2$O (1:1; 100 mL) and heated to 75°C for 6 h. The precipitate was filtered when hot, washed with plenty of H$_2$O and dried at 80°C to yield a blue solid (58 mg, 29 μmol, 94%).

IR (KBr): ν/cm^{-1}: 3435, 2963, 1608, 1588, 1478, 1459, 1420, 1351, 1297, 1272, 1197, 1094, 1051, 961. UV-vis (CHCl$_3$): λ_{max}/nm: 309, 338, 629, 698. MS (MALDI, dithranol as matrix): *m/z*: calcd. for [M+H]$^+$: 2001.04, found: 2001.04. CHN analysis: calcd. (%) for C$_{128}$H$_{140}$N$_{12}$O$_6$Co·3.5H$_2$O: C, 74.47; H, 7.18; N, 8.14, found: C, 74.44; H, 6.97; N, 8.20. TGA shows an overall weight loss of 2.9% (calcd. for 3.5 molecules of water: 3.1%).

[2,3,9,10,16,17-Hexakis(3,5-di-*tert*-butylphenoxy)-1',4',8',9'-tetraazatriphenyleno[2,3-*c$_1$*]phthalocyaninato]zinc(II) (20). A mixture of **17** (200 mg, 103 μmol) and Zn(OAc)$_2$·2H$_2$O (23 mg, 105 μmol) in DMF (20 mL) was heated at 100°C overnight under nitrogen. Then, ethylenediaminetetraacetic acid disodium salt dihydrate (50 mg, 134 μmol) was added. The blue reaction mixture was kept at 100°C for another 8 h. Upon the addition of CH$_3$OH-H$_2$O (1:1; 150 mL), the mixture was heated to 75°C for 6 h. The precipitate was filtered when hot, washed with plenty of boiling H$_2$O and dried at 80°C to yield a blue solid (203 mg, 101 μmol, 98%).

IR (KBr): ν/cm^{-1}: 3444, 2964, 1609, 1587, 1448, 1423, 1402, 1353, 1297, 1268, 1197, 1092, 1036, 962. UV-vis (CHCl$_3$): λ_{max}/nm: 377, 638, 708, 726. MS (MALDI, dithranol as matrix): *m/z*: calcd. for [M+H]$^+$: 2006.04, found: 2006.04. CHN analysis: calcd. (%) for C$_{128}$H$_{140}$N$_{12}$O$_6$Zn·1.2H$_2$O: C, 75.75; H, 7.07; N, 8.28, found: C, 75.62; H, 7.12; N, 8.22. TGA shows an overall weight loss of 1.0% (calcd. for 1.2 molecules of water: 1.1%).

5.7. Synthesis of phthalocyanines with peripherally coordinated Ru(II) complexes

Bis(2,2'-bipyridine){[2,3,9,10,16,17-Hexakis(3,5-di-*tert*-butylphenoxy)-1',4',8',9'-tetra-azatriphenyleno[2,3-*c$_1$*]phthalocyaninato]zinc(II)}ruthenium(II) dihexafluorophosphate (21). A mixture of **17** (66 mg, 34 μmol) and ZnCl$_2$ (19 mg, 139 μmol) in DMF (4 mL) was heated at 160°C for 3 h under nitrogen. Upon the addition of [Ru(bpy)$_2$Cl$_2$]·2H$_2$O (35 mg, 67 μmol), the blue reaction mixture was refluxed for another 4 h. Then, the DMF was removed under reduced pressure and the residue was dissolved in a minimum amount of CHCl$_3$. The green solution was subjected to a neutral alumina column. A blue and a purple fraction were removed by eluting with CH$_2$Cl$_2$-CH$_3$OH (20:1). The desired product was isolated using CH$_2$Cl$_2$-CH$_3$OH (15:1, R_f = 0.4) as eluent. After the solvents were removed, the green solid was dissolved in a minimum amount of EtOH and filtered. An aqueous solution of NH$_4$PF$_6$ (120 mg, 736 μmol) was added to the stirred green solution. The resulting precipitate was then

filtered and washed with plenty of H_2O. The green solid was collected and dried at 80°C (53 mg, 20 μmol, 58%).

IR (KBr): v/cm^{-1}: 2962, 1607, 1585, 1447, 1422, 1403, 1297, 1269, 1196, 1093, 1035, 961, 845, 558. UV-vis (CHCl$_3$): λ_{max}/nm: 287, 368, 637, 701. MS (ESI, CH$_3$OH): *m/z*: calcd. for $[M-2PF_6]^{2+}$: 1209.54, found: 1209.54. CHN analysis: calcd. (%) for C$_{148}$H$_{156}$N$_{16}$O$_6$F$_{12}$P$_2$RuZn·4H$_2$O: C, 63.86; H, 5.94; N, 8.05, found: C, 64.18; H, 5.92; N, 7.80. TGA shows an overall weight loss of 3.0% (calcd. for 4 molecules of water: 2.6%).
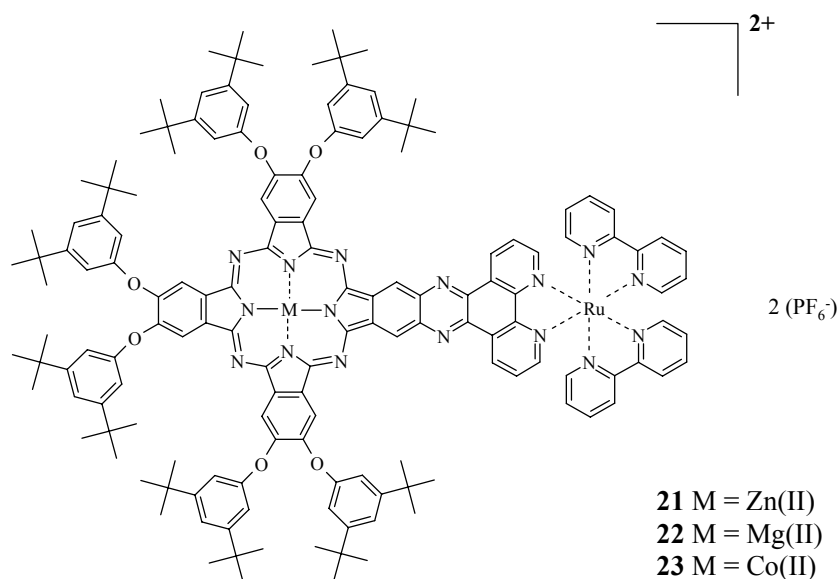
21 M = Zn(II)
22 M = Mg(II)
23 M = Co(II)

Bis(2,2'-bipyridine){[2,3,9,10,16,17-Hexakis(3,5-di-*tert*-butylphenoxy)-1',4',8',9'-tetra-azatriphenyleno[2,3-*c$_1$*]phthalocyaninato]magnesium(II)}ruthenium(II) dihexafluorophosphate (22). Magnesium chloride hexahydrate (62 mg, 305 μmol) and **17** (30 mg, 15 μmol) in DMF (3 mL) were refluxed at 160°C overnight under nitrogen. Then, [Ru(bpy)$_2$Cl$_2$]·2H$_2$O (16 mg, 31 μmol) was added and the reaction mixture was stirred at 160°C for an additional 10 h. The DMF was then removed by rotary evaporation and the crude product was dissolved in CHCl$_3$. The chromatographic procedure and the anion exchange process was carried out as described for **21**. The green solid was collected and dried at 80°C (28 mg, 11 μmol, 68%).

IR (KBr): v/cm^{-1} 3436, 2962, 1607, 1586, 1447, 1422, 1401, 1297, 1268, 1196, 1088, 1034, 960, 845, 558. UV-vis (CHCl$_3$): λ_{max}/nm: 286, 371, 640, 704. MS (ESI, CH$_3$OH): *m/z*: calcd. for $[M-2PF_6]^{2+}$: 1189.57, found: 1189.56. CHN analysis: calcd. (%) for C$_{148}$H$_{156}$N$_{16}$O$_6$F$_{12}$MgP$_2$Ru·5H$_2$O: C, 64.40; H, 6.06; N, 8.12, found: C, 64.56; H, 5.91; N, 7.88. TGA shows an overall weight loss of 3.4% (calcd. for 5 molecules of water: 3.3%).

Bis(2,2'-bipyridine){[2,3,9,10,16,17-Hexakis(3,5-di-*tert*-butylphenoxy)-1',4',8',9'-tetra-azatriphenyleno[2,3-*c₁*]phthalocyaninato]cobalt(II)}ruthenium(II) **dihexafluorophos-phate (23)**. A mixture of **19** (40 mg, 20 μmol) and *cis*-[Ru(bpy)$_2$Cl$_2$]·2H$_2$O (21 mg, 40 μmol) in DMF (3 mL) was refluxed at 160°C for 20 h under nitrogen. Then, the DMF was removed under reduced pressure and the bluish green solid was dissolved in a minimum amount of CHCl$_3$. The solution was chromatographed through a neutral alumina column. The eluent, CH$_2$Cl$_2$-CH$_3$OH, was changed from an initial ratio of 25:1 to 20:1 to 15:1 (R_f = 0.3). Solvents were removed from the bluish green fractions, the resulting solid was dissolved in a minimum amount of ethanol and filtered. An aqueous solution of NH$_4$PF$_6$ (100 mg, 613 μmol) was added to the green solution and stirred at r.t. until precipitation was complete. After adding 50 mL of water, the green suspension was filtered, washed with plenty of water and dried at 80°C (34 mg, 13 μmol, 63%).

IR (KBr): ν/cm^{-1}: 3435, 2956, 1607, 1586, 1448, 1416, 1396, 1350, 1296, 1272, 1196, 1097, 1052, 960, 843, 558. UV-vis (CHCl$_3$): λ$_{max}$/nm: 290, 336, 630, 693. MS (ESI, CH$_3$OH): *m/z*: calcd. for [M-2PF$_6$]$^{2+}$: 1207.04, found: 1207.04. CHN analysis: calcd. (%) for C$_{148}$H$_{156}$N$_{16}$O$_6$CoF$_{12}$P$_2$Ru·3H$_2$O: C, 64.43; H, 5.92; N, 8.12, found: C, 64.44; H, 5.92; N, 8.06. TGA shows an overall weight loss of 2.1% (calcd. for 3 molecules of water: 2.0%).

cis*-Bis(1,10-phenanthroline-5,6-dione)-dichlororuthenium(II) **(24).** A mixture of RuCl$_3$·3H$_2$O (187 mg, 715 μmol), 1,10-phenanthroline-5,6-dione (300 mg, 1.43 mmol) and lithium chloride (210 mg, 4.95 mmol) in DMF (4 mL) was heated at 140°C for 8h under nitrogen. After cooling to r.t., acetone (25 mL) was added to the purple-red solution, which was then stored at 0°C overnight. The precipitate was filtered, washed with water (until the filtrate was colorless) and dried at 50°C to yield a dark brown solid (250 mg, 422 μmol, 59%).[185]

^{1}H NMR: δ$_H$ (300 MHz, DMSO-d$_6$): 10.11 (dd, *J* = 5.6 Hz and 1.3 Hz, 2H), 8.48 (dd, *J* = 7.7 Hz and 1.3 Hz, 2H), 8.10 (dd, *J* = 7.9 Hz and 1.3 Hz, 2H), 8.01 (dd, *J* = 7.9 Hz and 5.6 Hz, 2H), 7.77 (dd, *J* = 5.6 Hz and 1.3 Hz, 2H), 7.34 (dd, *J* = 7.7 Hz and 5.6 Hz, 2H). IR (KBr): ν/cm^{-1}: 3422, 3068, 3005, 1692 (C=O), 1660, 1595, 1558, 1424, 1313, 1299, 1283, 1256, 1104, 1070, 938, 834, 729.

Bis(1,10-phenanthroline-5,6-dione){[2,3,9,10,16,17-Hexakis(3,5-di-*tert*-butylphenoxy)-1',4',8',9'-tetraazatriphenyleno[2,3-*c₁*]phthalocyaninato]zinc(II)}ruthenium(II) dichloride (25). A mixture of **20** (79 mg, 39 μmol) and **24** (46 mg, 78 μmol) in DMF (8 mL) was heated at 140°C for 8 h under nitrogen. After removing the DMF, the green residue was dissolved in toluene and unreacted **24** was filtered off. The filtrate was concentrated and then subjected to size exclusion chromatography. The product was purified several times by this procedure until all unreacted **20** could be removed (The purity of the different fractions was checked by TLC: Alox, CH_2Cl_2-CH_3OH 15:1). The obtained green solid was redissolved in a minimum of toluene and precipitated by the addition of hexane. The suspension was centrifuged, washed with hexane, and the pellet was dried at 50°C (72 mg, 23 μmol, 70%).

25
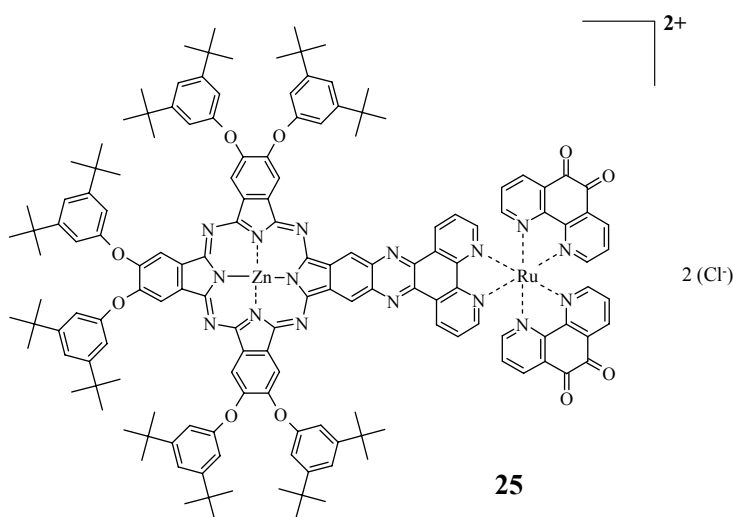
IR (KBr): ν/cm^{-1}: 3432, 2954, 2866, 1701 (C=O), 1607, 1585, 1446, 1422, 1401, 1362, 1350, 1296, 1267, 1194, 1091, 1033, 960, 902, 875, 707. UV-vis (CHCl₃): λ_{max}/nm: 279, 363, 653, 709. MS (ESI, CH_2Cl_2/CH_3OH): *m/z*: calcd. for [M-2Cl]$^{2+}$: 1263.51, found: 1263.53. CHN analysis: calcd. (%) for $C_{152}H_{152}N_{16}O_{10}Cl_2RuZn \cdot 4H_2O$: C, 68.32; H, 6.03; N, 8.39, found: C, 68.63; H, 5.85; N, 8.24. TGA shows an overall weight loss of 2.8% (calcd. for 4 molecules of water: 2.7%).

Bis[4',5'-bis(propylthio)tetrathiafulvaleno[4,5-*i*]dipyrido[3,2-*a*:2',3'-*c*]phenazine]{[2,3,9, 10,16,17-Hexakis(3,5-di-*tert*-butylphenoxy)-1',4',8',9'-tetraazatriphenyleno[2,3-*c₁*]-phthalocyaninato]zinc(II)}ruthenium(II) dichloride (26). To a supersonicated suspension of **25** (50 mg, 19 μmol) in EtOH (8 mL), 5,6-diamino-2-[4,5-bis(propylthio)-1,3-dithio-2-ylidene]-benzo[*d*]-1,3-dithiole (20 mg, 46 μmol) was added. This mixture was refluxed overnight under nitrogen. After removing the solvent, the residue was dissolved in CH_2Cl_2

and chromatographed through a neutral alumina column. The eluent, CH_2Cl_2-CH_3OH, was changed from an initial ratio of 40:1 to 30:1 to 20:1 to 15:1. After removing the solvents, the dark green solid was redissolved in a minimum of CH_2Cl_2 and precipitated by the addition of hexane. The suspension was centrifuged and washed with hexane. The pellet was dried at 50°C (21 mg, 6.2 μmol, 32%). Due to photoinstability in solution, compound **26** was kept in the dark during synthetic and purification procedures.

26
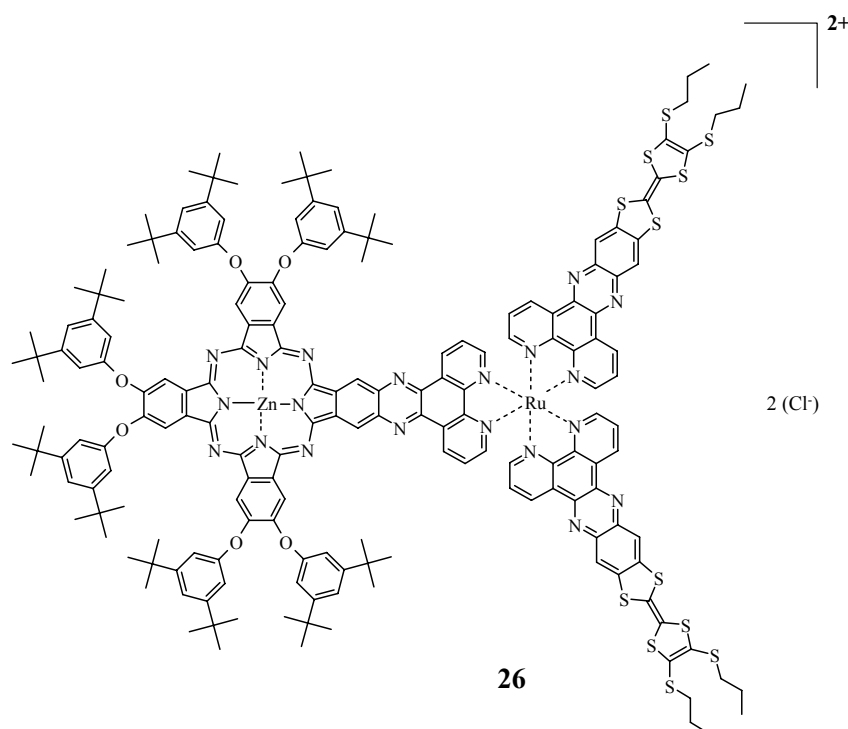
IR (KBr): ν/cm^{-1}: 3437, 2960, 2923, 2853, 1607, 1586, 1445, 1424, 1402, 1349, 1297, 1265, 1195, 1119, 1090, 1034, 961. UV-vis ($CHCl_3$): λ_{max}/nm: 300, 381, 649, 710. MS (ESI, CH_2Cl_2/CH_3OH): *m/z*: calcd. for [M-2Cl]$^{2+}$: 1659.4845, found: 1659.4849. CHN analysis: calcd. (%) for $C_{184}H_{184}N_{20}O_6S_{12}Cl_2RuZn·2H_2O$: C, 64.44; H, 5.52; N, 8.17, found: C, 64.21; H, 6.11; N, 7.23. TGA shows an overall weight loss of 1.0% (calcd. for 2 molecules of water: 1.1%).

5.8. Synthesis of a symmetric zinc phthalocyanine for STM imaging

[2,3,9,10,16,17,23,24-Octakis(3,5-di-*tert*-butylphenoxy)phthalocyaninato]zinc(II) (27). A mixture of **16** (200 mg, 93 μmol) and $Zn(OAc)_2·2H_2O$ (61 mg, 278 μmol) in 1-pentanol (10 mL) was heated at 100°C for 15 h under nitrogen. The reaction mixture was then poured into hexane (100 mL) and stored in the freezer for 1 h. The resulting precipitate was filtered and washed with hexane. Afterwards, the crude product was dissolved in $CHCl_3$ and subjected to

a silica column. Unreacted starting material **16** was removed by elution with CH_2Cl_2. The desired product **27** was isolated using CH_2Cl_2-CH_3OH (20:1) as eluent. After removing the solvents, the green solid was refluxed in CH_3CN (50 mL), filtered hot and washed with boiling CH_3CN. The product was dried at 80°C (130 mg, 59 μmol, 63%).

27
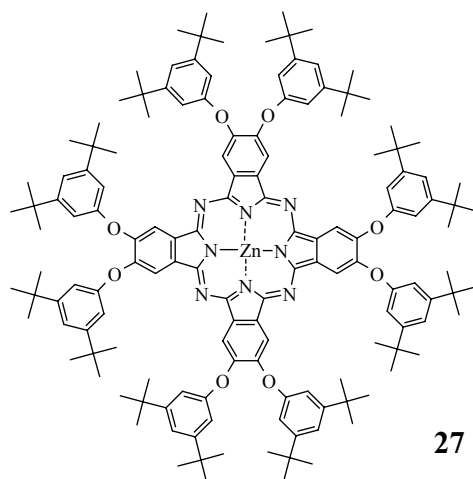
^{1}H NMR: δ_H (300 MHz, CDCl$_3$): 8.99 (s, 8H), 7.17 (t, J = 1.7 Hz, 8H), 7.05 (d, J = 1.7 Hz, 16H), 1.25 (s, 144H). IR (KBr): ν/cm^{-1}: 3436, 2964, 1609, 1587, 1479, 1450, 1422, 1401, 1297, 1270, 1198, 1090, 1036, 961. UV-vis (CHCl$_3$): λ_{max}/nm (log ε): 281 (4.8), 356 (4.9), 615 (4.2), 682 (5.3). MS (MALDI, DCTB as matrix): m/z: calcd. for [M+H]$^+$: 2210.30, found: 2210.25. CHN analysis: calcd. (%) for $C_{144}H_{176}N_8O_8Zn\cdot2H_2O$: C, 76.92; H, 8.07; N, 4.98, found: C, 76.90; H, 8.20; N, 4.85. TGA shows an overall weight loss of 1.4% (calcd. for 2 molecules of water: 1.6%).

References

[1]   N. B. McKeown, *Phthalocyanine Materials: Synthesis, Structure and Function*, Cambridge University Press, Cambridge UK, **1998**.

[2]   *The Porphyrin Handbook, Vol. 19* (Eds.: K. M. Kadish, K. M. Smith, R. Guilard), Academic Press, San Diego, California, **2003**.

[3]   K.-W. Poon, Y. Yan, X.-Y. Li, D. K. P. Ng, *Organometallics* **1999**, *18*, 3528.

[4]   M. Quintiliani, E. M. García-Frutos, A. Gouloumis, P. Vázquez, I. Ledoux-Rak, J. Zyss, C. G. Claessens, T. Torres, *Eur. J. Org. Chem.* **2005**, 3911.

[5]   C. Loosli, *PhD thesis* **2005**, University of Berne.

[6]   A. González-Cabello, P. Vázquez, T. Torres, D. M. Guldi, *J. Org. Chem.* **2003**, *68*, 8635.

[7]   M. Kimura, T. Hamakawa, T. Muto, K. Hanabusa, H. Shirai, N. Kobayashi, *Tetrahedron Lett.* **1998**, *39*, 8471.

[8]   M. Kimura, T. Hamakawa, K. Hanabusa, H. Shirai, N. Kobayashi, *Inorg. Chem.* **2001**, *40*, 4775.

[9]   S. M. Contakes, S. T. Beatty, K. K. Dailey, T. B. Rauchfuss, D. Fenske, *Organometallics* **2000**, *19*, 4767.

[10]   R. G. Wollmann, D. N. Hendrickson, *Inorg. Chem.* **1977**, *16*, 3079.

[11]   P. D. W. Boyd, A. K. Burrell, W. M. Campbell, P. A. Cocks, K. C. Gordon, G. B. Jameson, D. L. Officer, Z. Zhao, *Chem. Commun.* **1999**, 637.

[12]   Z. Jin, K. Nolan, C. R. McArthur, A. B. P. Lever, C. C. Leznoff, *J. Organomet. Chem.* **1994**, *468*, 205.

[13]   K.-W. Poon, W. Liu, P.-K. Chan, Q. Yang, T.-W. D. Chan, T. C. W. Mak, D. K. P. Ng, *J. Org. Chem.* **2001**, *66*, 1553.

[14]   M. J. Cook, G. Cooke, A. Jafari-Fini, *J. Chem. Soc., Chem. Commun.* **1995**, 1715.

[15]   A. Ambroise, R. W. Wagner, P. D. Rao, J. A. Riggs, P. Hascoat, J. R. Diers, J. Seth, R. K. Lammi, D. F. Bocian, D. Holton, J. S. Lindsey, *Chem. Mater.* **2001**, *13*, 1023.

[16]   A. González, P. Vázquez, T. Torres, *Tetrahedron Lett.* **1999**, *40*, 3263.

[17]   A. González-Cabello, C. G. Claessens, G. Martin-Fuch, I. Ledoux-Rack, P. Vázquez, J. Zyss, F. Agulló-López, T. Torres, *Synth. Met.* **2003**, *137*, 1487.

[18]   S. Dabak, Ö. Bekaroğlu, *New J. Chem.* **1997**, *21*, 267.

[19]   A. González-Cabello, P. Vázquez, T. Torres, *J. Organomet. Chem.* **2001**, *637-639*, 751.

[20]   T. G. Linssen, K. Dürr, M. Hanack, A. Hirsch, *J. Chem. Soc., Chem. Commun.* **1995**, 103.

[21]   K. Dürr, S. Fiedler, T. Linssen, A. Hirsch, M. Hanack, *Chem. Ber.* **1997**, *130*, 1375.

[22]   W. F. Qiu, Y. Q. Liu, C. Y. Pan, D. Zhu, *Chin. Chem. Lett.* **1997**, *8*, 811.

[23]   W. Huang, S. Wang, R. Liang, Q. Gong, W. Qiu, Y. Liu, D. Zhu, *Chem. Phys. Lett.* **2000**, *324*, 354.

[24]   Z. Tian, C. He, C. Liu, W. Yang, J. Yao, Y. Nie, Q. Gong, Y. Liu, *Mater. Chem. Phys.* **2005**, *94*, 444.

[25]   A. Gouloumis, S.-G. Liu, Á. Sastre, P. Vázquez, L. Echegoyen, T. Torres, *Chem. Eur. J.* **2000**, *6*, 3600.

[26]   D. M. Guldi, A. Gouloumis, P. Vázquez, T. Torres, *Chem. Commun.* **2002**, 2056.

[27]   D. M. Guldi, I. Zilbermann, A. Gouloumis, P. Vázquez, T. Torres, *J. Phys. Chem. B* **2004**, *108*, 18485.

[28]   D. M. Guldi, A. Gouloumis, P. Vázquez, T. Torres, V. Georgakilas, M. Prato, *J. Am. Chem. Soc.* **2005**, *127*, 5811.

[29]   E. Bruneau, D. Lavabre, G. Levy, J. C. Micheau, *J. Chem. Educ.* **1992**, *69*, 833.

[30]   A. de la Escosura, M. V. Martínez-Díaz, D. M. Guldi, T. Torres, *J. Am. Chem. Soc.* **2006**, *128*, 4112.

[31]   M. A. Loi, P. Denk, H. Hoppe, H. Neugebauer, C. Winder, D. Meissner, C. Brabec, N. S. Sariciftci, A. Gouloumis, P. Vázquez, T. Torres, *J. Mater. Chem.* **2003**, *13*, 700.

[32]   H. Neugebauer, M. A. Loi, C. Winder, N. S. Sariciftci, G. Cerullo, A. Gouloumis, P. Vázquez, T. Torres, *Sol. Energy Mater. Sol. Cells* **2004**, *83*, 201.

[33]   Á. Sastre, A. Gouloumis, P. Vázquez, T. Torres, V. Doan, B. J. Schwartz, F. Wudl, L. Echegoyen, J. Rivera, *Org. Lett.* **1999**, *1*, 1807.

[34]   Y. Chen, M. E. El-Khouly, M. Sasaki, Y. Araki, O. Ito, *Org. Lett.* **2005**, *7*, 1613.

[35]   B. Ballesteros, G. de la Torre, T. Torres, G. L. Hug, G. M. A. Rahman, D. M. Guldi, *Tetrahedron* **2006**, *62*, 2097.

[36]   K. N. Kim, C. S. Choi, K.-Y. Kay, *Tetrahedron Lett.* **2005**, *46*, 6791.

[37]   D. M. Guldi, J. Ramey, M. V. Martínez-Díaz, A. de la Escosura, T. Torres, T. Da Ros, M. Prato, *Chem. Commun.* **2002**, 2774.

[38]   M. E. El-Khouly, L. M. Rogers, M. E. Zandler, G. Suresh, M. Fujitsuka, O. Ito, F. D´Souza, *ChemPhysChem* **2003**, *4*, 474.

[39]   F. D´Souza, S. Gadde, M. E. El-Khouly, M. E. Zandler, Y. Araki, O. Ito, *J. Porphyrins Phthalocyanines* **2005**, *9*, 698.

[40]   M. V. Martínez-Díaz, N. S. Fender, M. S. Rodríguez-Morgade, M. Gómez-López, F. Diederich, L. Echegoyen, J. F. Stoddart, T. Torres, *J. Mater. Chem.* **2002**, *12*, 2095.

[41]   H. Imahori, Y. Sekiguchi, Y. Kashiwagi, T. Sato, Y. Araki, O. Ito, H. Yamada, S. Fukuzumi, *Chem. Eur. J.* **2004**, *10*, 3184.

[42]   Y. Kashiwagi, K. Ohkubo, J. A. McDonald, I. M. Blake, M. J. Crossley, Y. Araki, O. Ito, H. Imahori, S. Fukuzumi, *Org. Lett.* **2003**, *5*, 2719.

[43]   K. Ohkubo, H. Kotani, J. Shao, Z. Ou, K. M. Kadish, G. Li, R. K. Pandey, M. Fujitsuka, O. Ito, H. Imahori, S. Fukuzumi, *Angew. Chem. Int. Ed.* **2004**, *43*, 853.

[44]   J. Li, J. S. Lindsey, *J. Org. Chem.* **1999**, *64*, 9101.

[45]   S. Gaspard, C. Giannotti, P. Maillard, C. Schaeffer, T.-H. Tran-Thi, *J. Chem. Soc., Chem. Commun.* **1986**, 1239.

[46]   T. H. Tran-Thi, C. Desforge, C. Thiec, S. Gaspard, *J. Phys. Chem.* **1989**, *93*, 1226.

[47]   K. Dou, J. Zhang, W. Xu, S. Huang, J. Yu, X. Xu, *J. Lumin.* **1994**, 465.

[48]   H.-J. Tian, Q.-F. Zhou, S.-Y. Shen, H.-J. Xu, *Chin. J. Chem.* **1996**, *14*, 412.

[49]   X.-Y. Li, Q.-F. Zhou, H.-J. Tian, H.-J. Xu, *Chin. J. Chem.* **1998**, *16*, 97.

[50]   J. P. C. Tomé, A. M. V. M. Pereira, C. M. A. Alonso, M. G. P. M. S. Neves, A. C. Tomé, A. M. S. Silva, J. A. S. Cavaleiro, M. V. Martínez-Díaz, T. Torres, G. M. A. Rahman, J. Ramey, D. M. Guldi, *Eur. J. Org. Chem.* **2006**, 257.

[51]   S. I. Yang, J. Li, H. S. Cho, D. Kim, D. F. Bocian, D. Holten, J. S. Lindsey, *J. Mater. Chem.* **2000**, *10*, 283.

[52]   K. Kameyama, A. Satake, Y. Kobuke, *Tetrahedron Lett.* **2004**, *45*, 7617.

[53]   N. Kobayashi, Y. Nishiyama, T. Ohya, M. Sato, *J. Chem. Soc., Chem. Commun.* **1987**, 390.

[54]   N. Kobayashi, T. Ohya, M. Sato, S.-I. Nakajima, *Inorg. Chem.* **1993**, *32*, 1803.

[55]   J. Li, J. R. Diers, J. Seth, S. I. Yang, D. F. Bocian, D. Holten, J. S. Lindsey, *J. Org. Chem.* **1999**, *64*, 9090.

[56]   Z. Zhao, K. I. Ozoemena, D. M. Maree, T. Nyokong, *Dalton Trans.* **2005**, 1241.

[57]   Z. Zhao, A. O. Ogunsipe, M. D. Maree, T. Nyokong, *J. Porphyrins Phthalocyanines* **2005**, *9*, 186.

[58]   Z. Zhao, T. Nyokong, D. M. Maree, *Dalton Trans.* **2005**, 3732.

[59]   L. Li, S. Shen, Q. Yu, Q. Zhou, H. Xu, *J. Chem. Soc., Chem. Commun.* **1991**, 619.

[60] M. A. Miller, R. K. Lammi, S. Prathapan, D. Holton, J. S. Lindsey, *J. Org. Chem.* **2000**, *65*, 6634.

[61] C. C. Leznoff, S. Greenberg, S. M. Marcuccio, P. C. Minor, P. Seymour, A. B. P. Lever, K. B. Tomer, *Inorg. Chim. Acta* **1984**, *89*, L35.

[62] R. R. Durand Jr., C. S. Bencosme, J. P. Collman, F. C. Anson, *J. Am. Chem. Soc.* **1983**, *105*, 2710.

[63] Y. Le Mest, M. L'Her, J. P. Collman, N. H. Hendricks, L. McElwee-White, *J. Am. Chem. Soc.* **1986**, *108*, 533.

[64] C. C. Leznoff, S. M. Marcuccio, S. Greenberg, A. B. P. Lever, K. B. Tomer, *Can. J. Chem.* **1985**, *63*, 623.

[65] W. Liu, M. R. Hempstead, W. A. Nevin, M. Melník, A. B. P. Lever, C. C. Leznoff, *J. Chem. Soc., Dalton Trans.* **1987**, 2511.

[66] C. C. Leznoff, H. Lam, W. A. Nevin, N. Kobayashi, P. Janda, A. B. P. Lever, *Angew. Chem., Int. Ed.* **1987**, *26*, 1021.

[67] N. Kobayashi, H. Lam, W. A. Nevin, P. Janda, C. C. Leznoff, A. B. P. Lever, *Inorg. Chem.* **1990**, *29*, 3415.

[68] W. A. Nevin, W. Liu, S. Greenberg, M. R. Hempstead, S. M. Marcuccio, M. Melník, C. C. Leznoff, A. B. P. Lever, *Inorg. Chem.* **1987**, *26*, 891.

[69] W. A. Nevin, M. R. Hempstead, W. Liu, C. C. Leznoff, A. B. P. Lever, *Inorg. Chem.* **1987**, *26*, 570.

[70] P. Janda, N. Kobayashi, P. R. Auburn, H. Lam, C. C. Leznoff, A. B. P. Lever, *Can. J. Chem.* **1989**, *67*, 1109.

[71] S. Vigh, H. Lam, P. Janda, A. B. P. Lever, C. C. Leznoff, R. L. Cerny, *Can. J. Chem.* **1991**, *69*, 1457.

[72] C. C. Leznoff, *Can. J. Chem.* **2000**, *78*, 167.

[73] D. Lelièvre, O. Damette, J. Simon, *J. Chem. Soc., Chem. Commun.* **1993**, 939.

[74] J. Yang, M. R. van de Mark, *Tetrahedron Lett.* **1993**, *34*, 5223.

[75] N. Kobayashi, H. Lam, W. A. Nevin, P. Janda, C. C. Leznoff, T. Koyama, A. Monden, H. Shirai, *J. Am. Chem. Soc.* **1994**, *116*, 879.

[76] K. Ishii, N. Kobayashi, Y. Higashi, T. Osa, D. Lelièvre, J. Simon, S. Yamauchi, *Chem. Commun.* **1999**, 969.

[77] N. Kobayashi, T. Fukuda, D. Lelièvre, *Inorg. Chem.* **2000**, *39*, 3632.

[78] M. Calvete, M. Hanack, *Eur. J. Org. Chem.* **2003**, 2080.

[79] M. Handa, N. Kataoka, Y. Ito, T. Tonomura, I. Hiromitsu, T. Sugimori, K. Sogabe, K. Kasuga, *Bull. Chem. Soc. Jpn.* **2004**, *77*, 1647.

[80] M. J. F. Calvete, D. Dini, S. R. Flom, M. Hanack, R. G. S. Pong, J. S. Shirk, *Eur. J. Org. Chem.* **2005**, 3499.

[81] S. Makarov, C. Litwinski, E. A. Ermilov, O. Suvorova, B. Röder, D. Wöhrle, *Chem. Eur. J.* **2006**, *12*, 1468.

[82] A. de la Escosura, M. V. Martínez-Díaz, P. Thordarson, A. E. Rowan, R. J. M. Nolte, T. Torres, *J. Am. Chem. Soc.* **2003**, *125*, 12300.

[83] G. de la Torre, A. Gouloumis, P. Vázquez, T. Torres, *Angew. Chem., Int. Ed.* **2001**, *40*, 2895.

[84] D. González-Rodríguez, C. G. Claessens, T. Torres, S. Liu, L. Echegoyen, N. Vila, S. Nonell, *Chem. Eur. J.* **2005**, *11*, 3881.

[85] X. Li, L. E. Sinks, B. Rybtchinski, M. R. Wasielewski, *J. Am. Chem. Soc.* **2004**, *126*, 10810.

[86] S. Fukuzumi, K. Ohkubo, J. Ortiz, A. M. Gutiérrez, F. Fernández-Lázaro, Á. Sastre-Santos, *Chem. Commun.* **2005**, 3814.

[87] T. Ceyhan, A. Altindal, A. R. Özkaya, M. K. Erbil, B. Salih, Ö. Bekaroğlu, *Chem. Commun.* **2006**, 320.

[88] G. de la Torre, M.V. Martínez-Díaz, P. R. Ashton, T. Torres, *J. Org. Chem.* **1998**, *63*, 8888.

[89] A. Gouloumis, S.-G. Liu, P. Vázquez, L. Echegoyen, T. Torres, *Chem. Commun.* **2001**, 399.

[90] G. de la Torre, W. Blau, T. Torres, *Nanotechnology* **2003**, *14*, 765.

[91] Z. L. Yang, H. Z. Chen, L. Cao, H. Y. Li, M. Wang, *Chin. Chem. Lett.* **2004**, *15*, 717.

[92] H.-B. Xu, H.-Z. Chen, M.-M. Shi, R. Bai, M. Wang, *Mater. Chem. Phys.* **2005**, *94*, 342.

[93] N. B. McKeown, I. Chambrier, M. J. Cook, *J. Chem. Soc. Perkin Trans. 1* **1990**, 1169.

[94] J. A. Thompson, K. Murata, D. C. Miller, J. L. Stanton, W. E. Broderick, B. M. Hoffman, J. A. Ibers, *Inorg. Chem.* **1993**, *32*, 3546.

[95] D. Wöhrle, M. Eskes, K. Shigehara, A. Yamada, *Synthesis* **1993**, 194.

[96] C. C. Leznoff, T. W. Hall, *Tetrahedron Lett.* **1982**, *23*, 3023.

[97] M. S. Rodríguez-Morgade, G. de la Torre, T. Torres in *The Porphyrin Handbook, Vol. 15* (Eds.: K. M. Kadish, K. M. Smith, R. Guilard), Academic Press, San Diego, California, **2003**, 125.

[98] Y. Ikeda, H. Konami, M. Hatano, K. Mochizuki, *Chem. Lett.* **1992**, 763.

[99] T. G. Linssen, M. Hanack, *Chem. Ber.* **1994**, *127*, 2051.

[100] G. J. Clarkson, N. B. McKeown, K. E. Treacher, *J. Chem. Soc. Perkin Trans. 1* **1995**, 1817.

[101] K. E. Treacher, G. J. Clarkson, Z. Ali-Adib, N. B. McKeown, *Chem. Commun.* **1996**, 73.

[102] S. Rodríguez-Morgade, M. Hanack, *Chem. Eur. J.* **1997**, *3*, 1042.

[103] R. Polley, T. G. Linssen, P. Stihler, M. Hanack, *J. Porphyrins Phthalocyanines* **1997**, *1*, 169.

[104] R. P. Kingsborough, T. M. Swager, *Angew. Chem. Int. Ed.* **2000**, *39*, 2897.

[105] M. Haas, S.-X. Liu, A. Neels, S. Decurtins, *Eur. J. Org. Chem.* **2006**, published online, DOI: 10.1002/ejoc.200600619.

[106] N. Kobayashi, T. Ashida, T. Osa, *Chem. Lett.* **1992**, 2031.

[107] N. B. Subbotin, V. N. Nemykin, Y. Z. Voloshin, *Mendeleev Commun.* **1993**, 121.

[108] J. Yang, M. R. Van de Mark, *J. Heterocycl. Chem.* **1995**, *32*, 1521.

[109] N. Kobayashi, H. Miwa, V. N. Nemykin, *J. Am. Chem. Soc.* **2002**, *124*, 8007.

[110] N. Kobayashi, R. Kondo, S.-I. Nakajima, T. Osa, *J. Am. Chem. Soc.* **1990**, *112*, 9640.

[111] K. Kasuga, T. Idehara, M. Handa, *Inorg. Chim. Acta* **1992**, *196*, 127.

[112] E. Musluoglu, A. Gürek, V. Ahsen, A. Gül, Ö. Bekaroğlu, *Chem. Ber.* **1992**, *125*, 2337.

[113] S. Dabak, A. Gül, Ö. Bekaroğlu, *Chem. Ber.* **1994**, *127*, 2009.

[114] A. Weitemeyer, H. Kliesch, D. Wöhrle, *J. Org. Chem.* **1995**, *60*, 4900.

[115] Á. Sastre, T. Torres, M. Hanack, *Tetrahedron Lett.* **1995**, *36*, 8501.

[116] S. V. Kudrevich, S. Gilbert, J. E. van Lier, *J. Org. Chem.* **1996**, *61*, 5706.

[117] Á. Sastre, B. del Rey, T. Torres, *J. Org. Chem.* **1996**, *61*, 8591.

[118] S. Kudrevich, N. Brasseur, C. La Madeleine, S. Gilbert, J. E. van Lier, *J. Med. Chem.* **1997**, *40*, 3897.

[119] H. Ali, S. K. Sim, J. E. van Lier, *J. Chem. Res. (S)* **1999**, 496.

[120] N. Kobayashi, T. Ishizaki, K. Ishii, H. Konami, *J. Am. Chem. Soc.* **1999**, *121*, 9096.

[121] C. C. Leznoff, T. W. Hall, *Tetrahedron Lett.* **1982**, *23*, 3023.

[122] T. W. Hall, S. Greenberg, C. R. McArthur, B. Khouw, C. C. Leznoff, *Nouv. J. Chim.* **1982**, *6*, 653.

[123] A. Hirth, A. K. Sobbi, D. Wöhrle, *J. Porphyrins Phthalocyanines* **1997**, *1*, 275.

[124] J. G. Young, W. Onyebuagu, *J. Org. Chem.* **1990**, *55*, 2155.

[125] S. Dabak, Ö. Bekaroğlu, *J. Chem. Res. (S)* **1997**, 8.

[126] P. Stihler, B. Hauschel, M. Hanack, *Chem. Ber.* **1997**, *130*, 801.

[127] M. Hanack, P. Stihler, *Eur. J. Org. Chem.* **2000**, 303.

[128] W. J. Youngblood, *J. Org. Chem.* **2006**, *71*, 3345.

[129] C. C. Leznoff, S. Greenberg, B, Khouw, A. B. P. Lever, *Can. J. Chem.* **1987**, *65*, 1705.

[130] S. W. Oliver, T. D. Smith, *J. Chem. Soc. Perkin Trans. 2* **1987**, 1579.

[131] K. J. M. Nolan, M. Hu, C. C. Leznoff, *Synlett* **1997**, 593.

[132] N. Kobayashi, *Chem. Commun.* **1998**, 487.

[133] H. Miwa, N. Kobayashi, *Chem. Lett.* **1999**, 1303.

[134] I. Seotsanyana-Mokhosi, T. Nyokong, *J. Porphyrins Phthalocyanines* **2004**, *8*, 1214.

[135] M. Kimura, H. Ueki, K. Ohta, H. Shirai, N. Kobayashi, *Langmuir* **2006**, *22*, 5051.

[136] Ü. Salan, A. Altindal, M. Bulut, Ö. Bekaroğlu, *Tetrahedron Lett.* **2005**, *46*, 6057.

[137] E. M. Maya, P. Vázquez, T. Torres, *Chem. Commun.* **1997**, 1175.

[138] E. M. Maya, P. Vázquez, T. Torres, *Chem. Eur. J.* **1999**, *5*, 2004.

[139] M. J. Cook, M. J. Heeney, *Chem. Commun.* **2000**, 969.

[140] M. J. Cook, M. J. Heeney, *Chem. Eur. J.* **2000**, *6*, 3958.

[141] E. M. García-Frutos, F. Fernández-Lázaro, E. M. Maya, P. Vázquez, T. Torres, *J. Org. Chem.* **2000**, *65*, 6841.

[142] J. M. Sutton, R. W. Boyle, *Chem. Commun.* **2001**, 2014.

[143] E. M. Maya, P. Vázquez, T. Torres, L. Gobbi, F. Diederich, S. Pyo, L. Echegoyen, *J. Org. Chem.* **2000**, *65*, 823.

[144] R. Jung, K.-H. Schweikart, M. Hanack, *Eur. J. Org. Chem.* **1999**, 1687.

[145] K.-H. Schweikart, M. Hanack, *Eur. J. Org. Chem.* **2000**, 2551.

[146] D. P. Rillema, K. B. Mack, *Inorg. Chem.* **1982**, *21*, 3849.

[147] A. Escuer, T. Comas, J. Ribas, R. Vicente, X. Solans, C. Zanchini, D. Gatteschi, *Inorg. Chim. Acta* **1989**, *162*, 97.

[148] A. Escuer, S. B. Kumar, M. Font-Bardía, X. Solans, R. Vicente, *Inorg. Chim. Acta* **1999**, *286*, 62.

[149] J. Granifo, M. E. Vargas, M. T. Garland, R. Baggio, *Inorg. Chim. Acta* **2000**, *305*, 143.

[150] R. L. Williams, H. N. Toft, B. Winkel, K. J. Brewer, *Inorg. Chem.* **2003**, *42*, 4394.

[151] J. Granifo, M. T. Garland, R. Baggio, *Inorg. Chim. Acta* **2003**, *348*, 263.

[152] M. Cusumano, M. L. Di Pietro, A. Giannetto, F. Nicolò, B. Nordén, P. Lincoln, *Inorg. Chem.* **2004**, *43*, 2416.

[153] E. Rotondo, A. Rotondo, F. Nicolò, M. L. Di Pietro, M. A. Messina, M. Cusumano, *Eur. J. Inorg. Chem.* **2004**, 4710.

[154] M. Newell, J. A. Thomas, *Dalton Trans.* **2006**, 705.

[155] D. M. D'Alessandro, A. C. Topley, M. S. Davies, F. R. Keene, *Chem. Eur. J.* **2006**, *12*, 4873.

[156] J. I. Goldsmith, W. R. Hudson, M. S. Lowry, T. H. Anderson, S. Bernhard, *J. Am. Chem. Soc.* **2005**, *127*, 7502.

[157] C. Chiorboli, S. Fracasso, M. Ravaglia, F. Scandola, S. Campagna, K. L. Wouters, R. Konduri, F. M. MacDonnell, *Inorg. Chem.* **2005**, *44*, 8368.

[158] W. Lu, D. A. Vicic, J. K. Barton, *Inorg. Chem.* **2005**, *44*, 7970.

[159] A. Chouai, S. E. Wicke, C. Turro, J. Bacsa, K. R. Dunbar, D. Wang, R. P. Thummel, *Inorg. Chem.* **2005**, *44*, 5996.

[160] K. K.-W. Lo, C.-K. Chung, N. Zhu, *Chem. Eur. J.* **2006**, *12*, 1500.

[161] B. Carlson, G. D. Phelan, J. B. Benedict, W. Kaminsky, L. Dalton, *Inorg. Chim. Acta* **2006**, *359*, 1093.

[162] J. A. Weinstein, M. T. Tierney, E. S. Davies, K. Base, A. A. Robeiro, M. W. Grinstaff, *Inorg. Chem.* **2006**, *45*, 4544.

[163] C. Rajput, R. Rutkaite, L. Swanson, I. Haq, J. A. Thomas, *Chem. Eur. J.* **2006**, *12*, 4611.

[164] A. Delgadillo, M. Arias, A. M. Leiva, B. Loeb, G. J. Meyer, *Inorg. Chem.* **2006**, *45*, 5721.

[165] J. Rusanova, M. Pilkington, S. Decurtins, *Chem. Commun.* **2002**, 2236.

[166] J. Rusanova, S. Decurtins, E. Rusanov, H. Stoeckli-Evans, S. Delahaye, A. Hauser, *J. Chem. Soc., Dalton Trans.* **2002**, 4318.

[167] S. E. Maree, T. Nyokong, *J. Porphyrins Phthalocyanines* **2001**, *5*, 782.

[168] M. J. Plater, A. Jeremiah, G. Bourhill, *J. Chem. Soc., Perkin Trans. 1* **2002**, 91.

[169] N. Kobayashi, H. Konami in *Phthalocyanines: Properties and Applications, Vol. 4* (Eds.: C. C. Leznoff, A. B. P. Lever), VCH Publishers, New York, **1996**, 343.

[170] S. C. Rasmussen, M. M. Richter, E. Yi, H. Place, K. J. Brewer, *Inorg. Chem.* **1990**, *29*, 3926.

[171] A. Escuer, R. Vicente, T. Comas, J. Ribas, M. Gomez, X. Solans, *Inorg. Chim. Acta* **1990**, *177*, 161.

[172] F. Nicolò, M. Cusumano, M. L. Di Pietro, R. Scopelliti, G. Bruno, *Acta Crystallogr. Sect. C* **1998**, *54*, 485.

[173] O.-S. Jung, S. H. Park, Y. J. Kim, Y.-A. Lee, H. G. Jang, U. Lee, *Inorg. Chim. Acta* **2001**, *312*, 93.

[174] S. Y. Al-Raqa, M. J. Cook, D. L. Hughes, *Chem. Commun.* **2003**, 62.

[175] E. V. Kudrik, E. M. Bauer, C. Ercolani, A. Chiesi-Villa, C. Rizzoli, A. Gaberkorn, P. A. Stuzhin, *Mendeleev Commun.* **2001**, *11*, 45.

[176] M. J. Crossley, P. L. Burn, S. J. Langford, J. K. Prashar, *J. Chem. Soc., Chem. Commun.* **1995**, 1921.

[177] A. G. Montalban, E. G. Sakellariou, E. Riguet, Q. J. McCubbin, A. G. M. Barrett, B. M. Hoffman, *Inorg. Chim. Acta* **2001**, *317*, 143.

[178] K. Ishii, N. Kobayashi in *The Porphyrin Handbook, Vol. 16* (Eds.: K. M. Kadish, K. M. Smith, R. Guilard), Academic Press, San Diego, California, **2003**, 1.

[179] A. W. Snow in *The Porphyrin Handbook, Vol. 17* (Eds.: K. M. Kadish, K. M. Smith, R. Guilard), Academic Press, San Diego, California, **2003**, 129.

[180] R. R. Millard, B. I. Greene, *J. Phys. Chem.* **1985**, *89*, 2976.

[181] A. V. Nikolaitchik, M. A. J. Rodgers, *J. Phys. Chem. A* **1999**, *103*, 7597.

[182] A. A. Abdel-Shafi, F. Wilkinson, *Phys. Chem. Chem. Phys.* **2002**, *4*, 248.

[183] M. E. El-Khouly, O. Ito, P. M. Smith, F. D'Souza, *J. Photochem. Photobiol. C* **2004**, *5*, 79.

[184] C. Goze, S.-X. Liu, C. Leiggener, A. Hauser, S. Decurtins, *unpublished results*.

[185] C. A. Goss, H. Abruña, *Inorg. Chem.* **1985**, *24*, 4263.

[186] B. P. Sullivan, D. J. Salmon, T. J. Meyer, *Inorg. Chem.* **1978**, *17*, 3334.

[187] E. M. Bauer, C. Ercolani, P. Galli, I. A. Popkova, P. A. Stuzhin, *J. Porphyrins Phthalocyanines* **1999**, *3*, 371.

[188] N. Margiotta, V. Bertolasi, F. Capitelli, L. Maresca, A. G. G. Moliterni, F. Vizza, G. Natile, *Inorg. Chim. Acta* **2004**, *357*, 149.

[189] G. Torres-Garcia, H. Luftmann, C. Wolff, J. Mattay, *J. Org. Chem.* **1997**, *62*, 2752.

[190] C. Jia, S.-X. Liu, C. Tanner, C. Leiggener, L. Sanguinet, E. Levillain, S. Leutwyler, A. Hauser, S. Decurtins, *Chem. Commun.* **2006**, 1878.

[191] Z.-Y. Yang, S.-B. Lei, L.-H. Gan, L.-J. Wan, C. Wang, C.-L. Bai, *ChemPhysChem* **2005**, *6*, 65.

[192] J. K. Gimzewski, E. Stoll, R. R. Schlittler, *Surf. Sci.* **1987**, *181*, 267.

[193] P. H. Lippel, R. J. Wilson, M. D. Miller, C. Wöll, S. Chiang, *Phys. Rev. Lett.* **1989**, *62*, 171.

[194] K. W. Hipps, X. Lu, X. D. Wang, U. Mazur, *J. Phys. Chem.* **1996**, *100*, 11207.

[195] X. Lu, K. W. Hipps, X. D. Wang, U. Mazur, *J. Am. Chem. Soc.* **1996**, *118*, 7197.

[196] X. Lu, K. W. Hipps, *J. Phys. Chem. B* **1997**, *101*, 5391.

[197] G. V. Nazin, X. H. Qiu, W. Ho, *Science* **2003**, *302*, 77.

[198] C. Dekker, S. J. Tans, B. Oberndorff, R. Meyer, L. C. Venema, *Synth. Met.* **1997**, *84*, 853.

[199] D. E. Barlow, K. W. Hipps, *J. Phys. Chem. B* **2000**, *104*, 5993.

[200] I. Chizhov, G. Scoles, A. Kahn, *Langmuir* **2000**, *16*, 4358.

[201] M. C. Hersam, N. P. Guisinger, J. W. Lyding, *J. Vac. Sci. Technol. A* **2000**, *18*, 1349.

[202] S. F. Alvarado, L. Rossi, P. Müller, W. Riess, *Synth. Met.* **2001**, *122*, 73.

[203] K. Walzer, M. Hietschold, *Surf. Sci.* **2001**, *471*, 1.

[204] S. Yoshimoto, A. Tada, K. Suto, K. Itaya, *J. Phys. Chem. B* **2003**, *107*, 5836.

[205] T. G. Gopakumar, M. Lackinger, M. Hackert, F. Müller, M. Hietschold, *J. Phys. Chem. B* **2004**, *108*, 7839.

[206] A. Manivannan, L. A. Nagahara, K. Hashimoto, A. Fujishima, H. Yanagi, T. Kouzeki, M. Ashida, *Langmuir* **1993**, *9*, 771.

[207] M. Lackinger, T. Müller, T. G. Gopakumar, F. Müller, M. Hietschold, G. W. Flynn, *J. Phys. Chem. B* **2004**, *108*, 2279.

[208] X. Qiu, C. Wang, Q. Zeng, B. Xu, S. Yin, H. Wang, S. Xu, C. Bai, *J. Am. Chem. Soc.* **2000**, *122*, 5550.

[209] X. Qiu, C. Wang, S. Yin, Q. Zeng, B. Xu, C. Bai, *J. Phys. Chem. B* **2000**, *104*, 3570.

[210] S. Yoshimoto, K. Suto, A. Tada, N. Kobayashi, K. Itaya, *J. Am. Chem. Soc.* **2004**, *126*, 8020.

[211] P. Samorí, H. Engelkamp, P. de Witte, A. E. Rowan, R. J. M. Nolte, J. P. Rabe, *Angew. Chem. Int. Ed.* **2001**, *40*, 2348.

[212] S. Zhou, Y. Liu, Y. Xu, W. Hu, D. Zhu, X. Qiu, C. Wang, C. Bai, *Chem. Phys. Lett.* **1998**, *297*, 77.

[213] Y. J. Zhang, Y. Li, Q. Liu, J. Jin, B. Ding, Y. Song, L. Jiang, X. Du, Y. Zhao, T. J. Li, *Synth. Met.* **2002**, *128*, 43.

[214] S. Q. Zhou, Y. Q. Liu, W. F. Qiu, X. B. Huang, L. Jiang, D. B. Zhu, *Synth. Met.* **2003**, *135-136*, 857.

[215] S. B. Lei, C. Wang, S. X. Yin, C. L. Bai, *J. Phys. Chem. B* **2001**, *105*, 12272.

[216] S. B. Lei, S. X. Yin, C. Wang, L. J. Wan, C. L. Bai, *Chem. Mater.* **2002**, *14*, 2837.

[217] S.-B. Lei, K. Deng, D.-L. Yang, Q.-D. Zeng, C.Wang, *J. Phys. Chem. B* **2006**, *110*, 1256.

[218] B. Xu, S. Yin, C. Wang, X. Qiu, Q. Zeng, C. Bai, *J. Phys. Chem. B* **2000**, *104*, 10502.

[219] S. B. Lei, C. Wang, S. X. Yin, H. N. Wang, F. Xi, H. W. Liu, B. Xu, L. J. Wan, C. L. Bai, *J. Phys. Chem. B* **2001**, *105*, 10838.

[220] S. Lei, C. Wang, L. Wan, C. Bai, *J. Phys. Chem. B* **2004**, *108*, 1173.

[221] Z.-Y. Yang, L.-H. Gan, S.-B. Lei, L.-J. Wan, C. Wang, J.-Z. Jiang, *J. Phys. Chem. B* **2005**, *109*, 19859.

[222] K. W. Hipps, L. Scudiero, D. E. Barlow, M. P. Cooke Jr., *J. Am. Chem. Soc.* **2002**, *124*, 2126.

[223] L. Scudiero, K. W. Hipps, D. E. Barlow, *J. Phys. Chem. B* **2003**, *107*, 2903.

[224] K. Suto, S. Yoshimoto, K. Itaya, *J. Am. Chem. Soc.* **2003**, *125*, 14976.

[225] S. Yoshimoto, N. Higa, K. Itaya, *J. Am. Chem. Soc.* **2004**, *126*, 8540.

[226] Y. Liu, S. Lei, S. Yin, S. Xu, Q. Zheng, Q. Zeng, C. Wang, L. Wan, C. Bai, *J. Phys. Chem. B* **2002**, *106*, 12569.

[227] M. Stöhr, T. Wagner, M. Gabriel, B. Weyers, R. Möller, *Adv. Funct. Mater.* **2001**, *11*, 175.

[228] S. R. Wilson, S. MacMahon, F. T. Tat, P. D. Jarowski, D. I. Schuster, *Chem. Commun.* **2003**, 226.

[229]   F. J. Williams, O. P. H. Vaughan, K. J. Knox, N. Bampos, R. M. Lambert, *Chem. Commun.* **2004**, 1688.

[230]   O. P. H. Vaughan, F. J. Williams, N. Bampos, R. M. Lambert, *Angew. Chem. Int. Ed.* **2006**, *45*, 3779.

[231]   F. Moresco, G. Meyer, K.-H. Rieder, H. Tang, A. Gourdon, C. Joachim, *Phys. Rev. Lett.* **2001**, *86*, 672.

[232]   F. Moresco, G. Meyer, K.-H. Rieder, J. Ping, H. Tang, C. Joachim, *Surf. Sci.* **2002**, *499*, 94.

[233]   G. E. Bossard, M. J. Abrams, M. C. Darkes, J. F. Vollano, R. C. Brooks, *Inorg. Chem.* **1995**, *34*, 1524.

[234]   A. N. Cammidge, G. Berber, I. Chambrier, P. W. Hough, M. J. Cook, *Tetrahedron* **2005**, *61*, 4067.

[235]   J. H. Price, A. N. Williamson, R. F. Schramm, B. B. Wayland, *Inorg. Chem.* **1972**, *11*, 1280.

[236]   W. Paw, R. Eisenberg, *Inorg. Chem.* **1997**, *36*, 2287.

[237]   G. M. Sheldrick, SHELXS-97 Program for the Solution of Crystal Structures, University of Göttingen, Göttingen (Germany), **1997**.

[238]   G. M. Sheldrick, SHELXL-97 Program for the Refinement of Crystal Structures, University of Göttingen, Göttingen (Germany), **1997**.

[239]   A. L. Spek, *J. Appl. Crystallogr.* **2003**, *36*, 7.

[240]   M. Stöhr, M. Wahl, C. H. Galka, T. Riehm, T. A. Jung, L. H. Gade, *Angew. Chem. Int. Ed.* **2005**, *44*, 7394.

A1. Crystallographic data

Table A.1. Selected crystal data of compounds **1**, **4** and **15**.

	1	4	15
Chemical formula	$C_{20}H_{10}N_6$	$C_{20}H_{10}Cl_2N_6Pd \cdot C_2H_3N$	$C_{109}H_{99}N_{13}O_6Zn \cdot 7.5C_5H_5N$
Molecular weight [g/mol^{-1}]	334.34	552.69	2345.63
Crystal size [mm]	0.50 x 0.15 x 0.10	0.25 x 0.20 x 0.15	0.50 x 0.40 x 0.40
Crystal color	pale yellow	yellow	pink
Crystal shape	rod	block	block
Crystal system	triclinic	triclinic	monoclinic
Space group	P $\bar{1}$	P $\bar{1}$	P 2_1/c
a [Å]	7.582(1)	9.534(1)	27.097(1)
b [Å]	9.461(1)	9.902(1)	25.106(1)
c [Å]	12.205(2)	12.265(2)	19.666(1)
α [°]	102.74(2)	102.75(2)	90.00
β [°]	99.56(2)	97.34(1)	109.190(3)
γ [°]	104.69(2)	99.97(1)	90.00
Volume [Å^3]	802.8(2)	1095.6(2)	12635.3(9)
Z	2	2	4
Density (calculated) [g cm^{-3}]	1.383	1.675	1.233
μ [mm^{-1}]	0.088	1.116	0.260
F(000)	344	548	4948
Index ranges h	-9 → 9	-10 → 10	-29 → 29
k	-11 → 11	-12 → 12	-28 → 29
l	-14 → 14	-15 → 15	-23 → 23
θ range for data collection [°]	2.49-26.00	2.16-26.01	1.14-25.00
Reflections: collected	6345	8532	97937
independent	2922	3964	20611
observed	1786	3196	12193
Parameters/restraints	235/0	289/0	1072/27
R indices R1	0.0737	0.0539	0.1140
(all data) wR2	0.0903	0.1089	0.2098
Final R indices R1	0.0392	0.0428	0.0753
[I>2σ(I)] wR2	0.0815	0.1048	0.1949
Goodness-of-fit on F^2	0.848	0.976	0.944
Min. ρ_e [eÅ^{-3}]	-0.162	-1.061	-0.725
Max. ρ_e [eÅ^{-3}]	0.207	1.008 near Pd1	0.959
Temperature [K]	153	153	153
Wavelength [Å] (MoK$_\alpha$)	0.71073	0.71073	0.71073
Diffractometer used	Stoe IPDS I	Stoe IPDS I	Stoe IPDS II
Scan type	φ oscillation	φ oscillation	ω rotation
Solution	SHELXS-97	SHELXS-97	SHELXS-97
Refinement	SHELXL-97	SHELXL-97	SHELXL-97
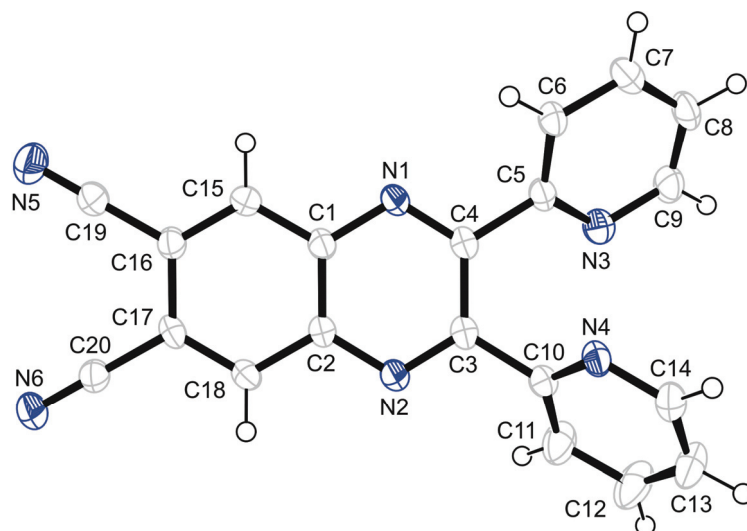
Figure A.1. ORTEP representation (ellipsoids at 50% probability) of the molecular structure of **1**.

Table A.2. Bond lengths [Å] of compound **1**.

N(1)-C(4)	1.308(2)	C(7)-H(7A)	0.929
N(1)-C(1)	1.372(2)	C(8)-C(9)	1.379(3)
N(2)-C(3)	1.317(2)	C(8)-H(8A)	0.93
N(2)-C(2)	1.365(2)	C(9)-H(9A)	0.9298
N(3)-C(5)	1.344(2)	C(10)-C(11)	1.367(3)
N(3)-C(9)	1.349(2)	C(11)-C(12)	1.384(3)
N(4)-C(14)	1.337(2)	C(11)-H(11A)	0.9282
N(4)-C(10)	1.343(2)	C(12)-C(13)	1.368(3)
N(5)-C(19)	1.137(2)	C(12)-H(12A)	0.9255
N(6)-C(20)	1.148(2)	C(13)-C(14)	1.372(3)
C(1)-C(15)	1.398(2)	C(13)-H(13A)	0.93
C(1)-C(2)	1.412(2)	C(14)-H(14A)	0.928
C(2)-C(18)	1.414(2)	C(15)-C(16)	1.373(2)
C(3)-C(4)	1.445(2)	C(15)-H(15A)	0.9292
C(3)-C(10)	1.491(2)	C(16)-C(17)	1.430(2)
C(4)-C(5)	1.491(2)	C(16)-C(19)	1.442(3)
C(5)-C(6)	1.366(3)	C(17)-C(18)	1.369(2)
C(6)-C(7)	1.385(2)	C(17)-C(20)	1.447(2)
C(6)-H(6A)	0.9295	C(18)-H(18A)	0.9297
C(7)-C(8)	1.364(3)		

Table A.3. Bond angles [°] of compound **1**.

C(4)-N(1)-C(1)	117.21(14)	C(8)-C(9)-H(9A)	118.4
C(3)-N(2)-C(2)	116.91(14)	N(4)-C(10)-C(11)	123.78(16)
C(5)-N(3)-C(9)	116.75(17)	N(4)-C(10)-C(3)	114.28(16)
C(14)-N(4)-C(10)	116.56(16)	C(11)-C(10)-C(3)	121.92(18)
N(1)-C(1)-C(15)	119.34(15)	C(10)-C(11)-C(12)	118.3(2)
N(1)-C(1)-C(2)	120.70(15)	C(10)-C(11)-H(11A)	120.9
C(15)-C(1)-C(2)	119.91(15)	C(12)-C(11)-H(11A)	120.8
N(2)-C(2)-C(18)	118.85(15)	C(13)-C(12)-C(11)	118.9(2)
N(2)-C(2)-C(1)	121.46(15)	C(13)-C(12)-H(12A)	120.6
C(18)-C(2)-C(1)	119.67(15)	C(11)-C(12)-H(12A)	120.5

N(2)-C(3)-C(4)	121.51(15)	C(12)-C(13)-C(14)	118.94(18)
N(2)-C(3)-C(10)	116.96(15)	C(12)-C(13)-H(13A)	120.6
C(4)-C(3)-C(10)	121.41(15)	C(14)-C(13)-H(13A)	120.5
N(1)-C(4)-C(3)	121.86(15)	N(4)-C(14)-C(13)	123.47(19)
N(1)-C(4)-C(5)	116.70(15)	N(4)-C(14)-H(14A)	118.4
C(3)-C(4)-C(5)	121.42(15)	C(13)-C(14)-H(14A)	118.1
N(3)-C(5)-C(6)	123.54(16)	C(16)-C(15)-C(1)	120.40(16)
N(3)-C(5)-C(4)	116.93(17)	C(16)-C(15)-H(15A)	119.7
C(6)-C(5)-C(4)	119.53(16)	C(1)-C(15)-H(15A)	119.9
C(5)-C(6)-C(7)	118.62(17)	C(15)-C(16)-C(17)	119.71(15)
C(5)-C(6)-H(6A)	120.6	C(15)-C(16)-C(19)	120.54(16)
C(7)-C(6)-H(6A)	120.7	C(17)-C(16)-C(19)	119.75(15)
C(8)-C(7)-C(6)	119.10(19)	C(18)-C(17)-C(16)	120.72(15)
C(8)-C(7)-H(7A)	120.5	C(18)-C(17)-C(20)	120.07(16)
C(6)-C(7)-H(7A)	120.4	C(16)-C(17)-C(20)	119.19(15)
C(7)-C(8)-C(9)	119.05(17)	C(17)-C(18)-C(2)	119.58(16)
C(7)-C(8)-H(8A)	120.4	C(17)-C(18)-H(18A)	120.1
C(9)-C(8)-H(8A)	120.5	C(2)-C(18)-H(18A)	120.3
N(3)-C(9)-C(8)	122.87(18)	N(5)-C(19)-C(16)	178.6(2)
N(3)-C(9)-H(9A)	118.7	N(6)-C(20)-C(17)	179.0(2)

Table A.4. Torsion angles [°] of compound **1**.

C(4)-N(1)-C(1)-C(15)	-179.47(18)	C(14)-N(4)-C(10)-C(11)	1.4(3)
C(4)-N(1)-C(1)-C(2)	-2.1(3)	C(14)-N(4)-C(10)-C(3)	179.83(15)
C(3)-N(2)-C(2)-C(18)	-178.40(18)	N(2)-C(3)-C(10)-N(4)	-128.36(18)
C(3)-N(2)-C(2)-C(1)	-0.1(3)	C(4)-C(3)-C(10)-N(4)	47.7(2)
N(1)-C(1)-C(2)-N(2)	3.8(3)	N(2)-C(3)-C(10)-C(11)	50.1(3)
C(15)-C(1)-C(2)-N(2)	-178.82(18)	C(4)-C(3)-C(10)-C(11)	-133.8(2)
N(1)-C(1)-C(2)-C(18)	-177.92(18)	N(4)-C(10)-C(11)-C(12)	-2.4(3)
C(15)-C(1)-C(2)-C(18)	-0.5(3)	C(3)-C(10)-C(11)-C(12)	179.3(2)
C(2)-N(2)-C(3)-C(4)	-4.9(3)	C(10)-C(11)-C(12)-C(13)	1.8(4)
C(2)-N(2)-C(3)-C(10)	171.19(17)	C(11)-C(12)-C(13)-C(14)	-0.4(3)
C(1)-N(1)-C(4)-C(3)	-2.9(3)	C(10)-N(4)-C(14)-C(13)	0.1(3)
C(1)-N(1)-C(4)-C(5)	175.68(17)	C(12)-C(13)-C(14)-N(4)	-0.5(3)
N(2)-C(3)-C(4)-N(1)	6.8(3)	N(1)-C(1)-C(15)-C(16)	177.45(19)
C(10)-C(3)-C(4)-N(1)	-169.13(18)	C(2)-C(1)-C(15)-C(16)	0.0(3)
N(2)-C(3)-C(4)-C(5)	-171.74(18)	C(1)-C(15)-C(16)-C(17)	0.5(3)
C(10)-C(3)-C(4)-C(5)	12.3(3)	C(1)-C(15)-C(16)-C(19)	-179.48(19)
C(9)-N(3)-C(5)-C(6)	2.5(3)	C(15)-C(16)-C(17)-C(18)	-0.5(3)
C(9)-N(3)-C(5)-C(4)	-178.56(16)	C(19)-C(16)-C(17)-C(18)	179.46(19)
N(1)-C(4)-C(5)-N(3)	-143.04(17)	C(15)-C(16)-C(17)-C(20)	178.1(2)
C(3)-C(4)-C(5)-N(3)	35.6(3)	C(19)-C(16)-C(17)-C(20)	-1.9(3)
N(1)-C(4)-C(5)-C(6)	35.9(3)	C(16)-C(17)-C(18)-C(2)	0.0(3)
C(3)-C(4)-C(5)-C(6)	-145.46(18)	C(20)-C(17)-C(18)-C(2)	-178.65(19)
N(3)-C(5)-C(6)-C(7)	-2.6(3)	N(2)-C(2)-C(18)-C(17)	178.84(17)
C(4)-C(5)-C(6)-C(7)	178.55(17)	C(1)-C(2)-C(18)-C(17)	0.5(3)
C(5)-C(6)-C(7)-C(8)	0.4(3)	C(15)-C(16)-C(19)-N(5)	92(9)
C(6)-C(7)-C(8)-C(9)	1.6(3)	C(17)-C(16)-C(19)-N(5)	-88(9)
C(5)-N(3)-C(9)-C(8)	-0.3(3)	C(18)-C(17)-C(20)-N(6)	87(12)
C(7)-C(8)-C(9)-N(3)	-1.7(3)	C(16)-C(17)-C(20)-N(6)	-92(12)
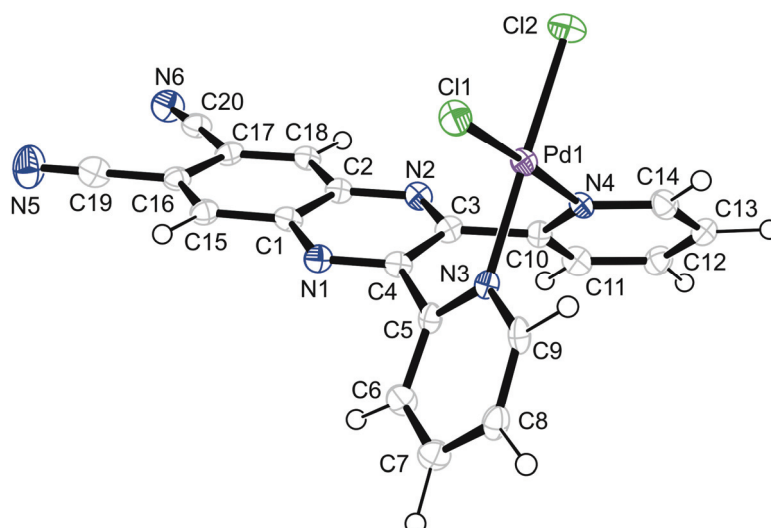
Figure A.2. ORTEP representation (ellipsoids at 50% probability) of the molecular structure of **4**. The co-crystallised CH_3CN molecule is omitted for clarity.

Table A.5. Bond lengths [Å] of compound **4**.

Pd(1)-N(3)	2.010(4)	C(7)-H(7A)	1.08
Pd(1)-N(4)	2.028(3)	C(8)-C(9)	1.371(7)
Pd(1)-Cl(1)	2.2834(10)	C(8)-H(8A)	1.08
Pd(1)-Cl(2)	2.2863(12)	C(9)-H(9A)	1.08
N(1)-C(4)	1.304(6)	C(10)-C(11)	1.376(6)
N(1)-C(1)	1.367(5)	C(11)-C(12)	1.383(7)
N(2)-C(3)	1.320(5)	C(11)-H(11A)	1.08
N(2)-C(2)	1.364(6)	C(12)-C(13)	1.398(7)
N(3)-C(9)	1.340(5)	C(12)-H(12A)	1.08
N(3)-C(5)	1.352(6)	C(13)-C(14)	1.375(6)
N(4)-C(14)	1.341(6)	C(13)-H(13A)	1.08
N(4)-C(10)	1.352(5)	C(14)-H(14A)	1.0799
N(5)-C(19)	1.142(7)	C(15)-C(16)	1.379(6)
N(6)-C(20)	1.136(6)	C(15)-H(15A)	1.08
C(1)-C(15)	1.410(6)	C(16)-C(17)	1.431(6)
C(1)-C(2)	1.411(6)	C(16)-C(19)	1.438(7)
C(2)-C(18)	1.421(5)	C(17)-C(18)	1.375(6)
C(3)-C(4)	1.440(6)	C(17)-C(20)	1.446(6)
C(3)-C(10)	1.506(6)	C(18)-H(18A)	1.08
C(4)-C(5)	1.501(5)	N(7)-C(21)	1.139(7)
C(5)-C(6)	1.377(6)	C(21)-C(22)	1.465(9)
C(6)-C(7)	1.392(6)	C(22)-H(22A)	0.98
C(6)-H(6A)	1.08	C(22)-H(22B)	0.98
C(7)-C(8)	1.386(7)	C(22)-H(22C)	0.9799

Table A.6. Bond angles [°] of compound **4**.

N(3)-Pd(1)-N(4)	86.95(13)	N(3)-C(9)-H(9A)	118.3
N(3)-Pd(1)-Cl(1)	89.95(9)	C(8)-C(9)-H(9A)	119.8
N(4)-Pd(1)-Cl(1)	176.18(10)	N(4)-C(10)-C(11)	121.5(4)
N(3)-Pd(1)-Cl(2)	175.95(9)	N(4)-C(10)-C(3)	117.6(3)
N(4)-Pd(1)-Cl(2)	89.23(10)	C(11)-C(10)-C(3)	120.8(4)

Cl(1)-Pd(1)-Cl(2)	93.92(4)	C(10)-C(11)-C(12)	119.3(4)
C(4)-N(1)-C(1)	117.6(4)	C(10)-C(11)-H(11A)	121.7
C(3)-N(2)-C(2)	116.8(4)	C(12)-C(11)-H(11A)	119
C(9)-N(3)-C(5)	119.0(4)	C(11)-C(12)-C(13)	119.0(4)
C(9)-N(3)-Pd(1)	121.9(3)	C(11)-C(12)-H(12A)	118.6
C(5)-N(3)-Pd(1)	119.1(3)	C(13)-C(12)-H(12A)	122.4
C(14)-N(4)-C(10)	119.4(3)	C(14)-C(13)-C(12)	118.7(4)
C(14)-N(4)-Pd(1)	118.3(3)	C(14)-C(13)-H(13A)	120.2
C(10)-N(4)-Pd(1)	122.3(3)	C(12)-C(13)-H(13A)	121.1
N(1)-C(1)-C(15)	118.2(4)	N(4)-C(14)-C(13)	122.1(4)
N(1)-C(1)-C(2)	120.8(4)	N(4)-C(14)-H(14A)	118.4
C(15)-C(1)-C(2)	121.0(4)	C(13)-C(14)-H(14A)	119.5
N(2)-C(2)-C(1)	121.2(4)	C(16)-C(15)-C(1)	118.8(4)
N(2)-C(2)-C(18)	119.1(4)	C(16)-C(15)-H(15A)	120.1
C(1)-C(2)-C(18)	119.7(4)	C(1)-C(15)-H(15A)	121.1
N(2)-C(3)-C(4)	121.8(4)	C(15)-C(16)-C(17)	120.4(4)
N(2)-C(3)-C(10)	114.7(3)	C(15)-C(16)-C(19)	119.6(4)
C(4)-C(3)-C(10)	123.4(3)	C(17)-C(16)-C(19)	120.0(4)
N(1)-C(4)-C(3)	121.5(4)	C(18)-C(17)-C(16)	121.2(4)
N(1)-C(4)-C(5)	114.4(4)	C(18)-C(17)-C(20)	121.7(4)
C(3)-C(4)-C(5)	123.8(4)	C(16)-C(17)-C(20)	117.1(4)
N(3)-C(5)-C(6)	121.9(4)	C(17)-C(18)-C(2)	118.8(4)
N(3)-C(5)-C(4)	118.7(4)	C(17)-C(18)-H(18A)	119.9
C(6)-C(5)-C(4)	119.3(4)	C(2)-C(18)-H(18A)	121.3
C(5)-C(6)-C(7)	118.8(4)	N(5)-C(19)-C(16)	179.3(5)
C(5)-C(6)-H(6A)	118.2	N(6)-C(20)-C(17)	175.4(5)
C(7)-C(6)-H(6A)	123	N(7)-C(21)-C(22)	179.2(6)
C(8)-C(7)-C(6)	118.7(4)	C(21)-C(22)-H(22A)	109.6
C(8)-C(7)-H(7A)	120.1	C(21)-C(22)-H(22B)	109.2
C(6)-C(7)-H(7A)	121.2	H(22A)-C(22)-H(22B)	109.5
C(9)-C(8)-C(7)	119.5(4)	C(21)-C(22)-H(22C)	109.7
C(9)-C(8)-H(8A)	118.3	H(22A)-C(22)-H(22C)	109.5
C(7)-C(8)-H(8A)	122.2	H(22B)-C(22)-H(22C)	109.5
N(3)-C(9)-C(8)	121.9(4)		

Table A.7. Torsion angles [°] of compound **4**.

N(4)-Pd(1)-N(3)-C(9)	109.7(3)	C(4)-C(5)-C(6)-C(7)	178.8(4)
Cl(1)-Pd(1)-N(3)-C(9)	-68.1(3)	C(5)-C(6)-C(7)-C(8)	1.3(6)
Cl(2)-Pd(1)-N(3)-C(9)	129.5(13)	C(6)-C(7)-C(8)-C(9)	1.5(6)
N(4)-Pd(1)-N(3)-C(5)	-69.2(3)	C(5)-N(3)-C(9)-C(8)	1.2(6)
Cl(1)-Pd(1)-N(3)-C(5)	113.0(3)	Pd(1)-N(3)-C(9)-C(8)	-177.7(3)
Cl(2)-Pd(1)-N(3)-C(5)	-49.3(16)	C(7)-C(8)-C(9)-N(3)	-2.8(6)
N(3)-Pd(1)-N(4)-C(14)	-111.4(3)	C(14)-N(4)-C(10)-C(11)	-0.3(6)
Cl(1)-Pd(1)-N(4)-C(14)	-75.7(17)	Pd(1)-N(4)-C(10)-C(11)	-179.1(3)
Cl(2)-Pd(1)-N(4)-C(14)	69.9(3)	C(14)-N(4)-C(10)-C(3)	-176.6(4)
N(3)-Pd(1)-N(4)-C(10)	67.3(3)	Pd(1)-N(4)-C(10)-C(3)	4.6(5)
Cl(1)-Pd(1)-N(4)-C(10)	103.1(16)	N(2)-C(3)-C(10)-N(4)	128.8(4)
Cl(2)-Pd(1)-N(4)-C(10)	-111.3(3)	C(4)-C(3)-C(10)-N(4)	-55.3(6)
C(4)-N(1)-C(1)-C(15)	-179.5(4)	N(2)-C(3)-C(10)-C(11)	-47.5(6)
C(4)-N(1)-C(1)-C(2)	3.0(6)	C(4)-C(3)-C(10)-C(11)	128.3(4)
C(3)-N(2)-C(2)-C(1)	0.0(6)	N(4)-C(10)-C(11)-C(12)	0.5(6)
C(3)-N(2)-C(2)-C(18)	-179.4(4)	C(3)-C(10)-C(11)-C(12)	176.6(4)
N(1)-C(1)-C(2)-N(2)	-3.6(6)	C(10)-C(11)-C(12)-C(13)	-0.7(6)

C(15)-C(1)-C(2)-N(2)	179.0(4)	C(11)-C(12)-C(13)-C(14)	0.8(6)
N(1)-C(1)-C(2)-C(18)	175.7(4)	C(10)-N(4)-C(14)-C(13)	0.4(6)
C(15)-C(1)-C(2)-C(18)	-1.7(6)	Pd(1)-N(4)-C(14)-C(13)	179.2(3)
C(2)-N(2)-C(3)-C(4)	4.0(6)	C(12)-C(13)-C(14)-N(4)	-0.7(6)
C(2)-N(2)-C(3)-C(10)	179.9(4)	N(1)-C(1)-C(15)-C(16)	-176.1(4)
C(1)-N(1)-C(4)-C(3)	0.9(6)	C(2)-C(1)-C(15)-C(16)	1.3(6)
C(1)-N(1)-C(4)-C(5)	-174.1(3)	C(1)-C(15)-C(16)-C(17)	0.3(6)
N(2)-C(3)-C(4)-N(1)	-4.7(6)	C(1)-C(15)-C(16)-C(19)	179.4(4)
C(10)-C(3)-C(4)-N(1)	179.7(4)	C(15)-C(16)-C(17)-C(18)	-1.6(6)
N(2)-C(3)-C(4)-C(5)	169.9(4)	C(19)-C(16)-C(17)-C(18)	179.3(4)
C(10)-C(3)-C(4)-C(5)	-5.7(6)	C(15)-C(16)-C(17)-C(20)	177.6(4)
C(9)-N(3)-C(5)-C(6)	1.7(6)	C(19)-C(16)-C(17)-C(20)	-1.5(6)
Pd(1)-N(3)-C(5)-C(6)	-179.3(3)	C(16)-C(17)-C(18)-C(2)	1.2(6)
C(9)-N(3)-C(5)-C(4)	179.9(3)	C(20)-C(17)-C(18)-C(2)	-178.0(4)
Pd(1)-N(3)-C(5)-C(4)	-1.1(5)	N(2)-C(2)-C(18)-C(17)	179.8(4)
N(1)-C(4)-C(5)-N(3)	-123.3(4)	C(1)-C(2)-C(18)-C(17)	0.4(6)
C(3)-C(4)-C(5)-N(3)	61.8(5)	C(15)-C(16)-C(19)-N(5)	-149(45)
N(1)-C(4)-C(5)-C(6)	54.9(5)	C(17)-C(16)-C(19)-N(5)	30(45)
C(3)-C(4)-C(5)-C(6)	-120.0(5)	C(18)-C(17)-C(20)-N(6)	167(6)
N(3)-C(5)-C(6)-C(7)	-3.0(6)	C(16)-C(17)-C(20)-N(6)	-12(6)
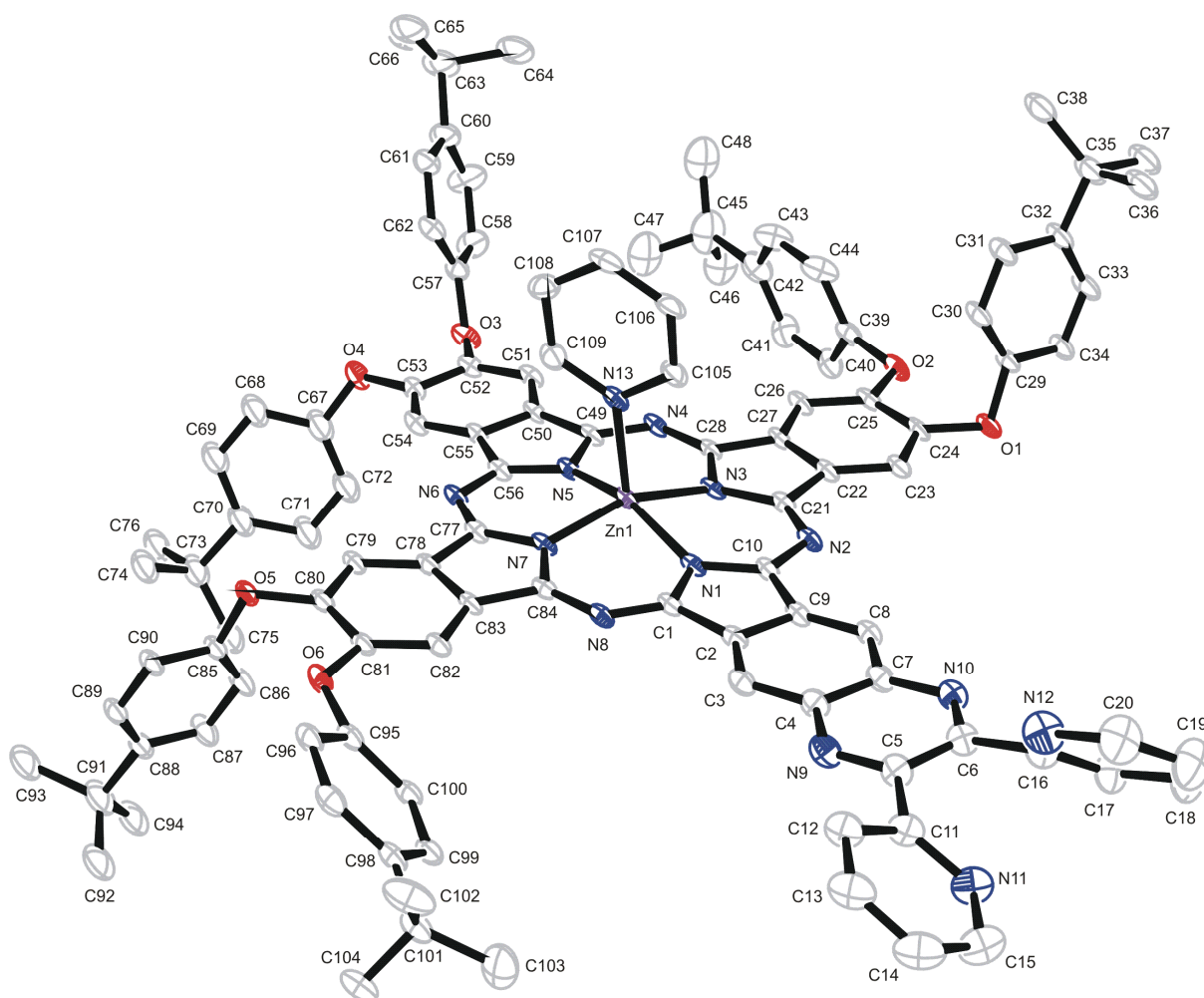
Figure A.3. ORTEP representation (ellipsoids at 20% probability) of the molecular structure of **15** with an axial pyridine ligand. Hydrogen atoms are omitted for clarity.

Table A.8. Bond lengths [Å] of compound **15**.

Zn(1)-N(7)	1.846(3)	C(35)-C(36)	1.653(13)
Zn(1)-N(3)	1.904(3)	C(35)-C(38A)	1.654(13)
Zn(1)-N(13)	2.068(3)	C(39)-C(40)	1.370(6)
Zn(1)-N(5)	2.197(3)	C(39)-C(44)	1.415(8)
Zn(1)-N(1)	2.240(3)	C(40)-C(41)	1.520(8)
O(1)-C(29)	1.312(5)	C(41)-C(42)	1.424(9)
O(1)-C(24)	1.360(5)	C(42)-C(43)	1.411(9)
O(2)-C(25)	1.330(4)	C(42)-C(45)	1.671(10)
O(2)-C(39)	1.546(6)	C(43)-C(44)	1.513(9)
O(3)-C(57)	1.388(5)	C(45)-C(47)	1.399(15)
O(3)-C(52)	1.457(5)	C(45)-C(46A)	1.455(14)
O(4)-C(67)	1.286(6)	C(45)-C(48A)	1.505(15)
O(4)-C(53)	1.480(5)	C(45)-C(48)	1.535(15)
O(5)-C(85)	1.298(5)	C(45)-C(47A)	1.565(15)
O(5)-C(80)	1.397(5)	C(45)-C(46)	1.616(15)
O(6)-C(81)	1.306(4)	C(49)-C(50)	1.580(6)
O(6)-C(95)	1.523(5)	C(50)-C(55)	1.305(5)
N(1)-C(1)	1.322(5)	C(50)-C(51)	1.457(6)
N(1)-C(10)	1.384(5)	C(51)-C(52)	1.463(6)
N(2)-C(10)	1.258(5)	C(52)-C(53)	1.301(6)
N(2)-C(21)	1.437(5)	C(53)-C(54)	1.445(6)
N(3)-C(28)	1.420(5)	C(54)-C(55)	1.465(6)
N(3)-C(21)	1.469(5)	C(55)-C(56)	1.585(5)
N(4)-C(49)	1.287(5)	C(57)-C(62)	1.351(7)
N(4)-C(28)	1.439(5)	C(57)-C(58)	1.377(7)
N(5)-C(49)	1.335(5)	C(58)-C(59)	1.374(8)
N(5)-C(56)	1.369(5)	C(59)-C(60)	1.385(9)
N(6)-C(56)	1.248(5)	C(60)-C(61)	1.361(8)
N(6)-C(77)	1.448(5)	C(60)-C(63)	1.514(8)
N(7)-C(84)	1.414(5)	C(61)-C(62)	1.378(7)
N(7)-C(77)	1.445(5)	C(63)-C(66A)	1.451(15)
N(8)-C(1)	1.278(5)	C(63)-C(65A)	1.503(13)
N(8)-C(84)	1.457(5)	C(63)-C(64)	1.566(14)
N(9)-C(5)	1.403(6)	C(63)-C(66)	1.567(15)
N(9)-C(4)	1.431(6)	C(63)-C(65)	1.582(15)
N(10)-C(6)	1.374(6)	C(63)-C(64A)	1.712(15)
N(10)-C(7)	1.462(6)	C(67)-C(68)	1.356(9)
N(11)-C(15)	1.367(7)	C(67)-C(72)	1.370(9)
N(11)-C(11)	1.438(7)	C(68)-C(69)	1.275(8)
N(12)-C(16)	1.355(6)	C(69)-C(70)	1.415(9)
N(12)-C(20)	1.426(8)	C(70)-C(71)	1.369(9)
N(13)-C(105)	1.307(5)	C(70)-C(73)	1.427(8)
N(13)-C(109)	1.406(6)	C(71)-C(72)	1.264(8)
C(1)-C(2)	1.594(6)	C(73)-C(74)	1.446(12)
C(2)-C(9)	1.327(5)	C(73)-C(75A)	1.471(12)
C(2)-C(3)	1.440(6)	C(73)-C(75)	1.523(14)
C(3)-C(4)	1.493(6)	C(73)-C(76A)	1.540(13)
C(4)-C(7)	1.342(6)	C(73)-C(74A)	1.606(13)
C(5)-C(6)	1.343(7)	C(73)-C(76)	1.726(13)
C(5)-C(11)	1.528(7)	C(77)-C(78)	1.349(5)
C(6)-C(16)	1.568(7)	C(78)-C(79)	1.391(6)

C(7)-C(8)	1.477(6)	C(78)-C(83)	1.541(6)
C(8)-C(9)	1.454(6)	C(79)-C(80)	1.309(5)
C(9)-C(10)	1.579(6)	C(80)-C(81)	1.539(6)
C(11)-C(12)	1.317(7)	C(81)-C(82)	1.385(6)
C(12)-C(13)	1.411(8)	C(82)-C(83)	1.339(5)
C(13)-C(14)	1.453(10)	C(83)-C(84)	1.396(5)
C(14)-C(15)	1.357(10)	C(85)-C(90)	1.314(5)
C(16)-C(17)	1.363(8)	C(85)-C(86)	1.349(6)
C(17)-C(18)	1.458(7)	C(86)-C(87)	1.303(6)
C(18)-C(19)	1.390(9)	C(87)-C(88)	1.305(6)
C(19)-C(20)	1.354(10)	C(88)-C(89)	1.371(7)
C(21)-C(22)	1.378(5)	C(88)-C(91)	1.433(7)
C(22)-C(23)	1.372(6)	C(89)-C(90)	1.289(6)
C(22)-C(27)	1.537(6)	C(91)-C(94)	1.540(9)
C(23)-C(24)	1.346(6)	C(91)-C(92)	1.570(10)
C(24)-C(25)	1.545(6)	C(91)-C(93)	1.599(9)
C(25)-C(26)	1.350(6)	C(95)-C(96)	1.358(6)
C(26)-C(27)	1.348(5)	C(95)-C(100)	1.445(6)
C(27)-C(28)	1.381(5)	C(96)-C(97)	1.486(7)
C(29)-C(34)	1.294(5)	C(97)-C(98)	1.451(7)
C(29)-C(30)	1.368(6)	C(98)-C(99)	1.376(6)
C(30)-C(31)	1.276(6)	C(98)-C(101)	1.647(7)
C(31)-C(32)	1.304(6)	C(99)-C(100)	1.482(6)
C(32)-C(33)	1.386(7)	C(101)-C(104)	1.385(6)
C(32)-C(35)	1.427(7)	C(101)-C(103)	1.554(9)
C(33)-C(34)	1.276(6)	C(101)-C(102)	1.567(8)
C(35)-C(37)	1.408(14)	C(105)-C(106)	1.325(6)
C(35)-C(37A)	1.428(13)	C(106)-C(107)	1.424(8)
C(35)-C(38)	1.518(15)	C(107)-C(108)	1.361(7)
C(35)-C(36A)	1.550(15)	C(108)-C(109)	1.354(7)

Table A.9. Bond angles [°] of compound **15**.

N(7)-Zn(1)-N(3)	155.97(14)	C(47)-C(45)-C(48)	104.6(13)
N(7)-Zn(1)-N(13)	101.59(13)	C(46A)-C(45)-C(47A)	111.2(11)
N(3)-Zn(1)-N(13)	102.40(13)	C(48A)-C(45)-C(47A)	84.5(13)
N(7)-Zn(1)-N(5)	86.91(12)	C(47)-C(45)-C(46)	85.4(13)
N(3)-Zn(1)-N(5)	89.84(13)	C(48)-C(45)-C(46)	117.4(10)
N(13)-Zn(1)-N(5)	94.64(13)	C(47)-C(45)-C(42)	120.6(9)
N(7)-Zn(1)-N(1)	90.64(13)	C(46A)-C(45)-C(42)	115.3(9)
N(3)-Zn(1)-N(1)	84.32(13)	C(48A)-C(45)-C(42)	100.5(8)
N(13)-Zn(1)-N(1)	105.38(12)	C(48)-C(45)-C(42)	116.8(9)
N(5)-Zn(1)-N(1)	159.91(11)	C(47A)-C(45)-C(42)	119.3(8)
C(29)-O(1)-C(24)	108.1(3)	C(46)-C(45)-C(42)	108.6(9)
C(25)-O(2)-C(39)	118.8(3)	N(4)-C(49)-N(5)	117.4(4)
C(57)-O(3)-C(52)	119.4(3)	N(4)-C(49)-C(50)	125.6(3)
C(67)-O(4)-C(53)	111.5(4)	N(5)-C(49)-C(50)	116.9(3)
C(85)-O(5)-C(80)	112.9(3)	C(55)-C(50)-C(51)	115.0(4)
C(81)-O(6)-C(95)	123.0(3)	C(55)-C(50)-C(49)	105.6(3)
C(1)-N(1)-C(10)	99.3(3)	C(51)-C(50)-C(49)	139.4(3)
C(1)-N(1)-Zn(1)	127.6(3)	C(50)-C(51)-C(52)	126.0(3)

C(10)-N(1)-Zn(1)	132.2(2)	C(53)-C(52)-O(3)	113.1(4)
C(10)-N(2)-C(21)	122.2(3)	C(53)-C(52)-C(51)	119.1(4)
C(28)-N(3)-C(21)	118.1(3)	O(3)-C(52)-C(51)	127.6(3)
C(28)-N(3)-Zn(1)	117.0(3)	C(52)-C(53)-C(54)	114.7(4)
C(21)-N(3)-Zn(1)	123.0(2)	C(52)-C(53)-O(4)	114.6(4)
C(49)-N(4)-C(28)	126.4(3)	C(54)-C(53)-O(4)	130.7(4)
C(49)-N(5)-C(56)	98.0(3)	C(53)-C(54)-C(55)	126.9(4)
C(49)-N(5)-Zn(1)	130.0(3)	C(50)-C(55)-C(54)	118.3(4)
C(56)-N(5)-Zn(1)	131.2(2)	C(50)-C(55)-C(56)	101.3(3)
C(56)-N(6)-C(77)	121.6(3)	C(54)-C(55)-C(56)	140.4(3)
C(84)-N(7)-C(77)	118.6(3)	N(6)-C(56)-N(5)	120.7(4)
C(84)-N(7)-Zn(1)	119.0(3)	N(6)-C(56)-C(55)	121.2(4)
C(77)-N(7)-Zn(1)	122.0(2)	N(5)-C(56)-C(55)	118.1(3)
C(1)-N(8)-C(84)	125.0(3)	C(62)-C(57)-C(58)	120.4(5)
C(5)-N(9)-C(4)	127.7(4)	C(62)-C(57)-O(3)	124.6(4)
C(6)-N(10)-C(7)	127.0(4)	C(58)-C(57)-O(3)	115.0(5)
C(15)-N(11)-C(11)	124.1(5)	C(59)-C(58)-C(57)	117.9(6)
C(16)-N(12)-C(20)	117.8(5)	C(58)-C(59)-C(60)	123.1(6)
C(105)-N(13)-C(109)	120.7(4)	C(61)-C(60)-C(59)	116.3(5)
C(105)-N(13)-Zn(1)	114.8(3)	C(61)-C(60)-C(63)	123.9(6)
C(109)-N(13)-Zn(1)	124.3(3)	C(59)-C(60)-C(63)	119.8(6)
N(8)-C(1)-N(1)	119.9(4)	C(60)-C(61)-C(62)	122.0(5)
N(8)-C(1)-C(2)	124.6(3)	C(57)-C(62)-C(61)	120.1(4)
N(1)-C(1)-C(2)	115.5(3)	C(66A)-C(63)-C(65A)	116.9(11)
C(9)-C(2)-C(3)	114.6(4)	C(66A)-C(63)-C(60)	116.0(8)
C(9)-C(2)-C(1)	106.7(3)	C(65A)-C(63)-C(60)	102.0(7)
C(3)-C(2)-C(1)	138.6(4)	C(60)-C(63)-C(64)	95.1(7)
C(2)-C(3)-C(4)	127.1(4)	C(60)-C(63)-C(66)	124.4(9)
C(7)-C(4)-N(9)	114.0(4)	C(64)-C(63)-C(66)	119.6(8)
C(7)-C(4)-C(3)	118.0(4)	C(60)-C(63)-C(65)	105.1(7)
N(9)-C(4)-C(3)	127.9(4)	C(64)-C(63)-C(65)	101.8(11)
C(6)-C(5)-N(9)	117.9(4)	C(66)-C(63)-C(65)	107.9(12)
C(6)-C(5)-C(11)	117.2(5)	C(66A)-C(63)-C(64A)	109.0(13)
N(9)-C(5)-C(11)	124.8(4)	C(65A)-C(63)-C(64A)	101.2(10)
C(5)-C(6)-N(10)	115.8(4)	C(60)-C(63)-C(64A)	110.8(8)
C(5)-C(6)-C(16)	118.1(4)	O(4)-C(67)-C(68)	112.4(6)
N(10)-C(6)-C(16)	125.9(4)	O(4)-C(67)-C(72)	120.3(6)
C(4)-C(7)-N(10)	117.4(4)	C(68)-C(67)-C(72)	127.3(6)
C(4)-C(7)-C(8)	113.8(4)	C(69)-C(68)-C(67)	115.0(7)
N(10)-C(7)-C(8)	128.7(4)	C(68)-C(69)-C(70)	119.0(6)
C(9)-C(8)-C(7)	126.9(4)	C(71)-C(70)-C(69)	123.4(5)
C(2)-C(9)-C(8)	119.4(4)	C(71)-C(70)-C(73)	118.9(6)
C(2)-C(9)-C(10)	100.1(3)	C(69)-C(70)-C(73)	117.6(6)
C(8)-C(9)-C(10)	140.5(3)	C(72)-C(71)-C(70)	117.2(7)
N(2)-C(10)-N(1)	120.2(4)	C(71)-C(72)-C(67)	118.1(6)
N(2)-C(10)-C(9)	121.4(4)	C(70)-C(73)-C(74)	104.1(7)
N(1)-C(10)-C(9)	118.3(3)	C(70)-C(73)-C(75A)	113.4(7)
C(12)-C(11)-N(11)	122.8(5)	C(70)-C(73)-C(75)	110.7(7)
C(12)-C(11)-C(5)	114.3(5)	C(74)-C(73)-C(75)	115.3(10)
N(11)-C(11)-C(5)	122.8(5)	C(70)-C(73)-C(76A)	107.1(7)
C(11)-C(12)-C(13)	113.0(6)	C(75A)-C(73)-C(76A)	120.9(9)
C(12)-C(13)-C(14)	125.6(6)	C(70)-C(73)-C(74A)	97.0(6)

C(15)-C(14)-C(13)	118.2(6)	C(75A)-C(73)-C(74A)	108.5(9)
C(14)-C(15)-N(11)	116.2(7)	C(76A)-C(73)-C(74A)	107.1(9)
N(12)-C(16)-C(17)	120.3(5)	C(70)-C(73)-C(76)	106.1(7)
N(12)-C(16)-C(6)	117.3(5)	C(74)-C(73)-C(76)	103.1(9)
C(17)-C(16)-C(6)	122.4(4)	C(75)-C(73)-C(76)	116.4(9)
C(16)-C(17)-C(18)	120.7(5)	C(78)-C(77)-N(7)	102.9(3)
C(19)-C(18)-C(17)	119.7(6)	C(78)-C(77)-N(6)	121.7(4)
C(20)-C(19)-C(18)	116.1(6)	N(7)-C(77)-N(6)	135.4(3)
C(19)-C(20)-N(12)	125.4(6)	C(77)-C(78)-C(79)	124.7(4)
C(22)-C(21)-N(2)	123.4(4)	C(77)-C(78)-C(83)	107.6(3)
C(22)-C(21)-N(3)	102.0(3)	C(79)-C(78)-C(83)	127.6(3)
N(2)-C(21)-N(3)	134.6(3)	C(80)-C(79)-C(78)	107.8(4)
C(23)-C(22)-C(21)	126.6(4)	C(79)-C(80)-O(5)	110.9(4)
C(23)-C(22)-C(27)	126.0(3)	C(79)-C(80)-C(81)	124.9(4)
C(21)-C(22)-C(27)	107.4(3)	O(5)-C(80)-C(81)	123.9(3)
C(24)-C(23)-C(22)	107.0(4)	O(6)-C(81)-C(82)	116.3(4)
C(23)-C(24)-O(1)	109.2(4)	O(6)-C(81)-C(80)	115.4(3)
C(23)-C(24)-C(25)	126.5(4)	C(82)-C(81)-C(80)	128.1(3)
O(1)-C(24)-C(25)	124.3(3)	C(83)-C(82)-C(81)	107.2(4)
O(2)-C(25)-C(26)	114.0(4)	C(82)-C(83)-C(84)	124.3(4)
O(2)-C(25)-C(24)	119.3(3)	C(82)-C(83)-C(78)	124.3(4)
C(26)-C(25)-C(24)	126.7(3)	C(84)-C(83)-C(78)	111.4(3)
C(27)-C(26)-C(25)	107.0(4)	C(83)-C(84)-N(7)	99.3(3)
C(26)-C(27)-C(28)	120.7(4)	C(83)-C(84)-N(8)	125.3(3)
C(26)-C(27)-C(22)	126.9(4)	N(7)-C(84)-N(8)	135.4(3)
C(28)-C(27)-C(22)	112.4(3)	O(5)-C(85)-C(90)	111.2(4)
C(27)-C(28)-N(3)	100.0(3)	O(5)-C(85)-C(86)	124.8(4)
C(27)-C(28)-N(4)	124.6(3)	C(90)-C(85)-C(86)	123.8(4)
N(3)-C(28)-N(4)	135.4(3)	C(87)-C(86)-C(85)	121.1(4)
C(34)-C(29)-O(1)	110.2(4)	C(86)-C(87)-C(88)	117.0(5)
C(34)-C(29)-C(30)	124.0(4)	C(87)-C(88)-C(89)	119.9(4)
O(1)-C(29)-C(30)	125.6(3)	C(87)-C(88)-C(91)	117.4(5)
C(31)-C(30)-C(29)	122.2(4)	C(89)-C(88)-C(91)	122.7(5)
C(30)-C(31)-C(32)	116.1(5)	C(90)-C(89)-C(88)	124.5(4)
C(31)-C(32)-C(33)	119.4(4)	C(89)-C(90)-C(85)	113.6(4)
C(31)-C(32)-C(35)	112.3(5)	C(88)-C(91)-C(94)	113.9(5)
C(33)-C(32)-C(35)	128.0(4)	C(88)-C(91)-C(92)	101.4(6)
C(34)-C(33)-C(32)	125.6(4)	C(94)-C(91)-C(92)	111.3(6)
C(33)-C(34)-C(29)	112.5(4)	C(88)-C(91)-C(93)	108.3(5)
C(37)-C(35)-C(32)	105.1(9)	C(94)-C(91)-C(93)	104.3(6)
C(32)-C(35)-C(37A)	108.6(9)	C(92)-C(91)-C(93)	118.0(6)
C(37)-C(35)-C(38)	115.0(13)	C(96)-C(95)-C(100)	118.0(4)
C(32)-C(35)-C(38)	117.4(8)	C(96)-C(95)-O(6)	112.7(4)
C(32)-C(35)-C(36A)	110.1(8)	C(100)-C(95)-O(6)	129.0(3)
C(37A)-C(35)-C(36A)	123.7(12)	C(95)-C(96)-C(97)	116.9(5)
C(37)-C(35)-C(36)	98.5(9)	C(98)-C(97)-C(96)	127.8(4)
C(32)-C(35)-C(36)	105.7(6)	C(99)-C(98)-C(97)	112.5(4)
C(38)-C(35)-C(36)	113.0(10)	C(99)-C(98)-C(101)	121.1(5)
C(32)-C(35)-C(38A)	111.4(6)	C(97)-C(98)-C(101)	126.4(4)
C(37A)-C(35)-C(38A)	97.8(9)	C(98)-C(99)-C(100)	121.7(4)
C(36A)-C(35)-C(38A)	104.3(10)	C(95)-C(100)-C(99)	122.9(4)
C(40)-C(39)-C(44)	113.6(5)	C(104)-C(101)-C(103)	108.8(5)

C(40)-C(39)-O(2)	122.3(4)	C(104)-C(101)-C(102)	107.3(5)
C(44)-C(39)-O(2)	124.0(4)	C(103)-C(101)-C(102)	105.0(6)
C(39)-C(40)-C(41)	122.2(5)	C(104)-C(101)-C(98)	103.9(4)
C(42)-C(41)-C(40)	125.9(5)	C(103)-C(101)-C(98)	119.8(4)
C(43)-C(42)-C(41)	110.5(6)	C(102)-C(101)-C(98)	111.6(5)
C(43)-C(42)-C(45)	122.4(7)	N(13)-C(105)-C(106)	115.9(5)
C(41)-C(42)-C(45)	127.0(6)	C(105)-C(106)-C(107)	123.4(5)
C(42)-C(43)-C(44)	123.5(6)	C(108)-C(107)-C(106)	122.5(5)
C(39)-C(44)-C(43)	124.1(5)	C(109)-C(108)-C(107)	110.6(5)
C(46A)-C(45)-C(48A)	122.6(13)	C(108)-C(109)-N(13)	126.9(5)

Table A.10. Torsion angles [°] of compound **15**.

N(7)-Zn(1)-N(1)-C(1)	-17.4(3)	O(2)-C(39)-C(44)-C(43)	-178.8(5)
N(3)-Zn(1)-N(1)-C(1)	-173.8(3)	C(42)-C(43)-C(44)-C(39)	-1.8(10)
N(13)-Zn(1)-N(1)-C(1)	84.8(3)	C(43)-C(42)-C(45)-C(47)	-104.9(15)
N(5)-Zn(1)-N(1)-C(1)	-100.1(4)	C(41)-C(42)-C(45)-C(47)	71.0(15)
N(7)-Zn(1)-N(1)-C(10)	175.6(3)	C(43)-C(42)-C(45)-C(46A)	122.1(12)
N(3)-Zn(1)-N(1)-C(10)	19.2(3)	C(41)-C(42)-C(45)-C(46A)	-62.0(13)
N(13)-Zn(1)-N(1)-C(10)	-82.2(3)	C(43)-C(42)-C(45)-C(48A)	-103.9(12)
N(5)-Zn(1)-N(1)-C(10)	92.9(4)	C(41)-C(42)-C(45)-C(48A)	72.0(13)
N(7)-Zn(1)-N(3)-C(28)	99.7(4)	C(43)-C(42)-C(45)-C(48)	23.8(12)
N(13)-Zn(1)-N(3)-C(28)	-77.0(3)	C(41)-C(42)-C(45)-C(48)	-160.3(9)
N(5)-Zn(1)-N(3)-C(28)	17.7(3)	C(43)-C(42)-C(45)-C(47A)	-14.4(13)
N(1)-Zn(1)-N(3)-C(28)	178.5(3)	C(41)-C(42)-C(45)-C(47A)	161.5(10)
N(7)-Zn(1)-N(3)-C(21)	-96.0(4)	C(43)-C(42)-C(45)-C(46)	159.3(9)
N(13)-Zn(1)-N(3)-C(21)	87.3(3)	C(41)-C(42)-C(45)-C(46)	-24.8(11)
N(5)-Zn(1)-N(3)-C(21)	-178.0(3)	C(28)-N(4)-C(49)-N(5)	2.9(6)
N(1)-Zn(1)-N(3)-C(21)	-17.2(3)	C(28)-N(4)-C(49)-C(50)	-176.4(3)
N(7)-Zn(1)-N(5)-C(49)	-176.7(4)	C(56)-N(5)-C(49)-N(4)	-178.1(4)
N(3)-Zn(1)-N(5)-C(49)	-20.5(3)	Zn(1)-N(5)-C(49)-N(4)	11.3(5)
N(13)-Zn(1)-N(5)-C(49)	81.9(3)	C(56)-N(5)-C(49)-C(50)	1.3(4)
N(1)-Zn(1)-N(5)-C(49)	-93.3(4)	Zn(1)-N(5)-C(49)-C(50)	-169.3(2)
N(7)-Zn(1)-N(5)-C(56)	15.7(3)	N(4)-C(49)-C(50)-C(55)	177.1(4)
N(3)-Zn(1)-N(5)-C(56)	171.9(3)	N(5)-C(49)-C(50)-C(55)	-2.2(5)
N(13)-Zn(1)-N(5)-C(56)	-85.7(3)	N(4)-C(49)-C(50)-C(51)	-1.8(7)
N(1)-Zn(1)-N(5)-C(56)	99.1(4)	N(5)-C(49)-C(50)-C(51)	178.9(4)
N(3)-Zn(1)-N(7)-C(84)	90.5(4)	C(55)-C(50)-C(51)-C(52)	-1.4(6)
N(13)-Zn(1)-N(7)-C(84)	-92.7(3)	C(49)-C(50)-C(51)-C(52)	177.4(4)
N(5)-Zn(1)-N(7)-C(84)	173.1(3)	C(57)-O(3)-C(52)-C(53)	95.1(5)
N(1)-Zn(1)-N(7)-C(84)	13.1(3)	C(57)-O(3)-C(52)-C(51)	-89.1(5)
N(3)-Zn(1)-N(7)-C(77)	-97.0(4)	C(50)-C(51)-C(52)-C(53)	-0.6(7)
N(13)-Zn(1)-N(7)-C(77)	79.7(3)	C(50)-C(51)-C(52)-O(3)	-176.2(4)
N(5)-Zn(1)-N(7)-C(77)	-14.4(3)	O(3)-C(52)-C(53)-C(54)	177.9(4)
N(1)-Zn(1)-N(7)-C(77)	-174.4(3)	C(51)-C(52)-C(53)-C(54)	1.6(6)
N(7)-Zn(1)-N(13)-C(105)	134.9(3)	O(3)-C(52)-C(53)-O(4)	-3.9(5)
N(3)-Zn(1)-N(13)-C(105)	-46.4(3)	C(51)-C(52)-C(53)-O(4)	179.8(4)
N(5)-Zn(1)-N(13)-C(105)	-137.3(3)	C(67)-O(4)-C(53)-C(52)	138.1(5)
N(1)-Zn(1)-N(13)-C(105)	41.0(3)	C(67)-O(4)-C(53)-C(54)	-44.0(7)
N(7)-Zn(1)-N(13)-C(109)	-50.1(3)	C(52)-C(53)-C(54)-C(55)	-1.0(7)
N(3)-Zn(1)-N(13)-C(109)	128.5(3)	O(4)-C(53)-C(54)-C(55)	-178.9(4)

N(5)-Zn(1)-N(13)-C(109)	37.7(3)	C(51)-C(50)-C(55)-C(54)	2.0(6)
N(1)-Zn(1)-N(13)-C(109)	-144.0(3)	C(49)-C(50)-C(55)-C(54)	-177.2(3)
C(84)-N(8)-C(1)-N(1)	0.9(6)	C(51)-C(50)-C(55)-C(56)	-179.1(3)
C(84)-N(8)-C(1)-C(2)	-177.9(3)	C(49)-C(50)-C(55)-C(56)	1.7(4)
C(10)-N(1)-C(1)-N(8)	-178.5(4)	C(53)-C(54)-C(55)-C(50)	-1.0(7)
Zn(1)-N(1)-C(1)-N(8)	11.3(5)	C(53)-C(54)-C(55)-C(56)	-179.4(5)
C(10)-N(1)-C(1)-C(2)	0.4(4)	C(77)-N(6)-C(56)-N(5)	-2.6(6)
Zn(1)-N(1)-C(1)-C(2)	-169.9(2)	C(77)-N(6)-C(56)-C(55)	178.8(3)
N(8)-C(1)-C(2)-C(9)	179.4(4)	C(49)-N(5)-C(56)-N(6)	-178.7(4)
N(1)-C(1)-C(2)-C(9)	0.6(5)	Zn(1)-N(5)-C(56)-N(6)	-8.3(6)
N(8)-C(1)-C(2)-C(3)	-3.1(8)	C(49)-N(5)-C(56)-C(55)	-0.1(4)
N(1)-C(1)-C(2)-C(3)	178.0(5)	Zn(1)-N(5)-C(56)-C(55)	170.4(3)
C(9)-C(2)-C(3)-C(4)	0.5(7)	C(50)-C(55)-C(56)-N(6)	177.4(4)
C(1)-C(2)-C(3)-C(4)	-176.8(4)	C(54)-C(55)-C(56)-N(6)	-4.1(8)
C(5)-N(9)-C(4)-C(7)	1.6(7)	C(50)-C(55)-C(56)-N(5)	-1.3(5)
C(5)-N(9)-C(4)-C(3)	-177.9(5)	C(54)-C(55)-C(56)-N(5)	177.3(5)
C(2)-C(3)-C(4)-C(7)	0.6(7)	C(52)-O(3)-C(57)-C(62)	-21.6(6)
C(2)-C(3)-C(4)-N(9)	-179.9(5)	C(52)-O(3)-C(57)-C(58)	161.2(5)
C(4)-N(9)-C(5)-C(6)	2.7(8)	C(62)-C(57)-C(58)-C(59)	4.5(9)
C(4)-N(9)-C(5)-C(11)	-174.6(5)	O(3)-C(57)-C(58)-C(59)	-178.1(6)
N(9)-C(5)-C(6)-N(10)	-4.2(7)	C(57)-C(58)-C(59)-C(60)	-1.3(12)
C(11)-C(5)-C(6)-N(10)	173.3(4)	C(58)-C(59)-C(60)-C(61)	-1.9(12)
N(9)-C(5)-C(6)-C(16)	170.9(4)	C(58)-C(59)-C(60)-C(63)	179.2(7)
C(11)-C(5)-C(6)-C(16)	-11.6(7)	C(59)-C(60)-C(61)-C(62)	2.1(10)
C(7)-N(10)-C(6)-C(5)	2.2(7)	C(63)-C(60)-C(61)-C(62)	-179.1(6)
C(7)-N(10)-C(6)-C(16)	-172.5(4)	C(58)-C(57)-C(62)-C(61)	-4.4(8)
N(9)-C(4)-C(7)-N(10)	-3.6(6)	O(3)-C(57)-C(62)-C(61)	178.5(4)
C(3)-C(4)-C(7)-N(10)	176.0(4)	C(60)-C(61)-C(62)-C(57)	1.0(8)
N(9)-C(4)-C(7)-C(8)	178.7(4)	C(61)-C(60)-C(63)-C(66A)	8.7(14)
C(3)-C(4)-C(7)-C(8)	-1.7(6)	C(59)-C(60)-C(63)-C(66A)	-172.5(12)
C(6)-N(10)-C(7)-C(4)	2.1(7)	C(61)-C(60)-C(63)-C(65A)	136.9(10)
C(6)-N(10)-C(7)-C(8)	179.3(4)	C(59)-C(60)-C(63)-C(65A)	-44.4(12)
C(4)-C(7)-C(8)-C(9)	2.2(6)	C(61)-C(60)-C(63)-C(64)	101.4(9)
N(10)-C(7)-C(8)-C(9)	-175.1(4)	C(59)-C(60)-C(63)-C(64)	-79.9(10)
C(3)-C(2)-C(9)-C(8)	-0.2(6)	C(61)-C(60)-C(63)-C(66)	-127.1(10)
C(1)-C(2)-C(9)-C(8)	178.0(3)	C(59)-C(60)-C(63)-C(66)	51.7(12)
C(3)-C(2)-C(9)-C(10)	-179.2(4)	C(61)-C(60)-C(63)-C(65)	-2.3(13)
C(1)-C(2)-C(9)-C(10)	-1.1(4)	C(59)-C(60)-C(63)-C(65)	176.4(11)
C(7)-C(8)-C(9)-C(2)	-1.2(6)	C(61)-C(60)-C(63)-C(64A)	-116.1(9)
C(7)-C(8)-C(9)-C(10)	177.3(4)	C(59)-C(60)-C(63)-C(64A)	62.6(11)
C(21)-N(2)-C(10)-N(1)	-2.5(6)	C(53)-O(4)-C(67)-C(68)	131.0(6)
C(21)-N(2)-C(10)-C(9)	178.2(3)	C(53)-O(4)-C(67)-C(72)	-50.6(8)
C(1)-N(1)-C(10)-N(2)	179.5(4)	O(4)-C(67)-C(68)-C(69)	175.9(7)
Zn(1)-N(1)-C(10)-N(2)	-11.0(6)	C(72)-C(67)-C(68)-C(69)	-2.5(13)
C(1)-N(1)-C(10)-C(9)	-1.2(4)	C(67)-C(68)-C(69)-C(70)	2.0(11)
Zn(1)-N(1)-C(10)-C(9)	168.4(2)	C(68)-C(69)-C(70)-C(71)	-0.5(13)
C(2)-C(9)-C(10)-N(2)	-179.1(4)	C(68)-C(69)-C(70)-C(73)	-177.7(7)
C(8)-C(9)-C(10)-N(2)	2.2(8)	C(69)-C(70)-C(71)-C(72)	-0.8(12)
C(2)-C(9)-C(10)-N(1)	1.6(5)	C(73)-C(70)-C(71)-C(72)	176.4(7)
C(8)-C(9)-C(10)-N(1)	-177.1(5)	C(70)-C(71)-C(72)-C(67)	0.5(12)
C(15)-N(11)-C(11)-C(12)	-1.8(9)	O(4)-C(67)-C(72)-C(71)	-177.1(7)
C(15)-N(11)-C(11)-C(5)	-176.8(5)	C(68)-C(67)-C(72)-C(71)	1.2(13)

C(6)-C(5)-C(11)-C(12)	148.2(5)	C(71)-C(70)-C(73)-C(74)	138.1(10)
N(9)-C(5)-C(11)-C(12)	-34.4(8)	C(69)-C(70)-C(73)-C(74)	-44.5(11)
C(6)-C(5)-C(11)-N(11)	-36.4(7)	C(71)-C(70)-C(73)-C(75A)	-144.7(9)
N(9)-C(5)-C(11)-N(11)	141.0(5)	C(69)-C(70)-C(73)-C(75A)	32.6(11)
N(11)-C(11)-C(12)-C(13)	1.5(8)	C(71)-C(70)-C(73)-C(75)	13.6(12)
C(5)-C(11)-C(12)-C(13)	176.9(5)	C(69)-C(70)-C(73)-C(75)	-169.0(9)
C(11)-C(12)-C(13)-C(14)	-2.0(10)	C(71)-C(70)-C(73)-C(76A)	-8.8(12)
C(12)-C(13)-C(14)-C(15)	2.7(11)	C(69)-C(70)-C(73)-C(76A)	168.5(9)
C(13)-C(14)-C(15)-N(11)	-2.5(10)	C(71)-C(70)-C(73)-C(74A)	101.5(9)
C(11)-N(11)-C(15)-C(14)	2.2(9)	C(69)-C(70)-C(73)-C(74A)	-81.1(9)
C(20)-N(12)-C(16)-C(17)	-0.4(9)	C(71)-C(70)-C(73)-C(76)	-113.5(9)
C(20)-N(12)-C(16)-C(6)	-177.8(5)	C(69)-C(70)-C(73)-C(76)	63.9(9)
C(5)-C(6)-C(16)-N(12)	-49.1(7)	C(84)-N(7)-C(77)-C(78)	2.9(5)
N(10)-C(6)-C(16)-N(12)	125.5(6)	Zn(1)-N(7)-C(77)-C(78)	-169.5(3)
C(5)-C(6)-C(16)-C(17)	133.6(6)	C(84)-N(7)-C(77)-N(6)	-175.5(4)
N(10)-C(6)-C(16)-C(17)	-51.8(8)	Zn(1)-N(7)-C(77)-N(6)	12.0(6)
N(12)-C(16)-C(17)-C(18)	-0.6(10)	C(56)-N(6)-C(77)-C(78)	-177.0(4)
C(6)-C(16)-C(17)-C(18)	176.6(6)	C(56)-N(6)-C(77)-N(7)	1.2(7)
C(16)-C(17)-C(18)-C(19)	2.7(11)	N(7)-C(77)-C(78)-C(79)	175.0(4)
C(17)-C(18)-C(19)-C(20)	-3.7(13)	N(6)-C(77)-C(78)-C(79)	-6.3(6)
C(18)-C(19)-C(20)-N(12)	2.8(14)	N(7)-C(77)-C(78)-C(83)	-3.1(4)
C(16)-N(12)-C(20)-C(19)	-0.8(12)	N(6)-C(77)-C(78)-C(83)	175.7(3)
C(10)-N(2)-C(21)-C(22)	179.3(4)	C(77)-C(78)-C(79)-C(80)	-179.0(4)
C(10)-N(2)-C(21)-N(3)	1.2(6)	C(83)-C(78)-C(79)-C(80)	-1.4(6)
C(28)-N(3)-C(21)-C(22)	0.3(4)	C(78)-C(79)-C(80)-O(5)	171.8(3)
Zn(1)-N(3)-C(21)-C(22)	-163.8(3)	C(78)-C(79)-C(80)-C(81)	-2.0(6)
C(28)-N(3)-C(21)-N(2)	178.6(4)	C(85)-O(5)-C(80)-C(79)	101.8(4)
Zn(1)-N(3)-C(21)-N(2)	14.5(6)	C(85)-O(5)-C(80)-C(81)	-84.3(5)
N(2)-C(21)-C(22)-C(23)	-0.4(6)	C(95)-O(6)-C(81)-C(82)	-15.1(6)
N(3)-C(21)-C(22)-C(23)	178.2(4)	C(95)-O(6)-C(81)-C(80)	169.8(3)
N(2)-C(21)-C(22)-C(27)	-178.8(3)	C(79)-C(80)-C(81)-O(6)	179.0(4)
N(3)-C(21)-C(22)-C(27)	-0.2(4)	O(5)-C(80)-C(81)-O(6)	6.0(6)
C(21)-C(22)-C(23)-C(24)	-178.2(4)	C(79)-C(80)-C(81)-C(82)	4.6(7)
C(27)-C(22)-C(23)-C(24)	0.0(6)	O(5)-C(80)-C(81)-C(82)	-168.4(4)
C(22)-C(23)-C(24)-O(1)	-177.8(3)	O(6)-C(81)-C(82)-C(83)	-176.9(4)
C(22)-C(23)-C(24)-C(25)	-1.5(6)	C(80)-C(81)-C(82)-C(83)	-2.5(6)
C(29)-O(1)-C(24)-C(23)	-113.0(4)	C(81)-C(82)-C(83)-C(84)	177.4(4)
C(29)-O(1)-C(24)-C(25)	70.6(5)	C(81)-C(82)-C(83)-C(78)	-0.9(5)
C(39)-O(2)-C(25)-C(26)	6.8(5)	C(77)-C(78)-C(83)-C(82)	-178.8(4)
C(39)-O(2)-C(25)-C(24)	-173.4(3)	C(79)-C(78)-C(83)-C(82)	3.2(7)
C(23)-C(24)-C(25)-O(2)	-177.6(4)	C(77)-C(78)-C(83)-C(84)	2.7(5)
O(1)-C(24)-C(25)-O(2)	-1.8(6)	C(79)-C(78)-C(83)-C(84)	-175.3(4)
C(23)-C(24)-C(25)-C(26)	2.1(7)	C(82)-C(83)-C(84)-N(7)	-179.4(4)
O(1)-C(24)-C(25)-C(26)	177.9(4)	C(78)-C(83)-C(84)-N(7)	-0.8(4)
O(2)-C(25)-C(26)-C(27)	179.1(3)	C(82)-C(83)-C(84)-N(8)	0.4(6)
C(24)-C(25)-C(26)-C(27)	-0.6(6)	C(78)-C(83)-C(84)-N(8)	178.9(3)
C(25)-C(26)-C(27)-C(28)	178.8(4)	C(77)-N(7)-C(84)-C(83)	-1.2(4)
C(25)-C(26)-C(27)-C(22)	-0.9(6)	Zn(1)-N(7)-C(84)-C(83)	171.5(3)
C(23)-C(22)-C(27)-C(26)	1.4(7)	C(77)-N(7)-C(84)-N(8)	179.1(4)
C(21)-C(22)-C(27)-C(26)	179.9(4)	Zn(1)-N(7)-C(84)-N(8)	-8.2(6)
C(23)-C(22)-C(27)-C(28)	-178.3(4)	C(1)-N(8)-C(84)-C(83)	176.9(4)
C(21)-C(22)-C(27)-C(28)	0.1(5)	C(1)-N(8)-C(84)-N(7)	-3.5(7)

C(26)-C(27)-C(28)-N(3)	-179.7(4)	C(80)-O(5)-C(85)-C(90)	143.2(4)
C(22)-C(27)-C(28)-N(3)	0.0(4)	C(80)-O(5)-C(85)-C(86)	-41.5(6)
C(26)-C(27)-C(28)-N(4)	-0.5(6)	O(5)-C(85)-C(86)-C(87)	-174.6(5)
C(22)-C(27)-C(28)-N(4)	179.3(3)	C(90)-C(85)-C(86)-C(87)	0.1(9)
C(21)-N(3)-C(28)-C(27)	-0.2(4)	C(85)-C(86)-C(87)-C(88)	2.2(10)
Zn(1)-N(3)-C(28)-C(27)	164.9(2)	C(86)-C(87)-C(88)-C(89)	-3.0(9)
C(21)-N(3)-C(28)-N(4)	-179.3(4)	C(86)-C(87)-C(88)-C(91)	177.9(6)
Zn(1)-N(3)-C(28)-N(4)	-14.2(5)	C(87)-C(88)-C(89)-C(90)	1.8(9)
C(49)-N(4)-C(28)-C(27)	179.6(4)	C(91)-C(88)-C(89)-C(90)	-179.2(6)
C(49)-N(4)-C(28)-N(3)	-1.5(7)	C(88)-C(89)-C(90)-C(85)	0.5(8)
C(24)-O(1)-C(29)-C(34)	-145.8(4)	O(5)-C(85)-C(90)-C(89)	173.9(4)
C(24)-O(1)-C(29)-C(30)	39.6(6)	C(86)-C(85)-C(90)-C(89)	-1.5(7)
C(34)-C(29)-C(30)-C(31)	1.6(8)	C(87)-C(88)-C(91)-C(94)	-9.4(9)
O(1)-C(29)-C(30)-C(31)	175.5(5)	C(89)-C(88)-C(91)-C(94)	171.5(6)
C(29)-C(30)-C(31)-C(32)	-3.9(8)	C(87)-C(88)-C(91)-C(92)	110.2(7)
C(30)-C(31)-C(32)-C(33)	4.3(8)	C(89)-C(88)-C(91)-C(92)	-68.9(7)
C(30)-C(31)-C(32)-C(35)	-170.2(5)	C(87)-C(88)-C(91)-C(93)	-124.9(7)
C(31)-C(32)-C(33)-C(34)	-2.5(10)	C(89)-C(88)-C(91)-C(93)	56.0(8)
C(35)-C(32)-C(33)-C(34)	171.0(6)	C(81)-O(6)-C(95)-C(96)	146.5(4)
C(32)-C(33)-C(34)-C(29)	0.1(9)	C(81)-O(6)-C(95)-C(100)	-40.4(6)
O(1)-C(29)-C(34)-C(33)	-174.2(4)	C(100)-C(95)-C(96)-C(97)	1.3(6)
C(30)-C(29)-C(34)-C(33)	0.4(8)	O(6)-C(95)-C(96)-C(97)	175.3(3)
C(31)-C(32)-C(35)-C(37)	-173.6(9)	C(95)-C(96)-C(97)-C(98)	1.3(7)
C(33)-C(32)-C(35)-C(37)	12.5(12)	C(96)-C(97)-C(98)-C(99)	-3.2(6)
C(31)-C(32)-C(35)-C(37A)	167.7(9)	C(96)-C(97)-C(98)-C(101)	179.6(4)
C(33)-C(32)-C(35)-C(37A)	-6.2(12)	C(97)-C(98)-C(99)-C(100)	2.5(6)
C(31)-C(32)-C(35)-C(38)	-44.4(13)	C(101)-C(98)-C(99)-C(100)	179.8(4)
C(33)-C(32)-C(35)-C(38)	141.7(12)	C(96)-C(95)-C(100)-C(99)	-1.9(6)
C(31)-C(32)-C(35)-C(36A)	-54.0(12)	O(6)-C(95)-C(100)-C(99)	-174.7(4)
C(33)-C(32)-C(35)-C(36A)	132.1(12)	C(98)-C(99)-C(100)-C(95)	-0.2(6)
C(31)-C(32)-C(35)-C(36)	82.8(7)	C(99)-C(98)-C(101)-C(104)	-98.5(5)
C(33)-C(32)-C(35)-C(36)	-91.2(8)	C(97)-C(98)-C(101)-C(104)	78.4(6)
C(31)-C(32)-C(35)-C(38A)	61.2(8)	C(99)-C(98)-C(101)-C(103)	23.1(7)
C(33)-C(32)-C(35)-C(38A)	-112.8(8)	C(97)-C(98)-C(101)-C(103)	-160.0(6)
C(25)-O(2)-C(39)-C(40)	-97.6(5)	C(99)-C(98)-C(101)-C(102)	146.2(5)
C(25)-O(2)-C(39)-C(44)	79.8(5)	C(97)-C(98)-C(101)-C(102)	-36.9(6)
C(44)-C(39)-C(40)-C(41)	2.4(6)	C(109)-N(13)-C(105)-C(106)	-0.2(7)
O(2)-C(39)-C(40)-C(41)	180.0(4)	Zn(1)-N(13)-C(105)-C(106)	175.0(4)
C(39)-C(40)-C(41)-C(42)	-0.9(8)	N(13)-C(105)-C(106)-C(107)	-0.6(8)
C(40)-C(41)-C(42)-C(43)	-2.0(8)	C(105)-C(106)-C(107)-C(108)	1.6(9)
C(40)-C(41)-C(42)-C(45)	-178.2(5)	C(106)-C(107)-C(108)-C(109)	-1.4(7)
C(41)-C(42)-C(43)-C(44)	3.2(9)	C(107)-C(108)-C(109)-N(13)	0.6(7)
C(45)-C(42)-C(43)-C(44)	179.6(6)	C(105)-N(13)-C(109)-C(108)	0.1(7)
C(40)-C(39)-C(44)-C(43)	-1.2(8)	Zn(1)-N(13)-C(109)-C(108)	-174.5(4)

A2. List of abbreviations

Å	Ångström
aPc	asymmetric phthalocyanine
Aq	anthraquinone
bpy	2,2′-bipyridine
c	concentration
C	compound
Calcd.	calculated
CCDC	Cambridge Crystallographic Data Centre
CE	crown ether
CNP	1-chloronaphthalene
CPA	chirped pulse amplification
CR	charge recombination
CS	charge separation
CV	cyclic voltammetry
DBA	dibenzylideneacetone
DBU	1,8-diazabicyclo[5.4.0]undec-7-ene
DCTB	*trans*-2-[3-(4-*tert*-butylphenyl)-2-methyl-2-propenylidene]malononitrile
DMAE	2-(dimethyl)-aminoethanol
DMF	*N,N*-dimethylformamide
DMSO	dimethyl sulfoxide
DNA	deoxyribonucleic acid
dppz	dipyrido[3,2-*a*:2',3'-*c*]phenazine
dpq	dipyrido[3,2-*f*:2',3'-*h*]quinoxaline
DSA	digital signal analyser
EDTA	ethylenediaminetetraacetic acid
EI	electron impact
ESI	electrospray ionisation
esu	electrostatic unit
ET	energy transfer
EtOH	ethanol
eV	electronvolt
Fc	ferrocene
Fc^+	ferrocenium
FT	Fourier transformation
FT-IR	Fourier transform infrared
FTMS	Fourier transform mass spectrometer
GCR	grade control receiver
h	hour or Planck constant
H_2Pc	metal-free phthalocyanine
HAT	hexaazatriphenylene
HOMO	highest occupied molecular orbital
HOPG	highly oriented pyrolytic graphite
HRS	hyper-Rayleigh light scattering
IPCE	incident photons to current efficiency
IPDS	image plate detector system
IR	infrared
ISC	intersystem crossing
J	coupling constant

K	Kelvin
LUMO	lowest unoccupied molecular orbital
M	molar or molecule
m.p.	melting point
m/z	mass to charge ratio
MALDI	matrix-assisted laser desorption ionisation
max.	maximum
MDMO-PPV	poly[2-methoxy-5-(3',7'-dimethyloctyloxy)-1-4-phenylene vinylene]
MeOH	methanol
Meph-tpy	4'-(*p*-tolyl)-2,2';6',2''-terpyridine
Min.	minimum
MLCT	metal-to-ligand charge transfer
MPc	metal phthalocyanine
MS	mass spectrometry
NLO	nonlinear optics
NMR	nuclear magnetic resonance
NOPA	noncollinear optical parametric amplifier
o	ortho
p	para
Pc	phthalocyanine
PDI	perylenediimide
PEDOT	poly(3,4-ethylenedioxythiophene)
PET	photoinduced electron transfer
Ph	phenyl
Phendione	1,10-phenanthroline-5,6-dione
Pn	phthalonitrile
Por	porphyrin
ppm	parts per million
PSS	poly(styrenesulfonate)
Pz	porphyrazine
r.t.	room temperature
R_f	retention factor
S	singlet
SAM	self-assembled monolayer
SAXS	small-angle X-ray scattering
SCE	saturated calomel electrode
SEC	size exclusion chromatography
SEM	scanning electron microscopy
STM	scanning tunneling microscopy
T	triplet
TEM	transmission electron microscopy
tert	tertiary
TFA	trifluoroacetic acid
TGA	thermal gravimetric analysis
THF	tetrahydrofuran
TLC	thin layer chromatography
TMS	tetramethylsilane
TPPor	*meso*-tetraphenylporphyrin
tpy	2,2';6',2''-terpyridine
TTF	tetrathiafulvalene

TTF-dppz	4',5'-bis-(propylthio)tetrathiafulvaleno[4,5-*i*]dipyrido-[3,2-*a*:2',3'-*c*]-phenazine
UHV	ultrahigh vacuum
UV-vis	ultraviolet-visible
XPS	X-ray photoelectron spectroscopy
YAG	yttrium aluminium garnet
Z	number of molecules (formula units) per unit cell
β_{HRS}	first-order hyperpolarisability determined by HRS
δ	chemical shift
ε	extinction coefficient
θ	Weiss constant
θ	diffraction angle
λ	wavelength
λ_{max}	wavelength of maximum absorption
μ	prefix or linear absorption coefficient
ν	frequency
ρ_e	electron density
Φ	quantum yield
Φ_F	fluorescence quantum yield

A3. Publications

- *Synthesis and Electrochemical and Photophysical Studies of Tetrathiafulvalene-Annulated Phthalocyanines*
  C. Loosli, C. Jia, S.-X. Liu, M. Haas, M. Dias, E. Levillain, A. Neels, G. Labat, A. Hauser, S. Decurtins, *J. Org. Chem.* **2005**, *70*, 4988.

- *A Synthetic Approach to Asymmetric Phthalocyanines with Peripheral Metal-Binding Sites*
  M. Haas, S.-X. Liu, A. Neels, S. Decurtins, *Eur. J. Org. Chem.* **2006**, published online, DOI: 10.1002/ejoc.200600619.

A4. Conferences and contributions

- Fall Meeting 2003 of the Swiss Chemical Society, October 9, 2003, Lausanne, Switzerland, poster presentation.

- 3rd International Conference on Porphyrins and Phthalocyanines (ICPP-3), July 11-16, 2004, New Orleans, USA, poster presentation.

- Fall Meeting 2004 of the Swiss Chemical Society, October 7, 2004, Zürich, Switzerland, poster presentation.

- NRP 47 Spring School on Supramolecular Chemistry of the Swiss National Science Foundation, April 11-15, 2005, Löwenberg Center, Murten, Switzerland, poster presentation.

- Fall Meeting 2005 of the Swiss Chemical Society, October 13, 2005, Lausanne, Switzerland, poster presentation.

- Summer School on Advanced Materials, September 18-22, 2005, Villars-sur-Ollon, Switzerland.

- OAMS06, workshop on Organising and Addressing Molecules on Surfaces, May 24-28, 2006, Platja d'Aro, Spain, poster presentation.

- 4th International Conference on Porphyrins and Phthalocyanines (ICPP-4), July 2-7, 2006, Rome, Italy, poster presentation.

- Fall Meeting 2006 of the Swiss Chemical Society, October 13, 2006, Zürich, Switzerland, poster presentation.

A5. Curriculum vitae

Family name: Haas

First name: Marco

Date of birth: May 25, 1978

Place of origin: Muntelier FR

Education

1985-1993	Primary and secondary school in Ittigen BE
1993-1998	Commercial high school, Bern-Kirchenfeld
1998-2002	Studies of Chemistry at the University of Berne
2002	Master of Science in Chemistry
2003-2006	PhD thesis directed by Prof. Dr. Silvio Decurtins at the University of Berne

Assistance

2003-2006	Assistant in the laboratory courses at the Department of Chemistry and Biochemistry, University of Berne

Erklärung (gemäss Art. 28 Abs. 2 RSL 05)

Name/Vorname: Haas Marco

Matrikelnummer: 98-105-455

Studiengang: Doktorat phil.-nat. in Chemie

Titel der Arbeit: A Synthetic Approach to Asymmetric Phthalocyanines with Peripheral Metal-Binding Sites and Their Divalent Ruthenium Complexes

Leiter der Arbeit: Prof. Dr. Silvio Decurtins

Ich erkläre hiermit, dass ich diese Arbeit selbständig verfasst und keine anderen als die angegebenen Quellen benutzt habe. Alle Stellen, die wörtlich oder sinngemäss aus Quellen entnommen wurden, habe ich als solche gekennzeichnet. Mir ist bekannt, dass andernfalls der Senat gemäss Artikel 36 Absatz 1 Buchstabe o des Gesetzes vom 5. September 1996 über die Universität zum Entzug des auf Grund dieser Arbeit verliehenen Titels berechtigt ist.

Ort/Datum   Marco Haas